Development of Design Guidelines for Hybrid Ground-Coupled Heat Pump Systems

by
Scott P. Hackel

A thesis submitted in partial fulfillment of the requirements for the degree of
MASTER OF SCIENCE
Mechanical Engineering

at the
UNIVERSITY OF WISCONSIN—MADISON

Advisors: Dr. Gregory F. Nellis and Dr. Sanford A. Klein
May, 2008

This thesis has been approved by

_____	_____
Dr. Sanford A. Klein, Professor	Date
_____	_____
Dr. Gregory F. Nellis, Assistant Professor	Date

Development of Design Guidelines for Hybrid Ground-Coupled Heat Pump Systems

Scott P. Hackel

Under the supervision of Professors Greg Nellis and Sanford Klein
and the University of Wisconsin – Madison

With Jeff Thornton – Thermal Energy Systems Specialists

Abstract

Hybrid ground-coupled heat pump systems (HyGCHPs) couple conventional ground-coupled heat pump (GCHP) equipment with supplemental heat rejection or extraction systems. In cooling- or heating-dominated climates, the use of these supplemental systems has been shown to significantly improve the economics and energy usage of the system. However, the design and operation of HyGCHPs are significantly more complex than GCHPs and there is currently relatively little information available in this regard that is accessible to the practicing engineer.

This project solves this problem through the development of a detailed simulation-based tool incorporating physics-based models of the HyGCHP system components using the TRNSYS simulation program. The simulation model has been used to develop a distributable software tool for use by the practicing engineer, as well as to complete a parametric study of many different scenarios varying in climate, building type, and economic and physical assumptions. The results of the parametric studies demonstrate a set of general design guidelines that can be used to select an equipment configuration, size equipment, and control the equipment of a typical HyGCHP system.

Acknowledgements

This thesis project was made possible through assistance from several other individuals. I would like to thank my advisors, Greg Nellis and Sanford Klein, for everything they've done over the past two years to make this project and my Master's degree successful. I am also tremendously grateful to Diego Arias for his software assistance, specifically in helping to develop the distributable version of my model. I'd also like to thank Jeff, David, and Tim at Thermal Energy Systems Specialists; they were a constant source of technical knowledge in completing this project.

I thank my family for being very supportive during one of the most demanding periods of my life so far; especially my wife Jenn, my parents Robert and Joyce, and my brothers Mike and Ben. Your patience is very much appreciated.

Finally, I would like to thank the American Society of Heating, Refrigeration, and Air-conditioning Engineers for their financial support, and the members of the ASHRAE Technical Committee on Geothermal Energy for their continuous review and critique of the project.

Executive Summary

Hybrid ground-coupled heat pump systems (HyGCHPs) couple conventional ground-coupled heat pump (GCHP) equipment with supplemental devices to reject or supply more heat than is possible with a stand-alone ground heat exchanger (GHX). In cooling- and heating-dominated climates, the use of these supplemental devices has been shown to significantly improve the economics and energy usage of the system. However, the design and operation of HyGCHPs are significantly more complex than GCHPs and there is currently relatively little information available in this regard. This research project has created a HyGCHP model, integrated it with an optimization algorithm, and exercised it over a range of conditions in order to identify the optimal (lowest life-cycle cost) sizing and control strategies for these systems. The goal of the project is to assist practicing engineers with selecting and designing HyGCHP systems by providing a powerful simulation/optimization tool as well as a series of more approximate design guidelines based on the parametric analysis.

The HyGCHP model is created using TRNSYS (Klein et al, 2006). Figure 1 shows a schematic of the model, with a cooling tower included as the supplemental device for this cooling-dominated system. In a heating-dominated system, the supplemental device (e.g., a boiler) would *add* heat to the fluid (and the location of the supplemental device and the GHX would be swapped). All components in this schematic are included in the TRNSYS model. The building is modeled independently to provide loads to the heat pumps; the heat pumps are appropriately sized so that they are capable of meeting the peak loads experienced by the building. This approach improves computational speed and therefore allows optimization of the equipment and control strategy (to find the design with the lowest life-cycle cost).

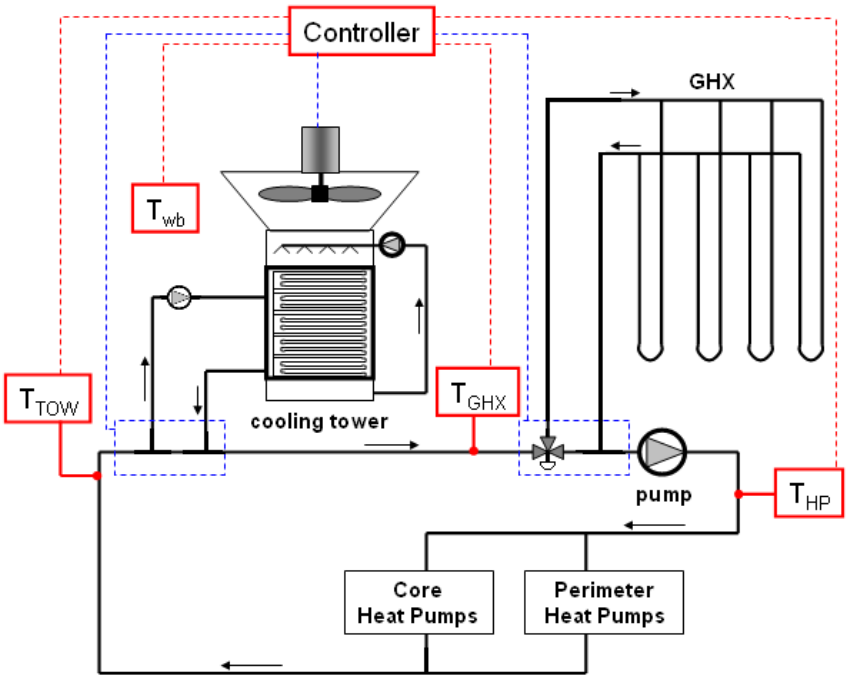

Figure 1. A schematic of a hybrid ground-coupled heat pump system, with a cooling tower as a supplemental heat rejection device. Temperature values show points where measurements are necessary for control.

The temperatures shown in Figure 1 represent the locations where measurements are necessary for control of the system. For the cooling-hybrid system using a cooling tower (shown in Figure 1), the cooling tower is activated when the difference between the fluid upstream of the tower (T_{TOW}) and the ambient wet-bulb temperature (T_{wb}) is greater than a control setpoint (ΔT_1). The GHX is operated when the temperature of the fluid upstream of the bore field (T_{GHX}) is greater than a control setpoint (T_{Cool2}) when the system is in cooling mode and less than a different control setpoint (T_{Heat1}) when the system is in heating. All these control set points are optimized to minimize life cycle cost. The optimizer also varies the equipment size (in the case shown in Figure 1, the equipment size includes the size of the cooling tower and the bore field). A distributable version of this HyGCHP model – integrated with the optimizer – represents one key deliverable from this project; it is a powerful design tool that can be used to specifically design a HyGCHP system for a particular project.

Additionally, the HyGCHP model and optimizer were utilized to develop design guidelines, which was the other major focus of this project. These guidelines are general observations regarding the optimal values of the control set points and equipment sizes as the type of building and climate changes. These guidelines are based on optimizing the system design and control set points in order to achieve the lowest life cycle cost over a 20 year time span for 20 different building/climate combinations using a set of nominal input parameters; the guidelines should be used with these limitations in mind. The purpose of the distributable program is to provide a design tool that is not constrained by these limitations. Building loads were generated using a model created in a previous ASHRAE project (ASHRAE TRP-1120, CDH and TESS, 2000). The climates were selected so that they span from cooling-dominated to heating-dominated (including a balanced case) and from wet to dry. In order to accomplish the simulation and the economic optimization, it is necessary to specify a set of parameters that characterize everything from the market conditions to the soil conditions to various aspects of equipment performance. These parameters vary according to location, year, manufacturer, designer, etc.; the value of the distributable simulation tool is that individual geothermal system designers can vary these parameters according to their situation and experience. However, for the parametric study, default values of the HyGCHP model parameters were used to carry out optimizations and develop the design guidelines. These values are based on literature research, and are summarized in Table 1.

Table 1. Summary of input parameters for the parametric study.

Category	Parameter	Baseline value
Bore field	Ground conductivity	1.4 Btu/hr-ft-F
	Ground diffusivity	1.1 ft^2/day
	Grout conductivity	0.8 Btu/hr-ft-F
	Initial ground temperature	varied according to climate
	Maximum drilling depth	300 ft
	Borehole diameter	4.5 inch
Other equipment	Pump efficiency	60%
	Boiler efficiency	85%
	Max. entering water temp. for heat pump	95°F
	Min. entering water temp. for heat pump	35°F
	EER of heat pump at ARI 13256-1 conditions	16
	COP of heat pump at ARI 13256-1 conditions	3.4
Economic	Life span	20 years
	Discount rate	8.5%
	Down payment	30%
	Loan interest rate (20 year loan)	6.0%
	Tax rate	35%
	Peak electricity rate	0.101 $/kW-hr
	Off-peak electricity rate	0.063 $/kW-hr
	Electricity demand charge	6.22$/kW, 15 minutes
	Gas price	0.99 $/therm
	Water price	4.0 $/100 ft^3
	Bore field cost	10 $/ft

For cases resembling the economic conditions and equipment summarized in Table 1, the results of the parametric study suggest the design guidelines detailed below.

Design Guidelines and Observations – Cooling Dominated Systems

- **GHX Sizing: size the ground heat exchanger (GHX) so that it is just capable of meeting the peak heating load**. Figure 2 illustrates the optimal size of the GHX (sum of all bore depths) as a function of the peak heating load (each point represents a different climate/building combination from the parametric study); notice that the optimal GHX size is essentially proportional to the peak heating load.

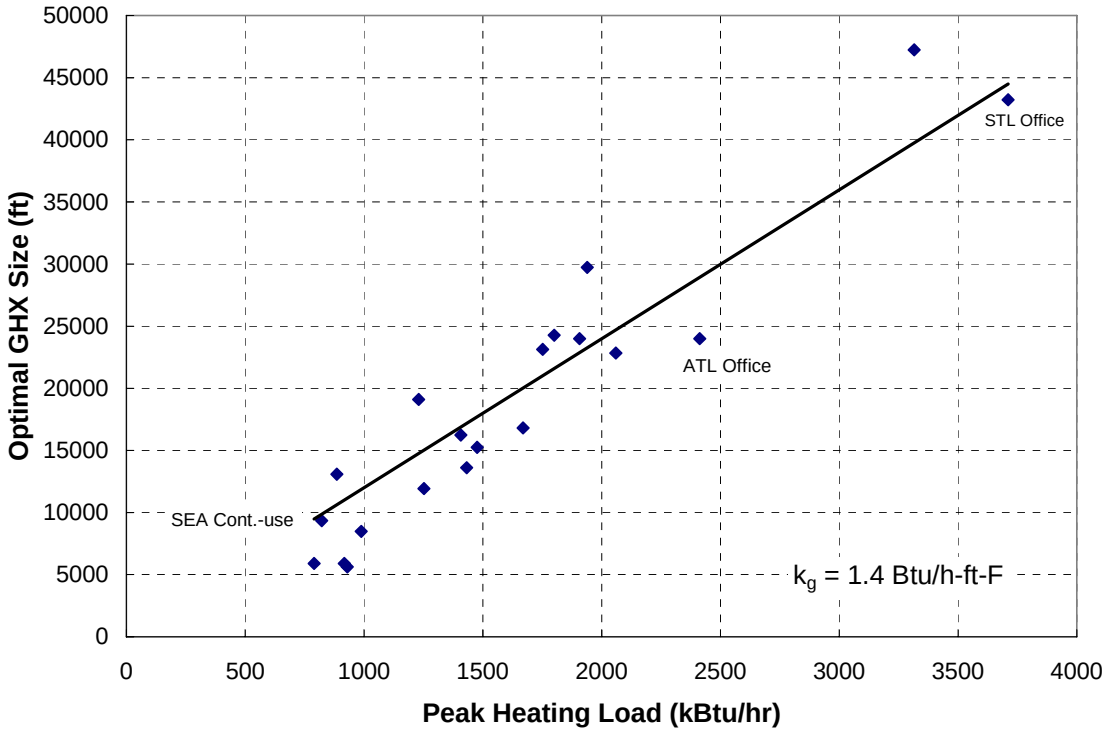

Figure 2. Optimal GHX size as a function of the peak heating load for each building/climate scenario.

The scatter in Figure 2 is partly due to the different initial ground temperatures associated with the various climates. Figure 3 illustrates the best fit regression of the ratio of the optimal GHX size to the peak heating load as a function of the initial ground temperature; as expected, less GHX length is required to meet a given heating load in regions with high ground temperature.

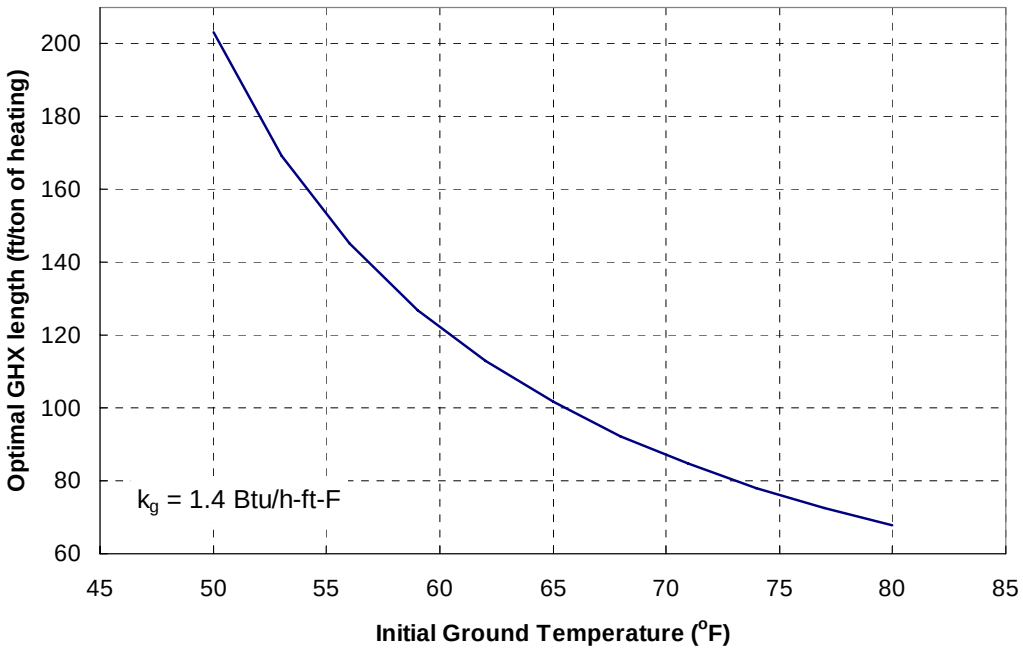

Figure 3. Ratio of the optimal GHX length for a cooling dominated system to the peak heating load as a function of the initial ground temperature (assumes k_g=1.4 Btu/hr-ft-^{o}F).

Some current methods/tools for sizing hybrid systems (such as the GCHPCalc program discussed below) already use this design guideline; it will be shown that the GCHPCalc software (Kavanaugh, 1997) arrives at a similar GHX size as shown here. The assumed ground conductivity (k_g) for these results is 1.4 Btu/hr-ft-^{o}F. Sensitivity studies were carried out on many of the parameters listed in Table 1, including k_g; these studies suggest that every 0.1 Btu/hr-ft-^{o}F decrease in k_g will result in a 5% increase in the optimal GHX size.

- **Supplemental Device Size: size the supplemental cooling device based on the peak cooling load that is not met by the GHX.**
    - The rated capacity of the optimally sized cooling tower (C_{CCCT}, in tons (12 kBtu/hr)), is 2.1x the unmet load ($q_{unmet,cool}$, in tons); the unmet load should be calculated according to Equation (1):

$$C_{CCCT} = 2.1 q_{unmet,cool} = 2.1 \left(q_{peak,cool} - \underbrace{\frac{L_{tot}}{3.05 T_{ground}}}_{q_{GHX,cool}} \right) \quad (1)$$

where T_{ground} is the initial ground temperature (in °F) and L_{tot} is the GHX length (in ft). The 2nd term in Eq. (1), $q_{GHX,cool}$, is the cooling capacity of the GHX; notice that the cooling capacity is proportional to length (a longer GHX provides more cooling) and inversely proportional to the initial ground temperature (a cooler ground provides more cooling). Equation (1) represents a best fit to the model predictions.

- For the cooling tower characteristics and economic conditions considered in the parametric study, it is economically attractive to oversize the tower and then use it less frequently, almost always operating it at low speed. Low speed was chosen here as 50% speed. (The setpoint temperature for high speed operation of the tower, T_{Cool1}, is therefore set to 5-8°F above the maximum entering heat pump temperature; this still allows the tower to meet the critical temperature limits). Alternatively, if a single-speed tower must be used, the tower is 1.3x the unmet cooling load; this unmet cooling load should then be calculated according to Equation (2).

$$C_{CCCT} = 1.3 q_{unmet,cool} = 1.3 \left(q_{peak,cool} - \underbrace{\frac{L_{tot}}{4.72 T_{ground}}}_{q_{GHX,cool}} \right) \quad (2)$$

- The optimal cooling tower size can also be estimated based on climate; specifically how balanced the building load is. Figure 4 illustrates the optimal cooling tower size (normalized by the building size) as a function of the ratio of the annual heating load to the annual cooling load of the building. Sizing the cooling tower according to Figure 4 should lead to approximately the same result as Eq. (1).

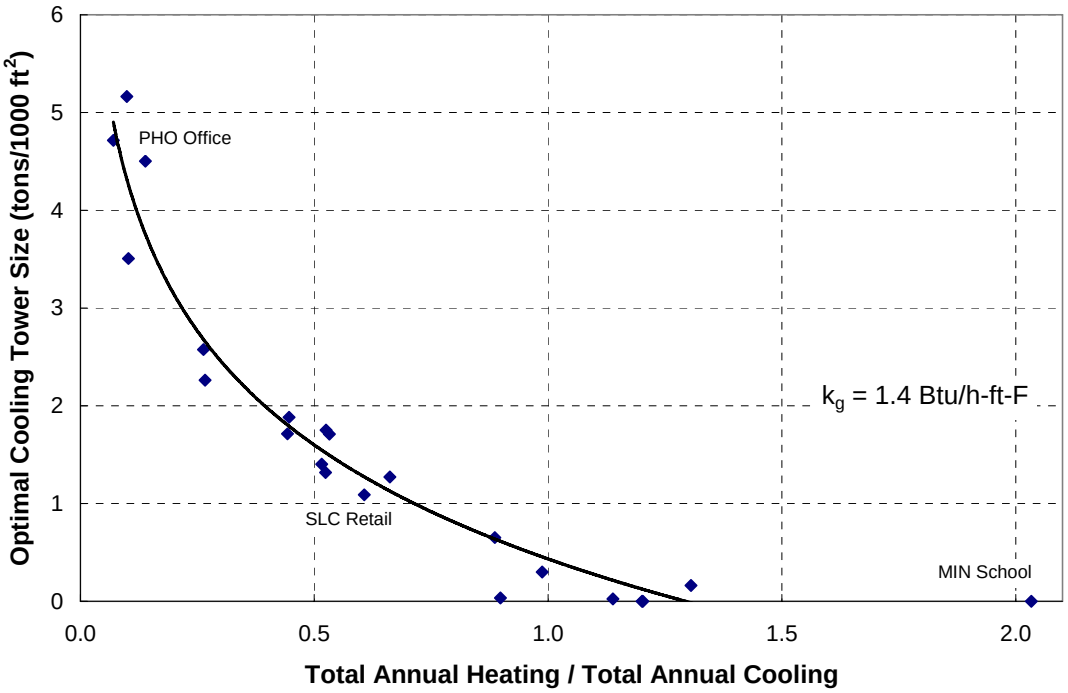

Figure 4. Optimal cooling tower size normalized by the building size as a function of the ratio of total annual heating load to peak cooling load.

- When using a dry fluid cooler as the supplementary device, the optimal sizes follow trends that are similar to those described above for cooling towers.

- **The optimal sizes and control setpoints identified here never balance the load on the ground**. Therefore, the ground temperature always increases over time (for the cooling-dominated climate) by an amount that is dependent on the ratio of the heating and cooling loads. The timespan of simulation (i.e., the timespan used to calculate the life cycle cost that is to be minimized) therefore has a significant impact on the results. All of the design guidelines shown here minimize the life cycle cost over 20 years. Designers concerned with sustainable design practices may wish to utilize the distributable software to optimize the results with an even longer life.

- **The optimal design of the system (especially GHX size) does not depend substantially on the economic parameters used in the model (although the life cycle costs do)**; the equipment is sized almost entirely based on meeting the specified loads and it is rarely economically attractive to purchase larger equipment (e.g., a GHX that is larger than what is just required to meet the peak heating load) or operate equipment more often in order to improve the system efficiency. The primary exception to this guideline is the selection of cooling towers that utilize the reduced fan power at low speed operation (fan laws) in order to justify the purchase of a larger tower.

The design guidelines therefore remain valid over a large range of economic parameters. For example, Figure 5 illustrates the optimal size of the GHX (for one particular case, the 76000 ft^2 continuous-use building in St. Louis) as a function of the initial fuel (electricity and natural gas) prices normalized by the base case prices that were summarized in Table 1. Figure 5 shows that the price of fuel must nearly double before it becomes more economic to increase the GHX size in order to reduce the operating cost of the system.

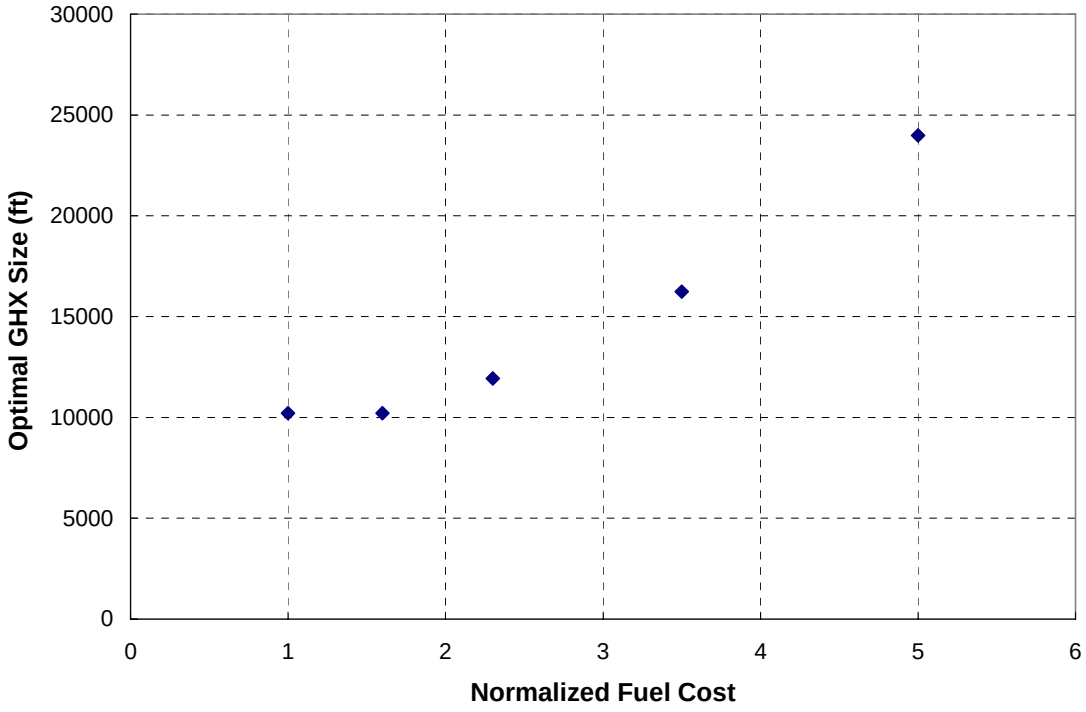

Figure 5. Sensitivity of optimal GHX size to fuel costs. The x-axis is the fuel cost normalized to the base case fuel cost (including electricity consumption, demand, and natural gas costs). Data is for a 76000 ft^2 continuous-use building in St. Louis.

- **Control setpoints**: c**hoose optimal control setpoints for hybrid systems as shown below. (See the example below for the control sequence formed by these setpoints.)**
    - Supplemental cooling device: operate this device when conditions are favorable; that is, when the fluid temperature entering the device is greater than the ambient wet bulb (dry bulb for dry fluid cooler) + ΔT_1, where:

ΔT_1 = 27°F for a cooling tower, where $T_{wb,July} < 70$°F

23°F for a cooling tower, where $T_{wb,July}$ 70 to 76°F

20°F for a cooling tower, where $T_{wb,July} > 76$°F

12°F for all dry fluid cooler scenarios

where $T_{wb,July}$ is the ASHRAE 1% design wet bulb temperature for the building's climate in July. (Users of these guidelines in the southern hemisphere should replace July conditions with January conditions.)

- GHX, cooling setpoint (T_{Cool2}): the GHX is bypassed only occasionally, generally in warmer climates (the optimal value of T_{Cool2} increases with more cooling dominated buildings, as shown in Figure 6)

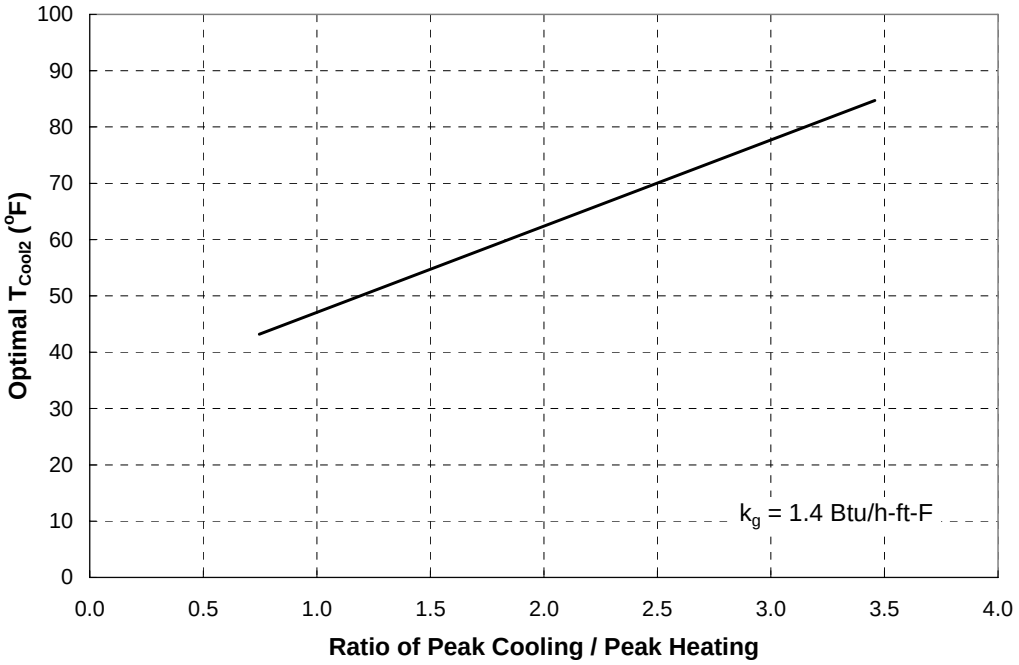

Figure 6. Optimal GHX cooling setpoint (T_{Cool2}) as a function of the ratio of peak cooling to peak heating load.

- GHX, heating setpoint (T_{Heat1}): the GHX is never bypassed in heating mode, so T_{Heat1} should be set to a high number that is never reached.

- **Operating temperature sensitivity: the lowest *LCC* for the HyGCHP model generally occurs at a minimum operating temperature below 35°F**. The limits on the temperature of the fluid entering the heat pump strongly drive the optimization; the equipment is sized in order to keep the entering fluid temperature within the specified limits (as presented in Table

1, the entering fluid temperature is not allowed to go below 35°F or above 95°F in the base cases). These base case temperature limits were selected with some guidance from the Project Monitoring Subcommittee and reflect "typical" design values. However, when the temperature limits are allowed to relax to 20°F and 110°F (within the manufacturers' stated operating limits) then the optimizer will typically choose an optimal minimum operating temperature that is lower than 35°F, trading off heat pump efficiency for reduced first cost (the size of the GHX is reduced by up to 50%). The effect of operating temperature limits is linked to the economic assumptions that were used for the parametric study, and it should be noted that a system designed using the more restrictive 35°F/95°F temperature limits will have some margin (against, for example, particularly severe weather or other uncertainties) that a system designed using relaxed temperature limits will not have.

Cost Comparisons – Cooling Dominated Systems

The parametric study considered and optimized a geothermal-only system, a boiler/tower system, and the hybrid geothermal system options for each building/climate combination. This provided an opportunity to make meaningful comparisons between these options based on life cycle costs.

- **In most moderate and southern climates, hybrid geothermal systems have a lower life cycle cost (*LCC*) than other options.**
    - The life cycle savings (*LCS*) of hybrid systems compared to geothermal-only systems is proportional to how unbalanced the climate is. Figure 7 illustrates the life cycle savings associated with a hybrid system compared to a geothermal only system (normalized by the building size) as a function of the ratio of the total annual heating load in the building to the total annual cooling load in the building, for each scenario.

Note that savings are negligible when the annual load ratio is greater than approximately 0.9.

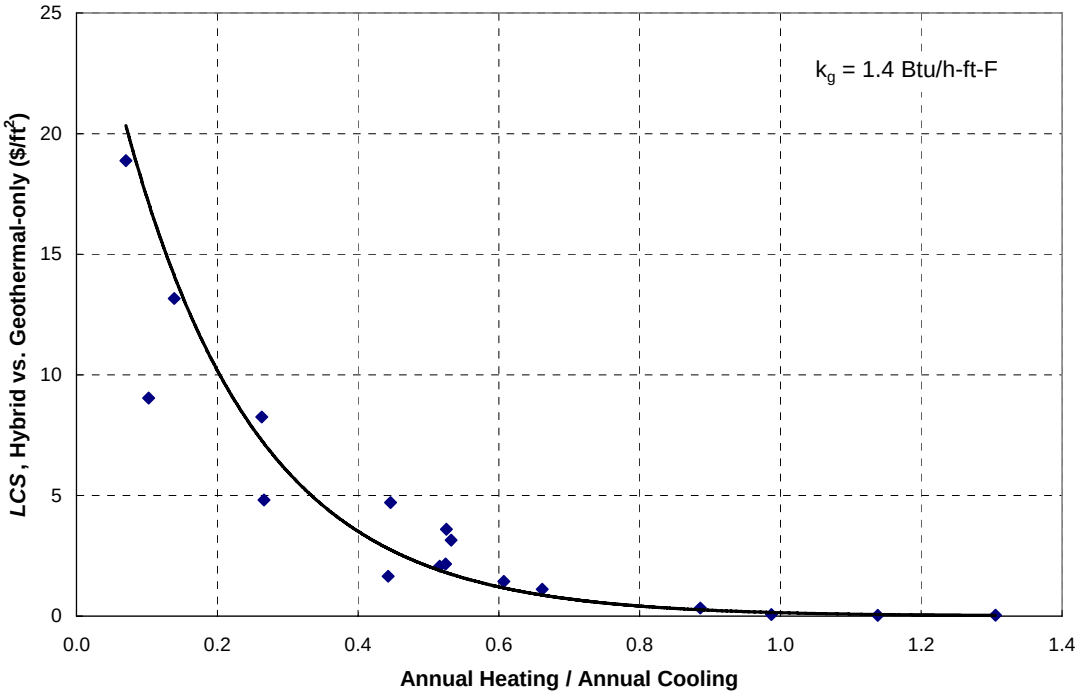

Figure 7. Life-cycle savings of hybrid systems over geothermal-only systems as a function of ratio of total annual heating load to total annual cooling load.

- The *LCS* of a hybrid system compared to a boiler/tower system is smaller than the *LCS* of a hybrid system compared to a geothermal only system (shown in Figure 7) and increases with peak heating load (the savings is negligible when the peak heating load is near zero).
- A smaller number of buildings were also studied with a dry fluid cooler used in place of a cooling tower in the hybrid system. In this study, the life cycle cost (LCC) generally changed very little from the hybrid that used a cooling tower. In some warmer climates, the LCC was slightly higher with the use of a dry fluid cooler.

- Unlike the optimal design parameters, the observed costs, and therefore *LCS*, are sensitive to economic parameters. For example, when fuel inflation is increased to 7.5% the *LCS* of hybrid systems as compared to boiler/tower systems *doubles*. The effect of GHX cost is also studied. The *LCS* changes as function of GHX cost as shown in Figure 8 (these results are normalized by building size and represent the average across five random building/climate scenarios).

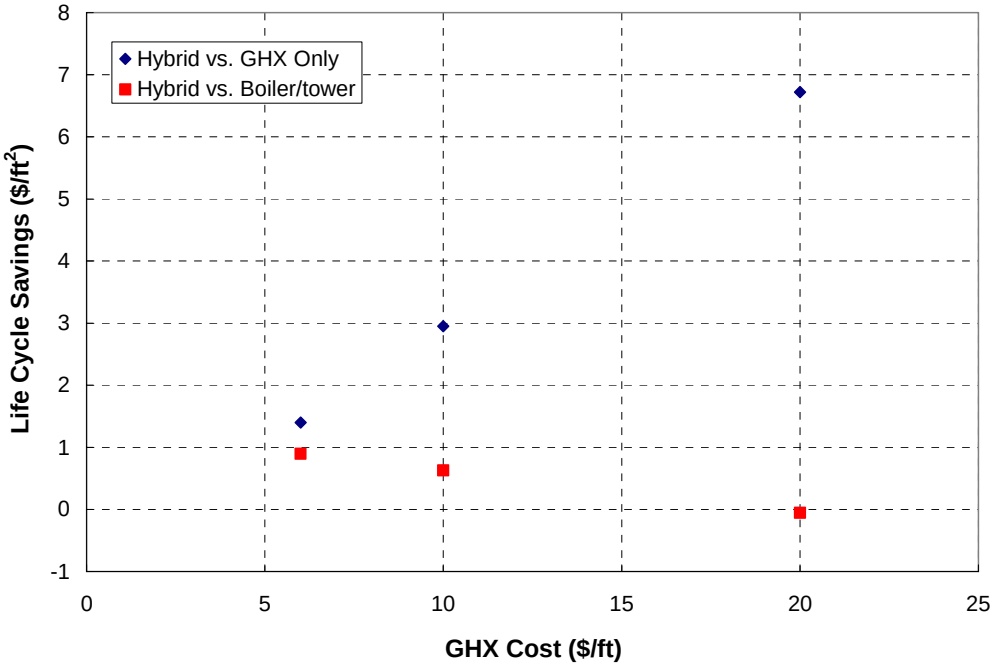

Figure 8. Life-cycle savings of hybrid systems as a function of the GHX cost. This plot shows the average values for five of the building/climate scenarios.

- **For northern climates (like Minneapolis, 7900 heating degree days (^{o}F), or colder) geothermal-only systems have a lower *LCC* than (cooling-dominated) hybrid or boiler/tower systems.**
- **In warm dry climates (like Phoenix), buildings with low heating loads have almost the same *LCC* for a hybrid and a boiler/tower system.**

- **In extreme climate cases featuring high ground temperatures and low wet bulb temperatures, it may be economically advantageous to place the ground heat exchanger upstream of the supplemental cooling device.**

Design Guidelines and Observations – Heating-Dominated Systems

Heating-dominated systems were also studied; the hybridization of these systems occurs through the addition of either a boiler or a solar collector array; otherwise the model and control strategy are very similar to those used for the cooling-dominated systems. The heating-dominated hybrid systems were studied for climates represented by Minneapolis and Edmonton (northern Alberta, Canada). **For the assumptions listed in Table 1, the results of the heating-dominated study suggest the design guidelines detailed below.**

- Geothermal-only systems should be sized based on heating in these climates. Note that the required ft/ton of heating is significantly greater than the values shown for cooling dominated systems. This is primarily due to the small temperature difference between the deep earth temperature and the minimum heat pump entering water temperature.
- Based on the economic assumptions used here, a solar/geothermal hybrid is never a viable option; including a solar component always resulted in a larger life cycle cost than a geothermal-only system (the solar component of a hybrid system was always optimized to zero). This is likely due to the high first cost of both devices utilized in this hybrid. Note that this statement does not apply to systems with direct solar heating systems that bypass the heat pumps.
- The boiler/geothermal hybrid has a slightly lower *LCC* than the geothermal-only system for a Minneapolis school; however, the boiler/geothermal hybrid was significantly more attractive

than the geothermal-only system for an Edmonton school. The boiler/geothermal hybrid option is likely to become increasingly attractive going north from Minneapolis.

- To optimally design a boiler/geothermal system, the GHX should be sized to meet the peak cooling load and the boiler is sized to meet the unmet heating load (this amounts to 69% of load in Minneapolis).

Example: Use of Design Guidelines

It is instructive to demonstrate the use of the design guidelines discussed above by applying them to an example building. For this demonstration, a typical cooling-dominated building was chosen: a large office building in Atlanta. This particular building has the characteristics summarized in Table 2.

Building area (1000 ft^2)	127
Peak cooling (tons)	222
Peak heating (kBtu/hr)	2413
Annual cooling (MMBtu/yr)	3683
Annual heating (MMBtu/yr)	1905
Ground temperature (^{o}F)	62.0
July wet bulb (^{o}F)	78.6

Table 2. Characteristics of the 127,000 ft^2 office building in Atlanta.

1. An optimal design for this building starts by choosing an equipment configuration. This report has demonstrated that an optimally designed hybrid system with a GHX and a cooling tower has the lowest *LCC* in Atlanta (which is a moderate climate with some heating load). Therefore, the system should be configured as shown in Figure 1.
2. In order to size the GHX for this system, Figure 3 is used; according to this plot, the GHX size required for this location (with an initial ground temperature of 62°F) is about 132 ft/ton of peak heating load. The resulting GHX size is then 26,543 ft.

3. Next, the cooling tower is sized using Equation (1). With an L_{tot} = 23,125 ft, $q_{peak,cool}$=222 tons, and T_{ground} = 62°F, the rated capacity of the cooling tower is 209 tons. Figure 4 can also be used to size the cooling tower; the ratio of the annual heating to annual cooling load is 0.52 which suggests a cooling tower size of about 1.5 tons/1000 ft^2, or about 190 tons. A size of 200 tons is chosen as the nearest 'nominal' size (this is an oversized tower; the optimal system operates mainly at half speed).
4. With the equipment configured and sized, the control setpoints are now chosen. Because the summer design wet bulb temperature in Atlanta is 78.6°F, the optimal value for ΔT_1 is identified as 20°F.
5. T_{Cool2} is chosen to be about 60°F based on Figure 6.
6. T_{Heat1} is set to 100°F so that the GHX is never bypassed in heating mode, and T_{Cool1} is set to 101°F (5-8°F above the maximum temperature limits as discussed in this summary) so that the cooling tower operates primarily at low speed.

The setpoints above form the following control sequence: The cooling tower will run at low speed whenever the fluid temperature exiting the heat pumps and entering the tower is 20°F above the ambient wet bulb, and it will run at high speed whenever the fluid temperature leaving the heat pumps and entering the tower is above 101°F. The fluid will pass through the ground heat exchanger whenever the leaving fluid temperature is above 60°F in cooling mode or whenever the heat pumps are in heating mode.

The hybrid system for this same building was explicitly optimized using the HyGCHP model. In Table 3, the optimal design values that were selected by the optimizer are compared with the more approximate values selected using the design guidelines, as calculated above. All values computed with the design guidelines are within 10% of the optimal for this scenario.

	Design Guidelines	HyGCHP Optimization	GCHPCalc
GHX Size (ft)	23125	23985	23600
Tower size (tons)	200	178	150
ΔT_1 (Δ^oF)	20	19.4	N/A
T_{Cool2} (^oF)	61	57.7	N/A
T_{Heat1} (^oF)	Never bypass		N/A

Table 3. Optimal design values determined with two different methods: 1) the design calculations discussed above and 2) the optimal design values determined by the HyGCHP model.

Additionally, the third column in Table 3 shows values for one commonly used GHX-sizing software that has a hybrid design feature. The software, GCHPCalc, allows for two methods of sizing the hybrid: 1) size and operate a cooling tower to meet the unmet peak cooling load or 2) size and operate a cooling tower to balance the load on the ground. As explained earlier, this report found that it is not economically optimal to balance the load on the ground if the objective is to minimize the 20 year life cycle cost, therefore method 1 is the preferable method, and is shown in Table 3. Note that the GHX size identified by GCHPCalc is consistent with the design guidelines presented here. The cooling tower size is somewhat smaller; however, this is at least partially an artifact of the control system that operates the cooling tower at low speed in order to achieve higher efficiency.

Synopsis

In cooling dominated climates, the use of a supplemental cooling device located upstream of the ground heat exchanger can provide significant life cycle savings compared to boiler/tower systems and geothermal-only systems. For almost all cases studied, the optimal size of the ground heat exchanger was found to be that which just meets the heating loads of the building (providing cooling as well but not enough to meet the peak cooling demand). For a wide range of climates and building types, the best control scheme for cooling operation was found to be one

where the cooling towers are operated at low speed whenever the ambient conditions are favorable (the fluid leaving the heat pumps is above the ambient wet bulb temperature by a prescribed amount). The tower fans are then operated at high speed whenever the temperature of the fluid leaving the heat pumps continues to rise and exceeds the maximum heat pump entering water temperature (design temperature) by 6-8^{o}F. Fluid flows through the ground heat exchanger whenever the fluid leaving the cooling tower is above a prescribed temperature setpoint. In heating mode, fluid flows through the ground heat exchanger whenever the temperature leaving the heat pumps falls below the set point for heating. Dry fluid coolers can be substituted for closed circuit cooling towers without substantial penalty in most cases.

In heating dominated climates, the use of a supplemental heating device located downstream of the ground heat exchanger can provide substantial life cycle savings compared to boiler/tower systems and stand-alone ground heat exchanger systems. For the cases studied, the optimal size of the ground heat exchanger was found to be that which just meets the cooling loads of the building (providing heating as well but not enough to meet the peak heating demand). The best control scheme for heating operation was found to be one where fluid flows through the ground heat exchanger whenever the temperature rises above or falls below prescribed temperature set points with a boiler being used at peak heating conditions to maintain the fluid at the minimum allowable heat pump entering water temperature.

Guidelines are presented for quick sizing and control of hybrid systems provided the parameters of the project closely match the default parameters presented earlier. Users are urged to exercise the distributable program to analyze specific projects more accurately (especially those deviating from default parameters); running quick comparison studies between design alternatives or a full-scale optimization.

Executive Summary References

CDH Energy Corp. and Thermal Energy Systems Specialists (TESS), Development of Equivalent Full Load Heating and Cooling Hours for GCHPs Applied in Various Building Types and Locations, Final Report, ASHRAE 1120-TRP (2000).

Kavanaugh, S. and K. Rafferty, *Design of Geothermal Systems for Commercial and Institutional Buildings.* ASHRAE, (1997).

Klein et al., *TRNSYS, A Transient System Simulation Program, User's Manual*, Version 16, Solar Energy Laboratory, University of Wisconsin-Madison (2006).

Table of Contents

List of Figures

List of Tables

Nomenclature

A	area
C	cost ($) or capacitance (kJ/K)
COP	coefficient of performance (-)
c_p	specific heat (J/kg-K)
D	percentage of the investment made as a down payment (-)
d	depth / distance (m) or discount rate (-)
ε	effectiveness (of a heat exchanger) (-)
EER	energy efficiency ratio (-)
F	scaling factor (-)
f	fraction of outside air (%)
γ	control signal (-)
h	heat transfer coefficient
η	efficiency
I_T	radiation incident on tilted collector
i	inflation rate (–)
k	thermal conductivity (Btu/ft-hr-^{o}F)
λ	variable, in this case representing enthalpy change ratio (-)
L	length (m)
LCC	life cycle cost ($)
LCS	life cycle savings ($)
$\dot{m}$	mass flow rate (kg/h)
MC	maintenance cost
N	number (of years, boreholes, etc.) (-)
n	timestep (-)
P	pressure (atm)
P_1	annual fuel cost multiplier in P1-P2 method (-)
P_2	equipment cost multiplier in P1-P2 method (-)
Q	volume flow rate (m^3/s)
q	heat transfer rate (W)

ρ	density (kg/m^3)
RH	relative humidity (%)
τ	time (s)
T	temperature (K)
t	time (yr) or time (hr)
UA	heat transfer coefficient (of heat exchanger) (W/K)
ω	humidity ratio (-)
$\dot{W}$	power (J/h)
w	power (W)
y	design exponent (-)

Subscripts

air	air (mixed or total, as opposed to return air or outside air)
actual	actual value, at off-design conditions
boil	boiler
bore	borehole
cap	capacity
coll	solar collector
cool	cooling mode
CCCT	closed circuit cooling tower
D	depreciation
db	dry bulb (temperature)
design	at design conditions
DFC	dry fluid cooler
e	evaluation
eff	efficiency
F	fuel
F1	fuel, in one year
fan	fan
fl	fluid (generally water or a glycol solution)
GHX	ground heat exchanger

Ground	ground property
heat	heating mode
in	an inlet parameter
lat	latent heat
max	maximum number
nom	at nominal size (where normalized size=1)
oa	outside air
out	an outlet parameter
return	return air
sat	saturated
sen	sensible heat
series	boreholes in series
surf	surface
tot	total
turb	turbulent flow
v	value (for resale)
wb	wet bulb (temperature)

1 Introduction

There has been a resurgence of interest in energy efficient technologies as fuel prices have risen and public awareness about the limited supply and environmental impacts of these fuels has grown. In the United States, 39% of all energy is used by residential and commercial buildings (EIA, 2007); a large portion of this energy is used for heating, cooling, and ventilation. One technology that has been proven to increase heating, cooling, and ventilation efficiency is the geothermal heat pump system.

Geothermal heat pump systems have been successfully providing efficient building air conditioning since the installation of the first ground-coupled heat pump in the 1940s (EERE, 2007b). Recently however, the technology has sustained extensive growth; Figure 9 shows the growth in the installed capacity of the ground-coupled heat pumps in the United States over the past 30 years (OIT, 2006). The growth of this technology can be attributed to its potential for energy savings; a geothermal heat pump system can save up to 50% of the energy that would be used by a conventional heating and cooling systems (EERE, 2007a). However, despite the tremendous growth in geothermal heat pump technology and the impact that it has made in some geographical niches and building categories (such as K-12 schools), geothermal heat pumps are still a secondary choice in most design scenarios, due in part to high system cost. In order to allow geothermal heat pump technology to capture an even larger portion of the heating and cooling market, innovations are needed which will allow this technology to be attractive in a wider range of climates, building sectors, and markets.

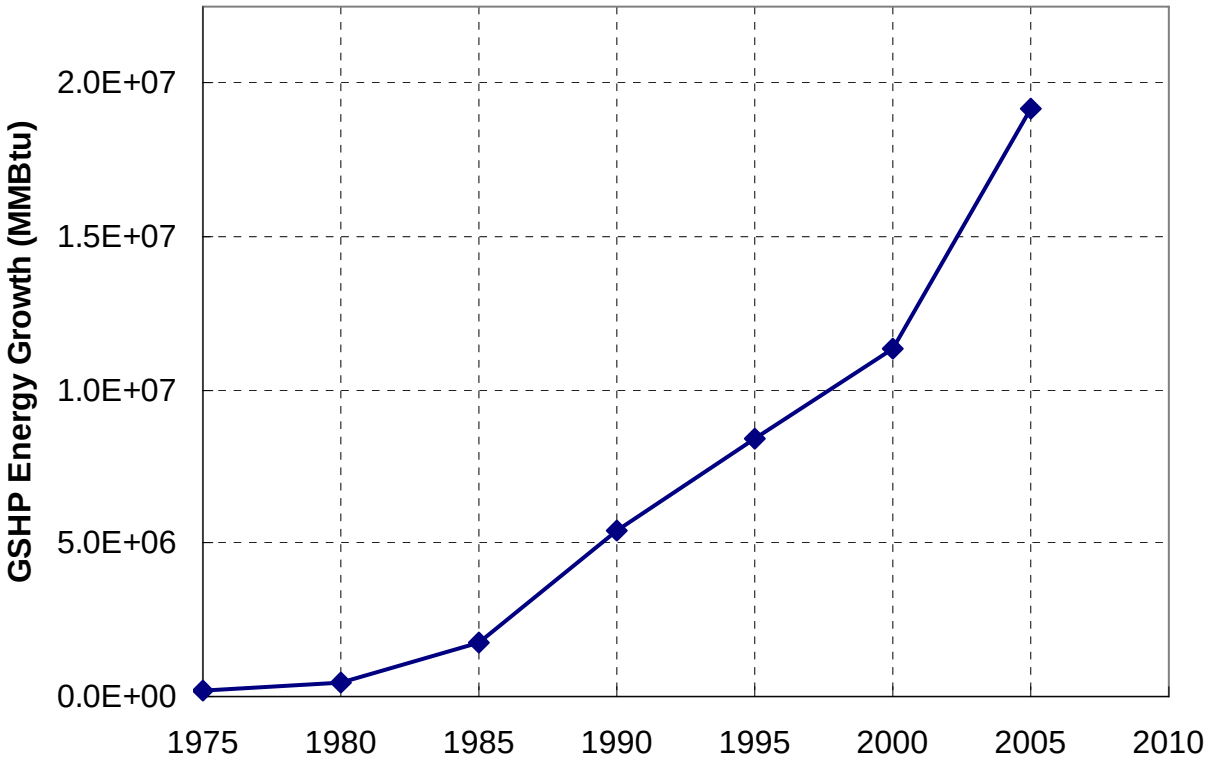

Figure 9. Growth in energy from GCHP systems in the U.S. (OIT, 2006); notice that the growth rate of ground-coupled heat pump systems has been increasing for 30 years.

One such innovation is the hybrid ground-coupled heat pump system. Hybrid ground-coupled heat pump systems (HyGCHPs) interface conventional ground-coupled heat pump (GCHP) equipment with supplemental heat rejection or extraction systems. Why add an additional device to the geothermal system? Let's consider a geothermal system in a heavily cooling-dominated climate (see a schematic in Figure 10), for example the Southeast U.S.. In such a cooling-dominated climate, the peak cooling loads are very large. In order to meet these large peak cooling loads using a geothermal heat pump system, a very large and therefore expensive ground heat exchanger (GHX) would be required. In the Southeast U.S., the heating loads are comparatively small; therefore, more heat is rejected to the ground during the cooling season than is extracted from the ground during the heating season. This difference (unbalance)

in the energy transported to the ground will tend to increase the ground temperature over time, causing the heat pump system to operate less efficiently (and therefore more expensively) during each subsequent year. It is these disadvantages that have limited the penetration of geothermal heat pump systems into heavily unbalanced climates.

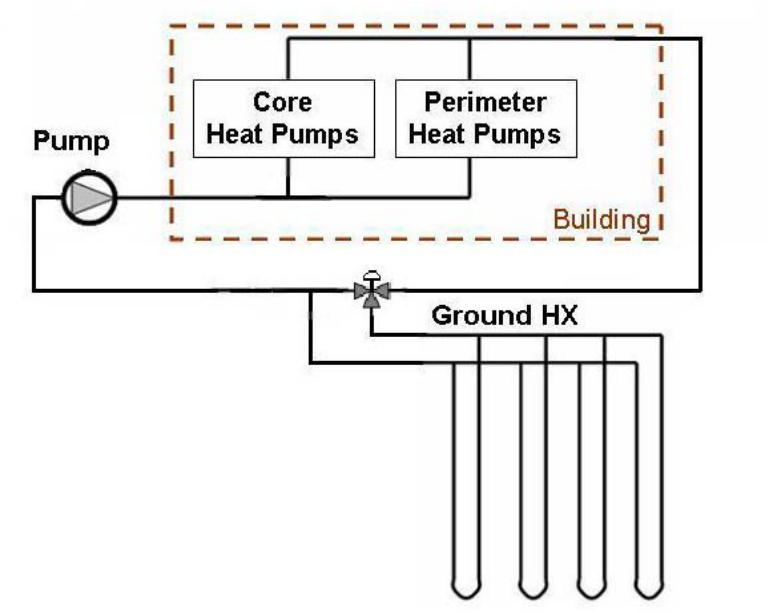

Figure 10. A schematic of a typical ground-coupled heat pump system.

In this situation, a hybrid geothermal heat pump system would integrate a supplemental heat rejection device, such as a cooling tower (see a schematic in Figure 11) with the system. The supplemental heat rejection device is operated during cooling in order to reduce the cooling load on the GHX.

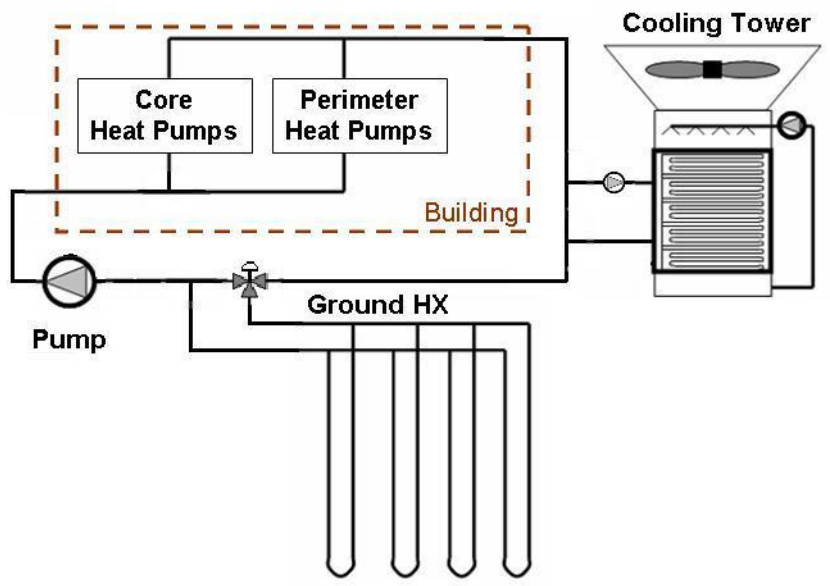

Figure 11. A schematic of a hybrid ground-coupled heat pump system, with a cooling tower as a supplemental heat rejection device.

This system results in a smaller, less expensive GHX that experiences a more balanced load (i.e., the heat rejection to the ground during the cooling season is more comparable to the heat extraction during heating season). The addition of the supplemental heat rejection system therefore mitigates the change in the ground temperature and leads to more efficient heat pump operation over time. The life-cycle savings associated with these two effects has been shown to more than offset the cost of buying and operating the cooling tower in many situations.

Similarly, in a heavily heating dominated building, adding a device that provides additional thermal energy, for example a boiler, may prove cost effective. The advantages are analogous to those discussed for the cooling dominated climate. The supplemental heat extraction device allows the size of the ground coupled heat exchanger (which is sized to meet the peak heating loads) to be reduced and also mitigates gradual reduction in the ground temperature that would otherwise be caused by the difference between the large heat extraction from the ground during heating season and small heat rejection during cooling season. In addition to saving money, HyGCHP systems operating in most climates using appropriate

control strategies have been shown to save energy overall. These benefits allow hybrid geothermal systems to be an attractive design choice in buildings and geographic regions where geothermal-only systems are not attractive.

1.1 Project Objective

The design and operation of HyGCHPs are significantly more complex than GCHPs and there is currently relatively little information available in this regard that is accessible to the practicing engineer. The overall objective of this research project is the development of tools that will allow engineers to better design and understand hybrid geothermal systems. One of the specific objectives is the development of a detailed simulation tool that integrates physics-based models of the HyGCHP system components. This computer tool is implemented using the TRNSYS simulation program and used to carry out a parametric study (using an optimization tool) of the characteristics of the optimal (lowest life-cycle cost) HyGCHP system design over a range of climates and building types. Results from this parametric study have been used to generate a set of design guidelines. Specifically, the results show how to size and control a hybrid geothermal system in cooling or heating dominated climates, as well as which climates benefit the most from implementation of a hybrid system.

However, it is clear from completing this parametric study that there is a large variation in building loads, climates, equipment parameters, and economic conditions that could be appropriate across the United States. Therefore, an additional objective of the project is the development of a distributable computer program based on the simulation tool which can be used by design engineers to consider specific case studies that are relevant to their climate/building/economic situation.

1.2 Report Outline

This report begins with a discussion in Chapter 2 of previous research related to hybrid geothermal systems in the areas of modeling and general design strategies. Details of the hybrid model are provided in Chapter 3. Chapter 3 begins with a discussion of the general modeling strategy for the hybrid systems. It goes on to describe the individual model components in detail and discuss how these components are interfaced. Finally, the optimization algorithm that operates on the simulation in order to minimize life cycle cost is discussed, and a distributable version of the model is described. Chapter 4 presents the parametric studies (and their results) that were accomplished in order to identify generally applicable but approximate trends in the results that can be used for first order design trade-offs. Finally, Chapter 5 summarizes the important conclusions that can be drawn from this study, including some general design guidelines for hybrid systems.

2 Literature Review

There has been a broad range of research projects related to geothermal heat pump systems in all areas of simulation, design, and operation.

2.1 Ground Heat Exchanger Modeling

This project relies heavily on prior work directed at simulating ground heat exchangers. The ground heat exchanger model used in this project is referred to as the duct storage model ('DST model') which was developed at the University of Lund, Sweden (Hellström, 1989); the DST model builds on previous Swedish research in ground heat storage and was modified for implementation in TRNSYS by Pahud et al. (1996). Validation of the model using experimental data has subsequently been accomplished by Shonder et al. (Shonder, 1999), McDowell and Thornton (McDowell and Thornton, 2008), and others.

2.2 Hybrid Geothermal Heat Pump Systems

Research directed at understanding hybrid geothermal heat pump systems represents only a small fraction of the total body of geothermal research. Several papers have presented details about actual hybrid systems (for example, Wrobel, 2004; Phetteplace and Sullivan, 1998, etc.). A few studies have also used simulation tools to model (Ramamoorthy et al., 2000) and even optimize hybrid systems; one example is the optimization of the hybrid geothermal system installed at Fort Polk (TESS, 2005). The model that is used in this project is based in part on the Fort Polk case study, in which a HyGCHP system was optimized for an administrative building in Louisiana. Both the equipment size and control methodology was optimized during the Fort Polk case study.

The HyGCHP model developed for this project is more general than these case studies because it is intended to be used to optimize systems over a wide range of buildings and climates, rather than for a specific building at a specific location. Work on *general* hybrid design methodology has been reported by Kavanaugh (Kavanaugh, 1998), who developed a methodology for sizing hybrid geothermal systems. Two studies have also focused on identifying effective control strategies for hybrids. One study was done by Yavuzturk and Spitler (2000), who identified economical method of controlling a cooling-dominated hybrid system, without adjusting the size of the equipment. The same conclusion on control methodology was reached in the Fort Polk study (TESS, 2005), in which several differing of control strategies were optimized and then compared.

Hybrid system studies have focused primarily on the design of cooling-dominated systems. However, some research has also been done relative to the design of hybrid systems for heating-dominated climates and buildings; primarily using solar collectors as the supplemental device (Chiasson and Yavuzturk, 20003 and Ozgener and Hepbasli, 2004). These research projects have tended to focus mainly on specific case studies rather than identifying more generally applicable design guidelines.

3 Model of a Hybrid Geothermal System

The objective of this project is to identify the optimal hardware and control methodology for a specific building/climate/economic situation. The building loads and ambient conditions vary dramatically during the day and the control system must make control decisions based on the instantaneous energy demand. Furthermore, the cost of energy may change based on time of day. All of these effects suggest that an energy simulation with sub-hourly time resolution is required to obtain meaningful results. In addition, the annual unbalance in the load and its effect on the ground temperature will substantially effect the long-term performance of the system. Therefore, it is necessary that the energy simulation consider multiple years. Specifically, the energy simulation must consider the entire operating life of the system, because a system is not useful if it ceases to operate correctly at any point in its life. Only a few software packages exist that can be used to model (in a straightforward manner) the variety of components and systems that must be considered by this project. The TRNSYS software – a component-based energy modeling package - was selected as the most appropriate simulation tool. TRNSYS has the ability to model geothermal systems, contains geothermal components that have been thoroughly validated, and is able to accomplish multi-year, sub-hourly simulations at reasonable speed (Klein, 2006).

The hybrid system model in TRNSYS (described in the remainder of this section) is made up of many different components models, each representing a discrete mechanical component or physical effect in an actual HyGCHP system (for example, components represent the behavior of the heat pumps, ground heat exchanger, cooling towers, etc.). These individual TRNSYS components interact with each other during simulation in much the same way that they

do in an actual system (Klein, 2006). This section begins by discussing some general strategy used to set up the model and then describes each component of the model in detail.

3.1 Model Strategy

3.1.1 Interaction with Building

The most complex and complete model of a hybrid geothermal system would explicitly model the building spaces, all the individual heat pumps, and the heat rejection and extraction systems outside the building; this type of model is possible using TRNSYS. However, the HyGCHP model developed for this project is based on several simplifying assumptions that are necessary so that the simulation can be applied to a wide range of buildings and climates *and* also be computationally efficient; these characteristics are necessary to facilitate the optimization exercises that are the focus of this project. First, the current hybrid study utilizes building models that are independent of the simulation of the HyGCHP system itself. This methodology of de-coupling the building simulation from the heating and cooling equipment was previously adopted and justified in the Fort Polk case study (TESS, 2005).

In the Fort Polk study, a building was explicitly modeled and interfaced with a well-designed GCHP system; the GHX was sized so that the entering fluid temperature (to the heat pump) was kept maintained within a 50^{o}F band during the entire year and the heat pumps were sized in order to meet the design loads of each building zone. This coupled building/equipment simulation was run using sub-hourly time steps in order to provide data at a resolution sufficient for use in the subsequent HyGCHP system simulations. The heating/cooling loads and air temperatures were recorded in a data file. The heating/cooling loads and air temperatures were subsequently used in a model that considered only the heating/cooling equipment and not, explicitly, the characteristics of the building. The removal of the building model substantially

accelerated the simulation. Several tests were carried out in order to determine whether there was a significant loss in accuracy associated with this approach of de-coupling the building from the heating/cooling equipment models. Several different hybrid systems were simulated using the coupled building/equipment model and it was found that “the heating and cooling loads met in each case were very similar (within 1%) (TESS, 2005)”. The same hybrid models were then re-run independently using the de-coupled strategy (i.e., using only the building loads recorded in the data files) and only “very small differences” in power consumption were observed (TESS, 2005). This ability to run the building model and the HyGCHP system model independently – without loss of accuracy – greatly reduces the computational requirements of the model, enabling a much deeper and broader study of HyGCHP systems.

In the current HyGCHP study, the strategy of de-coupling the building model from the model of the heating/cooling equipment is utilized. In some cases, existing building load files can be used in order to eliminate the need to create any building models provided that they are in the correct format for the HyGCHP model. A set of 20 different building types were modeled in a number of climates as part of an ASHRAE-sponsored study (ASHRAE TRP-1120, CDH and TESS, 2000). One additional assumption introduced in the ASHRAE TRP-1120 study was the assumption of specified indoor air conditions based on thermostat settings. This simplification necessarily assumes that the heating and cooling equipment is sized such that it can meet the peak loads so that indoor air conditions do not "drift" at any time during the day. In effect, this assumption requires that the heat pump and balance of plant be well-designed. And, unlike the Fort Polk study, in the current design study this assumption must hold true for different building types and climates.

3.1.2 Heat Pump System

The heat pump model developed for this project (Type 199 in TRNSYS, described in detail below) can be scaled to represent different heat pump models with a range of capacities (and performances, as explained in Section 3.2.1). Therefore, the heat pump model is more generally applicable and can be used to simulate the wide variety of buildings and climates (and therefore heating and cooling loads) that are being considered in this project; this is not possible with a heat pump component model that represents one specific heat pump model. This scalability is facilitated and justified to some extent by the fact that a principal outcome of a simulation of a specific hybrid case (with a particular building type/climate combination) is the comparison of that hybrid case with a more conventional water source heat pump system. Therefore, the systems that are being directly compared have the same building and heat pump setup regardless of the details of the heat sources and sinks that are used in the fluid loop.

A basic premise of this research is that it is not necessary to determine the specific size and quantity of all individual heat pumps that are installed in the system; e.g., an apartment building might utilize 10's or 100's of individual, small heat pump units to provide the required cooling and heating. In this model, the building loads are divided into two zones (perimeter and core) for a particular building/climate combination and the heat pump model servicing each zone uses these load *totals* as its input. The single "heat pump" used to condition each zone is sized to ensure that it can meet the maximum total cooling and heating load occurring during a year. As Figure 12 shows, the building load data file includes the heating and cooling loads associated with the perimeter and the core zone. The use of two separate zones (rather than a single-zone model) is required because there are often conditions where one of these zones is in heating mode while the other is in cooling mode (CDH and TESS, 2000). Although the total load in this

case might be zero, the energy consumption and fluid flow rate experienced by the system is not, as one of the heat pumps is transferring energy to the other during these times.

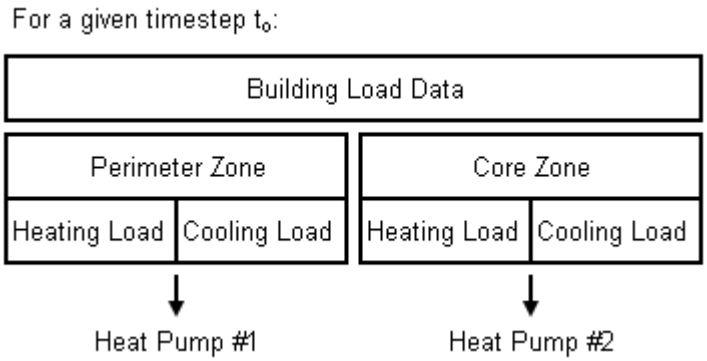

Figure 12. Division of loads as input to HyGCHP model.

As an example, consider an office building that requires 30 tons of cooling in its perimeter zone and 10 tons of heating in its core (1 ton = 12 kBtu/hr). This situation is represented in the model with one large heat pump providing the 30 tons of perimeter cooling and another large heat pump providing the 10 tons of core heating. In the actual office building, several different size heat pumps would likely be used, each turning on and off as the individual rooms or spaces changed temperatures.

As different building sizes, types, and climates are considered, these two heat pumps must be capable of being sized in order to meet the maximum possible *total* conditioning loads experienced by the core and perimeter zones over a modeled year. The performance of the heat pump system is modeled as the heat pump meets the actual loads during the year; part-load performance is not modeled but off-design conditions are considered. Section 3.2.1 will provide further details of the heat pump model and shows that this representation is accurate.

3.1.3 Configuration and Controls

Cooling Dominated System

The schematic in Figure 11 depicts a hybrid configuration with the cooling tower upstream of, and in series with, the GHX. This configuration is not arbitrary. The Fort Polk study examined several configurations as well as different control strategies and supplemental devices (for cooling-dominated buildings) and found that the series configurations always resulted in a lower life-cycle cost than the parallel configuration (TESS, 2005). Based on this observation, the HyGCHP model is always configured with the supplemental device in series with the ground coupled heat exchanger. However, note that the valve immediately upstream of the cooling tower allows only the rated amount of fluid to flow to the cooling tower. Depending on the size (and therefore the rated flow) of the cooling tower, in certain situations some of the fluid goes to the cooling tower while the remaining fluid circulates directly to the GHX (*after* being mixed with the fluid exiting the tower). Therefore, the optimal system can be a series configuration, but sometimes it is optimized to be neither strictly series nor strictly parallel. With the cooling tower placed in series with the GHX, the decision is then made to place the tower *upstream* of the GHX. This decision is based on the fact that the tower is the more expensive piece of equipment to operate (two pumps and a fan are turned on when it's operating). Therefore, when the tower is operating it should be doing so with the largest possible ΔT between the fluid and the ambient, to maximize heat transfer. The one known exception is for areas with extremely high ground temperature and low wet bulb temperatures; in these areas it can be beneficial to locate the tower downstream of the GHX.

For this type of configuration, what is the most cost effective method of controlling the loop pump and cooling tower? Two studies were found in the literature that looked at this question for cooling dominated systems. First, Yavuzturk and Spitler (2000) studied the hybrid

system control strategy for an office that resulted in the lowest life cycle cost. Five basic methods were considered and it was found that in both severe (Houston) and moderate (Tulsa) climates, one method resulted in the lowest cost – the difference between the heat pump exiting fluid temperature and the ambient wet bulb temperature is used to control the operation of the cooling tower. The ground heat exchanger flow is controlled using one setpoint for cooling and a different one for heating. The same conclusion with regard to control methodology was reached in the second study at Fort Polk (TESS, 2005); in this study, several different control strategies were individually optimized and then compared. This lowest-cost general control strategy is used in the current HyGCHP model; its sequence is explained in detail in Section 3.2.7.

Heating Dominated System

The heating-dominated system is configured differently than the cooling-dominated system. Figure 13 shows the configuration of the solar system within the hybrid model. This configuration consists of three fluid loops, labeled 1 through 3 in Figure 13. Loop 1 operates using a diverting valve that is placed in the system's main fluid loop; fluid is diverted from the loop, through a heat exchanger and is then returned, at higher temperature, to the main loop (this is the mechanism by which the collected solar energy is ultimately transferred to the heat pumps). Loop 2 circulates water from the thermal storage tank using a constant speed pump through a heat exchanger (labeled HX in Figure 13) that is interfaced to loop 1; the heated water is returned to the storage tank. Loop 3 circulates a fluid (water or propylene glycol depending on climate) through the other side of the tank using a constant speed pump; the fluid is circulated through a collector array and back to the tank (this type of configuration is sometimes called a

drain-back system). The thermal storage tank does not contain any auxiliary heating elements; its temperature is only affected by the liquid flows from the main loop and from the collector array.

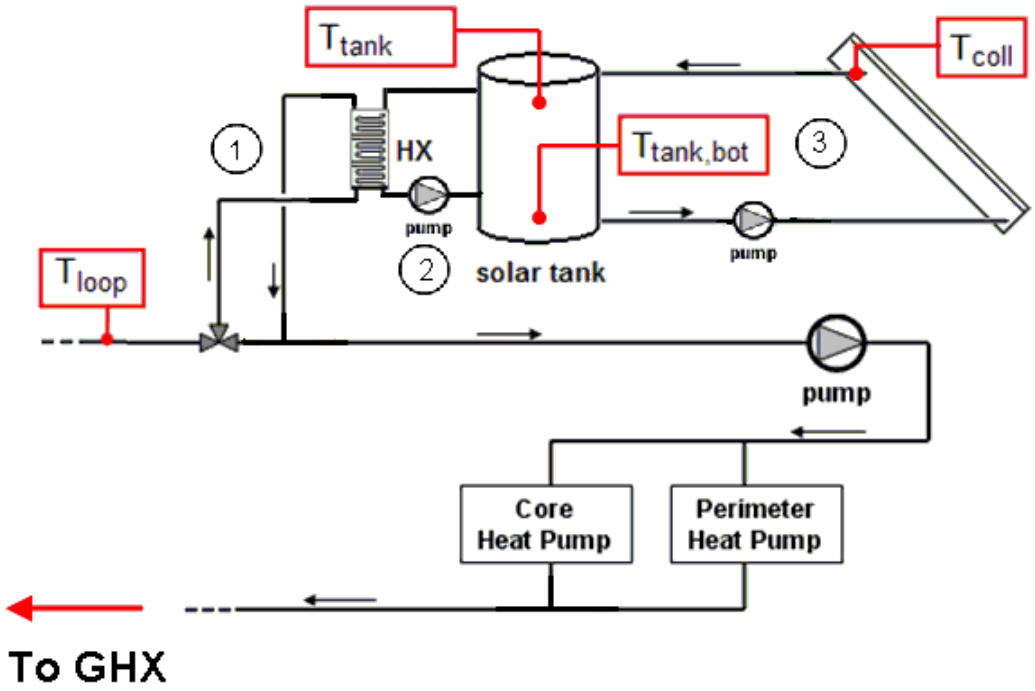

Figure 13. A schematic of a hybrid ground-coupled heat pump system with a solar thermal collection system as a supplemental heat absorption device.

The key difference between the cooling- and heating-dominated systems, other than the equipment itself, is the location of the supplemental heat transfer device. In the heating-dominated case, the solar collector (or boiler, discussed below) is placed *downstream* of the GHX. This choice is made because the temperature change associated with the boiler or solar system is much higher than the temperature change produced by the supplemental cooling devices. In fact, with a boiler or reasonably sized solar system the fluid temperature is likely to increase above the ground temperature which would render the GHX useless from a heating standpoint if it were placed downstream of these supplemental heating devices.

A number of alternative solar collector system configurations could have been specified; for example, multiple tanks or jacketed tanks might also have been used. The rationale behind

the system configuration that was selected (i.e., the system shown in Figure 13) is that it is simple and commonly used and can therefore provide at least an idea of the potential for the use of solar in a HyGCHP system. The benefits of different or more complex solar system configurations could be investigated in further studies; however, the analysis of this simple system shows that solar thermal collection may not be a practical method to hybridize geothermal systems in heating dominated climates.

The other device tested for use in the heating-dominated systems is a boiler. The configuration for the boiler is similar to that of the solar hybrid, with a boiler placed in the position of the solar tank in Figure 13.

3.2 Model Components

3.2.1 Heat Pump Component

A ground-source heat pump is a heat pump that uses a ground heat exchanger (GHX) as the heat source (in heating mode) or sink (in cooling mode). In the case of the hybrid system considered here, a fluid loop interfaces the GHX with the heat pump and the supplemental heat rejection or extraction device. The heat pump transfers heat (in either direction) between this fluid loop and the conditioned air inside the building envelope (see Figure 14).

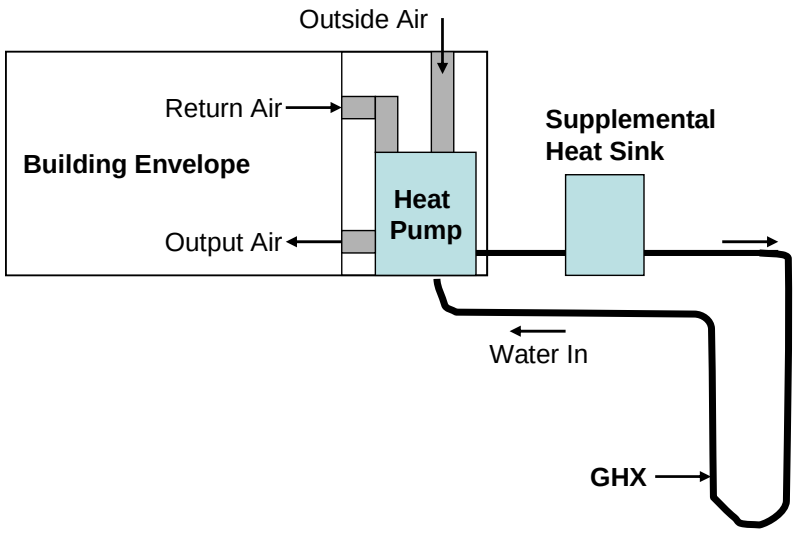

Figure 14. Standard layout of the heat pump, supplemental equipment, and ground heat exchanger (GHX). Note the heat pump has separate interfaces with air and fluid sides.

TRNSYS provides several ways to model a water-source heat pump. Initially, this project used the water source heat pump model coded into component Type 209. The Type 209 heat pump component is an empirical (rather than physics-based) model of a heat pump; its interaction with both the air and the fluid is based on interpreting catalog data provided by the user (ostensibly obtained from manufacturer's data). For example, in the Fort Polk HyGCHP study the performance data for a two-ton ClimateMaster heat pump were used. The input files include the cooling (sensible and total) and heating capacity and power consumption of the unit as a function of air flow rate, fluid flow rate, entering fluid temperature, and air conditions (dry-bulb and wet-bulb temperatures). For the current study, data files (or more optimally a set of equations fit to data files) must be provided that are applicable over a broader range of loads and flow rates than can be covered by any one model of heat pump. This is a unique challenge to the current, design-focused project; therefore, a different heat pump model that encompasses a sufficiently broad range of capacities has been developed.

The new heat pump model, Type 199, differs from the standard model in the way that it adjusts its performance in order to meet the building load. In the Type 209 model, the heat pump represents a single discrete heat pump and therefore assumes that the fluid flow rate is at its constant design value for the full time step (if there is any load at all during that timestep). The temperature difference (ΔT) of the fluid flowing through the heat pump is then controlled as necessary to meet the load. Alternatively, the heat pump can be controlled to be off or on over relatively short time steps. The control method used in Type 209 is convenient for systems that have a known quantity of heat pumps, all discretely modeled and sized to meet a specific load. However, the current HyGCHP model utilizes two heat pumps that can be of any size (as discussed in Section 3) and must be operated to meet different loads during each time step. With this diversity of loads, the strategy of varying ΔT would require large fluctuations in ΔT, which physically does not occur in actual heat pumps. A new strategy is therefore needed for Type 199.

Operation Method

The heat pump model needs to reject (in heating) or absorb (in cooling) a quantity q_{tot} of heat during each timestep. Note that q_{tot} is a function of the time step as well as both the load and the power consumption of the heat pump. (Most of the power consumption ends up as heat, which affects the energy flows). This load is assumed to be met entirely by the HyGCHP fluid loop (i.e., no domestic water heating or other streams are modeled); therefore, the total heat transfer to/from the loop is equal to

$$q_{tot} = \dot{m}_{fl}\, c_p\, \Delta T\, \tau_{on} \tag{3}$$

where $\dot{m}_{fl}$ is the mass flow of the fluid, c_p is the specific heat of the fluid, ΔT is the change in temperature from inlet to outlet, and τ_{on} is the length of time that the heat pump operates during

the time step. Although actual heat pumps operate intermittently (i.e., with varying τ_{on}), this control cannot be simulated using this model; it is not possible to model the process of turning individual heat pumps on and off during a time step because we are not sizing and discretely modeling each heat pump in a given building/climate scenario. It is therefore necessary to simulate the actual, intermittent part-load operation using an equivalent steady-state operating condition (i.e., a constant fluid mass flow rate and temperature difference, $\dot{m}_{wat,sim}$ and ΔT_{sim}) that is modeled as occurring continuously during the time step (i.e., with duration Δt). In order for energy to be conserved, it is necessary that the values of $\dot{m}_{fl,sim}$ and ΔT_{sim} be consistent with the total energy transferred to the loop:

$$q_{tot} = \dot{m}_{fl,sim}\, c_p\, \Delta T_{sim}\, \Delta t = \dot{m}_{fl}\, c_p\, \Delta T\, \tau_{on} \tag{4}$$

or

$$\dot{m}_{fl,sim}\, \Delta T_{sim} = \dot{m}_{fl}\, \Delta T \left(\frac{\tau_{on}}{\Delta t} \right) \tag{5}$$

where the factor in parentheses in Eq. (5) represents the fraction of the time step that a single heat pump would need to operate at design conditions in order to meet the load. The question then is whether it is most appropriate to hold $\dot{m}_{fl,sim} = \dot{m}_{fl}$ and adjust ΔT_{sim} according to:

$$\Delta T_{sim} = \Delta T \left(\frac{\tau_{on}}{\Delta t} \right) \tag{6}$$

as was done for the Type 209 model or, alternatively, hold $\Delta T_{sim} = \Delta T$ and adjust $\dot{m}_{wat,sim}$ according to:

$$\dot{m}_{fl,sim} = \dot{m}_{fl} \left(\frac{\tau_{on}}{\Delta t} \right) \tag{7}$$

Type 199 is based on the assumption that Eq. (7) provides a more appropriate representation of the intermittent process than does Eq. (6); this is justified below.

Equations (4) and (5) both result in the same integrated load. The difference in these methods is related to the impact of the fluid conditions on the performance of the ground source heat exchanger and other heat rejection/extraction devices. These balance of plant components have performance that is sensitive to temperature and flow rate and therefore the response of these components to a continuous flow at a constant ΔT is different than the response to the actual, intermittent operation; this is true regardless of whether the method described by Eq. (6) or Eq. (7) is used.

The Type 199 model simulates the actual intermittent part-load operation by varying the fluid flow rate, $\dot{m}_{fl}$, according to Eq. (7) while maintaining a fixed temperature difference from inlet to outlet. In an actual, large building, the load will usually be met by several smaller heat pumps that are turned on or off as needed with a corresponding change in the circulating fluid flow. In the simulation, the net effect of these individual heat pumps (both in terms of power consumption and flow rate) are represented by a single, large heat pump. The simplification associated with lumping these individual heat pumps into a single unit is appropriate from the standpoint of power consumption because heat pump performance and operating characteristics are relatively independent of full-load capacity and therefore the power consumed by 10 small heat pumps is nominally the same as one heat pump that is 10x larger if the same total load is met.

The strategy of adjusting the fluid flow rate in order to match the load more closely matches real HyGCHP operation as the number of actual heat pumps represented by the single large heat pump increases. To illustrate this conclusion, consider Figure 15(a) which shows the volumetric flow rate in the fluid loop as a function of time during a single, 1 hour interval for a single 8-ton heat pump operating at 50% load by cycling on and off. When the single heat pump

is on, it requires 17 gpm; note that the dashed line at 8.5 gpm reflects the average fluid flow rate that would be consistent with a single heat pump providing 4 tons of continuous cooling during the one hour timestep. In this lower-limit, where the actual system has a single heat pump, there is a significant difference between the modeled (dashed line) and actual (solid line) flow rates during the time step; this discrepancy could impact the simulated vs. actual performance of the components, particularly the performance of the ground heat exchanger.

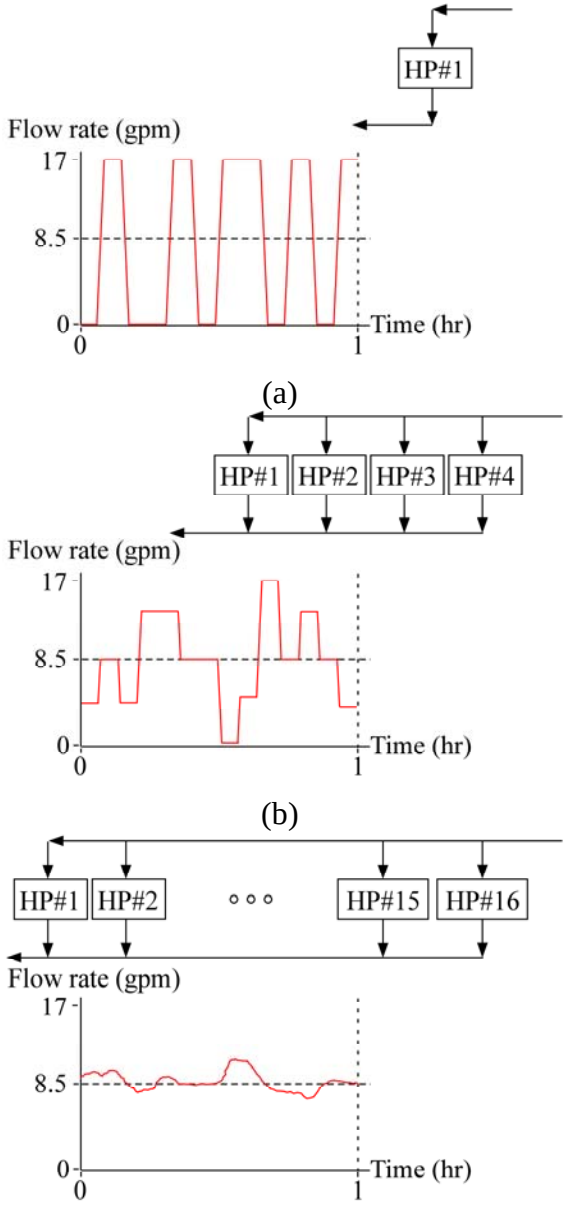

Figure 15. Volumetric flow rate as a function of time during a 1 hour operating period for (a) a single 8-ton heat pump meeting a 4 ton load, (b) for four, 2-ton heat pumps meeting the same 4 ton load, and (c) for 16 heat pumps with 0.5 ton capacity meeting the same 4 ton load. Notice that the flow rate becomes more consistent with the modeled flow (in Type 199) as the number of heat pumps increases.

As more and more heat pumps are used to meet the same load, their cumulative impact on the loop fluid flow begins to approach the constant 8.5 gpm value that is consistent with the model. Figure 15(b) illustrates the combined flow rate associated with an actual zone that is serviced by four, 2-ton heat pumps (each heat pump has a full-load capacity that is 25% of the single 8-ton heat pump). Notice that each heat pump turns on and off during the one hour time step in order to meet the 4-ton load. The times that the heat pumps turn on and off are likely not correlated strongly over short periods of time (i.e., as the time step becomes smaller, the actual operating time period for each heat pump becomes stochastically distributed throughout the time step). Therefore, the cumulative flow rate associated with the four heat pumps will average out to 8.5 gpm with some "noise" or standard deviation that is reduced as the number of heat pumps increases. To first order, the standard deviation of the flow rate should be related to the ratio of the average flow rate to the number of heat pumps.

Figure 15(c) illustrates the situation where a single zone requiring 4 tons of cooling is serviced by 16 heat pumps, each with 0.5 ton capacity; Notice that the cumulative flow rate is very nearly 8.5 gpm and the variation is small (on the order of 8.5 gpm/20 heat pumps). Clearly then, for zones serviced by more than a couple heat pumps, the average flow model is a good one.

It is necessary to establish the validity of the modeling many individual heat pumps with one single component model; specifically, the underlying assumption that performance and operating characteristics of the simulated individual heat pumps are linear and therefore can be

simulated without any knowledge of the precise number of heat pumps. The performance specifications for several different heat pump models (over a range of rated full-load capacity) are used; these heat pump models include several different manufacturers (see Table 4).

Manufacturer	Models
ClimateMaster	GLV: 8 - 20 tons
	GRV: 1 - 5 tons
Trane	Axiom: 0.5 - 5 tons
	GEH: 6 - 25 tons
Water Furnace	E series: 2 - 6 tons

Table 4. Heat pump manufacturer and models used in heat pump model creation and validation.

First, the assumption that the ΔT across the heat pump is independent of capacity is investigated. Figure 16 illustrates the heat pump temperature difference as a function of heat pump capacity, where capacity is taken to be the maximum q_{tot} that the heat pump could meet at an entering fluid temperature of $T_{fl,in}$ = 90°F. Note that ΔT varies by only ±10% over all models, which is acceptable relative to the variance in heat pump capacity that is modeled. The same trend holds at other entering fluid temperatures.

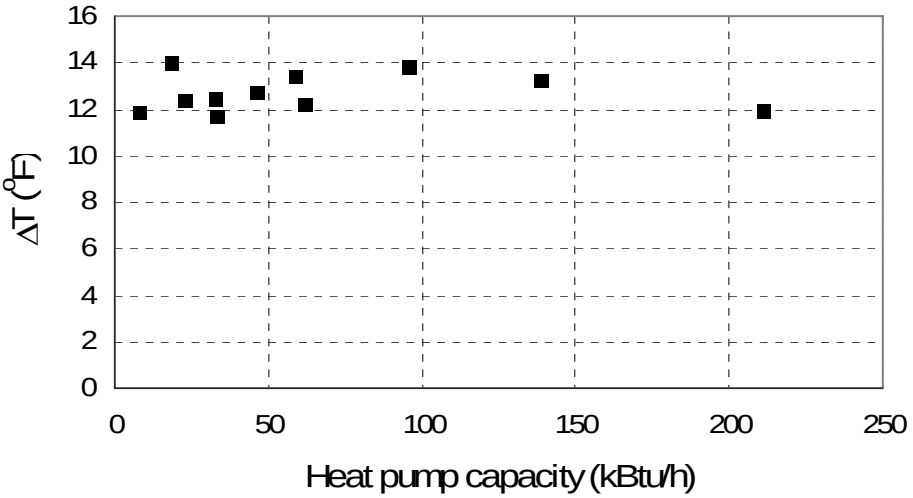

Figure 16. ΔT as a function of heat pump cooling capacity (for $T_{fl,in}$=90°F) as a function of the heat pump capacity for several heat pump models.

The volumetric flow rate of the fluid (which is directly proportional to the mass flow rate of the fluid under the anticipated operating conditions) is shown in Figure 17 as a function of heat pump cooling capacity. Note that the fluid flow rate is directly proportional to the cooling capacity of the heat pumps; this linear relationship justifies the assumption that the total fluid flow rate associated with many small heat pumps is consistent with the fluid flow rate required by a single large heat pump and allows the fluid flow rate to be computed according to the total heat pump capacity using only a simple, linear curve fit (as discussed in Section 4.3). Heat pump flow rates do not vary as air and fluid loop properties vary, therefore this equation is valid under any operating conditions.

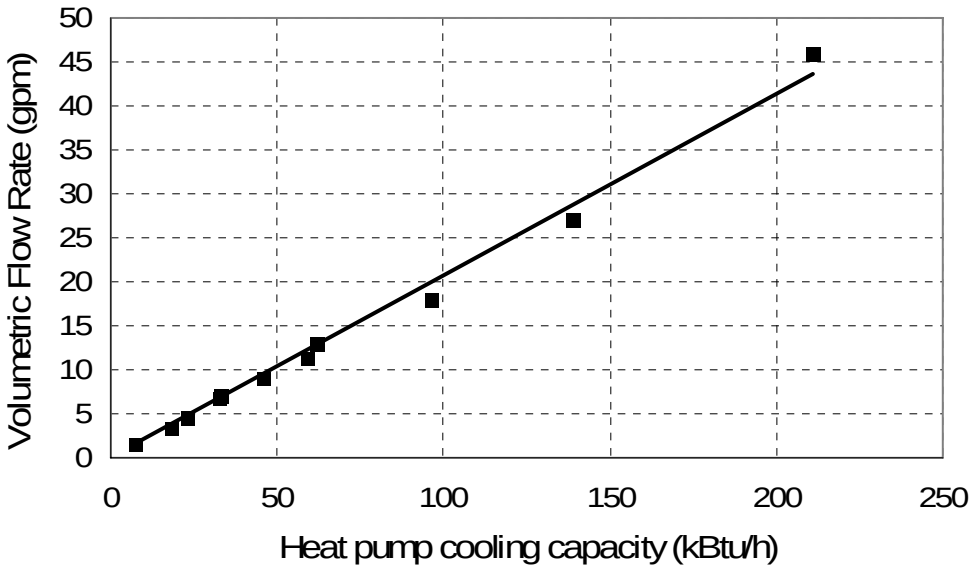

Figure 17. Fluid flow rate as a function of heat pump cooling capacity for different manufacturers.

The regression equation for the volumetric flow as a function of cooling capacity for these data is:

$$Q_{fl} = 0.207 q_{cap,cool} \tag{8}$$

where Q_{fl} is the flow rate in gpm and $q_{cap,cool}$ is the cooling capacity in kBtu/h. Figure 18 illustrates the flow rate as a function of the heating capacity of the heat pump (again, for different models and manufacturers) and shows that the volumetric flow rate is a linear function of the heating capacity as well.

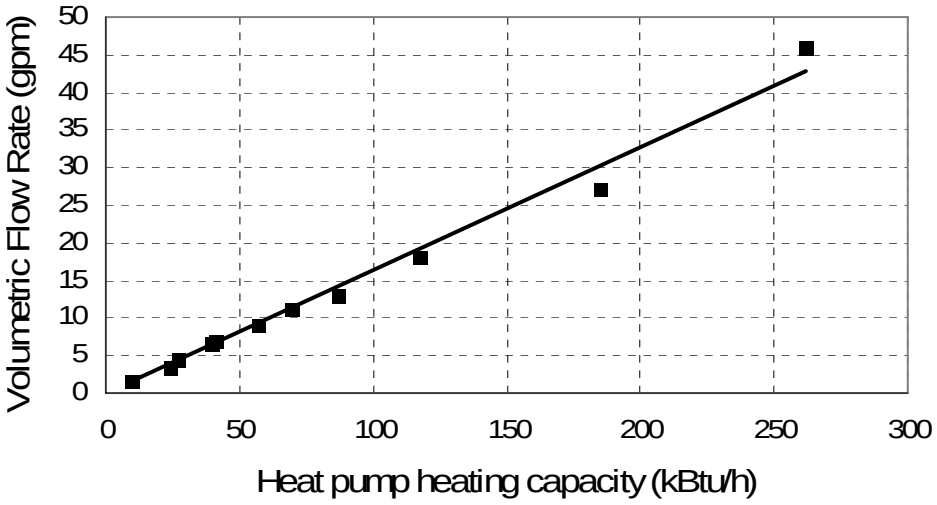

Figure 18. Fluid flow rate as a function of heat pump heating capacity.

The regression equation for the volumetric flow as a function of heating capacity for this data is:

$$Q_{fl} = 0.163\, q_{cap,heat} \tag{9}$$

where Q_{fl} is volumetric flow rate in gpm and $q_{cap,heat}$ is the heating capacity in kBtu/h. Equations (8) and (9) are used by the Type 199 model to calculate the volumetric (and subsequently the mass) flow rate as a function of capacity (cooling and heating, respectively).

In addition to fluid flow rate and temperature difference, it is necessary to verify that the performance of a heat pump unit (i.e., the efficiency) is independent of the capacity of that unit; again, this is required if a single equivalent heat pump is used to represent multiple actual heat pumps without any knowledge of the number of heat pumps. The heat pump efficiency is used to calculate power consumption, which has a significant impact on the economic results of the

simulation. Figure 19 illustrates the performance (in terms of EER – the Energy Efficiency Rating) as a function of the heat pump capacity for several heat pump sizes and manufacturers; note that efficiency is essentially independent of capacity. Higher quality (and generally higher cost) heat pumps that operate at higher efficiency at reduced loads do exist. Based on the variation in efficiency that is evident in Figure 19 and the impact that efficiency has on the economics of the system, the heat pump efficiency is taken to be 12.76 (at 90°F) for the parametric study but is a variable that can be set by the user for the distributable program. The modeling strategy used with Type 199 assumes that the heat pump system efficiency will remain constant as the size of the load changes during simulation. Additionally, note that there is no method of determining the part load of the heat pump system; the average efficiency assumed therefore accounts for degradation in efficiency due to part load operation.

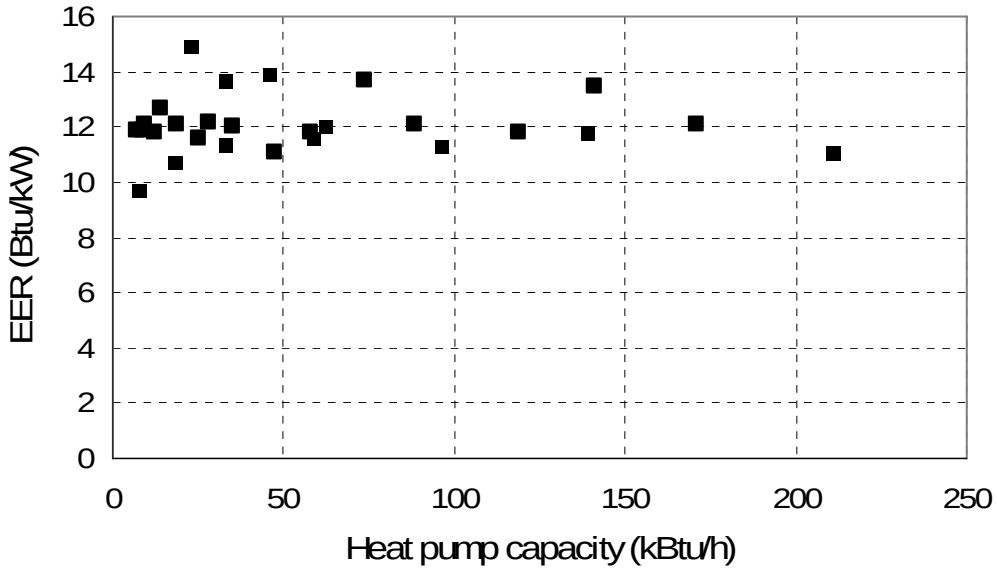

Figure 19. Energy Efficiency Rating (for cooling) as a function of heat pump capacity. Plots of efficiency for heating (COP in that case) show a similar trend.

During simulation, the manufacturer's catalog data (plotted throughout this section) is also used to directly calculate the heat flows that characterize the interaction of the heat pump

component with the HyGCHP model. To improve the computational speed of the model, it is desirable to fit the manufacturer's data to equations rather than interpolating large lookup tables of these data. For example, note the trend lines in Figure 17 and Figure 18; the corresponding linear equations are used for calculating the fluid flow rate for a given heat pump size during simulation. For this study, the catalog data used as the basis of the Type 199 model is taken from ClimateMaster, WaterFurnace, and Trane heat pumps. A wide range of sizes has been used from each manufacturer and product line.

Heat Pump Performance

Relationships are provided above to relate heat pump capacity, fluid flow rate, and efficiency. However, both capacity and efficiency are also functions of entering fluid temperature ($T_{fl,in}$). As with most energy conversion systems, heat pumps operate most efficiently when absorbing heat (in heating mode) from a higher temperature source and when rejecting heat (in cooling mode) to a lower temperature sink. In order to find an equation that captures this effect, the cooling capacity and efficiency are normalized with respect to their values at $T_{fl,in}$=90^{o}F and plotted as a function of $T_{fl,in}$ (see Figure 20 and Figure 21) for different models of heat pump. Note that there is an approximately linear relationship between efficiency and $T_{fl,in}$. However, there is considerable scatter at low $T_{fl,in}$ which occurs because there is also some effect of heat pump size on this function. The effect is judged to be small enough to be ignored; this is justified because the fluid loop rarely – if ever – operates at these low temperatures in cooling mode.

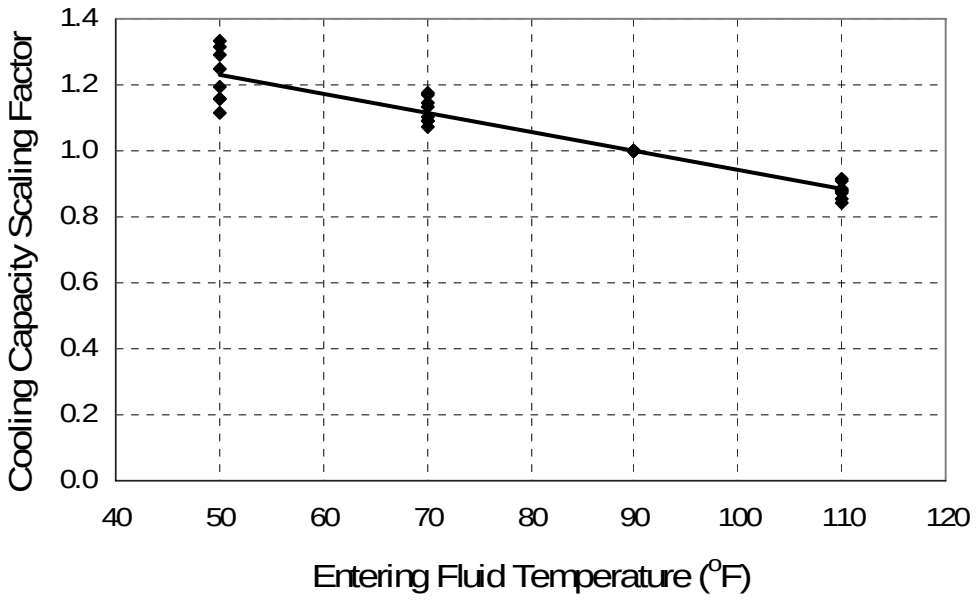

Figure 20. Cooling capacity scaling factor as a function of $T_{fl,in}$.

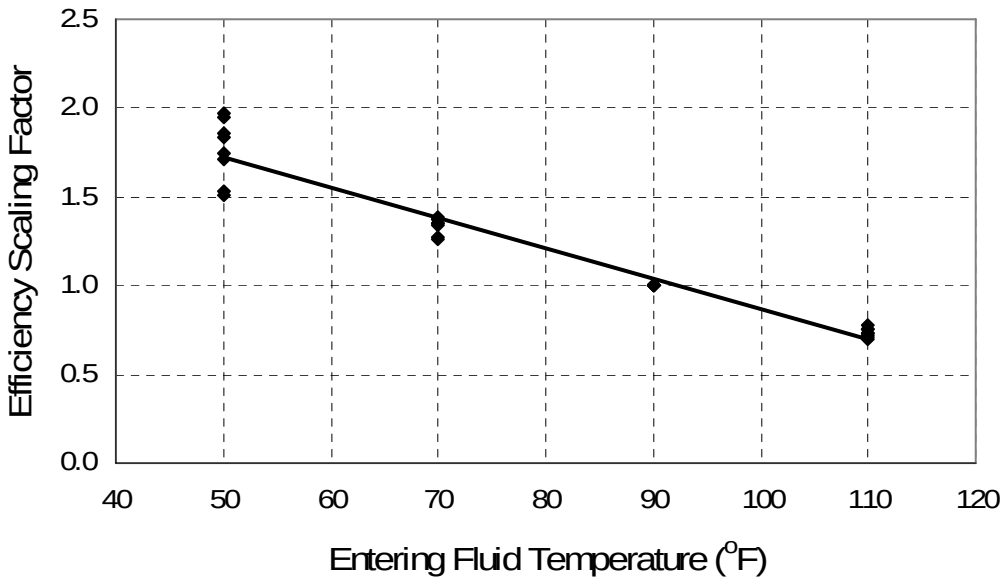

Figure 21. Efficiency (in cooling) scaling factor as a function of $T_{fl,in}$.

The regression equation for the cooling capacity scaling factor ($F_{cap,cool}$) as a function of entering fluid temperature ($T_{fl,in}$ in °F) is:

$$F_{cap,cool} = -0.0058(T_{fl,in}) + 1.522 \quad (10)$$

The regression equation for the efficiency scaling factor as a function of entering fluid temperature is:

$$F_{eff,cool} = -0.0171(T_{fl,in}) + 2.579 \quad (11)$$

Equations (10) and (11) are used to calculate the scaling factors for entering fluid temperature in the heat pump model. Similar curves for heating capacity and efficiency as a function of entering fluid temperature are shown in Figure 22 and Figure 23.

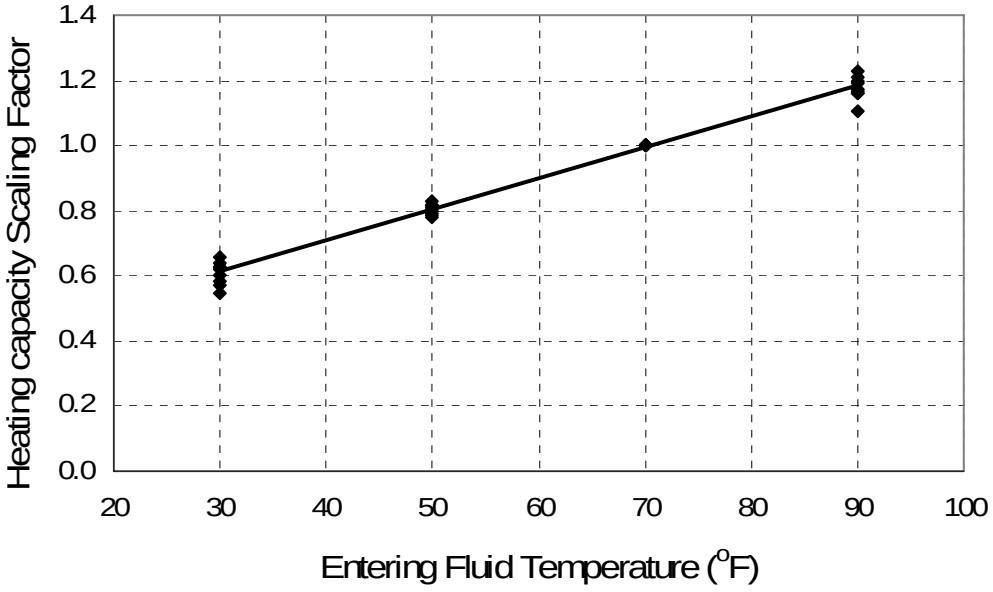

Figure 22. Heating capacity scaling factor as a function of $T_{fl,in}$.

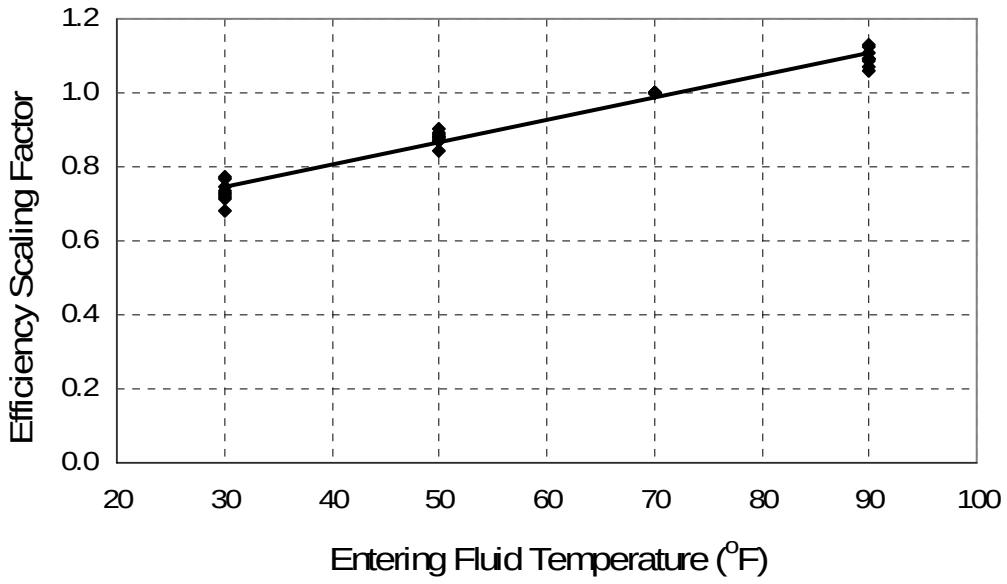

Figure 23. Efficiency (in heating) scaling factor as a function of $T_{fl,in}$.

The regression equation for the heating capacity scaling factor ($F_{cap,heat}$) as a function of entering fluid temperature ($T_{fl,in}$ in ^{o}F) is:

$$F_{cap,heat} = 0.0095(T_{fl,in}) + 0.326 \quad (12)$$

The regression equation for the efficiency scaling factor (in heating) as a function of entering fluid temperature is:

$$F_{eff,heat} = 0.0061(T_{fl,in}) + 0.562 \quad (13)$$

Equations (12) and (13) are used to calculate the scaling factors for entering fluid temperature in the heat pump model.

Indoor air temperature and humidity also affect the power consumption and capacity of the heat pump; therefore additional scaling relationships are required when off-design air conditions are present. There is no straightforward relationship between these parameters and therefore manufacturers' catalog look-up files must be used. These files (shown in Figure 24) include scaling factors (defined relative to 67^{o}F) as a function of dry-bulb and wet-bulb

temperatures for cooling (the heating mode modifications require only dry bulb temperature). As explained in Section 3, the heat pump model is not run coupled to a detailed building model. Therefore the return air conditions are specified by the user and not changed during the simulation. (This is a reasonable assumption because the small, sub-hourly fluctuations in indoor air temperature are just noise in a 20-year simulation).

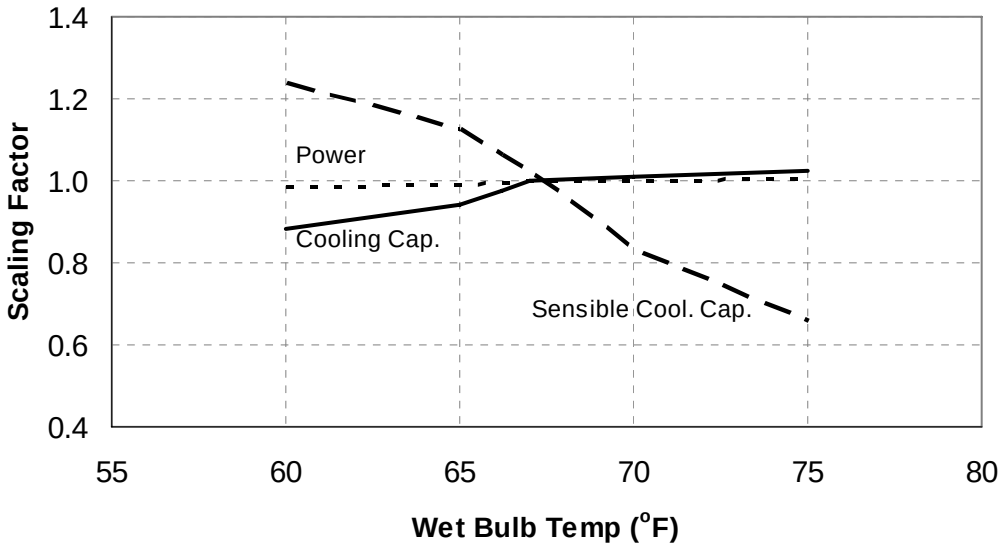

Figure 24. Scaling factors for capacity and power as a function of wet bulb temperature (T_{wb}) at dry bulb temperature (T_{db}) =81°C. Different curves exist in the model for a few different dry bulb air temperatures.

Operation Within Simulation

A flow chart that describes the internal calculations carried out by the Type 199 heat pump model is presented in Figure 25 and illustrates where and how the information and strategy discussed in Sections 4.1 and 4.2 are implemented.

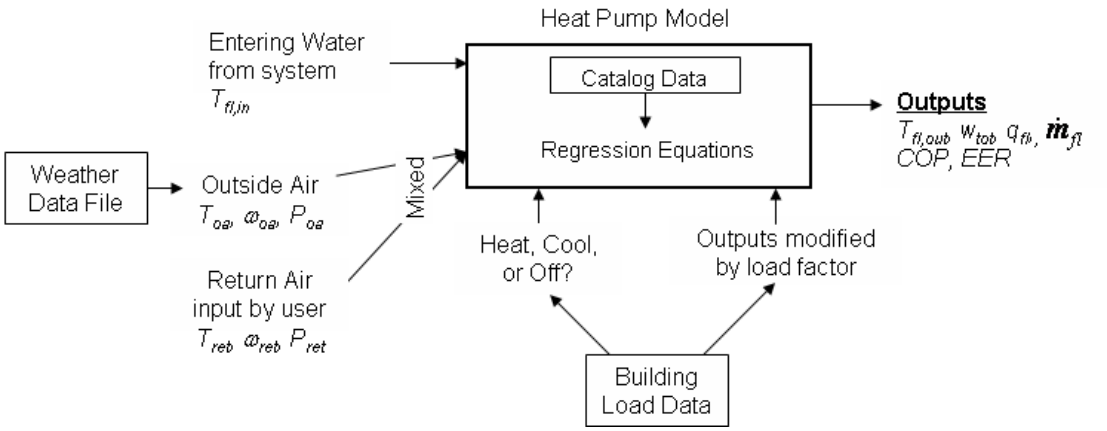

Figure 25. Flowchart of the basic heat pump model operation, with variables explained in this section (note that exiting air conditions are not part of this model – details in section 4).

When the heat pump component is called by TRNSYS with the inputs shown above, the following sequence of computations occurs:

1. The heat pump determines whether it is in heating or cooling mode based on the control signal provided by the building load (from the load data file). Cooling mode is assumed for this example sequence.
2. The state of the heat pump fan is determined for cases when the heat pump is neither in heating or cooling mode; in this model the fan is off during these periods.
3. A subroutine is called to determine all psychrometric properties of the return and outside air streams; the air stream volumetric flow rate is a fixed parameter that is set by the user. The inputs to the subroutine are obtained from the building load and weather data and include the pressure *P*, temperature *T*, and a humidity property (humidity ratio ω or relative humidity *RH*). The outputs of the subroutine are the enthalpy (*h*) and the remaining humidity property (*RH* or ω) of the air.
4. The mixed air enthalpy (h_{air}), humidity ratio (ω_{air}), and pressure (P_{air}) are calculated using a fixed fraction of outside air flow (*f*):

$$h_{air} = (1-f)h_{return} + fh_{oa} \quad (14)$$

$$\omega_{air} = (1-f)\omega_{return} + f\omega_{oa} \quad (15)$$

$$P_{air} = \min(P_{oa}, P_{return}) \quad (16)$$

where h is the enthalpy and ω is the humidity ratio and the subscripts *return* and *oa* refer to the return and outside air streams, respectively. The parameters P_{oa} and P_{return} are the pressure of the outside and return air streams, respectively. The parameter f is set to 15% for this study (but is changed to 0% in the distributable to give the user full control over air conditions at the heat pump).

5. A subroutine is called to determine all psychrometric properties of the mixed air stream; the subroutine inputs are the pressure (P), enthalpy (h), and humidity ratio (ω) while the outputs are the wet bulb temperature (T_{wb}), relative humidity (RH), and density (ρ).
6. The dry air mass flow rate ($\dot{m}_{air}$) is determined:

$$\dot{m}_{air} = Q_{air}\rho_{air} \quad (17)$$

where Q_{air} is the volumetric flow rate (a fixed input set by the user) of the mixed air and ρ_{air} is the density of the mixed air.

7. The volumetric flow rate of fluid (Q_{fl}) is calculated according to:

$$Q_{fl} = \frac{\dot{m}_{fl}}{\rho_{fl}} \quad (18)$$

where ρ_{fl} is the density of the fluid. These values correspond to heat pump operation at full capacity.

8. The rated cooling capacity (q_{tot}) and efficiency (using coefficient of performance, COP) of the heat pump are determined based on $T_{fl,in}$, Q_{fl}, and Q_{air} using the relationships (i.e., the equations based on plots of catalog data) determined in Section 4.

9. Power consumption (w_{tot}) of the heat pump is calculated using the *COP*:

$$w_{tot} = \frac{q_{tot}}{COP} \tag{19}$$

10. The rated cooling capacity and power consumption are corrected for off-design air conditions using the data file that contains scaling factors (see Figure 24). The inputs for this process are the T_{wb} and T_{db} of the air stream and the outputs are scaling factors for q_{tot} and w_{tot}. q_{tot} and w_{tot} are subsequently multiplied by these scaling factors.
11. A building load file is called; the building load file contains heating/cooling loads as a function of time for the entire duration of the simulation (these loads are based on a separate analysis, for example a detailed simulation of the building coupled to weather data). The instantaneous value of the building load (q_{load}) is used to compute a load factor ($Fraction_{runtime}$) which is nominally equal to the fraction of the current time step that the heat pump must be activated in order to meet the building load.

$$Fraction_{runtime} = \frac{q_{load}}{q_{tot}} \tag{20}$$

The main heat pump parameters – q_{tot}, w_{tot}, and $\dot{m}_{fl}$ – are then multiplied by this load factor. This is the strategy discussed in depth in the second part of Section 4.1.

12. The condenser heat rejection (q_{cond}) is calculated:

$$q_{cond} = q_{tot} + (w_{tot} - w_{cont}) \tag{21}$$

where w_{cont} is the power consumption of the controls (control power is not transferred as heat into the pump fluid).

13. The outlet fluid temperature $T_{fl,out}$ is calculated:

$$T_{fl,out} = T_{fl,in} + \frac{q_{cond}}{\dot{m}_{fl}\, c_{p,fl}} \tag{22}$$

where $c_{p,fl}$ is the specific heat of the fluid.

14. Finally, the coefficient of performance (COP) and energy efficiency rating (EER) are calculated; these values are computed by accounting for all of the heat pump power consumption including parasitic power consumption such as blower and controls as well as the compressor power.

In the standard heat pump model distributed with TRNSYS (Type 209), the outlet air properties would also be calculated for use as an output. Because the Type 199 version interacts only with a data file representing a building, the outlet air properties are not needed. The building air conditioning load is assumed to be entirely met by the equipment and the building set point is assumed to remain constant over the duration of the simulation. A useful extension of this model would be to include a desuperheater to meet some domestic hot water load; the scope of this project did not include this feature.

3.2.2 Ground Heat Exchanger

The ground heat exchanger (GHX) is perhaps the most important component model in the HyGCHP simulation. The size of the GHX has the largest effect on the initial cost of the system and the behavior of the GHX directly impacts the temperature of the fluid passing through the heat pumps, which controls their performance. The temperatures in the fluid loop are sensitive to several of the input parameters that specify the GHX model.

Model Basis

The GHX consists of a piping system that is buried in the ground through which the system's working fluid flows. The parameters used in the GHX component model (which is an existing TRNSYS component, Type 557) were initially based on the work done in the Fort Polk study and the ASHRAE design guidelines (Kavanaugh, 1997) for commercial/institutional

buildings. The heat exchanger geometry used in this analysis is based on the most common setup currently being used, which is a vertical ground heat exchanger with U-tube piping. This configuration is illustrated in Figure 26 (TESS, 2005). The thermal interaction between the fluid and the ground is simulated using the duct storage (*DST)* model of a vertical GHX field, which was created at the University of Lund in Sweden. The *DST* model calculates the transient temperature distribution as the superposition of three solutions; a global temperature solution (at the scale of the entire field), a local solution (at the single borehole scale, accounting for short time-scale effects), and a steady-flux solution (at the single borehole scale, accounting interaction between both scales). The global and local problems are solved using a finite difference technique which steps forward in time using an explicit integration method, whereas the steady flux part is given by analytical solution. The total temperature at any location and time is obtained by superposition of these three parts (Hellström, 1989).

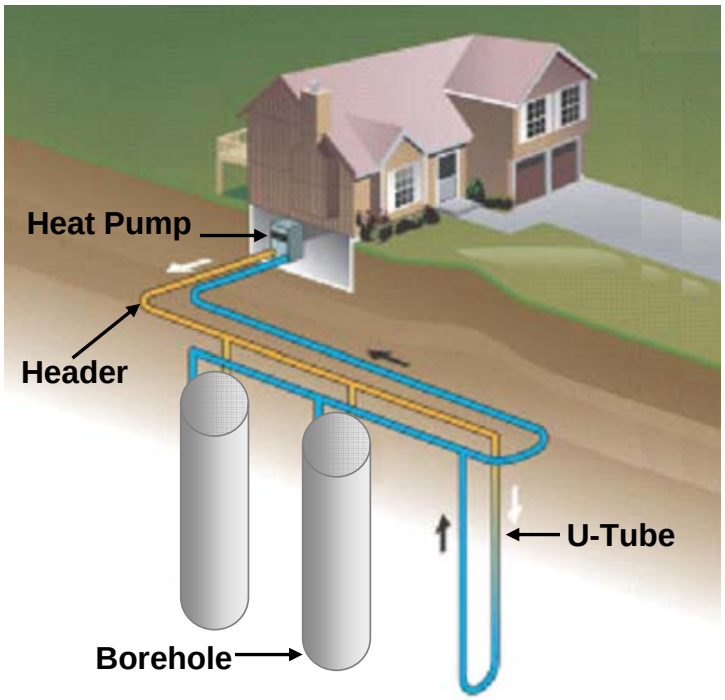

Figure 26. A basic ground heat exchanger system with three boreholes on a single header, one U-tube per borehole (adapted from Darling, 2006).

Ground Heat Exchanger Parameters

There are dozens of parameters needed to specify the GHX model. The overall size of the heat exchanger requires specification of the bore depth and the number of bores. The thermal capacitance and conductivity of the ground heat exchanger materials (including the ground) must be specified as well as the details regarding the configuration and geometry of the boreholes and associated piping. Finally, the initial temperatures of the components and the ground must be provided in order to initialize the static description of the GHX at the beginning of simulation. During the simulation, the fluid flow rate ($\dot{m}_{wat}$), inlet fluid temperature ($T_{GHX,in}$), ambient air temperature ($T_{air,db}$), and the surface temperature above the GHX (T_{surf}) are dynamic inputs which vary according to the operating conditions.

Several of the ground parameters that are required by the GHX model are known to vary significantly depending on the geographic region of interest (e.g., thermal properties of soil, drilling depth, borehole spacing, and initial ground temperatures). These parameters are therefore left as inputs in the distributable version of the model. In the parametric study, typical values of 300 ft and 23 ft are assumed for drilling depth and spacing, respectively. A conductivity value of 1.4 Btu/h-ft-^{o}F and thermal diffusivity value of 1.1 ft^2/day, were used in the simulation studies since geothermal systems are more likely to be installed in regions with favorable ground properties. The initial ground temperature in the parametric study is varied depending on the geographic location of each scenario. The parameters that dictate the overall size of the GHX, total bore length, number of bores, etc., are controlled by the optimizer and varied during the optimization (using an algorithm discussed below) in order to arrive at the most optimal GHX design. The configuration and construction of the individual bore holes can be adjusted by the user in the distributable model, but the configuration is specified and not changed in the

parametric study. The piping is assumed to be 1 inch SDR-11 PE pipe (which has an inner diameter of 1.06 inch); this is a standard size that is consistent with the most basic installation equipment. Some installers do not have the capability to install pipe greater than 1 inch diameter or must rent special equipment to do so (Kavanaugh, 1997). The bore diameter is assumed to be 4.5 inch, which leads to a U-tube spacing of 3 inch. The borehole fill material is assumed to be Thermal Grout 85, which has a thermal conductivity of 0.85 Btu/hr-ft-^{o}F.

The overall size of the GHX is controlled by the optimizer and varied during the optimization process. The parameters controlling the GHX size include the borehole depth, the number of boreholes, and the number of boreholes that are piped in series. An algorithm has been developed in order to set these parameters based on the total length of the boreholes specified by the optimizer (based on TESS, 2005):

1. The number of boreholes in series is set. If the maximum drilling depth is greater than 150 ft, then all boreholes are placed in parallel with on another. If the maximum drilling depth is less than 150 ft, then the boreholes are arranged with two in series in each parallel circuit. This configuration is based on a rule of thumb discussed in the ASHRAE manual and is meant to minimize pumping power consumption (Kavanaugh, 1997).
2. A maximum number of boreholes (N_{max}) is set based on the requirement that the fluid flow be sufficiently high that a turbulent flow condition is achieved. Turbulent flow creates a much higher heat transfer coefficient than laminar flow:

$$N_{max} = \frac{\dot{m}_{max} N_{series}}{\dot{m}_{turb}} \tag{23}$$

where $\dot{m}_{max}$ is the total mass flow through the GHX at the maximum building load, N_{series} is the number of bores in series, and $\dot{m}_{turb}$ is the mass flow that is required to reach turbulent flow conditions; turbulent flow is reached at a Reynolds number greater than the transition Reynolds number of 2300.

3. An initial estimate for the total number of bores (*N'*) is calculated as the ratio of total borehole length to maximum drilling depth, rounded up to the nearest integer value.
4. The actual total number of bores (*N*) is set according to the minimum of the two values *N'* and N_{max} calculated in steps (2) and (3) in order to assure that N_{max} is adhered to and also that the flow is turbulent in the U-tubes. Note that this choice may sometimes result in a violation of the maximum drilling depth that is set by the user. However, because flow rate increases proportionally to total building load and therefore is approximately proportional to the total borehole length, N_{max} and *N'* vary in a similar way and therefore any violation of the maximum drilling depth criterion is small.
5. The borehole depth (d_{bore}) is calculated:

$$d_{bore} = \frac{L_{tot}}{N} \tag{24}$$

where L_{tot} is the total borehole length.

In the DST model, this GHX is then laid out assuming a cylindrical storage volume, symmetrical about the center axis, with uniform spacing (as specified above) between all boreholes of depth of d_{bore} (for more details, see Hellström, 1989). The global solution calculates the temperature distribution of this storage volume and the local solution calculates the temperature distribution at the borehole level (with the specified spacing).

Validation and Laminar Flow Treatment

The Type 557 GHX model has been compared to analytical models and experimental data and shown to provide accurate predictions of the heat transfer and fluid temperature (Shonder et al., 1999; McDowell and Thornton, 2008). Type 557 requires that an average flow rate be specified in order to determine the average thermal resistance between the fluid and the soil; this average thermal resistance is used for the duration of the simulation. In this project, however, the flow rate changes significantly as the simulation progresses; during some of the time steps (33% in one typical simulation) the mass flow rate is low enough to be in the laminar flow regime (i.e., the Reynolds number < 2300, or $\dot{m}_{fl}$ <0.63 gpm in the 1" U-tubes). However, during these periods of low flow, the building load is also very small and therefore the impact of the degradation in the heat transfer coefficient associated with laminar flow is minimal.

In order to verify that the impact of the occasional laminar flow in the GHX is indeed small, the effect on the overall thermal resistance (between the fluid and the soil) was calculated using a simple model developed in EES as well as using the Type 557 model in TRNSYS. The Type 557 model reports only the resistance between the fluid and the wall of the borehole, including the resistance of the pipe wall and grout; this thermal resistance increases by 36% in laminar flow. In the EES model, the thermal resistance of the soil very near the bore hole (the 9 inches of soil adjacent to the bore hole, which corresponds to twice the bore diameter) was included in order to obtain a more realistic estimate of the short time scale thermal resistance. The total resistance calculated using the EES model increased by only 25% in laminar flow compared to the turbulent flow value. Based on this analysis, we can expect that the thermal resistance associated with the GHX is under-estimated by the Type 557 Model in TRNSYS by a quarter to a third during periods of laminar flow.

A typical hybrid simulation was carried out in TRNSYS; the histogram plotter feature was used to record the total energy flow that occurs during each of the two flow regimes. The total value of the energy flow during the two regimes (laminar and turbulent) was calculated by time integration over the 20-year simulation. The result of this analysis is shown in Figure 27; notice that the heat transferred during periods of laminar flow is only 1.5% of the total heat transfer; additionally, note that none of this 1.5% of the energy flow occurs during the peak load periods that directly drive design. Therefore, the change in thermal resistance will affect only 1.5% of the load; the effect of laminar flow on the GHX calculation is on the order of 0.4% and therefore can correctly be neglected.

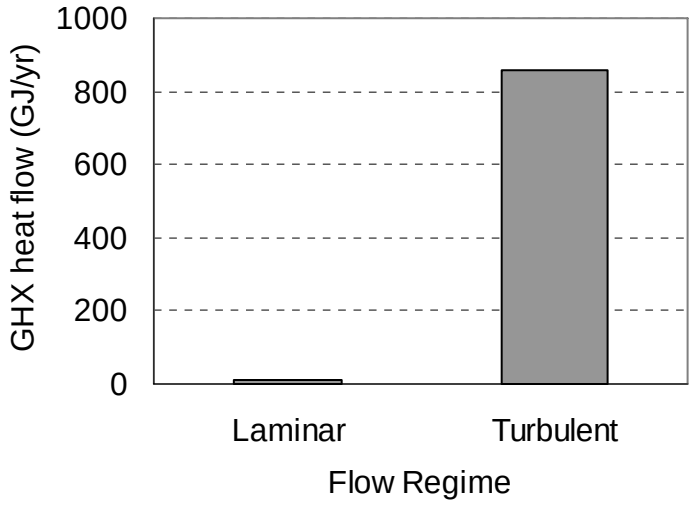

Figure 27. Total heat flow (average per year, absolute value) to and from the GHX during a typical 20-year simulation, categorized by flow regime.

3.2.3 Closed Circuit Cooling Tower

By definition, a HyGCHP system has a supplemental device that assists the ground heat exchanger (GHX) in heat rejection or absorption. One of the supplemental heat rejection devices that considered in this project is a closed-circuit cooling tower (CCCT), represented in TRNSYS by component model Type 510 (and alternately referred to in this report as simply a 'cooling tower'). Heat rejection in a CCCT is accomplished primarily by the evaporation of water that is

sprayed on the outside of tubes containing the working fluid stream (see Figure 28). The working fluid never comes in contact with the outside air or the water that is sprayed on the coil. This type of unit is sometimes referred to as an indirect evaporator.

Figure 28. A closed circuit cooling tower. Fans are shown on the bottom of the device, spray water is pumped into the top and runs through a coil of pipes inside the device (Adapted from Baltimore Air Coil, 2005).

The TRNSYS Type 510 component model is based on an algorithm developed by Zweifel et al. (Zweifel et al., 1995). The simulation algorithm is based on the assumption that the temperature of the fluid at the CCCT outlet is equal to the average temperature of the spray water; this is an approximation, but as Zweifel demonstrates, it is a good approximation for all cooling towers of the size used in HVAC applications. The CCCT component model requires one set of design conditions (i.e., the air and fluid properties at inlet and outlet, as well as their flow rates) for a particular model; these design conditions can be found in manufacturers' catalogs. The CCCT model extrapolates from these design conditions using a set of semi-empirical but phenomenological equations in order to calculate the performance over a range of off-design conditions.

In the CCCT model, the basic equations for a heat exchanger are iteratively solved for varying values of $T_{fl,out}$ (the fluid temperature leaving the CCCT) until the enthalpy of saturated

air at $T_{fl,out}$ (the left side of equation (25)) is equal to the enthalpy of outlet air based on an energy balance for the heat exchanger (the right side of equation (25)):

$$h_{sat}(T_{fl,out}) = h_{air}(T_{air,in}) + \frac{\dot{Q}_{fl}}{\dot{m}_{air}\left(1-\exp\left[-\lambda_{design}\left[\frac{\dot{m}_{air}}{\dot{m}_{air,design}}\right]^{y-1}\right]\right)} \quad (25)$$

where h_{sat} is the enthalpy of saturated air (evaluated at $T_{fl,out}$ in Eq. (25)), h_{air} is the enthalpy of the ambient air entering the cooling tower (evaluated at the ambient temperature, $T_{air,in}$, in Eq. (25)), $\dot{Q}_{fl}$ is the rate of heat transfer in the CCCT (in this case from fluid to air), $\dot{m}_{air}$ is the mass flow rate of the air through the CCCT, $\dot{m}_{air,design}$ is the mass flow rate of air at design conditions, y is an empirical constant that is set to 0.6 for cooling tower applications, and λ_{design} is a constant based on design conditions according to (Zweifel et al., 1995):

$$\lambda_{design} = \ln\left[\frac{h_{sat}(T_{fl,out,design}) - h_{air}(T_{air,in,design})}{h_{sat}(T_{fl,out,design}) - h_{air}(T_{air,out,design})}\right] \quad (26)$$

The outlet fluid temperature can be computed for any off-design condition using this algorithm provided that the following inputs are provided during simulation (see Figure 29): inlet air temperature ($T_{air,in}$), air humidity ($RH_{air,in}$), fan control signal, inlet fluid temperature ($T_{fl,in}$), and fluid flow rate ($\dot{m}_{fl}$). The fan control signal is the speed setting provided by the controller based on the control algorithm discussed in Section 3.2.7.

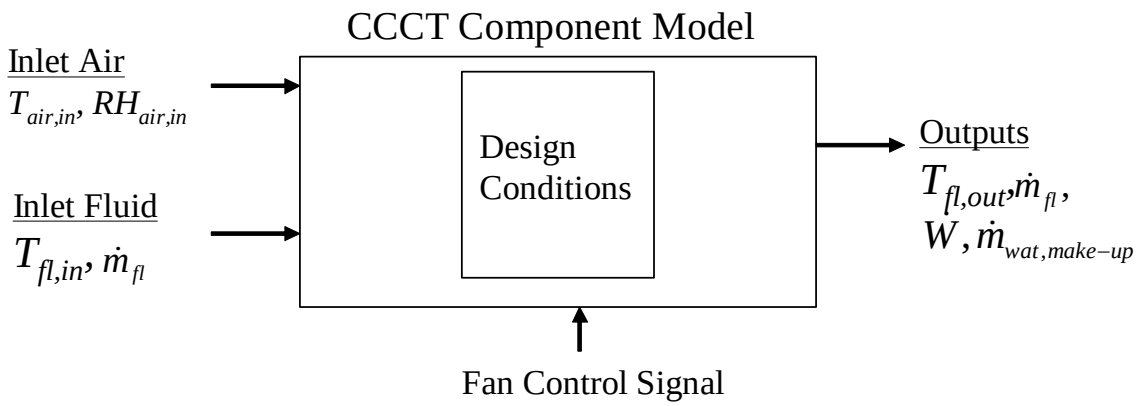

Figure 29. Flowchart of the basic operation of the CCCT component model.

Two additional values are calculated within the CCCT component model in order to facilitate an economic analysis of the larger system. First, an estimate of the required make-up water is obtained using the conservative assumption that all of the heat transfer in the tower goes to evaporate water. Second, the total power consumed by the CCCT is calculated as the sum of spray pump power and fan power; these parasitic power quantities are computed based on design curves for the spray pump and the fan. In this simulation model, both the fan curve data and the CCCT design conditions are taken from the Baltimore Air Coil Series V cooling tower.

A more detailed derivation of equations (25) and (26) description of the parameters describing the CCCT can be found in the Appendix of the Final Report on the Fort Polk Study (TESS, 2005). Thermal Energy Systems Specialists (TESS) was responsible for creating the CCCT component model as part of the Fort Polk Study.

In the HyGCHP simulation model, one of the optimization variables is the size of the secondary heat rejection/absorption equipment. The optimizer adjusts the size of the CCCT continuously (although practically this will correspond to discrete changes in the installed device) during optimization. It is therefore necessary to modify the design inputs to the Type 510 TRNSYS component (which models a specific CCCT unit) so that it models a series of

CCCT units from a particular manufacturer based on the size specified by the optimizer. An algorithm that describes the performance of the CCCT as its size is changed is required; there are four parameters that must change as the CCCT size is adjusted: air flow rate ($\dot{m}_{air}$), maximum water flow rate, spray pump power ($\dot{W}$), and fan power ($\dot{W}_{fan}$). The maximum fluid flow rate is directly proportional to the size of the CCCT. The other three parameters are scaled based on manufacturer's data (the data shown in Figure 22 are from Baltimore Air Coil Series V units). A normalized CCCT size of unity corresponds to a nominal CCCT unit which is the Baltimore Air Coil Model VF1-009, which has a 2 hp fan rated at 4780 cfm with a 1/3 hp spray pump rated at 35 gpm; the nominal cooling capacity of the Model VF1-009 is 10 tons. Figure 22 illustrates the ratio of the fan power, spray pump power, and air flow rate to these characteristics for the nominal CCCT unit as a function of the cooling tower's size.

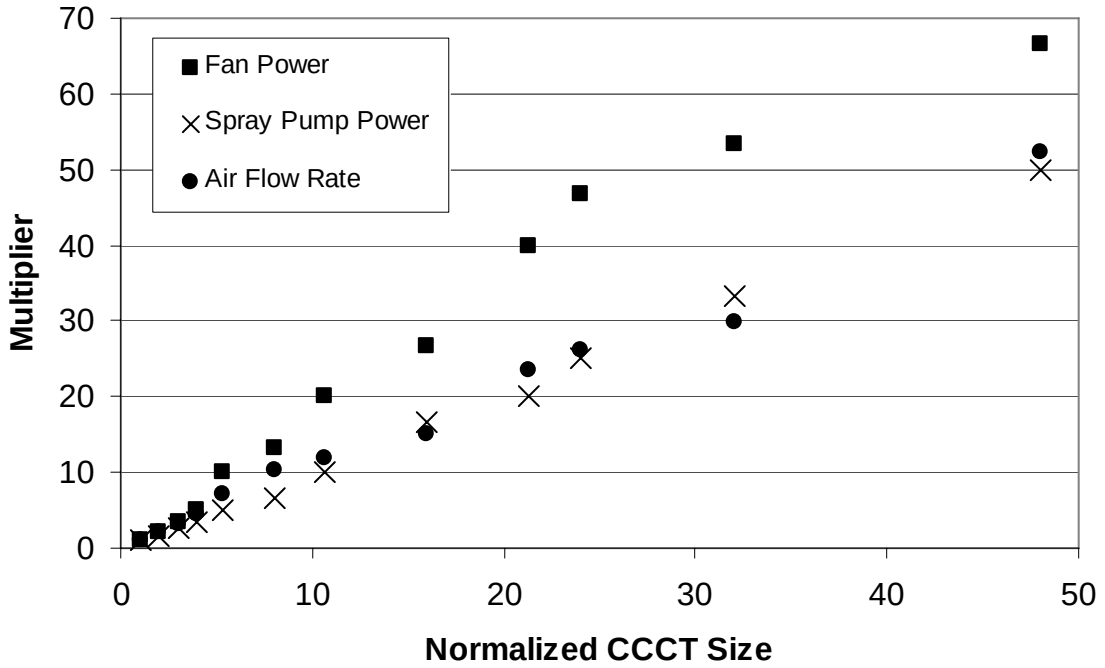

Figure 30. Multipliers for cooling tower parameters as a function of normalized cooling tower size. Data from Baltimore Air Coil Series V cooling towers.

The resulting regression curves for each of the multipliers shown in Figure 22 are:

$$\dot{W}_{fan} = (0.0183 f^2 + 1.4886 f) * \dot{W}_{fan,nom} \quad \text{if } f <= 18.64$$

$$\dot{W}_{fan} = (-0.014 f^2 + 2.091 f) * \dot{W}_{fan,nom} \quad \text{if } f > 18.64 \tag{27}$$

$$\dot{W} = (0.9884 f) \dot{W}_{nom} \tag{28}$$

$$\dot{m}_{air} = (1.0808 f) \dot{m}_{air,nom} \tag{29}$$

where *f* is the normalized size of the CCCT (TESS 2005) which is the ratio of the design capacity to the design capacity of the nominal CCCT unit.

Figure 30 shows the cooling tower parameters for units up to 520 tons, represented by a scaling factor of 50; larger sizes encountered during simulation require extrapolation. Note that this is not a problem for the standard set of buildings that is considered in the parametric study (schools, offices, and research facilities); however, users running the distributable program may want to investigate a larger range of building sizes. Therefore it is possible to adjust the curves provided by Eqs. (27) through (29) in the user distributable program.

3.2.4 Dry Fluid Cooler

Another supplemental heat rejection device that can be used to hybridize a geothermal system is a dry fluid cooler (DFC), represented in TRNSYS by component model Type 511. Heat rejection in a DFC is accomplished by blowing air across tubes through which the working fluid is flowing (see, for example, Figure 31). The working fluid never comes into contact with the outside air. This type of supplemental heat rejection device is sometimes referred to as a dry or air fluid cooler.

Figure 31. A dry fluid cooler. Fans are shown on the top of the device; the working fluid runs through coils inside the device (Adapted from General Air Products).

The TRNSYS Type 511 component model assumes that the fluid cooler device acts as a simple cross-flow heat exchanger (TESS, 2005). The total conductance, *UA*, of the heat exchanger is determined from the manufacturer's design specifications using the effectiveness-*NTU* method. Since the heat transfer surface area does not change for a specific model during a simulation, the TRNSYS component recalculates only the *U*-value as the air and fluid properties and flow rates change and then determines the heat transfer from the resultant *UA* using the appropriate ε-*NTU* solution. The *U*-value for such a heat exchanger is given by Eq. (30), which assumes the DFC coils are constructed from thin wall, high conductivity tubes:

$$U = \frac{1}{\frac{1}{\bar{h}_{fl}} + \frac{1}{\bar{h}_{air}}} \tag{30}$$

where $\bar{h}_{fl}$ and $\bar{h}_{air}$ are the average heat transfer coefficients associated with the fluid and the air, respectively. The McAdams correlation for air flow across unbaffled tubes (ASHRAE, 2001) is used to determine $\bar{h}_{air}$ based on air properties and flow rates. The Dittus-Boelter equation is

used to find $\overline{h}_{fl}$ (Incropera and DeWitt, 1996), resulting in the following ratio between *UA* at actual and design conditions:

$$\frac{UA_{design}}{UA_{actual}} = \frac{\left(\frac{1}{\overline{h}_{fl,design}} + \frac{1}{\overline{h}_{air,design}}\right)^{-1}}{\left(\frac{\left(\dot{m}_{fl,design}\right)^{0.8}}{\left(\dot{m}_{fl}\right)^{0.8}\overline{h}_{fl,design}} + \frac{1}{\gamma_{air}^{0.6}\overline{h}_{air,design}}\right)^{-1}} \tag{31}$$

where $\overline{h}_{fl,design}$ and $\overline{h}_{air,design}$ are the heat transfer coefficients on the fluid and air sides evaluated at design conditions, $\dot{m}_{fl}$ and $\dot{m}_{fl,design}$ are the fluid flow rates at actual and design conditions, respectively, and γ_{air} is the ratio of actual air flow rate to the design air flow rate; the value of γ_{air} is based on the fan control signal which comes from the controller.

After the conductance is computed (UA_{actual} in Eq. (31)), the effectiveness-*NTU* method is used to determine the outlet fluid temperature (from the heat exchanger effectiveness at the given conditions), which is the primary output of the model. The secondary outputs of the model are the outlet fluid flow rate (which is equal to the inlet flow rate) and the power consumed by the fan ($\dot{W}$), which is required for economic calculations; the fan power consumption is related to the rated fan power (another design parameter) according to the cube of the fan speed control signal. The heat transferred to the fluid (q) is also calculated, for informational purposes.

All design parameters in the DFC component model are set at the start of simulation based on manufacturer's data. The data used for this HyGCHP model are taken from a General Air Products air fluid cooler (General Air Products, 2007). The dynamic inputs to the model provided during the simulation include the inlet air temperature ($T_{air,in}$), fan control signal, inlet fluid temperature ($T_{fl,in}$), and fluid flow rate ($\dot{m}_{fl}$). The fan control signal is provided by the HyGCHP controller and is set based on the control algorithm. The fluid inputs come from the

fluid loop in the model, and the air temperature is determined by the weather data file associated with the climate being simulated. Figure 32 summarizes the inputs and outputs of the DFC component model.

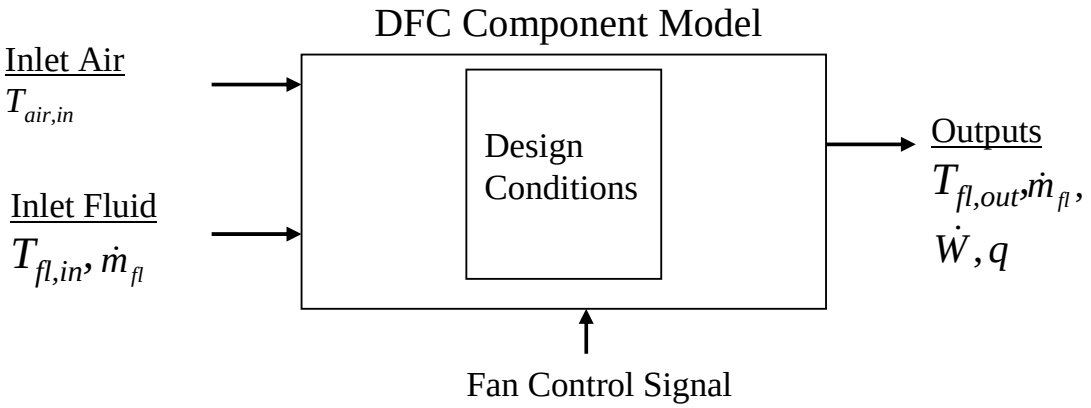

Figure 32. Flowchart of the basic operation of the DFC component model.

A more complete derivation of Eqs. (30) and (31) as well as a more detailed description of the parameters describing the DFC can be found in the Appendix of the Final Report on the Fort Polk Study (TESS, 2005). TESS was responsible for creating the DFC component model as part of the Fort Polk Study.

Note that the Type 511 TRNSYS model simulates a particular model of DFC, but the size of that DFC model is changed by the optimizer. Therefore, the design inputs to the DFC model have to be adjusted so the characteristics of a series of different DFC's can be simulated as the optimizer changes the size of the equipment. To facilitate the required scaling of the size of the DFC (continuously, although practically this will correspond to discrete changes in the installed device) during optimization, an algorithm that adjusts the performance of the DFC as its size changes is required. There are three design parameters that must change as the DFC size is adjusted: the design air flow rate ($\dot{m}_{air,design}$), the maximum allowable fluid flow rate, and the rated fan power ($\dot{W}_{design}$). The maximum fluid flow rate is assumed to be directly proportional to

the size of the DFC. The design air flow rate and fan power are scaled based on manufacturers data over a range of sizes corresponding to different models for a particular product line. Figure 30 illustrates fan power and air flow rate, normalized against these values for a nominal unit, for the General Air Products DFC series as a function of the normalized capacity. A DFC size of unity corresponds to the nominal model, General Air Products Model AFC14CX, which has a 0.5 hp fan rated at 6000 cfm and a nominal cooling capacity of 16 tons.

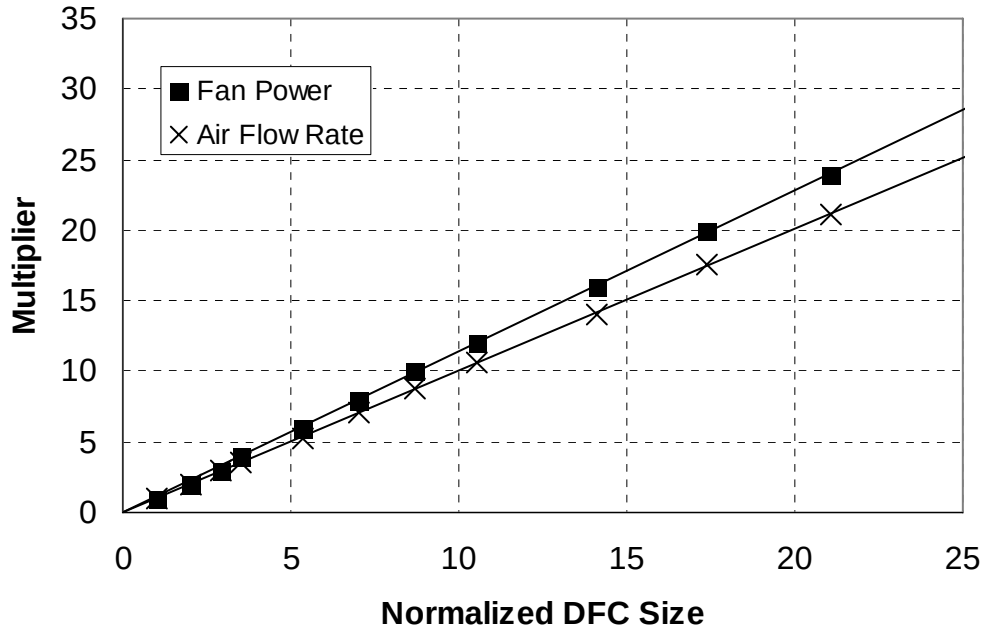

Figure 33. Multipliers for fluid cooler parameters as a function of normalized device size. Data from General Air Products air fluid coolers.

The regression curves for the multipliers shown in Figure 25 are:

$$\dot{W}_{design} = (1.1405 f)\dot{W}_{nom} \tag{32}$$

$$\dot{m}_{air,design} = (1.0045 f)\dot{m}_{air,nom} \tag{33}$$

where f is the normalized size of the DFC (TESS 2005), the capacity of the model relative to the capacity of the nominal model (16 tons). Figure 30 shows fluid cooler parameters for units up to

340 tons, represented by a scaling factor of 21. Sizes beyond this are extrapolated; therefore, the curves for fan power and air flow rate can be adjusted by the user in the distributable program.

3.2.5 Boiler Component

A boiler component is required in the model to provide the heat required by a conventional water-source heat pump configuration with no GHX. Additionally, the boiler is used as the supplemental device in one heating dominated hybrid configuration. The boiler is represented by TRNSYS component Type 659, which models a natural gas boiler with constant efficiency. The boiler is located in the HyGCHP model between the heat rejection device (cooling tower, etc.) and the heat pumps. The boiler is activated by the controller according to the control algorithm. The model is flexible relative to the control algorithm; in this study, the boiler is activated when the heat pumps are in heating mode and the fluid temperature falls below a specific set point (note that the set point is an optimized parameter).

Several static input parameters are required to describe the boiler model at the start of a simulation. The rated capacity (q_{CAP}) is the maximum rate of heat transfer that the boiler is capable of delivering to the fluid stream; this is an optimization parameter. The set point temperature (i.e., the temperature under which the boiler will operate to heat the fluid) is also a static parameter. Other parameters include the boiler efficiency (η_{boil}) which is assumed to be 85% for this study, the fluid specific heat (c_p), and a coefficient for calculating heat loss, which is set to zero for this study.

The boiler calculates the energy input required (obtained by burning natural gas) based on how much time it must run at full capacity in order to keep the fluid temperature above the given set point. The model outputs are then:

- fluid flow rate, which is equal to the fluid flow rate into the boiler,

- heat transfer provided by natural gas, which at a maximum is the boiler's rated capacity, and
- outlet fluid temperature ($T_{fl,out}$), which is calculated based on equation (34):

$$T_{fl,out} = T_{fl,in} + \frac{\eta_{boil}\gamma q_{CAP}}{\dot{m}_{fl} c_p} \tag{34}$$

where $T_{fl,in}$ is the inlet fluid temperature and γ is the control signal, which is fraction of rated heat input used to raise the fluid to the set point temperature (set to one by the controller when the boiler is on, set to zero when it is off). For more information on the boiler component, see TRNSYS documentation regarding Type 659.

3.2.6 Solar Thermal System

For heating dominated systems, a configuration using solar thermal collectors is an option for the supplemental heat absorption device (as discussed in Section 3.1.3). A few additional components are required to make up the solar collection system.

The solar collector itself is modeled as a flat plat collector using TRNSYS Type 1b. The collector model calculates heat gain in the fluid (q_{coll}) using the following equation:

$$q_{coll} = \eta_{coll} A I_T \tag{35}$$

where η_{coll} is the efficiency of the collector, A is the total area of the collector, and I_T is the total radiation per unit area that is incident on the solar collector during an hourly period. I_T is determined from several of the weather outputs, including ambient temperature, incident radiation, horizontal radiation; diffuse radiation, and incidence angle (Klein, 2006). The efficiency of the collector, η_{coll}, is determined using the Hottel-Whillier equation (Duffie and Beckman, 2006), which requires test data from the collector manufacturer. The collector data

used in this model are shown in Table 5. The only additional parameter describing the collector array is the number of collectors (the collectors are placed in parallel); this is the parameter that is optimized in this study in order to determine the optimal collector array size.

Tested flow rate	0.9	gpm
Intercept efficiency	0.8	--
Efficiency slope	0.64	Btu/hr-ft^2-R
Efficiency curvature	0.0014	Btu/hr-ft^2-R^2
Collectors in series	1	
Area of one collector	38	ft^2
Slope	45	degrees
Azimuth	0	degrees

Table 5. Parameters for flat-plate collector model. Slope is set to 45^o to correspond to northern U.S. latitudes (primarily Minneapolis). All other parameters are based on American Energy Technologies collector model CF-50-SGC (SRCC, 2007).

The other key solar component is the solar tank. In this system, the tank is modeled as a fully-mixed (single-node) tank with no auxiliary heating, two inlets, and two outlets. Fully mixed tanks are reasonable approximations of actual tanks (Duffie and Beckman, 2006), and allow for smaller tanks to be modeled while maintaining a reasonable timestep (in a multi-node tank, the timestep has to be small enough so that the volume of fluid flowing through the tank in one timestep is smaller than the volume contained in each tank node). Because the tank is fully mixed, the location of the inputs and the outputs is immaterial. The only other thermal interaction is tank losses. For the purpose of calculating tank losses, the heat transfer coefficient associated with each tank wall is assumed to be 0.44 Btu/hr-ft^2. The size of the tank depends on the size of the collector array; in this model, the ratio of collector array area to tank size is 3 ft^2/ft^3; this ratio is in the middle of the range 1.5 to 6 ft^2/ft^3 which is suggested by Duffie and Beckman (2006) as a range of ‘broad optima’ for solar thermal storage.

In addition to the collector and storage tank, a simple plate heat exchanger and two pumps are required to exchange fluid between the collectors and the tank, as shown in Figure 13.

The heat exchanger model is a simple, constant effectiveness heat exchanger with an effectiveness of 60%. The additional pumps are modeled with the sole purpose of estimating the pumping power; the same pumping power calculations that were described for the main loop pump are used for the collector loop pumping losses (see Equations (36) and (37)). The pump efficiency is assumed to be 60% with a motor efficiency of 90%. The heat exchanger loop and the collector loop pumps are both assumed to operate at the collector's tested flow rate. While this flow rate does not necessarily maximize either the collector outlet temperature or the collected energy, it is selected for simplicity and for the sake of reducing optimization run times. Parametric studies for the heating-dominated systems will assume a climate at least as cold as Minneapolis, so the collector side of the system is assumed to have a water/propylene glycol solution with a concentration of 25% in order to avoid freezing. The pumping power of the solar system is observed to be very small in comparison to all other power consumptions, so these simplifications do not have a significant effect on results.

3.2.7 Controller

The scope of this simulation study requires that the model be both distributable and capable of optimization. In order to meet these two objectives (as well as for simplicity), it is advantageous to contain all of the TRNSYS computations within one simulation model. The single simulation model must therefore contain the heat pump system, building load input, ground heat exchanger, and all supplemental heat rejection/extraction devices. No existing controller component in TRNSYS is setup to control all of these components based on the building load files; therefore a new controller component has been developed (Type 198).

Cooling Dominated System Control

As discussed in Section 3.1.3, one general control strategy has been selected for this project that has proven to be the most cost effective in most situations. Within this general strategy, several set points can be changed by the optimizer; therefore different buildings can still have very different control sequences even though they use the same general strategy. The general control strategy works with the supplemental device in series with, and upstream of, the GHX; it then operates the supplemental device when ambient temperatures are favorable (the set point temperatures determining 'favorable' conditions are adjusted within the optimization, but the strategy is unchanged). Temperature measurements and flow controls are required in the locations shown in Figure 34 in order to operate the controller:

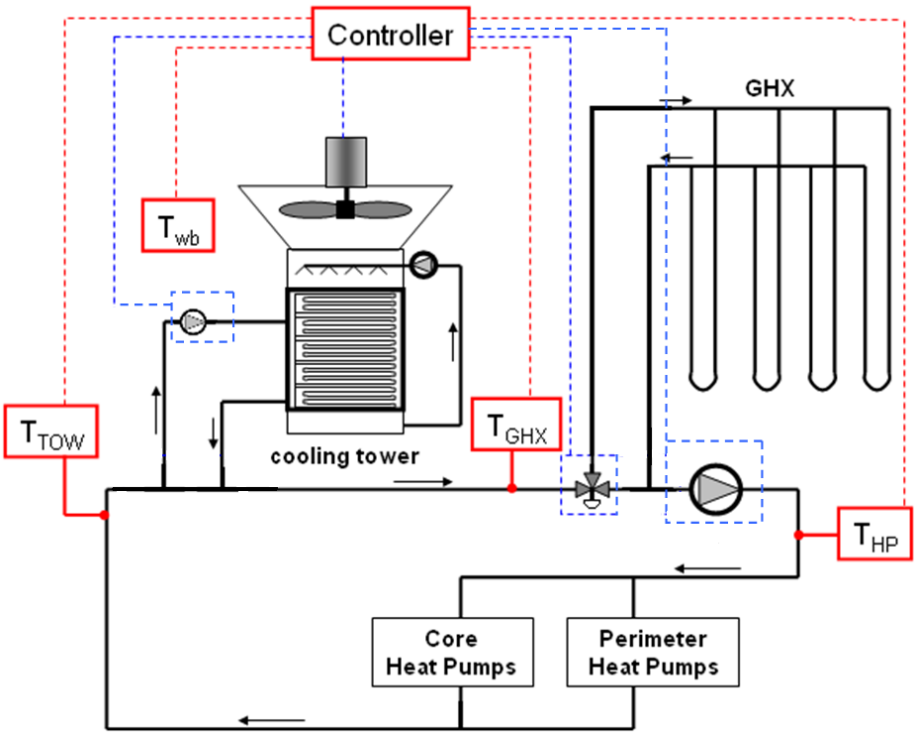

Figure 34. Temperature measurements (shown in red) and flow controls (shown in blue) that are part of the hybrid controller.

The controller operates in the following sequence (also illustrated in Figure 35):

1. At the start of simulation, the type of supplemental device is chosen and passed to the controller. The controller contains different (but similar) code for each device, and immediately jumps to the code for the device being used. This explanation will assume a cooling tower is used as a supplemental heat rejection device.
2. The controller determines whether heating is needed based on the temperature entering and leaving the heat pump. If heating is required, then the fluid is diverted through the GHX whenever the temperature falls below some set point control temperature, $T_{Heat1.}$ The controller stops here if heating is needed, if not (i.e., if cooling is required) then it continues.
3. The cooling tower is turned on (at low fan speed and flow rate) if the fluid temperature leaving the heat pumps is above the ambient wet bulb temperature plus some set point temperature difference, ΔT_1. The tower loop pump is activated whenever the tower is on.
4. If the fluid temperature leaving the heat pumps is also above some higher set point temperature, T_{Cool1}, then the cooling tower is switched to high fan speed and flow rate.
5. If the fluid temperature leaving the cooling tower remains above some set point temperature T_{Cool2}, then the fluid is diverted through the GHX as well.

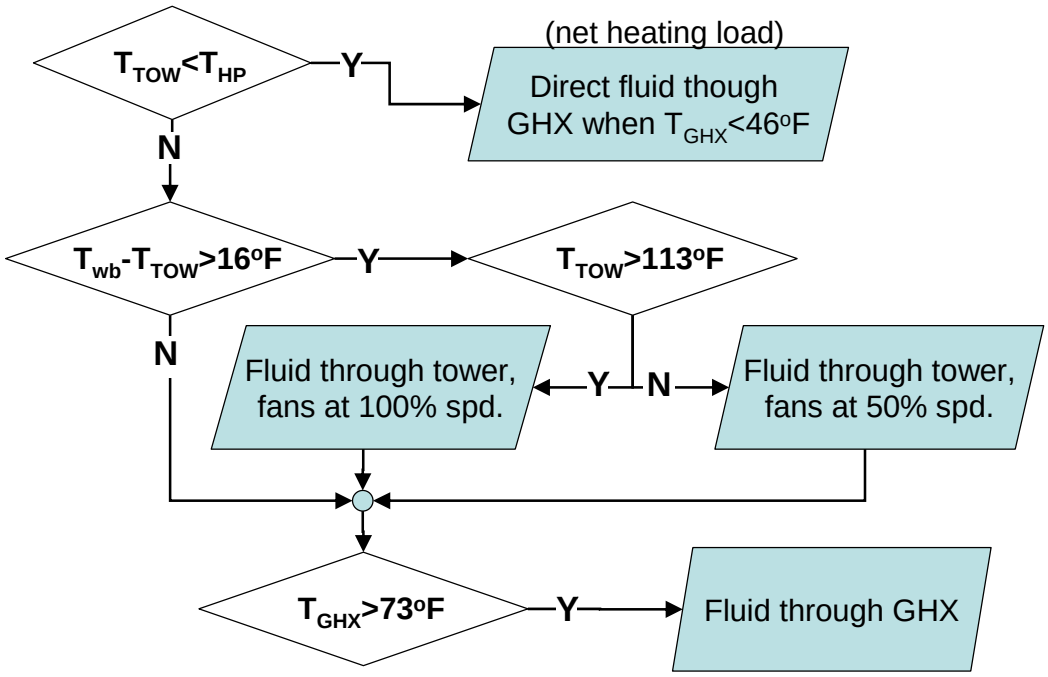

Figure 35. Flowchart representation of an example control sequence. This sequence is for a cooling dominated building with a cooling tower as the supplemental device. Temperature variables correspond to those shown in Figure 34.

Note that the values of the temperature set points in the control system described above (i.e., T_{Cool1}, etc.) are specified only once at the beginning of the simulation. These set points can be controlled by optimization algorithm and are, eventually, an output of the optimization process. The control system operates using a dead band temperature difference, $\Delta T_{deadband}$ *that* is set to 4.5°C in this study. Having a dead band temperature difference at each set point prevents the controller from cycling the equipment on and off too frequently. The set of calculations for this strategy discussed above is taken from the more complex, multi-strategy controller model (Type 216) in order to form the standalone control component model (Type 198) which is used in the HyGCHP model. Also note that this somewhat simplified control sequence does not include any predictive control capabilities such as preheating/precooling. Further research would be required to investigate the viability of including such a feature.

Heating Dominated System Control

The configuration and control of a heating dominated hybrid system is different from that of a cooling dominated system. As discussed in Section 3.1.3, the supplemental device (boiler or solar collector) is placed downstream of the GHX (in contrast with the supplemental devices for cooling dominated climates, which are placed upstream of the GHX); this change in the system configuration also changes the basic control strategy slightly.

In the case of boiler hybrid, the GHX is operated using the same control strategy discussed in the previous section for a cooling dominated hybrid system. The only addition is a second heating control setpoint, T_{Heat2}, which controls the operation of the boiler. When the temperature of the fluid leaving the GHX is below T_{Heat2} then fluid is diverted through the boiler and heated until the fluid reaches the heating control setpoint temperature, T_{Heat2}.

Control of the solar hybrid is more complex, requiring control of the fluid flow on both sides of the tank (i.e., the main system side and the collector side). The collector loop pump (on the collector side) is activated when the temperature of liquid at the collector array outlet is 18^{o}F higher than the average temperature of the fluid in the solar tank and continues to operate until the temperature at the collector outlet falls to 3.6^{o}F above the average fluid temperature in the solar tank. The 18^{o}F and 3.6^{o}F dead band temperatures were chosen to ensure that the controller does not enter an oscillatory state in which the pumps are continually turned on and off.

The control of main system loop fluid flow (through the heat exchanger (including flow on either side of the heat exchanger) is somewhat more complex as there are a number of conditions that affect the diverter valve setting; these conditions are dealt with in the order set below:

1. The first condition is that the temperature of the fluid in the main loop entering the diverter valve must be less than the average temperature of the liquid in the thermal storage tank by a certain amount; this value, designated ΔT_S, is an additional control setpoint that is optimized.
2. Fluid continues to flow from the main loop until the temperature in the tank falls to 1^oF above the temperature of the fluid entering the diverter (the main loop temperature).
3. The heat pumps have a high limit on their allowable inlet temperature; if the temperature of the liquid in the thermal storage tank is very hot, then a tempering controller placed on the diverting valve ensures that the temperature of the remixed liquid (i.e., some from the solar tank loop and some from the main loop) does not exceed the heat pumps' maximum allowable inlet temperature; this is done by modulating the fraction of the flow that is diverted to the solar tank loop.
4. The final condition that determines the diverter valve setting is the tank size. Diverting a large amount of fluid through a very small tank will lead to control stability problems (as well as inaccurate results) in TRNSYS. Therefore, the upper bound on the total amount of liquid that can be diverted through the tank's loop in one timestep is equal to the size of the tank. With the parametric study using 15 minute timesteps, this is not only a modeling consideration but a practical limit as well; it forces the amount of fluid flowing from the loop through the solar heat exchanger to be on the same order of magnitude as the amount of fluid flowing through the tank from the collector side (since the tank size is set using a ratio to collector area).

3.2.8 Pump and Pumping Power

A pump is needed in any HyGCHP system in order to circulate the fluid through the fluid loop. In this simulation model, a simple variable speed pump component model (Type 742 in TRNSYS) represents the characteristics of the pump. The pump must operate over a range of speeds because of the changing mass flow rate in the system. In the simulation model the pump is located between the GHX and the heat pumps.

The Type 742 component model can be simple because it is not involved in the *control* of the fluid loop. The heat pump component models determine the fluid flow rate for the entire fluid loop, and this total flow is required from the variable speed pump; the flow rate is therefore an input to the pump model rather than an output. The other input required by the pump model is the entering fluid temperature. Fluid flow rate is passed to the next component (the heat pumps) without modification. Temperature is passed to the next component after an increase is made for heat transfer due to pump inefficiency; no heat is transferred from the motor or drive (which is assumed outside the fluid stream) but mechanical pumping inefficiencies result in some heat transfer. The main role of the pump component, however, is to calculate pumping power. The pump component model calculates pumping power based on fluid flow rate and temperature inputs, a constant pump efficiency parameter, and a calculated pressure rise for the fluid loop.

The calculation of pump power consumption begins with a calculation of the power that goes into actually pumping the fluid ($\dot{W}_{pumping}$):

$$\dot{W}_{pumping} = \frac{\dot{m}_{fl}\Delta P}{\rho_{fl}} \tag{36}$$

where $\dot{m}_{fl}$ is the mass flow rate of fluid through the pump, ρ_{fl} is the density of the fluid, and ΔP is the pressure rise required to overcome losses in the entire fluid loop (see pressure drop

calculated below). The total power consumed by the pump ($\dot{W}_{tot}$) is then calculated as the ratio of the pumping power to the pump efficiency (η_{pump}):

$$\dot{W}_{tot} = \frac{\dot{W}_{pumping}}{\eta_{pump}} \tag{37}$$

The pump efficiency is set by default to 60%; however, it is a user-controlled variable in the distributable program. The heat transferred to the fluid (q_{pump}) due to pumping inefficiencies is then:

$$q_{pump} = \dot{W}_{tot}\eta_{motor} - \dot{W}_{pumping} \tag{38}$$

where η_{motor} is the efficiency of the motor (including the variable frequency drive), which is set to 90%. Though q_{pump} is taken into account in the energy and temperature calculations in the model, it is so small that its effect on temperature is negligible.

The constant-efficiency assumption is based on the fact that a single, variable-speed pump is used for the outdoor loop and GHX (note that indoor loop pumping power is not considered here), with a separate tower pump providing pumping power through the cooling tower. A variable speed pump can be selected so that the pump curve matches reasonably well to the system curve in both cases; this is occurs for a system with no static head (such as a GHX system). Such a well-designed pump will have a relatively constant efficiency over a wide range of flow rates (see Figure 36). The pump efficiency will decrease at very low flow rates; however, the energy consumption associated with these low flow rates is also small and therefore the change in efficiency during those periods does not have a significant effect on the total energy consumed.

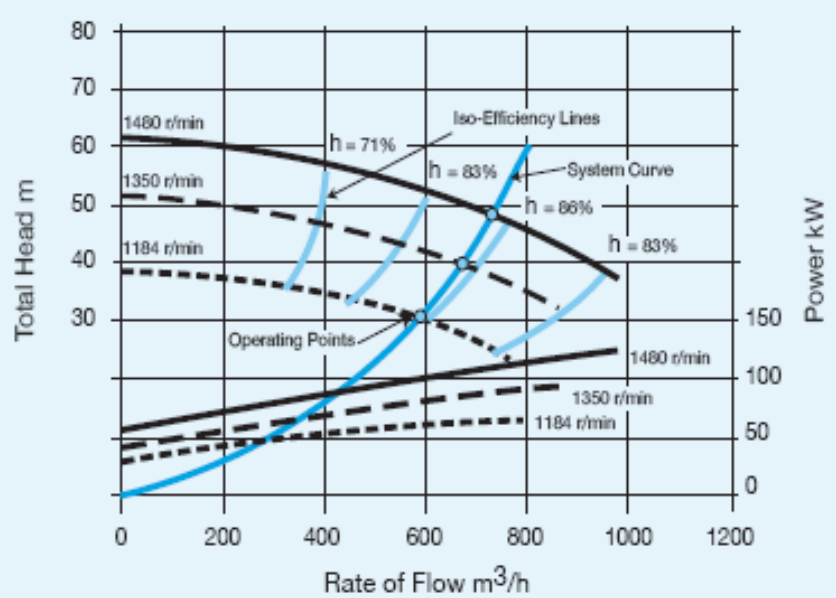

Figure 36. Example pump curves for a variable speed pump, plotted with a general system curve. Note that as pump speed changes with flow rate, the efficiency remains constant. This is only true for systems with zero (or low) static head, such as a GHX (EERE, 2004).

Pressure Drop Calculation

The pressure rise that is required to estimate the pumping power is based on a summation of the pressure drops that are calculated individually across each component in the fluid loop. Most of the pressure drop is caused by pipe friction losses, including the piping through the GHX. The pipe friction losses are calculated in TRNSYS component Type 586 which uses empirical (Haaland) friction factor formulas (White, 2000). The dynamic inputs to these formulas during simulation include fluid properties, temperature, and flow rate. Additionally, parameters describing the length and diameter of each individual section of pipe are required. The user provides an estimate of the length of piping between components; however, the layout and geometry of the GHX piping is a more complicated problem.

The GHX layout changes as the total borehole length changes during optimization, so an algorithm is developed in this study to calculate pipe geometries (length and diameter) based on

the outputs of the GHX sizing algorithm (sizing algorithm discussed in Section 3.2.2; total borehole length is the only variable). To calculate the GHX pressure drop (using TRNSYS component Type 586), the length, diameter, and flow rate associated with each piece of pipe between the building supply and return is required (see Figure 37). The pressure drop in the GHX is then equivalent to the pressure drop in a borehole on the furthest sub-header from the building. A length is input for the distance of the furthest sub-header from the building ($d_{borefield}$); this length corresponds to the lengths of each of the first and last sections of pipe. The diameter of the first (section '1' as shown in Figure 37) and last section (section '*n*') is based on the mass flow rate through the header (using ASHRAE guidelines for minimum diameter per flow rate). The other *n*-2 sections of pipe are equal in length to the spacing between boreholes ($d_{spacing}$), with the diameters of these intermediate sections decreasing as the flow rate decreases as fluid is diverted through successive bore holes. The one exception is section '*n*-1'; the length of this section is increased by twice the borehole depth (representing pressure drop in the U-tube that is set down in the bore). The number of sections (*n*) is determined by the number of bores per sub-header.

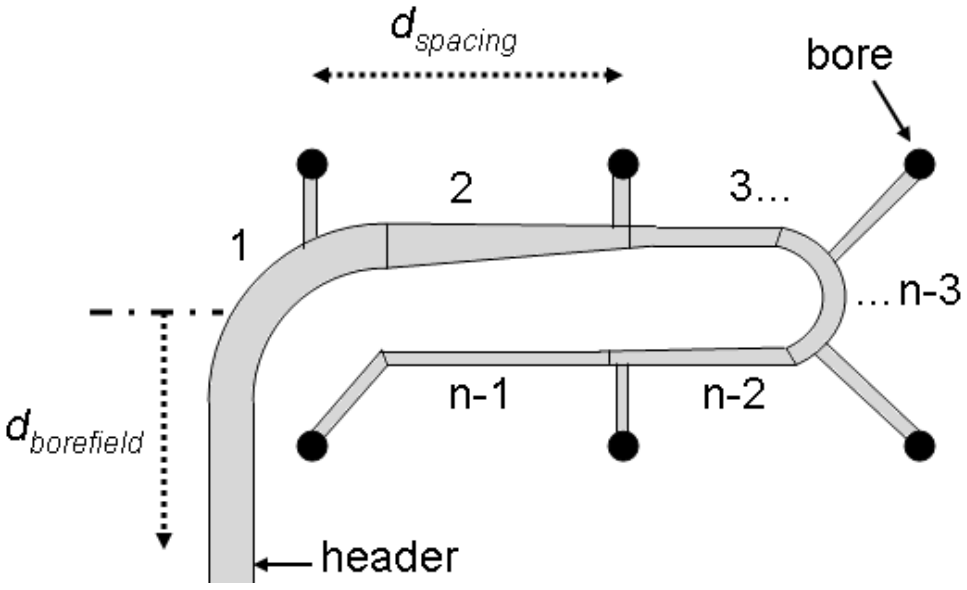

Figure 37. Standard layout of GHX surface piping (supply); each bore contains one u-tube that carries fluid to the bore depth. Note that an identical return piping system is also necessary, but not shown here.

This algorithm does not specify the layout of the headers nor does it consider how many bores each header would serve. For example, if there are only a few boreholes then they will all be grouped together with one header pipe running out from the main fluid loop. However, if there are dozens or even hundreds of boreholes in a large installation, then the bores should be divided into groups, each on its own sub-header. This flow arrangement allows smaller groups of bores to be isolated for flushing or for other maintenance procedures and also leads to a simpler ground installation. The layout of the bore field will affect the GHX pressure drop; however if the layout is well-designed (as is assumed here), different header configurations will lead to a small impact on the calculated pressure drop because the distance of the furthest sub-header from the building will not change substantially and the pipe sizes will be selected chosen based on achieving a similar figure of merit given by the pressure drop per length of pipe (i.e., ΔP per 100 ft of pipe). In this study we assume a header for every 40 gpm based on anecdotal comparison with published installations.

In addition to piping and GHX losses in the fluid loop, there is some pressure drop associated with the supplemental devices in the fluid loop. In the Fort Polk study, relationships between pressure drop and flow rate were identified for a number of supplemental devices. These same pressure drop formulas are used in this study. For the closed circuit cooling tower, for example, the pressure drop (ΔP_{CCCT}) in psi is calculated as:

$$\Delta P_{CCCT} = 0.006Q^2 + 0.23Q \tag{39}$$

where Q is the flow rate of fluid, in gpm, through the cooling tower (TESS, 2005). The flow rate is divided by the nominal size of the CCCT (f) to account for the fact that as the CCCT increases

in size, the heat exchanger piping increases in size, resulting in a decreased pressure drop for a given flow rate.

3.2.9 Economic Model

In order to perform an optimization it is necessary to define a figure of merit to be maximized. For a building energy system, such as the heat pump systems considered in this project, the life cycle cost (*LCC*) is the most logical figure of merit because the *LCC* includes the size (i.e., capital cost) and efficiency (i.e., operating costs) of the system equipment. All energy systems incur these two types of costs over their operational life; these costs cannot be compared directly due to the effect of the time value of money, which depend on both the inflation rate (*i*) and the required rate of return (used for the discount factor, *d*). The life cycle cost combines all of these considerations into a single number, which represents the present value of all costs that are associated with owning and operating the system over its economic life. One method for determining the *LCC* associated with an energy system is the P_1-P_2 method developed by Duffie and Beckman (Duffie and Beckman, 2006) and supplemented by Mitchell and Braun (Mitchell and Braun, 1997). All calculations needed to implement the P_1-P_2 method have been included in a TRNSYS component (Type 582) that can be integrated with the HyGCHP system model.

The P_1-P_2 method embodied by this TRNSYS component simplifies the entire life cycle cost calculation to:

$$LCC = P_1 C_{F1} + P_2 C_E \tag{40}$$

where C_{F1} is the cost of fuel (i.e., electricity and gas for the heat pump system) in the first year and C_E is the initial cost of the equipment. The parameter P_1 is then the ratio of the life-cycle fuel cost to the first-year fuel cost and P_2 is the ratio of the life cycle equipment cost to the initial

equipment cost. The P_1-P_2 method condenses all of the costs incurred over the life of the HyGCHP system into the two parameters P_1 and P_2.

P_1 reflects the change in fuel cost in the future, and is calculated as:

$$P_1 = (1 - c\bar{t})PWF(N, i_f, d) \tag{41}$$

where c is a binary flag (i.e., it is either 0 or 1) indicating whether fuel costs are deducted from taxes as a business expense, $\bar{t}$ is the income tax rate, and *PWF* is a present-worth function (Duffie and Beckman, 2006). The *PWF* function returns a multiplier that modifies a given periodic cost to account for the summation of N periodic costs over time including the inflation of these costs and the discounting of those costs. The *PWF* function is defined as:

$$PWF(N, i, d) = \frac{1}{d - i}\left[1 - \left(\frac{1+i}{1+d}\right)^N\right] \tag{42}$$

where i is the general inflation rate (i_f in the case of Eq. (41) because it is inflation of *fuel* cost) and d is the discount rate.

P_2 is a measure of the amount of the equipment cost that is *not* required up front (e.g., financed equipment cost, insurance, etc.), and is calculated as:

$$\begin{aligned} P_2 = {} & D + (1-D)\frac{PWF(N_{\min}, 0, d)}{PWF(N_L, 0, m)} \\ & -\bar{t}(1-D)\left[PWF(N_{\min}, m, d)\left(m - \frac{1}{PWF(N_L, 0, m)} + \frac{PWF(N_{\min}, 0, d)}{PWF(N_L, 0, m)}\right)\right] \\ & + I + \left[t(1-\bar{t}) + M_s(1 - c\bar{t})\right]PWF(N_e, i, d) - \frac{c\bar{t}}{N_D}PWF(N'_{\min}, 0, d) - R - \frac{R_v}{(1+d)^{N_e}} \end{aligned} \tag{43}$$

where the previously undefined variables represent the following parameters (Duffie and Beckman, 2006):

D = Percentage of the investment made as a down payment

N_{min} = Number of years that mortgage contributes to analysis (minimum of N_e and N_L)

N_L = Number of years over which the loan is paid

m = Interest rate paid on the mortgage

I = Installation cost, expressed as a fraction of equipment price excluding installation

t = Property tax rate

M_s = Ratio of first-year miscellaneous costs (insurance, etc.) to initial investment

i = General inflation rate

N_e = Period of economic analysis

N_D = Number of years over which (straight line) depreciation occurs

$N'_{\min}$ = Number of years of depreciation in the analysis (minimum of N_e and N_D)

R = A rebate or discount on the purchase price, expressed a fraction of the purchase price

R_v = Ratio of resale value at the end of analysis period to initial investment

The equations provided above are implemented in the Type 582 TRNSYS model based on a number of user inputs, each of which are described in detail in Section 3.2. In this study, the economics component is used to analyze a single simulation as the optimizer adjusts parameters. Therefore, only the *LCC* is calculated within the HyGCHP model. After several optimizations are completed and the associated *LCC* has been identified for a number of case studies, additional calculations can be accomplished (outside of TRNSYS) in order to determine the life cycle savings (*LCS* - the difference in the *LCC* between an optimized system and a baseline system) and other economic figures of merit. For example, after complete optimization of one HyGCHP system (case 1) and one conventional heat pump system (case 2), the life cycle savings associated with the selection of the hybrid system can be calculated:

$$LCS_{\text{hybrid}} = LCC_{\text{case2}} - LCC_{\text{case1}} \tag{44}$$

Note that a negative *LCS* indicates that the hybrid system has a higher life cycle cost than the conventional system and would therefore be considered to be economically unfavorable *in comparison to the conventional GCHP system*. It is important to note that the *LCC* results output by the model (including those presented at the end of this study) can only be used to compare different systems for a given building. Due to simplifying assumptions (discussed in Section 3.1.2), the equipment within the building – including the initial cost of the heat pumps themselves – are not considered in the base-case economics. (In the distributable version of the model, the user can enter an approximation of these costs to get closer to having a full cost for comparison with other types of systems – standard VAV, etc.). Therefore, the *LCC* calculated here can only be compared with other simulations done using HyGCHP or with other economic calculations that contain the same elements as the HyGCHP model.

The Type 582 component model keeps a running total of operating, fuel, and maintenance costs. Details associated with these costs are provided in Section 3.2. Throughout the simulation, these individual costs are passed to the Type 582 component at each time step and Type 582 adds both fuel and maintenance cost to a running cumulative operating cost:

$$C_{CumOp,t=n} = OperatingCost_{n-1} + FuelCost_n + MaintenanceCost_n \tag{45}$$

At the end of simulation, the annual fuel cost (C_{F1}) is calculated based on this cumulative operating cost:

$$C_{F1} = \frac{C_{CumOp}}{N_e} \tag{46}$$

A more detailed description of the Type 582 component model can be found in the TRNSYS documentation (Bradley, 2004).

As with most economic analyses, the specific inputs that are provided to the *LCC* calculation are likely to have a strong impact on the results. A large number of economic parameters (discussed in the previous section) are required for any economic analyses, including the P_1-P_2 method described above. In the distributable version of this model, these parameters are user inputs because the values for the economic parameters will vary substantially depending on location and application. However, for simulations run within the current study, the economic parameters are fixed at a set of nominal values (which also provide the default value for the user distributable) in order to simplify the optimization. A sensitivity analysis does investigate the impact of varying some of these economic parameters; this study is discussed in Section 4.6.2. All of the required economic parameters are discussed below.

First Cost

In the HyGCHP model, C_E is the total first cost of the heat rejection devices, including both the ground heat exchanger and any supplemental device. It is assumed that the cost of the heat pumps, internal piping, and fluid loop pump is identical for any of the cases that are compared during an optimization (note that the size and therefore expense of these components is not included in the optimization). It is also assumed that installation costs are included in this first cost; therefore, the value of I in Eq. (43) is set to zero.

The first costs associated with the installation of a GHX can vary widely depending on location and these costs are shifting significantly over time as the use of GCHP systems gains acceptance. The first cost of a GHX ranges from $6-20 per foot of installed borehole (Kavanaugh, 1997 – adjusted to 2007 values for inflation); in systems measuring thousands of feet, this range represents a large uncertainty in the total first cost of the system. Therefore the first cost of the GHX is a user input in the distributable version of the HyGCHP model (entered

in terms of cost per foot of installed borehole); in the parametric study, the sensitivity of the results to the first cost of the GHX is investigated.

The first cost of the supplemental devices is determined from the R.S. Means Mechanical Cost Data guide (R.S. Means, 2006) in order to ensure that the costs are near the industry average and not tied to a specific manufacturer. The first costs taken from the R.S. Means Guide correspond to the fully installed cost of each device. Costs are provided over a range of sizes and these costs are normalized and curve fit for each device that is of interest to this project. For the dry fluid cooler, a nominal unit with 16-ton capacity has an installed cost (C_{DFC}) of \$4425; the cost for other sizes of *DFC* are represented by Eq. (47):

$$C_{DFC} = 4425\$\left(0.0354 f^2 + 0.720 f + 0.217\right) \tag{47}$$

where f is the normalized size factor (i.e., the ratio of the capacity to the nominal capacity, with f=1 corresponding the nominal size). Fluid cooler costs are only documented in R.S. Means up to a normalize size of f = 10 (i.e.,, 160 tons); however, the data over this range shows no signs of deviating from the trend given by Eq. (47). For all equipment other than the DFC, cost data (including maintenance data) are available which cover the entire range of equipment sizes that the component models are technically capable of representing (for these technical limits, see individual component descriptions).

For the cooling tower, a nominal unit was selected with a size of 10-ton tower; this unit has an installed cost (C_{CCCT}) of \$4500. The cost for other sizes of cooling towers is given by Eq.(48):

$$C_{CCCT} = 4500\$\left(-0.00210 f^2 + 0.288 f + 0.868\right) \tag{48}$$

where f is the ratio of the cooling tower size to the size of the nominal unit (10 ton).

For the boiler, a 122 MBH boiler unit was selected as the nominal unit; this unit has an installed cost (C_{boil}) of \$3825. The cost associated with other boiler sizes is given by Eq.(49):

$$C_{boil} = 3825\$\left(-0.00430 f^2 + 0.411 f + 0.692\right) \text{ if } f <= 31.20$$

$$C_{boil} = 3825\$\left(0.118 f + 5.64\right) \text{ if } f > 31.20 \quad (49)$$

There is an additional cost associated with the addition of propylene glycol to the HyGCHP system (see Section 3.3 for a discussion of fluids used in the model, including antifreeze). This cost includes both a first cost component related to the cost of the antifreeze as well as a maintenance cost component related to checking, draining, and replacing the antifreeze periodically. The first cost associated with propylene glycol is estimated to be \$0.12 per foot of borehole based on information provided on the Geothermal Bore Technologies website (GBT, 2007). This estimate is reasonable based on a calculation using the current price of propylene glycol and an estimation of borehole volume leading to a range of \$0.10 - \$0.16 per foot. A 30% additional cost is added to account for the volume of the indoor piping (also based on estimating the associated volume). Maintenance costs associated with checking the antifreeze (and replacing the solution every several years) are found in the R.S. Means Maintenance cost guide (Means, 2002). An estimate of 0.22 annual hours is listed as the combined annual time (on average) required for these tasks; this value is for a small system and is therefore doubled here. An estimate can be used because this cost is so small when compared to other maintenance costs that the *LCC* calculated for a system will be insensitive to the exact value of the maintenance cost associated with using propylene glycol. Finally, the cost of draining and replacing the propylene glycol solution every 10 years is included in the maintenance costs.

When simulating heating dominated systems, the hybrid boiler configuration uses the same boiler model and costs as the cooling dominated system. An additional cost function is

needed for the cost of the solar system. A nominal 38 ft^2 unit was selected; this unit has an installed cost (C_{coll}) of \$5096 including piping and pumps. The cost for other sizes of collector arrays is given by Eq.(50):

$$C_{coll} = 5096\$\left(0.135N_{coll} + 0.865\right) + C_{tnk} \tag{50}$$

where N_{coll} is the number of nominal collectors in the array and C_{tnk} is the first cost of the solar tank, which is given by Eq. (51):

$$C_{tnk} = 960\$(0.691f + 0.316) \tag{51}$$

where f is the ratio of the tank size to the size of the nominal unit (100 gallons).

Maintenance Costs

Maintenance costs are added to the operating cost (and subsequently C_{F1}) as shown in Eq. (45). The maintenance costs are calculated on an annual basis and added to the cumulative operating cost at the end of each year. Maintenance costs will only be included for the equipment that varies between different heat pump systems (e.g. HyGCHP and boiler/tower; this approach is consistent with the approach used to calculate the first cost). The equipment includes the GHX and exterior piping, for which no (or negligible) maintenance is needed, leaving the maintenance costs associated with the supplemental heating and cooling devices. The maintenance costs associated with this supplemental equipment are estimated using the R.S. Means guide. For cooling towers, an additional nominal maintenance cost is added to account for costs related to water treatment.

Maintenance costs from the R.S. Means guide are separated into annual maintenance and repair time, with wages specified for various types of labor (R.S. Means, 2002). Some additional cost is also listed for parts. The wage for general maintenance is taken to be \$46.05/hour. The annual maintenance and repair time for each device varies with device size; these times are first

multiplied by \$46.05/hour and then added to the annual parts cost before they are finally normalized and fit to a simple curve that represents each device (i.e., larger devices require more maintenance). The cost of replacing the supplemental devices is not included; it is assumed that each piece of equipment will last the 20-year length of the simulations. For the dry fluid cooler, it was found that a nominal 16-ton cooler has an annual maintenance cost (MC_{DFC}) of \$115; the cost associated with a dry fluid coolers with a different size is given by Eq. (52):

$$MC_{DFC} = 115\$\left(-0.00430 f^2 + 0.209 f + 0.796\right) \tag{52}$$

where f is the normalized size of the cooler. For the cooling tower, a nominal 10-ton tower had an annual maintenance cost (MC_{CCCT}) of \$290; the cost for other sizes of cooling towers is given by Eq. (53):

$$MC_{CCCT} = 290\$\left(-1E-5 f^2 + 0.055 f + 1.059\right) \tag{53}$$

where f is the normalized size of the cooling tower. For the boiler, a nominal 122 MBH boiler had an annual maintenance cost (MC_{boil}) of \$759; the cost of other sizes of boilers is given by Eq. (54):

$$MC_{boil} = 759\$\left(-0.0009 f^2 + 0.0648 f + 0.952\right) \text{ if } f <= 11$$

$$MC_{boil} = 759\$\left(0.0196 f + 1.367\right) \text{ if } f > 11 \tag{54}$$

where f is the normalized size of the boiler. For the solar system, a system with a nominal 38 ft^2 collector has an annual maintenance cost (MC_{coll}) of \$759; the cost for systems with other array sizes is given by Eq.(55)

$$MC_{coll} = 438\$\left(0.105 N_{coll} + 0.895\right) \text{ if } f > 11 \tag{55}$$

where N_{coll} is the number of nominal collectors in the array.

Electricity Costs

The cost of electricity is included in the fuel cost and therefore is part of C_{F1} in Eq. (45). There are two components to the monthly cost of electricity: a usage charge and a demand charge. The demand charge is calculated based on the monthly peak power consumption of the system (the TRNSYS periodic integrator is used to find this maximum power during each month). This maximum power is multiplied by the marginal power demand charge associated with the location being studied. The monthly demand cost is then added to the electricity cost at the end of each month (using a TRNSYS forcing function). The usage charge is the sum of the total electrical energy consumption during each timestep multiplied by the marginal cost of electricity (which may change according to time-of-day rate structures).

Both of the demand and usage electricity costs depend on the total power consumption predicted by the HyGCHP system model. The power consumption associated with each component is added at each timestep in order to determine the total power consumption; this includes the power that is consumed by the supplemental heating and cooling devices (e.g., to run the fans, pumps, and motors that are associated with these devices), the fluid loop pump power (which is based on pressure drop in the system, as discussed in the pump component description), and all heat pumps.

Electric rates (and energy rates in general) vary widely throughout the country; therefore, electric rates and demand charges are user inputs for the distributable program, and the sensitivity of the results to these parameters is studied in this report. In order to determine a reasonable range of electricity cost parameters and establish a meaningful baseline set of parameters, a survey of the electric rate structures around the nation was carried out. To assure a representative sample, electric rates (for commercial customers) have been obtained from

electricity providers in five different regions of the contiguous United States: East Coast, West Coast, Gulf Coast/South, Midwest, and Mountain; the demand charge and usage charge parameters are summarized in Figure 38. Note that usage charge in many areas changes from peak to non-peak times of day; a time of day rate structure is an option in the HyGCHP model. The average rates are $0.101/kWh for on-peak usage (10 am – 9 pm), $0.063/kWh for off-peak usage, and $6.22/kW for demand; these are the default rates used for parametric study.

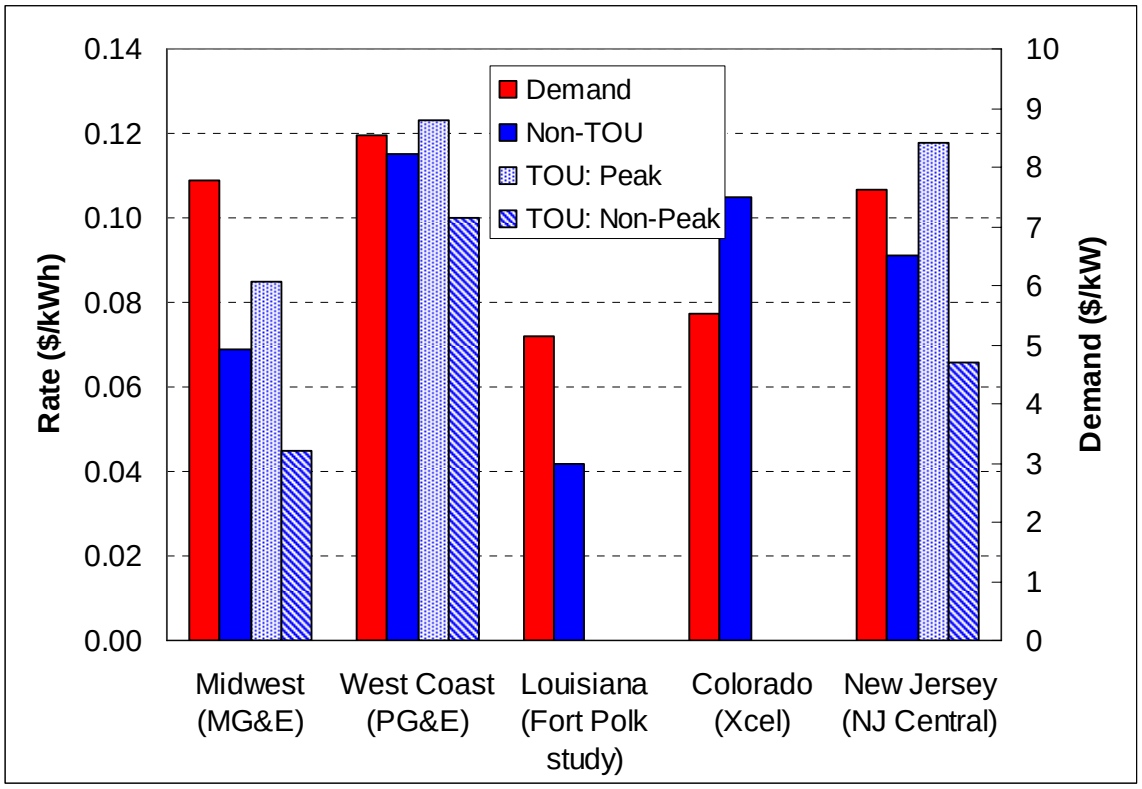

Figure 38. Electric rates (both demand and usage charges) in various regions of the United States. Sources are given below each region. Note that TOU indicates time of use rates.

Other Utility Costs

Electricity costs represent the largest portion of the fuel cost; however other utility costs such as gas and water are also make up a portion of the operating costs. Natural gas is needed for gas fired supplemental devices, specifically a boiler. The power (i.e., fuel) consumption is an output of the gas boiler component model. This power consumption is multiplied by the

marginal cost of natural gas, which is provided by the user. For the parametric studies, a nominal cost of $0.99/therm is used, based on the current natural gas prices in the Midwest. Because these prices vary across regions and by the season (as well as from year to year), the cost of natural gas is also included an input in the distributable version.

The cost related to water consumption is specifically required for cooling towers which require makeup water; the water used for cooling in the closed circuit cooling tower is lost by evaporation, drift (water carried away by air flow), and blow-down (bleeding of the tower sump to prevent mineral build-up). The calculation of these the makeup water consumption for this study are based on the methods used in the Fort Polk study (TESS, 2005). The Fort Polk study assumed that 0.01% of the spray water was consumed in drift (a value that is based on a literature review), evaporation consumption as calculated and reported by the cooling tower component model, and blow-down consumption is assumed to be equal to the evaporation rate (this assumption is based on data from Fort Polk maintenance records). Water cost is determined by multiplying the total water consumption by the price of water, which is the related both to the direct cost of water cost as well as sewer charges. Water cost information is generally provided on a per-cubic-foot-consumed basis. Water rates across the country have been investigated by surveying providers across the country; however, data on water costs is less easily attained than those for electricity. The cost of using water was approximately $\$1.40/m^3$ ($4 per 100 ft^3) for several cities in the United States and therefore this is the default water cost rate used in the model. The water cost is also a user input in the distributable program so that users in regions with particularly high water rates can include this in their design study.

All of these utility costs are included in fuel costs (and subsequently C_{F1}) as shown in Eq. (45).

Market Parameters

Market parameters such as discount rate and tax rates are key input parameters for any economic analysis. In the TNRSYS model, these types of parameters are used to calculate the P_1 and P_2 parameters used in Eq. (40). In the distributable version of the model, the user has control over all of the market parameters; this is necessary because market parameters can change significantly depending on the owner of the building, the region, and the economic health of the nation. The market parameters include:

- Number of years in the evaluation (N_e)
- Rate (m) and length (N_L) of mortgage/loan, and percentage paid up front (D)
- Income tax ($\overline{t}$) and local property tax rate (t)
- Whether or not expenses are tax deductible (c)
- Required discount rate (d)
- Rates of inflation; general (i) and fuel (i_F)
- Rebate fraction (R)
- Salvage (resale) fraction (R_v)

The sensitivity of the results to some of these parameters is discussed in this report. The initial strategy was to study a baseline case (which is discussed below) and then vary P_1 and P_2, separately, away from this baseline case in order to examine their impact. If the results showed a clear trend that could be expressed in terms of P_1 and P_2 then the impact of changing *any* of the market parameters could be extracted easily. The effect of changing any market parameter can be mapped onto an associated change in P_1 and/or P_2 and therefore the net result on the HyGCHP design can be understood without running additional simulations. However, as we will see in Section 4.6.2, the optimal design values show no clear trend across building/climate

types with regard to changing P_1 and P_2; therefore, this strategy did not provide useful results. Instead, some additional parametric studies on P_1 and P_2 were added to the simulation matrix.

The baseline case for the parametric study is chosen based largely on anecdotal evidence and national averages (where possible), with an additional goal of arriving at a good distribution of P_1-P_2 cases to use for the study. The simulations have been run for 20 years, which is a standard period of analysis in the geothermal industry. This period is also assumed to be the length of the loan for the system. The loan interest rate is assumed to be 6% in order to reflect typical national interest rates. A single baseline discount rate and down payment are more difficult to identify since these parameters depend strongly on the financial situation of the owner. The discount rate is set at 8.5%, based on the average cost of capital for organizations in sectors that typically use geothermal (financial, retail, etc.) (Value Line, 2006). The down payment is set at 30%.

The general inflation rate is identified in the annual Federal Energy Management Program report on economic indices; over the next two decades it is expected to average 1.6% (Rushing and Fuller, 2006). According to the same report, the cost of fuel during that time period is expected to keep pace with inflation (due in large part to an expected near term drop in fuel costs by FEMP). The income tax rate is assumed to be 35%, which is based on the federal rate for businesses, and the property tax rate is set at 3.0%, which is approximately the average in the United States. Resale and rebate values are set to zero, the installation cost fraction (I) and annual expenses ratio (M_s) are also fixed at zero (installation costs are included in the first cost and annual expenses are all handled by the P_1 term), and the number of years assumed for straight-line depreciation (N_D) is fixed at 4.55 years. This value of N_D results in straight-line depreciation that is equivalent to the IRS' current modified accelerated cost recovery system

(MACRS) depreciation method for 5-year assets. Geothermal systems are in the 5-year asset category in order to promote investment and defray risk; however, the actual systems last significantly longer than five years.

3.3 Additional Model Features

Some additional features and effects are included in the model in order to add to the accuracy and usability of the model; these are discussed below.

3.3.1 Weather

Weather information is required by the HyGCHP model to determine the temperature and humidity of the outside air, which interacts with several of the supplemental devices as well as the geothermal heat exchanger. Additionally, solar data are required for those configurations that include solar panels. The weather data used within the HyGCHP model is read from a TMY2 data file. These files are available for many cities in the US, and are compiled from the National Solar Radiation Data Base. The TMY2 data files contain hourly weather data (temperature, humidity, solar radiation, etc.) for a 'typical meteorological year' in the given location. Note that in the distributable program, weather must be supplied with the building load data files; this was done to assure that users did not use a different weather file for the building loads than they use for the simulation.

3.3.2 Thermal Inertia: Input Recall Device

In any water-based heat pump system, there is a significant amount of thermal capacity associated with the water side of the system. This thermal capacity causes heat inputs (and outputs) to change the loop temperature over several minutes instead of a few seconds, giving the fluid temperature some thermal 'inertia'. It is important to include this inertia in the simulation model in order to yield realistic results; this is particularly true since one of the key constraints

on the system are limits placed on the instantaneous value of the water entering the heat pump system. The thermal inertia has the additional practical advantage of allowing the system equations and controller algorithm to converge to a physical solution more easily at each time step. Without any thermal inertia, the controller – which diverts the water to the various devices as necessary – has difficulty converging to a control decision because its choice of outputs affects the water temperature in the current time step, which also happens to be the basis of the controller input.

In a transient, explicit simulation such as the HyGCHP model, consistent and robust convergence requires a minimum amount of thermal capacity that is equivalent to the amount of water that can flow through the system in one time step. This amount of inertia creates sufficient separation between changes in the water temperature (i.e., the input to the decision process) and control of the equipment (i.e., actions resulting from the decision process). There are several components in TRNSYS that can simulate this thermal inertia: a simple pipe model, a tank, or the input recall device (Type 93). Type 93 saves the value of fluid temperature (upstream of the heat pumps) for one full time step before passing it on to the heat pumps during the subsequent time step. All of these methods for simulating thermal inertia were implemented in the HyGCHP model and tested with two objectives in mind: accuracy and computational speed. In these comparisons, computational speed is affected by both the ability of the system to converge at each time step as well as the additional computation time required by the thermal inertia component.

After running a few simulations with each of the three components, it appeared that the tank and pipe model were identical in function for the purpose of simulating inertia (i.e., they both affected simulation results in exactly the same way), which was expected. Additionally,

both of these devices required considerably more computation time than the Type 93 input recall device (also expected, due to the relative simplicity of the Type 93). Another observation was that the pipe and Type 93 were not functionally equivalent and resulted in slightly different temperature and heat flow outputs during the course of a simulation. This difference was also expected and is due to the fact that, for any given time step, the pipe model and Type 93 simulate a different amount of thermal capacity. The pipe (and similarly the tank) are sized to hold enough fluid for one time step at the maximum flow rate that will occur during the simulation; therefore, the thermal inertia simulated by the pipe is fixed and does not change during the simulation. The Type 93 has the same effect as a pipe that holds the amount of flow used in each time step and therefore the thermal inertia simulated by the Type 93 varies during the simulation according to the flow rate in each time step. The most accurate model of the actual thermal inertia in the system is a pipe that is sized so that it contains the amount of water that is actually held in the GCHP system being simulated. However, this approach would dramatically increase the computational time associated with the simulation because (1) the pipe model is fundamentally slower than the Type 93 model and (2) the time step used in the simulation would need to be reduced to be consistent with the size of the pipe (on the order of a few minutes) in order to reliably converge. Therefore, a test was carried out in order to see if the results obtained using the Type 93 are sufficiently accurate for this project.

Tests were run for two different cases, the Atlanta continuous-occupancy building and the St. Louis retail building (see Section 4.2 for building descriptions). The volume of water that would fill the pipes in the geothermal field for each building was estimated. The time step that matched the inertia associated with the actual volume of water present in the buildings is about 7.5 minutes; this time step was used for the simulation.

For the St. Louis model, the amount of heat flow, power consumption, temperature, and most importantly, life-cycle cost, varied by less than 1% between the physically correct pipe model described above, and the much faster model with the input recall device and 30 minute time steps. This latter model is the approach used in the current HyGCHP model to generate the results presented in this report. For the Atlanta model, values for heat flow, power consumption, temperature, and most importantly, life-cycle cost, varied by 2-3% between the accurate pipe model described above, and the model using an input recall device with 30 minute time steps. The inertia in the current HyGCHP model (using Type 93 and 30 minute time steps) is therefore sufficient to represent an actual GCHP system.

3.3.3 Heat Pump Temperature Limits

When the fluid returning from the geothermal system is outside of the operating temperature range of the heat pump units, they will automatically shut off, leaving the building without cooling or heating. This problem would not occur in a viable system design, so it is necessary to prevent the optimizer from selecting a system design in which the heat pumps ever experience fluid temperatures outside set limits (high and low). These temperature limits may be based on the manufacturer's stated operating range or, more likely, the designer's experience (a system designer may elect to use a more narrow temperature range to protect against uncertainties in design and the occasional year of particularly severe weather). The choice of these temperature limits will be discussed in more detail in later sections.

In order to constrain the optimization process so that the heat pump temperature limits are not violated, a penalty function is applied during simulation relative to the heat pump entering fluid temperature. When the value of the entering fluid temperature ($T_{fl,in}$) is less than a lower temperature limit $T_{fl,min}$ or greater than a temperature limit $T_{fl,max}$, a large cost penalty is added to

the utility costs. If the entering fluid temperature is between these temperature limits then no additional cost is added. This additional cost is not real; it is used in order to constrain the optimization process and therefore ensure that the heat rejection and absorption equipment selected by the optimizer are large enough to meet the requirements of the heat pumps. The additional cost is prohibitive so that a system cannot be optimal if it violates these temperature limits for any time step. This technique assures that all optimized designs presented in the results of this study always operate with fluid temperatures between $T_{fl,min}$ and $T_{fl,max}$. The values of these limits were varied during parametric study in order to study the effects of fluid loop temperatures limits on energy consumption, cost, and performance. Section 4.4.3 discusses the impacts of changing these temperature limits. In the distributable program, these temperature limits can be modified by the user.

In an actual GCHP system, the heat pumps would trip out if the fluid temperature fell outside the manufacturer's values for these temperature limits, causing a considerable problem for both the tenants and operators of the building being conditioned (TESS, 2005). Therefore, the manufacturer's limits can be considered the absolute maximum and minimum setting for these values.

3.3.4 Propylene Glycol

Antifreeze must be added to HyGCHP systems if the loop encounters freezing or near-freezing temperatures during the year. One common antifreeze that is added to GCHP systems is propylene glycol, which has low environmental and safety risks while only increasing operating costs slightly (2%) over other antifreeze solutions (Heinonen et al., 1997). The HyGCHP model is therefore designed to run with either water or a propylene glycol solution as the simulated working fluid. The concentration of propylene glycol is set based on the minimum temperature

expected in the system (with a goal of preventing freezing at this temperature); this minimum expected temperature is specified and the HyGCHP model calculates the associated concentration that avoids freezing.

The fluid properties for the specified working fluid are passed to each of the component models that require fluid properties (propylene glycol properties are based on Melinder, 1997; see below). For example, the pressure drop calculations require fluid density and viscosity; these properties are calculated based on the fluid type and temperature during simulation. Additionally, all component models in the fluid loop require both fluid density and specific heat capacity in order to calculate heat transfer characteristics. Other than viscosity, these parameters cannot be changed during simulation; therefore, these properties are calculated based on average temperatures. Note that both specific heat and density are only weakly dependent on temperature in the temperature range of interest (see Figure 39); a constant, average value is therefore reasonable. Viscosity on the other hand, *is* heavily dependent on temperature. The only calculation in the model that requires viscosity is pressure drop, and the component that calculates pressure drop is able to modify the viscosity for changes in temperature at each timestep.

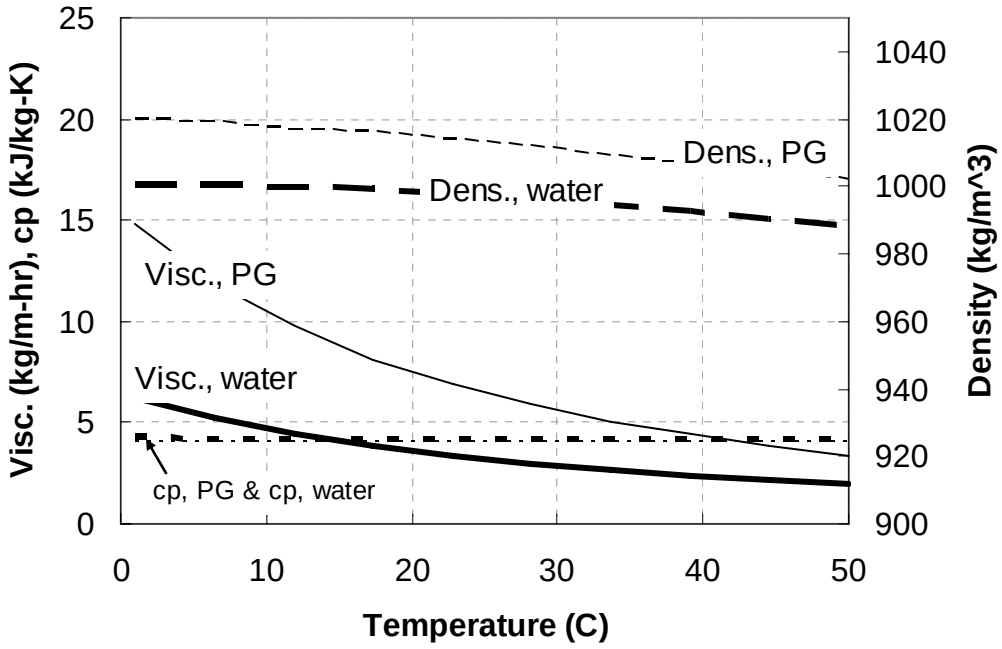

Figure 39. Properties of water and 20% propylene glycol / water solution (PG). Note that viscosity is the only property that depends significantly on temperature.

An additional study was carried out in order to determine which parametric study cases should use propylene glycol as the default working fluid and which should use water (in the distributable program, this decision is made by the user). It is assumed in the heating dominated cases that ambient temperatures are cold enough to warrant inclusion of antifreeze. For the cooling dominated buildings, however, further analysis is needed. These buildings were studied both with and without antifreeze for the main configurations (boiler/tower, geothermal, and hybrid). In the boiler/tower configuration, the boiler is typically operated often enough to prevent the fluid from dropping below 39^{o}F, eliminating the need for antifreeze. Similarly in the geothermal-only configuration, the geothermal loop is sized for cooling and therefore keeps the fluid temperature warm enough in the winter to avoid needing antifreeze. There were some cases (in more moderate climates) in which the geothermal-only case did not keep the temperature sufficiently above freezing; the parametric study was then re-run for these cases with a propylene glycol solution. In the hybrid system configurations, fluid temperatures often

drop below 32°F since all heating is done by the bore field. Therefore, antifreeze is used for hybrid configurations. As the parametric study progressed, these general trends held for most cases that were considered.

3.4 Optimization

In order to determine what the optimal HyGCHP system is for any given building/climate/economic scenario, there are a number of different independent design parameters that can be selected for optimization. These include the design variables listed below (for a hybrid configuration using a cooling tower):

- Ground heat exchanger (total borehole) length (**GHX**)
- Cooling tower size (**Tower size**)
- Cooling tower control set point; the difference between working fluid and ambient temperature at which to activate the cooling tower in cooling mode (ΔT_1)
- GHX control set points (T_{Cool2} – the temperature at which to activate the GHX in cooling mode, T_{Heat1} – the temperature at which to activate the GHX in heating mode).

Due to the large design variable space and the wide array of scenarios that must be studied, the use of a computerized optimization algorithm is the only practical way to accomplish the objectives of this project. The software TRNOPT is packaged with TRNSYS; TRNOPT interfaces TRNSYS with the optimization package GENOPT (Wetter, 2007). GENOPT is a general optimization tool that was developed at Lawrence Berkeley National Laboratory and is freely distributed.

The typical design parameters adjusted during optimization are the equipment sizes and control set points listed above. The optimal design of a HyGCHP system therefore corresponds

to the values of these parameters that result in a minimum life cycle cost (*LCC*) for a given scenario. This design is identified by running an initial TRNSYS simulation and calculating a *LCC*, then allowing GENOPT to change the parameters (in some intelligent direction, decided by the algorithm) after which the simulation is run again; this process is repeated many times until the GENOPT algorithm is satisfied that a minimum *LCC* has been identified. This iteration process is facilitated by the TRNOPT interface which initializes the optimization parameters in both TRNSYS and GENOPT and establishes the links between these two programs (see Figure 40).

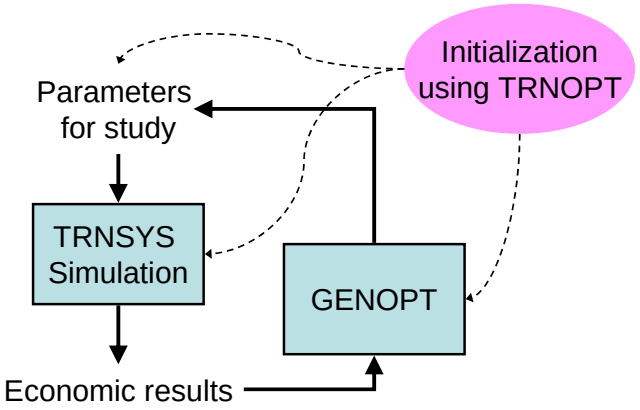

Figure 40. A flowchart depiction of the optimization cycle using TRNSYS and GENOPT, with the TRNOPT interface used to initialize the cycle.

As the parametric study progressed, an additional program was added to run multiple optimizations successively, allowing batch runs of several optimizations without any user input. The optimization sequence was modified further for the distributable program; in this case TRNOPT was eliminated and a direct communication is established between the HyGCHP model and GenOpt.

Prior to using the optimizer for the parametric studies, the model settings were checked in order to ensure that the individual simulations were running with as little computational time as possible (while maintaining appropriate accuracy). Dozens of simulations are required to

accomplish a single optimization and therefore tens of thousands of simulations must be run in order to accomplish the complete parametric study; therefore, even some small improvement in model speed results in a substantial saving in time. With a faster model, more parametric studies could be concluded, distributable versions would be more convenient to use, etc. For example, the current version of the model runs in a few minutes on a new PC, resulting in optimizations that take a few hours. If this optimization time were cut significantly, it would be of great benefit to the research and make design more feasible with the distributable version of the program.

Order of Components. The first step in speeding up the simulation was to optimize the order in which the components in TRNSYS are solved. This order is adjustable in TRNSYS, and it is most efficient to solve the components in the same order that the working fluid flows through the system. All input equations that are not dependent on the working fluid (such as those defining occupancy, building load, weather, etc.) are solved first, followed by the controller, and then each component from upstream to downstream, starting at the heat pumps. Finally, all economic calculations and output components (integration and printing components) are solved. Optimizing the order reduced computational time significantly – by about 40% compared with the default order that was pre-determined by TRNSYS.

Selection of Optimized Control Setpoints. The impact of the control set points were also studied in an initial set of parametric runs in order to determine if optimization was required for all of them (i.e., are there some set points that are not significantly changed based on operating parameters?). It is observed that T_{Cool1}, the fluid temperature at which the supplemental device switches from low speed to high speed operation (controlled speed includes both fan speed and flow rate), remains roughly constant for all of the optimized building/climate

scenarios when using the cooling tower. The set point T_{Cool1} was always optimized to be between 99°F and 105°F, or 4 - 10°F above the input temperature limit for the heat pumps in these scenarios. The high speed setting on the cooling tower is therefore typically only used when the fluid is near the high temperature limit of the heat pumps. The T_{Cool1} control set point is therefore set to 6.5°F above the input temperature limit for all cooling tower scenarios in the parametric study. A dry fluid cooler is also studied here (though not as heavily), but the same relationship does not hold true for that equipment; optimal values of T_{Cool1} will therefore be studied for the dry fluid cooler.

Simulation timestep. The initial timestep choice for the HyGSHP model was 15 minutes. This was on the same order of magnitude as the thermal inertia of the fluid system, and had a good balance of accuracy and computational speed. Testing was done to determine whether this timestep could be increased to speed up the model. In a couple scenarios, the heat flows and energy consumption values changed by about 2% when changing from 15 to 30 minutes. When going to 60 minutes, the inaccuracy was closer to 10%. The conclusion of this study was to use 30 minute time steps, as 2% error is acceptable in this type of model.

Optimization algorithm parameters. The Hooke-Jeeves optimization algorithm is used to optimize the HyGSHP model. The algorithm was researched in more depth. The key conclusion of this study was that the number of step size cuts (m) could be reduced.

The optimizer begins with a base step size (this is different than timestep sizes, which are in the simulation, not the optimization). As the optimizer nears the minimum, it narrows down the size of these steps until it reaches the desired precision (discussed above). The number of times this step size is cut (m) was reduced from 4 to 2, resulting in faster optimization (Wetter, 2007). Because the final precision of the optimization variables was already set to its maximum,

the choice of *m* was based largely on getting an initial step size that was large enough to reach the optimal area quickly. Tests were run on several models to assure no change in the accuracy of optimization. Computation time was also tested, and the value of *m*=2 reduced this time significantly (26% in one model). In addition to speeding up the model, this adjustment also created a lower likelihood of the algorithm ending in local minima of life cycle cost.

Extrapolation of cost streams. In a typical energy simulation, life-cycle cost is determined by calculating economic results based on one typical year. Geothermal models, however, change from year to year due to the change in temperature of the ground in and near the GHX (due to the imbalance of heating and cooling loads in the building). The model is therefore run for multiple years to accurately represent operating costs over time, which increase or decrease proportionately to this temperature change. Therefore, if the long-term temperature change can be accurately predicted, the future costs may also be predicted, allowing the simulation to model only the first few years of system operation, and predict the results of the remaining years. This theory was tested with the objective of reducing simulation time by well over half.

The cost results were plotted for several building and climate scenarios; all showed results similar to those in Figure 41. Costs for both consumption (of water and electricity) and demand (demand charge for electricity, based on the peak kW used by the building each month) increased roughly logarithmically with time. This corresponds to the observed increase in operating temperature; this can be seen by the maximum entering fluid temperature plotted in Figure 42. It is also important to accurately predict the maximum or minimum operating temperature – depending on whether operating temperatures are increasing or decreasing – to determine if the system will violate the heat pump's temperature limits (see 'Optimization'

above). These costs and temperature trends are shown below for a specific building, but all other simulated systems showed a similar pattern of results.

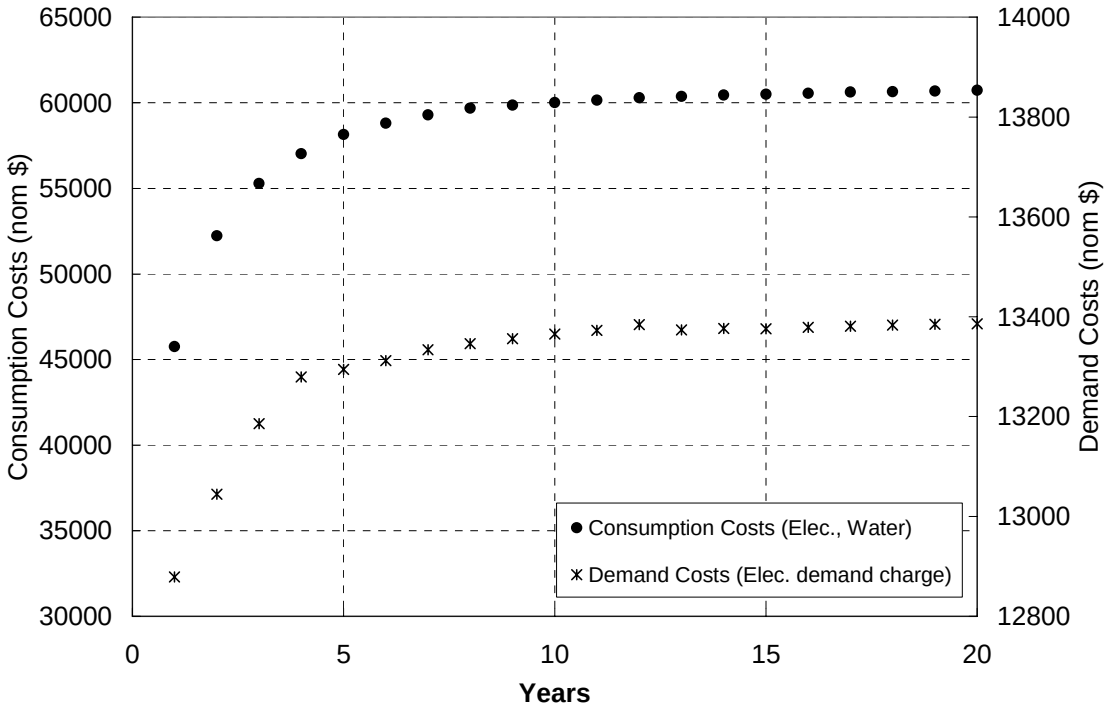

Figure 41. Annual costs of operating a hybrid ground-coupled heat pump system as a function of time (results are for an retail building in Atlanta).

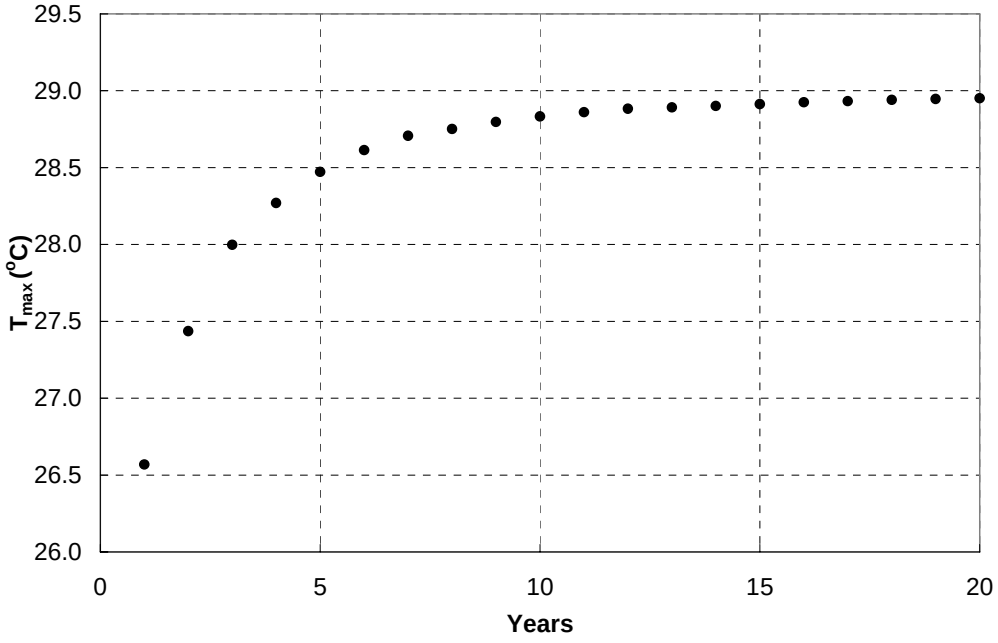

Figure 42. Increase in maximum operating temperature of the hybrid geothermal heat pump system with time.

Extrapolation is the most straightforward method of predicting the operating costs and temperatures of these systems. A few years would need to be simulated in order to extrapolate these values over 20 years. A basic equation form was postulated to represent the results:

$$Cost = A + Bt - C\exp\left(\frac{-t}{D}\right) - E\exp\left(\frac{-t}{F}\right) - \ldots \quad (56)$$

This assumes that the data will eventually decay to a linear equation, which has been found to generally be true. Additionally, it was found that data could be predicted with reasonable accuracy (a couple percent) by only expanding the equation to the first exponential term (all coefficients beyond *D* could be zero). Therefore, to predict the life-cycle cost of the system, the coefficients in the following equations would be required:

$$Cost_{Consumption} = A_1 + B_1 t - C_1 \exp\left(\frac{-t}{D_1}\right)$$
$$Cost_{Demand} = A_2 + B_2 t - C_2 \exp\left(\frac{-t}{D_2}\right) \quad (57)$$
$$T_{\min/\max} = A_3 + B_3 t - C_3 \exp\left(\frac{-t}{D_3}\right)$$

These coefficients would need to be predicted based on results from a shortened simulation, running from t=0 to t=N, where N is the shortest length of time that will allow for an accurate prediction of results. The slope of the linear portion of the costs (coefficient B) proved difficult to solve or regress correctly with only the first few years of data, because the function does not generally become near-linear until the latter half of the simulation. Therefore, B is first estimated based on $\Delta Cost$ from year 1 to year N, according to:

$$B_1 = \beta_1 (Cost_{Consumption,N} - Cost_{Consumption,1}) \quad (58)$$

and similarly for B_2 and B_3, where β is a constant. A study of dozens of simulations yielded constants of β_1=0.015, β_2=0.033, β_3=0.025.

With three more coefficients to be determined for each equation, it was decided that it would be most computationally efficient to solve for the three unknowns with three data points, rather than attempting to regress each equation from several years of data. An algorithm was developed using a type of successive substitution to solve each of the equations. This algorithm is demonstrated here with a solution of T_{max}. Three data points from the simulation results are used in this solution, based on three early simulation years (though not necessarily years 1, 2, and 3).

First, each data point was modified to subtract the slope of the linear component, which is the previously-estimated B_3 (as shown in equation (58)); for each data point *i* the following then applies:

$$T_{\max,\mathrm{mod},i} = A_3 - C_3 \exp\left(\frac{-t_i}{D_3}\right) \text{ for i=1..3} \tag{59}$$

Two values of A were then guessed:

$$\begin{aligned} A_{low} &= \max(T_{\max,\mathrm{mod},1}, T_{\max,\mathrm{mod},2}, T_{\max,\mathrm{mod},3}) + 0.1 \\ A_{high} &= 1.5 A_{low} \end{aligned} \tag{60}$$

Values for C_3 and D_3 were then calculated based on A_{low} and then based on A_{high}, according to the algebraic solution of equation set (59); the solution based on A_{low} is demonstrated here:

$$\begin{aligned} C &= \frac{A_{low} - T_2}{\exp\left(\frac{-t_2}{D}\right)} \\ D &= \frac{t_2 - t_1}{\ln(A_{low} - T_1) - \ln(A_{low} - T_2)} \\ A_{new} &= T_3 + C \exp\left(\frac{-t_3}{D}\right) \end{aligned} \tag{61}$$

If A_{new} is greater than the midpoint between A_{low} and A_{high}, then A_{low} is set equal to that midpoint; if A_{new} is less than the midpoint, A_{high} is set equal that midpoint. The process is repeated until A_{low} and A_{high} converge; then A, C, and D have been determined.

As mentioned above, this process can be completed using any three data points. It is desirable to simulate as few years as possible, but in order to achieve prediction error of only a couple percent, 6-7 years of simulation are required, with the third data point being the final year. The life-cycle cost is then determined using the actual simulation results, with the remaining years being predicted with the method above.

3.4.1 Optimization Parameter Sensitivity

One final speed improvement involved a significant study to determine the sensitivity of the results to each of the design parameters. This study was carried out by varying each of the optimized design parameters and evaluating the associated impact on the figure of merit - the life-cycle savings (LCS) of the HyGCHP system (relative to a constant cost of a base case boiler/tower system). Such a study allows for a comparison of the sensitivity of optimized parameters with the precision settings in the optimization algorithm. Adjustments can be made to speed up optimization by lowering precision if allowable. A second result of this study is a better understanding of the dependence of overall cost on each of the optimized parameters, in order to identify the most important of these parameters.

To accomplish these goals, two specific hybrid geothermal (with cooling towers) scenarios are chosen and optimized. The optimized values are then varied one at a time to 'map' out the solution surface near the optimal point. Both the magnitude of the variation and the resulting impact on life cycle savings (*LCS)* are plotted in the figures below. Figure 43 and Figure 44 show the sensitivity of the *LCS* of a hybrid system over a conventional boiler/tower (reported in terms of the % change in the life cycle savings), for a retail building in Salt Lake City. Figure 45 and Figure 46 show the sensitivities for a hybrid system in an Atlanta school building (note that the axes scales are consistent in all four plots in order to allow for easy comparisons).

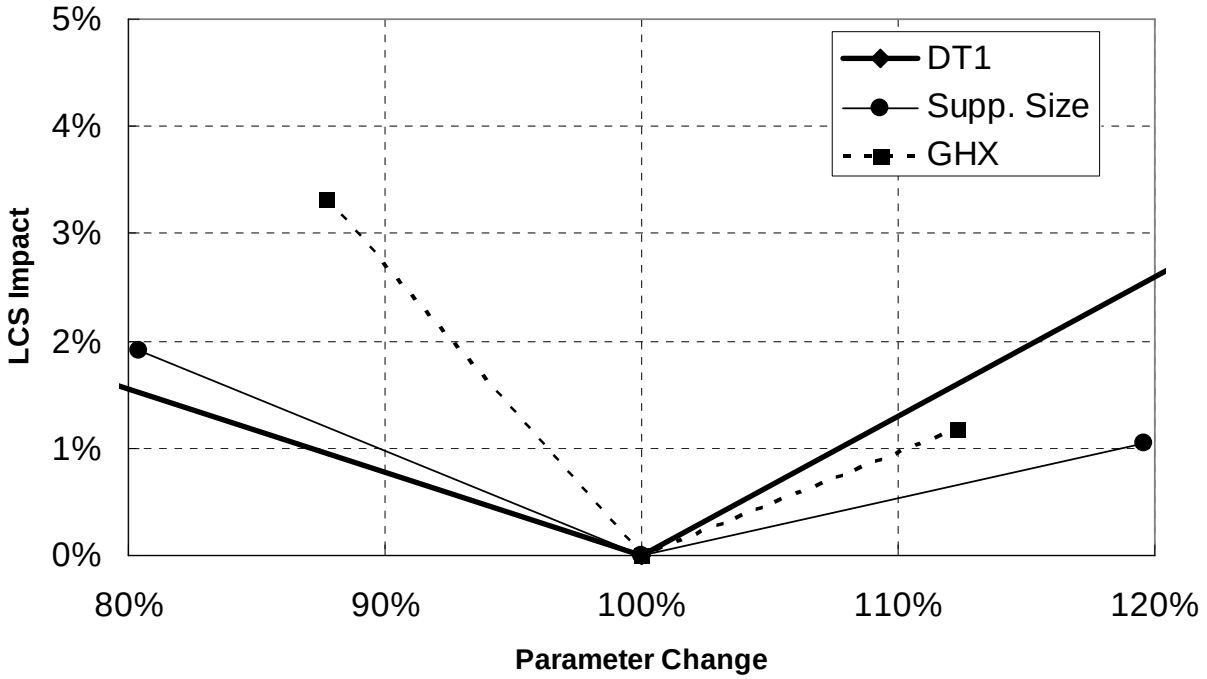

Figure 43. Sensitivities to optimized values: GHX length, supplemental size, and control setpoint of the supplemental device (DT1). Results are from the retail building, Salt Lake City climate.

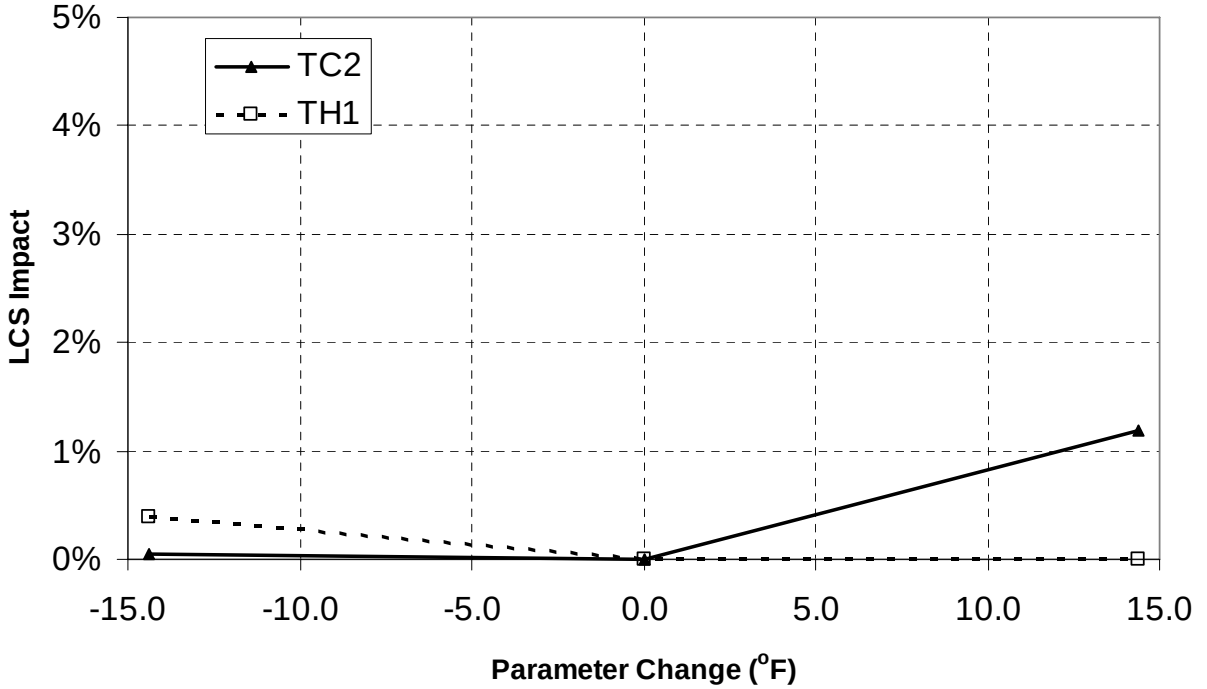

Figure 44. Sensitivities to optimized values: T_{Cool2} (GHX control setpoint for cooling) and T_{Heat1} (GHX control setpoint for heating). Results are from the retail building, Salt Lake City climate.

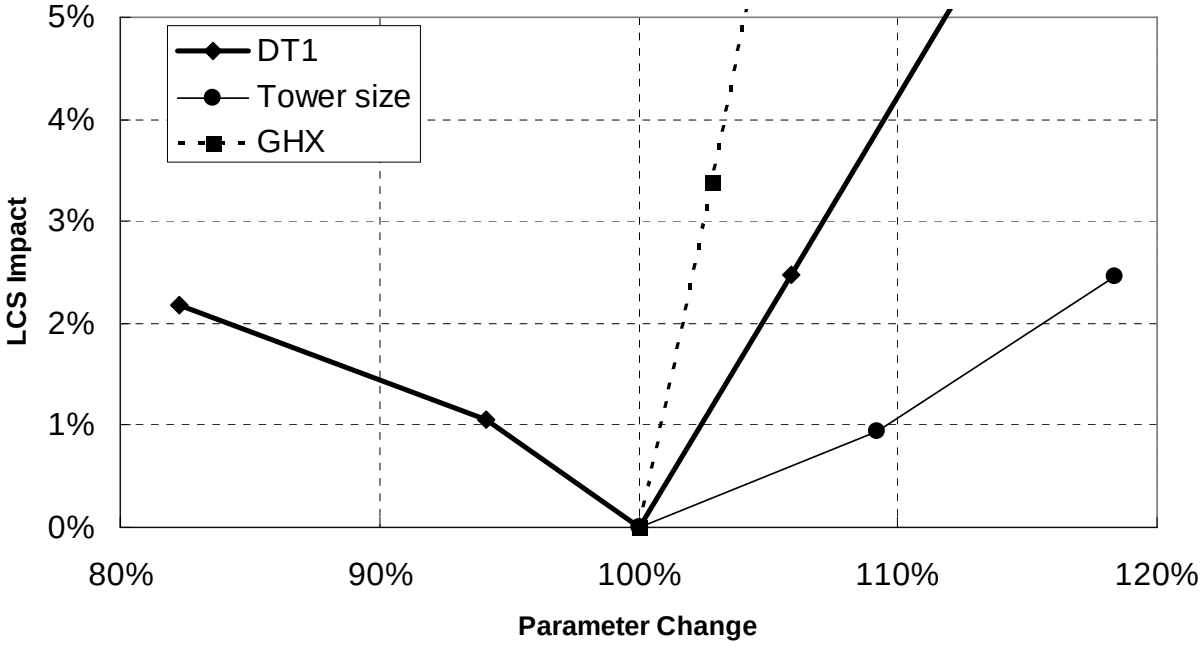

Figure 45. Sensitivities to optimized values: GHX length, supplemental size, and control setpoint of the supplemental device. GHX length and cooling tower size are not simulated below 100% because the heat pump temperature limit would be violated for this case. Results are from the school building, Atlanta climate.

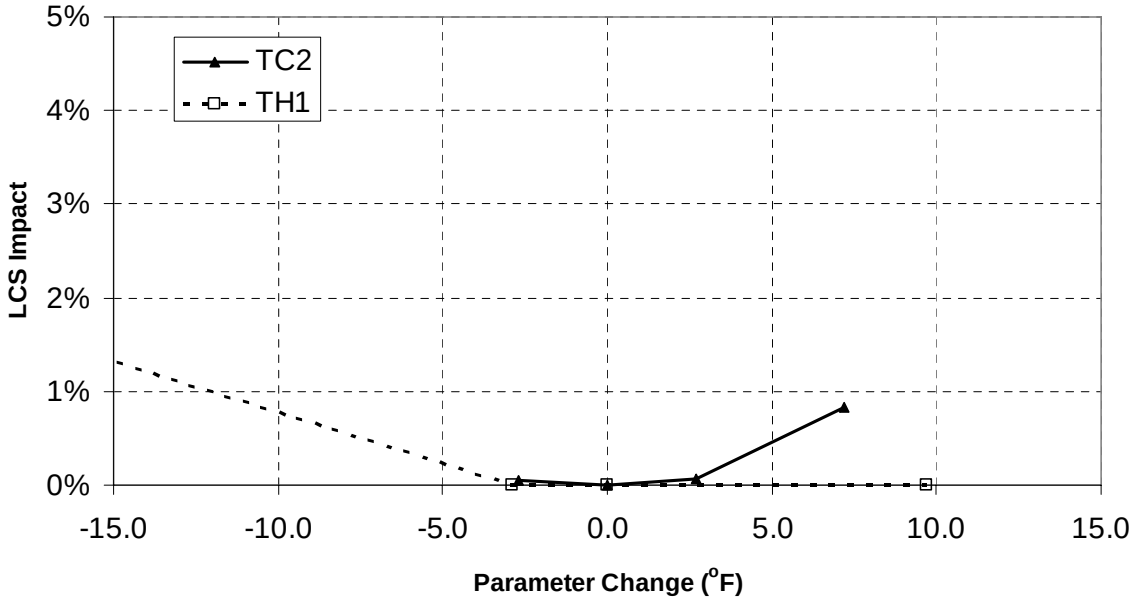

Figure 46. Sensitivities to optimized values: T_{Cool2} (GHX control setpoint for cooling) and T_{Heat1} (GHX control setpoint for heating). Results are from the school building, Atlanta climate.

It is apparent from Figure 44 and Figure 46 that the control set points, T_{Cool2} and T_{Heat1}, have a relatively small effect on the *LCS* of the system. This observation provides insight into some of the results regarding optimal control sequences; in several cases, small changes in the system configuration have led to large differences in the optimized set points, T_{Cool2} and T_{Heat1}. The impact of these control set points is still sufficiently large (and their values sufficiently different for various climates and buildings) in order to warrant keeping them in the optimization algorithm; however, the precision associated with their optimal value can be 'coarser' than the other parameters such as ΔT_1 and the GHX length which (according to Figure 43 and Figure 45) have a large impact on *LCS*. Notice that the impact of the cooling tower size is somewhere between these two extremes. A non-hybrid geothermal system showed even less *LCS* sensitivity to the various parameters and a similar relationship between relative magnitudes of the impact of the parameters.

The magnitude of each parameter on the *LCS* can be compared to the precision with which they are controlled in the optimization algorithm. Precision of the optimization is then adjusted in order to increase computational speed and still make *LCC* comparisons with reasonable resolution. The levels of precision used in this study (resulting from the fastest optimization settings) are listed below (percentages are given for the Salt Lake City example):

- GHX length: 300 ft (3%, also ~1 bore)
- Tower size: 4 tons (3%)
- ΔT_1 control setpoint: 0.9 ^{o}F (2%)
- T_{Cool2} control setpoint: 1.4 ^{o}F
- T_{Heat1} control setpoint: 1.4 ^{o}F

Because these settings are small relative to their *LCS* impact (i.e., in Figure 43 through Figure 46, these values all yield *LCS* differences of less than 1%), the optimization settings are acceptable. These sensitivity results will also be valuable in analyzing parametric results; the relative sensitivity of the economics to each parameter will help understand why the optimized values differ between various scenarios.

3.4.2 Potential Computational Speed Improvements

After the studies discussed in the previous sections, potential still remained for improvement in computational speed. The following potential ideas either did not yield significant results or remain to be attempted in future work.

Faster optimization algorithm. With the knowledge that Hooke-Jeeves is a fairly simple optimization algorithm, several other algorithms were tested. These included Armijio, Coordinate Search, and Nelder. Hooke-Jeeves was as fast as any of the other algorithms. Methods such as Particle Swarm and Hybrid did not work for this particular type of optimization (see Wetter, 2007 for more details).

Choosing good starting values. The possibility of speeding up optimization by choosing starting values that are closer to optimal was considered. The starting values for the optimization parameters were varied, but it was found that even starting with values that are exactly equal to the optimal values resulted in only a small reduction in optimization time and starting with values that are very near the optimum barely affected the optimization time at all. This result demonstrates that improving the starting values does not provide a viable method for decreasing run-time; the result also shows that the optimizer is likely doing a reasonably thorough search of the parameter space regardless of the initial conditions selected by the user.

GHX component model. Using a faster ground heat exchanger model would speed up the TRNSYS model. The ground heat exchanger model takes significantly more computation time than any other model component during a simulation (though it does not take a majority of the computation time), so it was considered most heavily for substitution. After studying some possible models to substitute for the DST and discussing the issue with TESS, no changes were made. The component model being used (Type 557) is the fastest of its kind for anything close to the degree of accuracy being considered.

Seasonal modeling. It may be possible to simulate a year of building operation by only running the model for a few 'typical' weeks, then extrapolating energy flows and temperature changes to approximate a full year of operation. This method is a possibility, but there is likely too much difficulty in choosing the representative weeks for this approximation.

Extrapolation of ground temperature. This idea was based on the fact that the annual energy input or output of the ground is the constant. The TRNSYS GHX component (DST model) models the ground as a radially symmetrical two-dimensional grid of temperatures. If the changes in this grid over time could be predicted based on one or two years of simulation, the modeling time could be reduced by an order of magnitude. This method has potential, though it would require a thorough study to assure accuracy (outside the scope of the current project), and would require modification of the ground model. This is possibly a good area for future research.

Different Method of Parametric Study. Another method considered for decreasing the computation time of the parametric study was to store the electricity, gas, and water consumption results for each time step, for every simulation in each scenario (building/climate) optimization (there are anywhere from 50-200 simulations run per optimization). Because the economic

variables do not affect these power consumption results, saving the data from these runs might allow their corresponding *LCC* results to be mapped against the non-economic inputs (e.g., bore field length, supplemental unit size, control set-points, etc.). This could potentially form the basis of a curve-fit based model that can be used to quickly optimize a particular climate/building situation for any given set of economic parameters. However, it was decided not to utilize this strategy because each optimization only explores a small fraction of the possible optimization parameter combinations (ground heat exchanger (GHX) size, control setpoints, etc.) with the resolution needed to choose an optimal design. For example, for a given building/climate scenario, the GHX size is widely explored with coarse resolution, but is then narrowed down to a specific range before any of the control set points are (see Figure 47). As a result, one optimization run only maps a very small portion of the possible GHX sizes. Economic studies on this data would be restricted to that small number of GHX sizes.

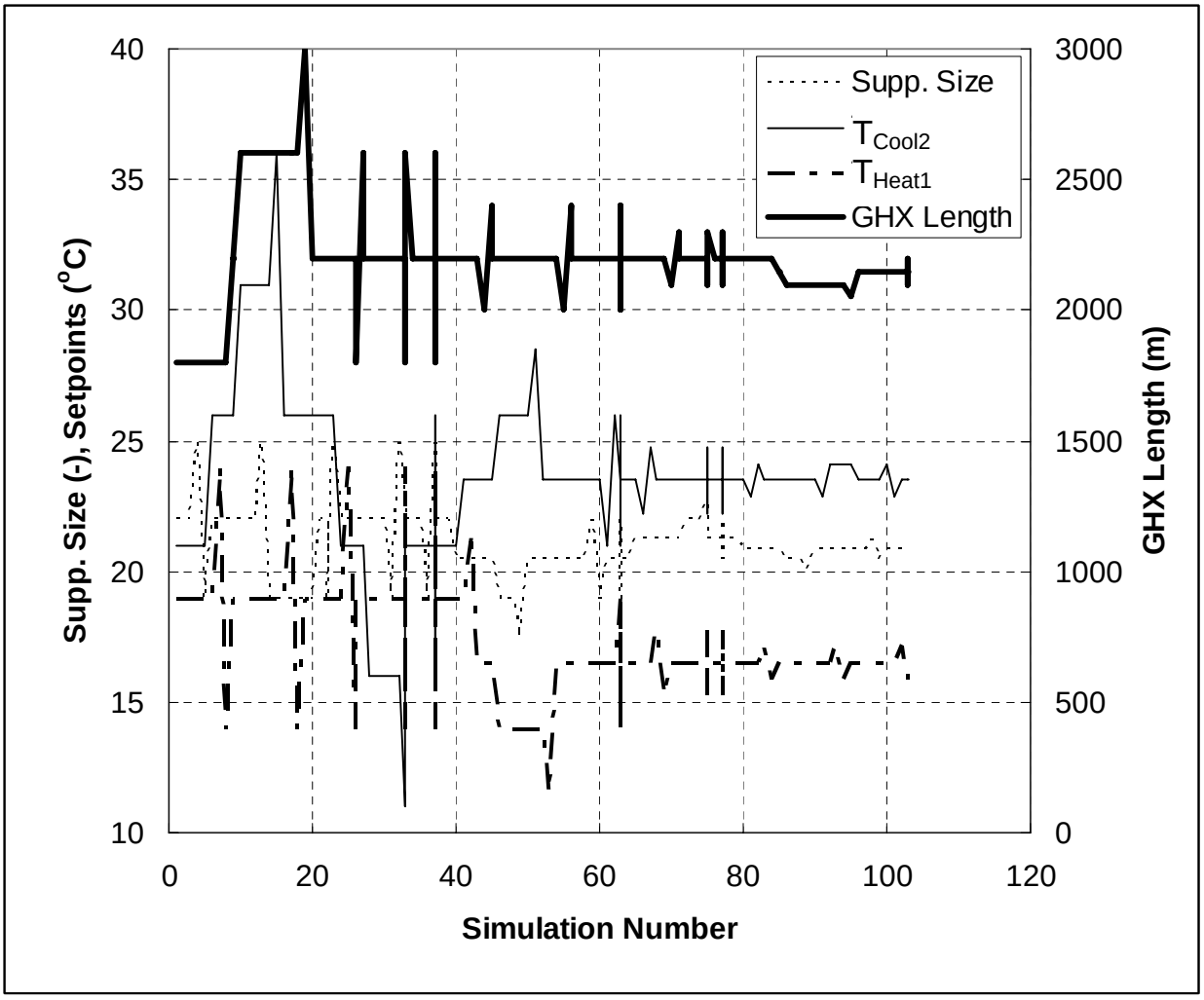

Figure 47. Optimization parameters as a function of simulation number during one optimization (for one building/climate scenario). T_{Cool2} and T_{Heat1} are control setpoints being optimized, the other two optimized variables are the equipment sizes.

3.5 Validation

Many informal tests were conducted during the development of the HyGCHP model. With each new component added, the model is run using different building loads and weather conditions in order to check that the results are reasonable (i.e., the temperatures are changing in the correct direction, power consumption was at the correct order of magnitude, etc.). These tests assure that the components are linked correctly in the model. Each existing TRNSYS component has also been independently validated as part of its development process. For

example, as mentioned in the GHX model description, several studies have been done that show that the GHX component model matches experimental data (for example Shonder et al., 1999).

A second level of testing was carried out upon completion of the initial system model. The similarities between this study and the Fort Polk study (TESS, 2005) made a comparison between these simulations convenient. The building loads (summed into one total load) and weather data used in the Fort Polk study were linked to the model, the optimization values were set equal to the Fort Polk study inputs, and a 20-year simulation was run (using the closed circuit cooling tower). The *LCC* calculated using the HyGCHP model was $51,806, only about 2% more than the Fort Polk study (TESS, 2005) result for the GHX and closed circuit cooling tower ($50,840). The observed temperatures were a couple degrees higher than the Fort Polk study due to the changes in heat pump model; recall that the heat pump model was changed so that the temperature difference was held constant during any time step while the flow rate is varied to match load. However, even with this change the fluid carries a similar magnitude of energy through the fluid loop, and therefore results in only a small difference in the demand charge and a negligible difference between all other costs.

After optimization was added to the model, optimal design parameters could be generated to compare with other design tools. All typical industry design tools output the required GHX length for a given building, so it is useful to compare this design parameter between HyGCHP and a commonly used industry tool. In this case the comparison is done with the GCHPCalc software (Kavanaugh, 1997). This software calculates GHX lengths analytically, using G-functions as described in the ASHRAE handbook's method (ASHRAE, 2003). The results of this comparison are shown in Figure 49 for three different building/climate pairs. These results represent a heating-constrained GHX with a 35^{o}F minimum entering water temperature (the

results section will demonstrate that most optimal HyGCHP GHXs are sized based on the heating loads). Note that the cases have an average difference of 7%, with a maximum difference of 17%. It is accepted that there is inherent differences in the modeling of GHXs in the two tools (in fact, the GHX model in TRNSYS is often considered a benchmark for these other design tools), so this comparison only goes to show that the rest of the system model, as well as the entire optimization process, arrive at reasonable results.

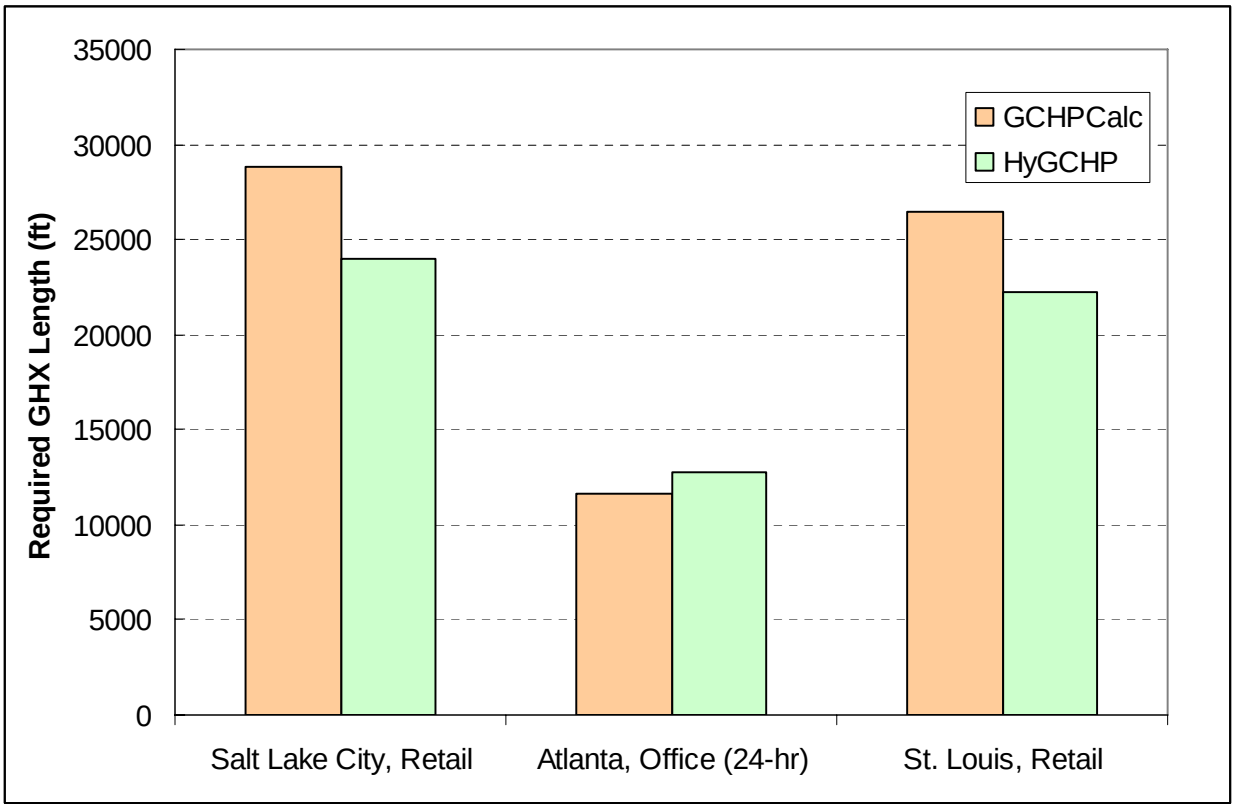

Figure 48. Comparison of HyGCHP optimal design results to those from a typical industry design tool, GCHPCalc.

All other system properties are equal, with the exception of the building loads. Loads for HyGCHP are given in 8760-hour format, but GCHPCalc uses a 'design' day made up of 4-hour-averaged loads. Four-hour averages were calculated from the 8760-hour loads, but this difference in inputs will still cause some degree of difference in the comparison.

Consideration of cooling-constrained GHX would require comparison of multiple-year geothermal-only scenarios. Since GCHPCalc and the GHX component in TRNSYS treat heat storage over multiple years very differently, there is less similarity in those cases.

3.6 Distributable Version

Results of the parametric study show that even a broad parametric study would create only very general design guidelines, due to the large number of variables (especially economic variables) that affect the design of each system. If an engineer wants to design a hybrid system for a specific building with a specific set of economic parameters then it may be more valuable to have access to the model itself, rather than the results of a parametric study. With this in mind, a version of the TRNSYS HyGCHP model (from herein called *HyGCHP*) has been created that can be distributed to other engineers.

This distributable version is functionally equivalent to the TRNSYS model, but is integrated with a graphical user interface (GUI) in which users enter values for the key variables and can run the simulation without ever having to directly access the TRNSYS code (or Studio program). The units in the GUI allow for both inputs and outputs to be in either SI or IP systems in order to match industry standard. The user can enter any loads (generated using separate software) for any building that they are interested in, though a full year of hourly building loads (heating and cooling) is required. The optimization algorithm was integrated to this distributable file in order to allow users to run either a single simulation or carry out an optimization (still using GENOPT as the optimization engine). Summary results and help screens were created to make the program more user-friendly. The results screen displays the life-cycle cost, cost break-down, energy consumption by component, and a few other key results such as temperature and pressure data. Finally, the results screen shows the design parameters used in the simulation.

For an optimization, these design parameters are a key result because they represent the *optimal* design parameters (i.e. those resulting in lowest life-cycle cost) for the given scenario. For a single simulation, the design parameters on the results screen simply reflect the parameters input by the user for that simulation.

A few modifications to the TRNSYS model have been made to facilitate its interaction with the user interface, and some cost and performance constants have been updated based on initial analysis of the parametric study results. Due to these modifications, some parametric study results may not match exactly with results given by the distributable program. However, the two models should agree within reasonable design uncertainty.

In addition to allowing the user to modify most key input values, it is valuable for the HyGCHP distributable program to allow modification of more complex functions. Several important parameters, such as first cost, cooling tower power consumption, etc., vary with optimization parameters like equipment size; therefore, these parameters vary during the optimization process according to an equation (generally based on a curve fit of manufacturer's data). For example, the first cost of a boiler increases as a quadratic function of the size of the boiler. In order to allow users to model scenarios with different equipment manufacturers and models (and corresponding costs), the user interface must allow for some control over these curves. Several possible methods have been considered:

1) Allow the user to enter the coefficients of a polynomial for each curve
   (or only allow modification of linear curves; allow slope to be entered as a constant)
2) Allow the user to enter the value for each parameter at one given size (e.g. 10 tons); linearly scale all coefficients until the curve meets this point
3) Link each curve to a data file which the user can modify

4) Allow the user to enter data for 2-3 sizes, and have the software perform the curve fit

5) Allow the user to enter a ‘multiplier’ that scales all coefficients of the curve (see below)

In a typical application, for example, the user might have cost data for a specific series of cooling towers that they would choose from for a specific project. Options 1 and 3 would be fairly unwieldy for the user to perform. Option 4 is reasonable for the user, but would be difficult to implement in a robust manner in the software. Option 2 and 5 are very similar, both linearly scale the curve’s coefficients to approximate the desired data. Option 5 was chosen because it demonstrates to the user the fact that the parameter – in this case cooling tower cost – is represented by a curve and not a constant, and that adjusting the curve can have a large effect on certain sizes if the equation is non-linear.

This method is documented in the distributable program’s help. For example, the online help page for the Cooling Tower First Cost Multiplier is:

Cooling Tower First Cost Multiplier

The cost of the cooling tower is based on the size of the tower, according to the curve shown below in Figure 49 (with Multiplier=1.00). The data at 1.00 are from R.S. Means average data, and include installation costs (Means, 2006). However, these data do not include the cost of any sump that may need to be added. The multiplier for cooling tower cost can be modified by the user to adjust this curve to match the cooling tower cost that is desired. The equation of the curve is simply multiplied by the Multiplier value.

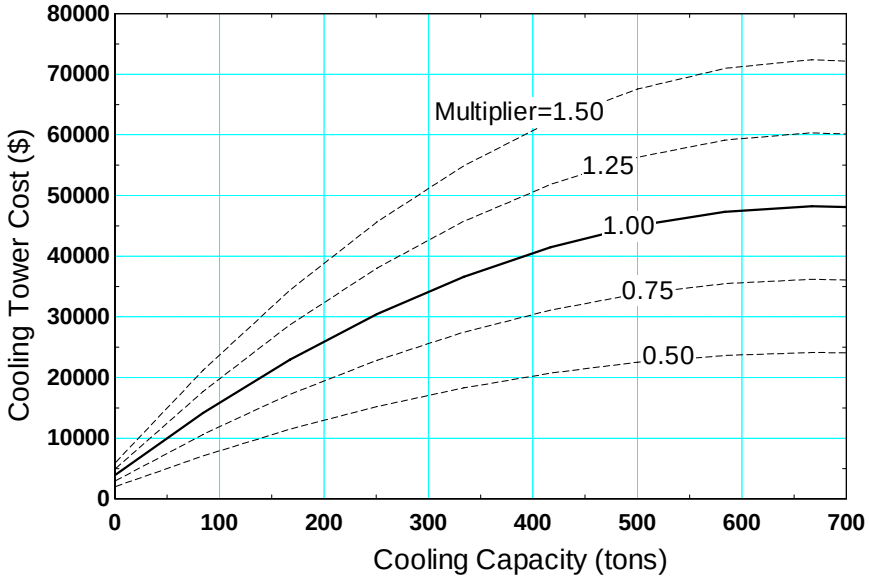

Figure 49. Cooling tower cost as a function of cooling tower size and cost multiplier.

Multipliers >1 lead to a greater cost (e.g. Multiplier=1.25), while multipliers <1 lead to lower cost (e.g. Multiplier=0.75). The user should look at the point on the curve specifically at the size of cooling tower that is expected for the building being modeled.

Multipliers like the one shown in Figure 49 are included for all initial and maintenance cost inputs. Additionally, multipliers are included for important supplemental device design parameters, such as fan power, air flow, and fluid flow.

The online help is the main tool for the user to explore the program and its many features. The help has been designed to be easily accessed from all points in the GUI and be very thorough, covering all input, output, and functionality of the model. In order to use this program, the user only needs two supplemental pieces of information: 1) a document called 'Getting Started' that will be packaged with the software and describe installation and beginner use and 2) total building loads in an 8760-hour format. If the user does not have a model that creates 8760

loads, one convenient source for approximate loads is the distributable program created by the ASHRAE-sponsored study (TRP-1120) of equivalent full-load hours (CDH and TESS, 2000).

4 Parametric Study

4.1 Overview

In order to develop guidelines for the design of hybrid ground source heat pump systems, a parametric study was carried out using the HyGCHP model discussed in Section 3. Simulations were run across a range of building load scenarios that included various climates and building types of interest. The climates were selected in order to span from cooling to heating dominated (including a balanced case) and wet to dry; the specific locations are listed in Table 6.

Climate	Location	
Heavily heating dom.	Minneapolis,	MN
Balanced	St. Louis,	MO
Wet, cooling dom.	Atlanta,	GA
Dry, cooling dom.	Phoenix,	AZ
Dry, heating dom.	Salt Lake City,	UT
Wet, heating dom.	Seattle,	WA

Table 6. Climates that were studied and the associated location of weather data.

The building types that were studied in each climate are:

1) 95,000 ft^2 retail building,
2) 92,000 ft^2 school (9-month),
3) 127,000 ft^2 six-story office, and a
4) 76,000 ft^2 six-story continuous-use building.

The continuous-use building is similar to the office building, but it is occupied 24 hours a day, 7 days a week.

For each building climate scenario, at least three main equipment configurations have been simulated:

A. Boiler/tower: a conventional boiler/tower heat pump system,

B. GCHP: a geothermal heat pump system, and

C. Hybrid: a hybrid geothermal heat pump system (with a cooling tower, in the base case).

Other equipment configurations have been studied, but only for a subset of the building/climate scenarios, and compared with the three base configurations. These additional equipment configurations include:

D. Boiler/DFC: a conventional boiler/dry fluid cooler heat pump system,

E. Hybrid DFC: a hybrid geothermal heat pump system with a dry fluid cooler,

F. Hybrid solar: a hybrid geothermal heat pump system with solar panels (for heating dominated buildings), and

G. Hybrid boiler: a hybrid geothermal heat pump system with a boiler (for heating dominated buildings).

By far the widest use of hybrid systems in the United States is for cooling-dominated building systems. Remember that in a cooling dominated system, the GHX-only system is sized primarily based on the cooling load (the heating load has an effect, but it is secondary) and secondary heat rejection equipment (e.g., a cooling tower or dry fluid cooler) is used to make these systems hybrids. This prevalence of cooling dominated systems in the U.S. can be attributed to many factors, including the nation's climate, typical building design, heat pump performance, and ground temperature. In fact, due to the energy lost as heat from inefficiency of heat pumps, a geothermal *system* can often be cooling dominated (require greater heat rejection than absorption) even if the heating load for the *building* is slightly larger than its cooling load. This study therefore focuses more effort on cooling dominated geothermal systems; heating dominated systems were also studied, but the most important results and guidelines discussed below are for cooling-dominated systems.

4.2 Creation of Building Loads for Study

The HyGCHP model does not include a building model. Instead, the HyGCHP model requires externally generated building loads (see Section 3.1.1) and the HyGCHP system is sized to meet the peak loads. The parametric studies were carried out using building loads created using a program that was developed by ASHRAE research project TRP-1120. ASHRAE TRP-1120 modeled a suite of buildings in order to provide expected hourly building loads for GCHP systems in different buildings and climates (CDH and TESS, 2000). One of the results of ASHRAE TRP-1120 was a TRNSYS-based executable file that allows parameters such as insulation, infiltration, and occupancy to be varied for a range of different building sizes and types in various climates. A one-year simulation using the TRP-1120 program provides a full year's worth of hourly building model data which can be used by simulations such as the HyGCHP model.

As discussed in Section 4.1, four different building types are studied. The TRP-1120 executable includes several different buildings that can be selected from within these four types. The goal of this parametric study is to create general-use design guidelines (while more specific designs are facilitated by the distributable program). Therefore, although there is no 'typical' building, the buildings that were selected from each category are as 'typical' as possible. The TRP-1120 study presents average values of the peak load and annual load for each of the four building categories that are studied here. These average values across a building category provide useful metrics that are used to identify specific buildings within each category that can be considered 'typical' (closest to the averages) and these are used in the parametric studies (it should again be noted that the user can choose from any of the buildings in TRP-1120 to create loads for the HyGCHP distributable model). Slight modifications were made to building

parameters (e.g. a 20% increase in internal generation, a 20% reduction in solar gain, etc.) so that the specific buildings corresponded even more closely to the category averages. The resulting four building models were then simulated at all six of the climates listed in Table 6. The total loads are summarized in Table 7 and Table 8 for the resulting buildings used in the parametric study; values are shown for the Atlanta and Salt Lake City climates, respectively.

	Peak Load (Btu/ft^2)		Annual Load (kBtu/yr/ft^2)	
	Cooling	Heating	Cooling	Heating
Retail	22	15	44	12
School (9 month)	23	16	20	9
Continuous-use	24	16	74	19
Office	21	19	29	15

Table 7. Loads used for building models used in the parametric study, shown for Atlanta's climate.

	Peak Load (Btu/ft^2)		Annual Load (kBtu/yr/ft^2)	
	Cooling	Heating	Cooling	Heating
Retail	24	20	37	22
School (9 month)	24	21	17	15
Continuous-use	25	19	63	33
Office	22	26	24	28

Table 8. Loads used for building models used in the parametric study, shown for Salt Lake City's climate.

4.3 Input Parameters for Study

In order to carry out a parametric study of each building and climate scenario, it is necessary to identify an appropriate set of the input parameters required by the HyGCHP model. Most of these inputs are discussed in the sections in Section 3 that describe the economic calculations and details of the physical component models. A summary of the key parameters used for the parametric study (i.e., quantities that are not optimized but rather set and used as the basis for an optimal system design) is shown in Table 9:

Ground:	Ground conductivity (Btu/h-ft-F)	1.4
	Ground diffusivity (ft^2/day)	1.1
	Grout conductivity (Btu/h-ft-F)	0.81
	Initial ground temp. (^oF)	by climate
	Drilling depth (ft)	300
	Borehole diameter (in.)	4.5
Fluid:	Pumping efficiency (%)	60
Equipment:	Boiler efficiency (%)	85
	Low-speed setting of tower/cooler (%)	50
	EER @ ARI 13256-1 conditions	16
	COP @ ARI 13256-1 conditions	3.4
Economic:	Discount rate (%)	8.5
	Down payment (%)	30
	Loan interest rate (20 yr. loan) (%)	6
	Tax rate (%)	35
	Inflation (%)	1.6
	Peak elec. rate ($/kWh)	0.101
	Off-peak elec. rate ($/kWh)	0.063
	Elec. demand charge ($/kW, 15 minutes)	6.22
	Gas price ($/therm)	0.99
	Water price ($/100 ft^3)	4
	GHX cost ($/ft)	10

Table 9. Summary of input parameters for the parametric study.

4.4 Results – Cooling Dominated System

The results of the parametric study have been compiled and analyzed with the goal of identifying trends that can lead to design guidelines. The key results from the study include the life cycle cost (*LCC*) and the optimized set of design parameters (i.e., the optimal values of the GHX size, tower size and control set points ΔT_1, T_{Cool2}, and T_{Heat1}, as described in Section 3.4) for each scenario.

4.4.1 System with Cooling Tower

Optimal Design Trends

In this section, the trends that have been identified for cooling-dominated hybrids with cooling tower will be discussed. For results that are presented in this section, the entering fluid

temperature is constrained by optimization to a minimum temperature of 35^{o}F and a maximum temperature of 95^{o}F. Scenarios with these assumptions are the 'base case' for this study (in Section 4.4.3, the effect different operating fluid temperature constraints are investigated – recall that for optimization, the limits of the entering fluid temperature at the heat pump have a large effect on size of the ground source loop that is required and thus the life cycle cost).

GHX Size. The most important variables for initial design of a hybrid system are the sizes of the equipment. In the case of the base configuration, these variables are the size of the cooling tower and ground heat exchanger. The optimal size of the GHX (in ft of total borehole) depends most strongly on the peak heating load of the building for cooling dominated hybrid systems. Figure 51 illustrates the optimal size of the GHX as a function of the peak heating load; notice that the optimal GHX size increases almost linearly with the peak heating load. The strong dependence on peak heating load indicates that in most of these cases the optimal GHX is sized so that it just meets the heating load of the building without violating the 35°F minimum fluid temperature constraint (i.e., the minimum entering fluid temperature during the entire 20 year simulation will be just slightly higher than the minimum temperature limit; a check of the temperatures in each case verifies this). In most of these simulations, there is a net heat addition to the ground over each year and therefore even though the simulation is run for 20 years, the minimum entering fluid temperature is experienced during the first year of simulation (and therefore, the optimal size of the ground heat exchanger could be identified using only a single year of simulation). This net heat addition occurs due to the optimal control sequence, even with the addition of the supplemental heat rejection device.

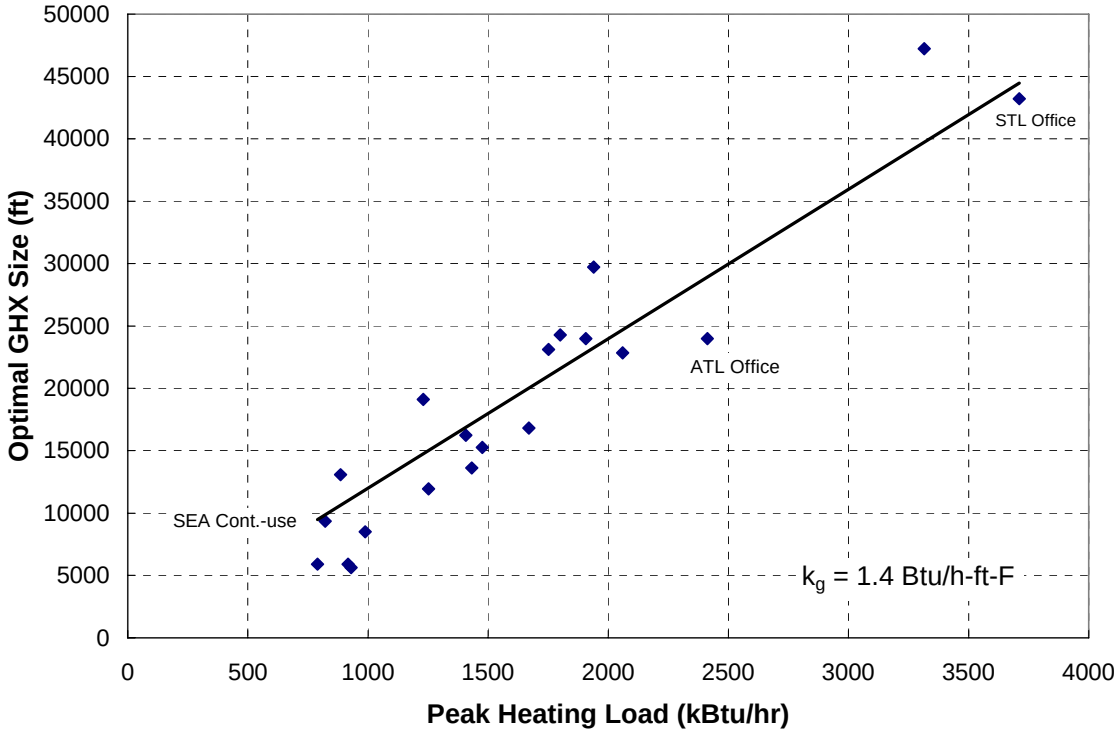

Figure 50. Optimal GHX size as a function of the peak heating load for each building/climate scenario.

A regression equation provides the optimal size (length, L_{tot} in feet) of the GHX as a function of heating load ($q_{load,heat}$ in kBtu/hr) as shown in Figure 50:

$$L_{tot} = 12.09 q_{load,heat} \tag{62}$$

Note that Eq. (62) forces a zero intercept (i.e., L_{tot} = 0 when $q_{load,heat}$ = 0). Equation (62) can be used as a very general design guideline; it corresponds to 145 ft of GHX per ton of heating.

There is of course some scatter around the best fit line in Figure 50 due to differences in the characteristics of the load and ground temperature. For ground temperature specifically, it is expected that GHX length would decrease with higher ground temperature in these cases, since geothermal heating is more efficient in locations with warmer ground. The effect of ground temperature was studied by plotting the optimal GHX size against the ratio of the peak heating load to the initial ground temperature (the x-axis in Figure 50 is normalized by an initial ground

temperature term equal to T_{ground} minus the minimum value of $T_{fl,in}$ (35°F). Figure 51 illustrates that this approach reduces the scatter in the data relative to Figure 50; buildings are described for a few sample data points.

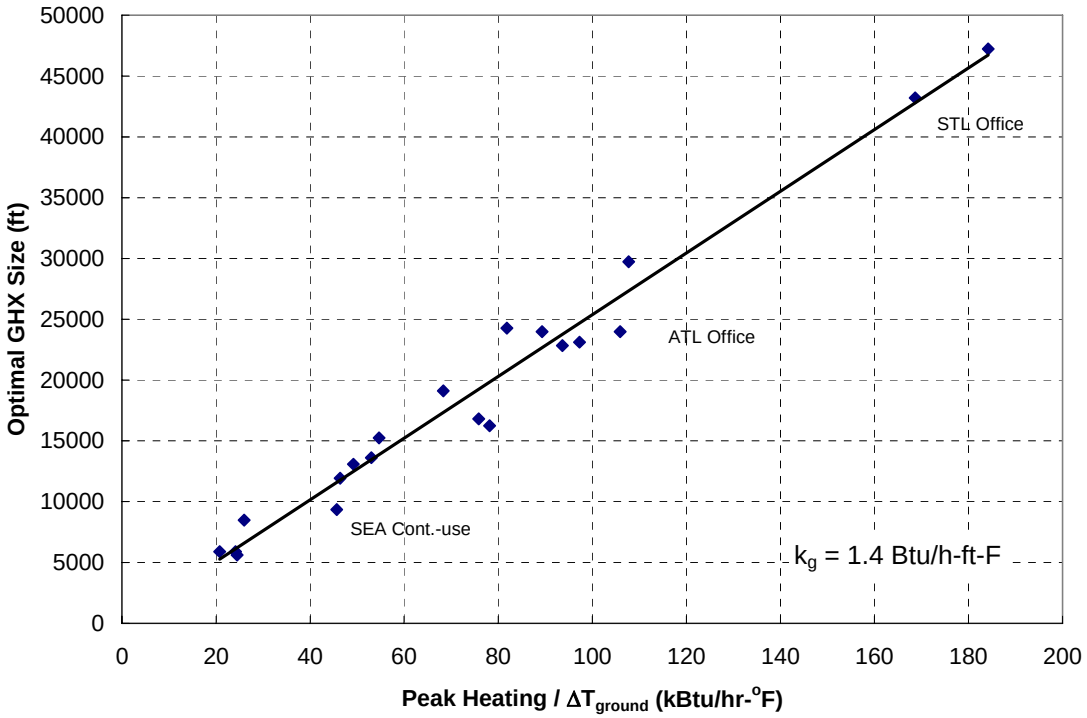

Figure 51. Optimal GHX size as a function of the ratio of the peak heating load to the difference between the initial ground temperature and the minimum value of $T_{fl,in}$ (35°F).

The regression equation for the optimal total size (length, L_{tot} in feet) of the GHX as a function of $q_{load,heat}/\Delta T_{ground}$ (in kBtu/hr-°F) is:

$$L_{tot} = \frac{254}{\Delta T_{ground}} q_{load,heat} \tag{63}$$

Equation (63) could also be used as a design guideline for hybrid geothermal heat pump systems in cooling dominated climates. A simpler design guideline is created by rearranging this equation and converting $q_{load,heat}$ to tons of heating; the result is shown in Figure 52. This plot

demonstrates the ft/ton (of heating load) of GHX required in a cooling dominated hybrid system for various ground temperatures.

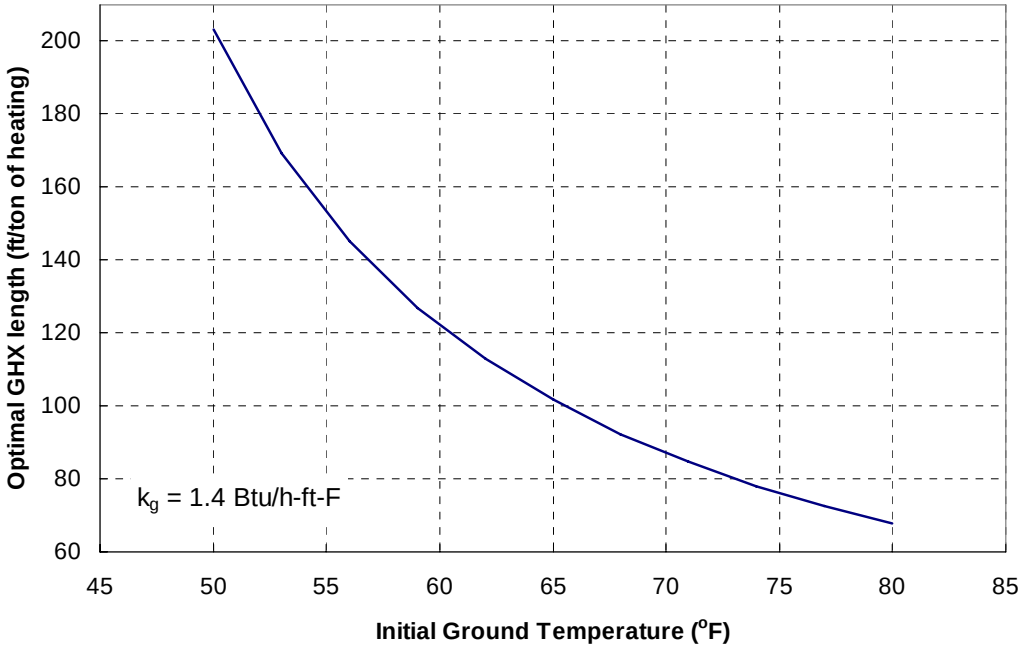

Figure 52. Design guideline for sizing a GHX in a cooling-dominated system as a function of the initial ground temperature.

The key conclusion of the results discussed above is that the optimal size of the GHX for a cooling-dominated hybrid system is one that is just large enough to meet the peak heating load. Additionally, the optimal control sequence and equipment sizes result in a net annual rejection of heat to the ground, so this constraint on GHX size occurs in the first year of simulation.

Design strategies described in this section are obviously driven by the economic assumptions. Although care was taken to choose 'typical' economic parameters for the parametric study, it is very possible that alternate parameters, such as higher fuel prices, for example, may yield a different conclusion. However, in the study of such sensitivities in Section 4.6.2; one of the key conclusions is that moderate changes in economic parameters do not have a significant effect on the optimal design values.

Cooling Tower Size. For hybrid systems in which the supplemental device is a cooling tower, the cooling tower must then be appropriately sized, as there is some cooling load that is not met by the GHX. Trends in the optimal size of the cooling tower are presented in this section. Since the GHX is sized based on the peak heating load, it would seem logical that the optimal size of the cooling tower would depend strongly on the remaining cooling load (i.e., the cooling load that is not met by the GHX). Figure 53 illustrates the optimal cooling tower size (C_{CCCT}, in tons) for each of the building/climate scenarios as a function of the unmet cooling load ($q_{unmet,cool}$), which is the difference between the peak cooling load ($q_{load,cool}$) and the amount of cooling provided by the GHX ($q_{GHX,cool}$). The peak cooling load is taken from the building data; to estimate the value of $q_{GHX,cool}$ for the modeled cases, we assume an equation for GHX length with the same form as that for heating:

$$L_{tot} = XT_{ground}q_{GHX,cool} \tag{64}$$

where X is a coefficient with units of ft/ton-^{o}F. The value of the coefficient X in Equation (64) was initially set assuming 155 ft/ton, based on basic ASHRAE recommended bore length for 1" vertical u-tubes (ASHRAE, 2003) at moderate temperatures (56-59^{o}F, and the base case conductivity). This yielded a plot similar to that in Figure 53. However, it is more accurate to adjust X based on the model results to a value at which the y-intercept of Figure 53 becomes 0; at this point the model should predict a cooling tower size of 0 if the GHX is meeting the entire cooling load. The resulting value for X in this case is 3.05 ft/ton-^{o}F; which, for example, corresponds to 174 ft of bore per ton of cooling from the GHX for 57^{o}F initial ground temperature.

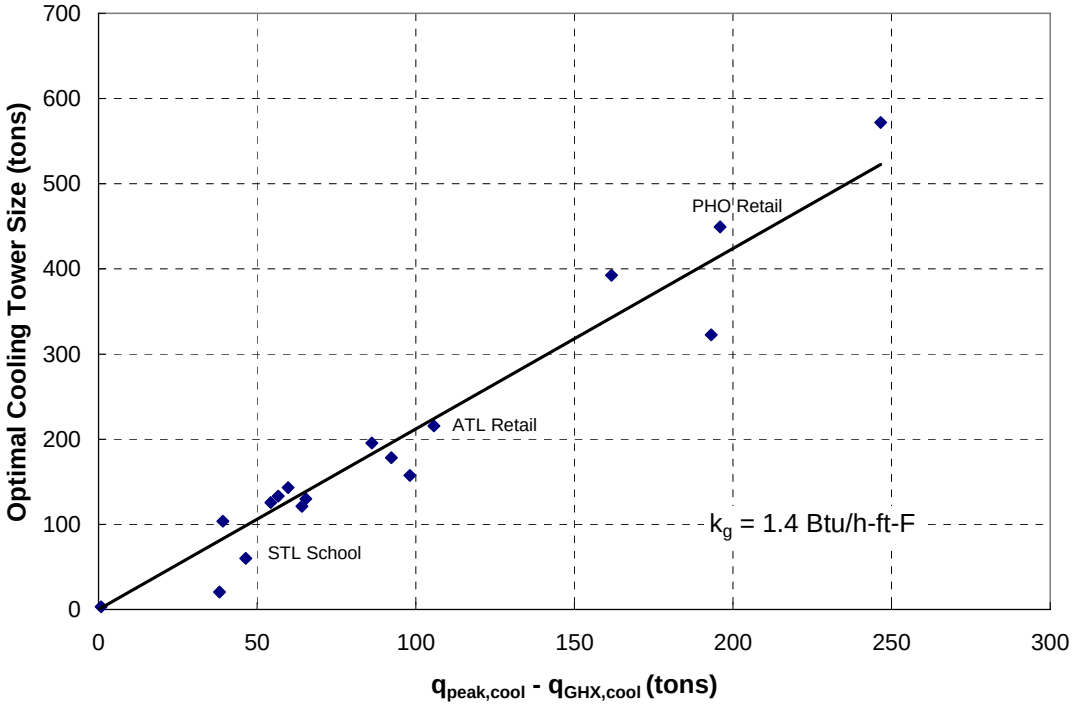

Figure 53. Optimal cooling tower size plotted as a function of the cooling load not met by the GHX.

The resulting regression equation for the optimal total size, C_{CCCT} (in tons) of the cooling tower as a function of $q_{unmet,cool}$ (in tons) is:

$$C_{CCCT} = 2.1 q_{unmet,cool} = 2.1\left(q_{peak,cool} - \frac{L_{tot}}{3.05 T_{ground}} \right) \tag{65}$$

Note that the optimal cooling tower size is larger than the unmet cooling load by a factor of 2.1. This is a surprising result, until we consider the optimal control sequence, which is discussed in the following section. With the assumed economic parameters, the optimizer has found that it is more cost effective to buy a very large cooling tower and operate it at half-speed the majority of the time than it is to buy a cooling tower that exactly matches the unmet load at full speed. (This result is due to the fact that fan power increases with speed to the third power while cost exhibits a dependence on cooling tower size that is more linear). Therefore, the

optimal cooling tower ‘size’ (its nominal rated capacity at full fan speed) is larger than its capacity under its typical half-speed operating condition (by about 60%). Several of the scenarios above were also analyzed with the cooling tower permanently set to full speed (to simulate a single-speed tower). With the single-speed results plotted in a manner similar to Figure 53, the equation for sizing the cooling tower becomes:

$$C_{CCCT} = 1.3 q_{unmet,cool} = 1.3 \left(q_{peak,cool} - \frac{L_{tot}}{4.72 T_{ground}} \right) \quad (66)$$

The optimal size of a single-speed tower is therefore still slightly oversized, at 1.3 times the size of the unmet cooling load. This equates to roughly 68% of the size of the two-speed tower that is operated mainly at low speed.

Optimal cooling tower size also has a relationship with climate. Figure 54 illustrates the optimal cooling tower size (normalized by the building size) as a function of the annual load imbalance; the imbalance is quantified as the ratio of the total annual heating load (in the building) to the total annual cooling load.

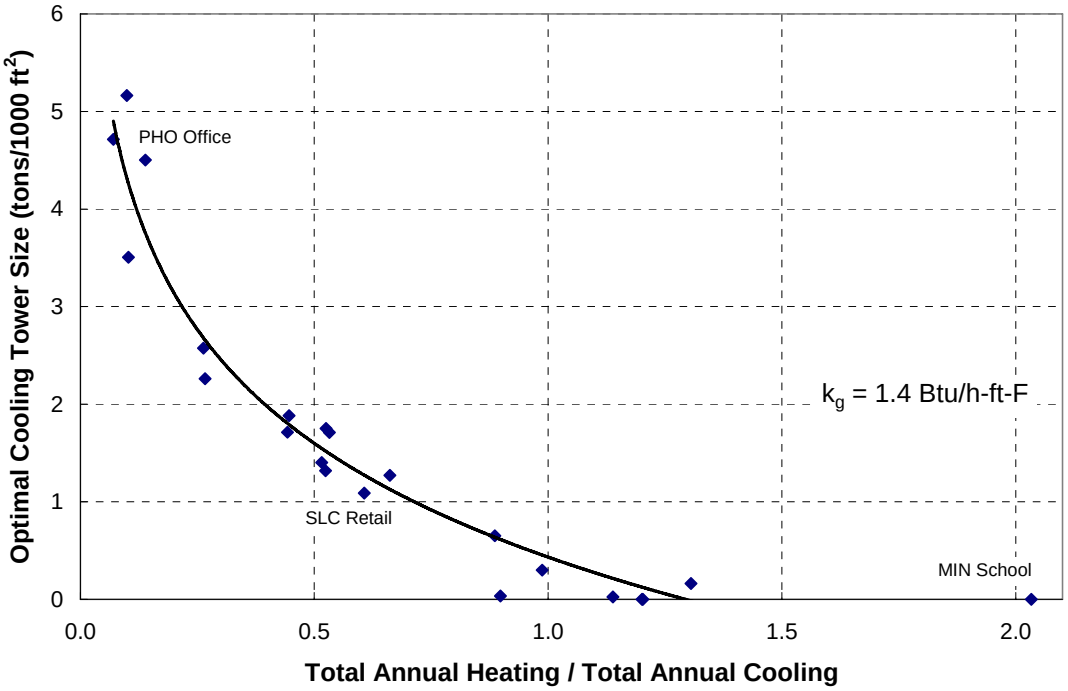

Figure 54. Optimal cooling tower size normalized by the building size as a function of the ratio of total annual heating load to peak cooling load.

In some cases (specifically in colder climates), the building loads are dominated by heating so that a GHX sized to meet the heating load also meets the entire cooling load. In these cases, the optimal size of the cooling tower approaches zero; the cooling tower is optimized away for an unbalanced heating/cooling ratio above about 1.2. This trend has a direct impact on the *LCS* of these systems, because the cooling tower is the key difference between hybrid and geothermal-only systems. This trend in *LCS* of hybrid systems versus geothermal-only systems is demonstrated in Figure 58, and shows a similar trend to Figure 54; however, note that the relationship to climate is even stronger for *LCS* (Figure 58) because the climate affects not only the size of the equipment but also how often it must operate.

Control Setpoints. In addition to the trends for equipment size, the optimal control setpoints are also investigated; refer to Section 3.2.7 for further information on the control strategy. The setpoint for operation of the cooling tower is ΔT_1; that is, the cooling tower is in

operation whenever the difference between the fluid leaving the heat pumps and the outdoor wet bulb air temperature is greater than ΔT_1.

The optimal values for ΔT_1 is relatively constant for all of the hybrid systems studied here. Figure 55 shows the optimal value of ΔT_1 for each building/climate scenario plotted as a function of ft^2/ton (ft^2 of building area) of cooling load. Generally, a value of 20 to 25^{o}F is appropriate for ΔT_1 and this appears to be fairly close to optimal for all cases. At very low cooling loads of 600 to 700 ft^2/ton, there may be a reason to increase the setpoint slightly, but this study does not have enough data in this range to be conclusive.

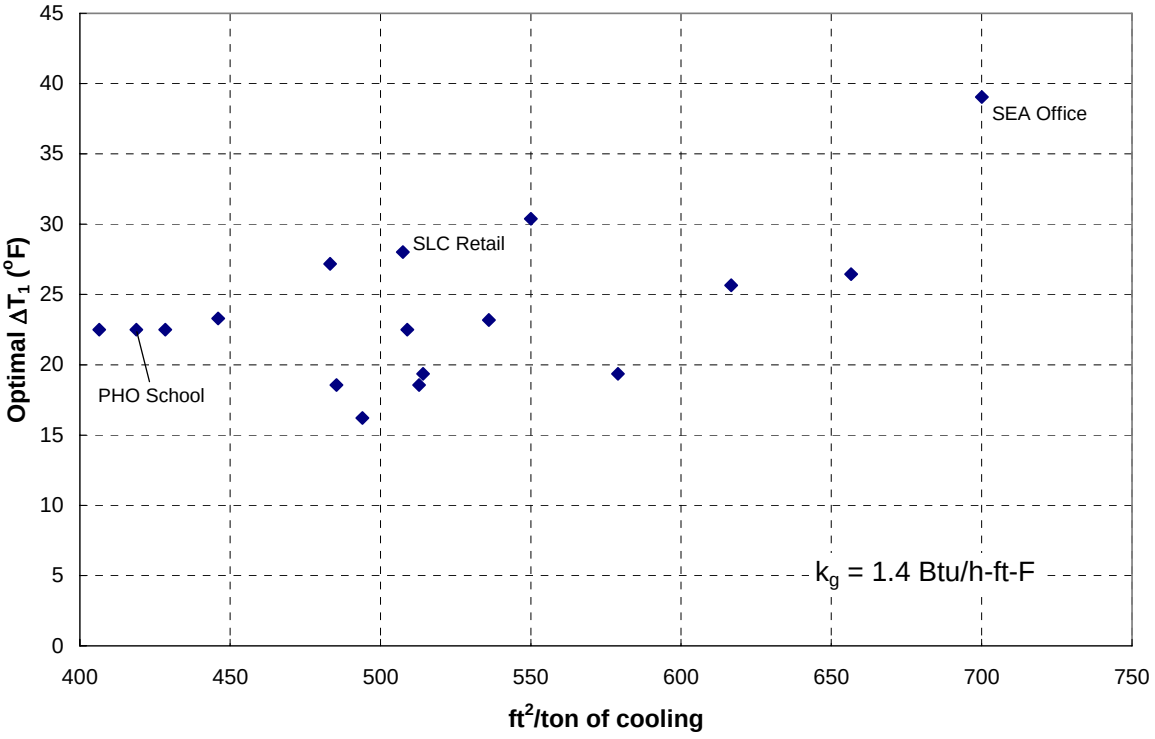

Figure 55. Optimal cooling tower control setpoint plotted as a function of ft^2/ton of cooling.

The cooling tower is sized based on the building loads, but its capacity during operation changes with ambient temperature and humidity. Therefore, a relationship between the setpoint

ΔT_1 and wet bulb temperature (T_{wb}) is also investigated. Figure 56 illustrates the optimal value of ΔT_1 as a function of T_{wb} (the wet bulb for July, according to the ASHRAE 1% value). Figure 56 suggests that for low summer T_{wb} locations (e.g., Seattle and Salt Lake City), a setpoint of 25 to 30°F should be chosen, while for higher summer T_{wb} locations (e.g., Atlanta), a value of about 19 to 23°F is likely to be closer to optimal.

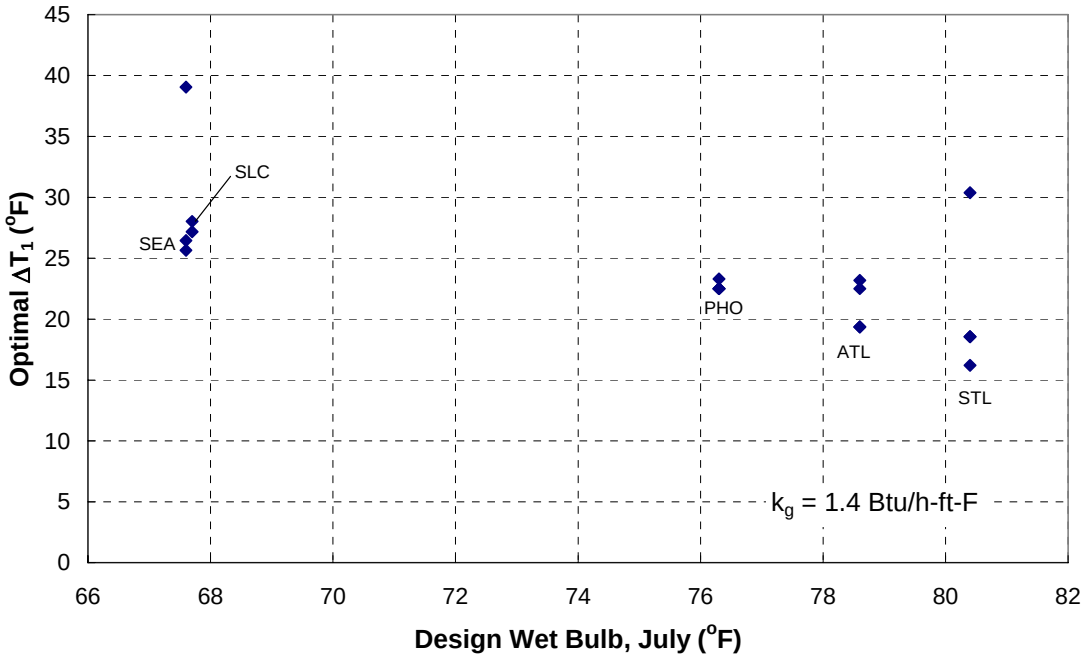

Figure 56. Optimal values of ΔT_1 plotted as a function of the ASHRAE design wet bulb temperature in July for the location in each scenario.

The other cooling tower control setpoint is T_{Cool1}, which controls when the cooling tower is operated in high speed as opposed to low speed. Recall that this setpoint was eliminated from optimization early in the study because it was found that the optimal value of T_{Cool1} is always a few degrees above the high limit for the entering fluid temperature. The value of T_{Cool1} has been set to 101.3°F for this parametric study and should generally be set about 5 to 8°F above the high limit for the entering fluid temperature (for economic parameters close to those used in this baseline study).

The remaining cooling control algorithm setpoint is T_{Cool2}, which controls flow through the GHX during cooling periods. Recall that flow is diverted through the GHX whenever the fluid temperature entering the GHX is above T_{Cool2}. Unlike the cooling tower, simulation data has shown that the GHX is *rarely* bypassed when there is a significant cooling load on the system. In some scenarios, once T_{Cool2} is set below a certain value it will have no effect at all on the results (because the GHX will never be bypassed in cooling), resulting in relatively arbitrary optimal values for T_{Cool2}. In fact, the only reasonable relationship between T_{Cool2} and other parameters is its relation to peak loads, specifically to the ratio of the peak cooling load to the peak heating load (as shown in

Figure **57**). The higher this ratio, the greater the fraction of the total cooling that will come from the cooling tower; this result reflects an increase in the amount of time observed in which the GHX is bypassed in favor of using the cooling tower. This type of operation seems to occur primarily in the shoulder seasons, when the heating and cooling loads are both smaller.

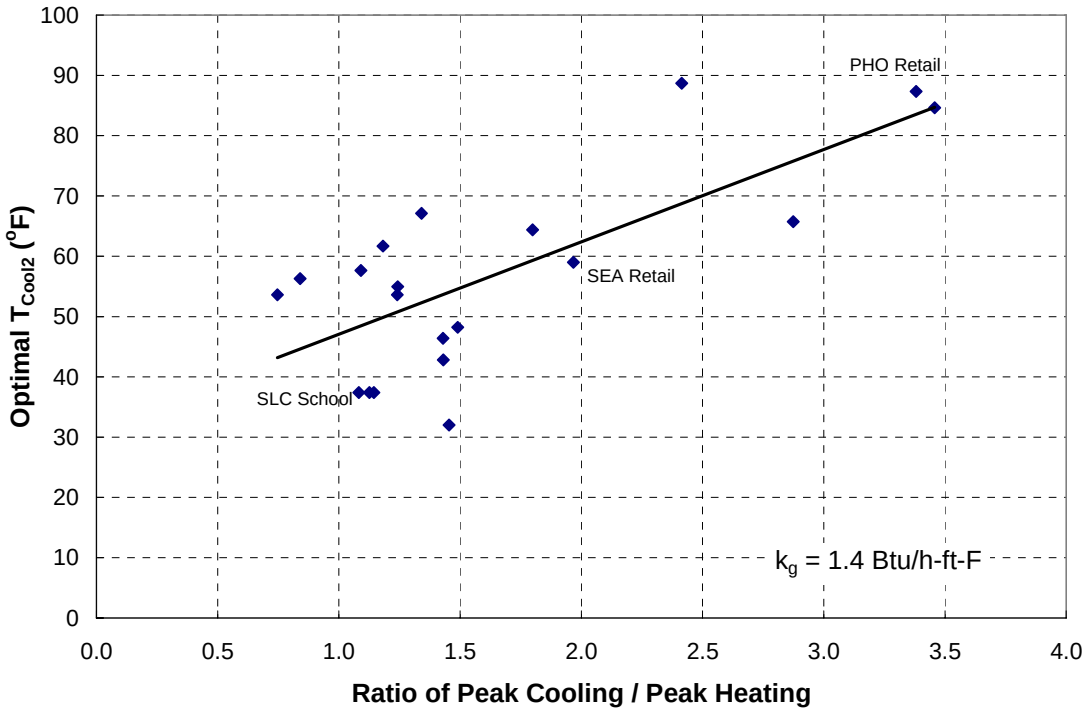

Figure 57. T_{Cool2} plotted as a function of the ratio between peak cooling and peak heating loads.

Note that when the temperature limits on the entering fluid temperature are relaxed, the optimal setpoints for both ΔT_1 and T_{Cool2} both change significantly; see 4.4.3 for a discussion of these trends.

The final control setpoint that must be optimized for hybrid geothermal systems is T_{Heat1}, which controls when fluid is diverted through the GHX for heating purposes. When the fluid temperature upstream of the GHX is below T_{Heat1}, the fluid is diverted through the GHX. Observations of simulation show that during heating, the GHX is *always* utilized. As expected, analysis of parametric study results show that T_{Heat1} is always set to a relatively high and relatively arbitrary value. Therefore, for cooling dominated systems, T_{Heat1} can therefore be set to a high value to allow the GHX to be utilized at all times that there is a heating load on the

system. In the distributable program, T_{Heat1} has been removed from optimization and is set to a high value.

Life Cycle Cost Trends

A secondary result of the parametric study is the relative life cycle costs of the cooling-dominated configurations (hybrid, geothermal-only, and conventional boiler/tower) for each of the building/climate scenarios. The relative life cycle costs can be compared in order to identify the most cost-effective configuration for each building and location and also to determine the magnitude of the savings associated with selecting the most attractive configuration. For example, in the 127,000 ft^2 office building in Atlanta, the hybrid system is the least expensive option (by a $73,000 margin over the next best configuration), followed by the boiler/tower system; the geothermal-only is the most expensive system using the baseline economic parameters.

It is instructive to examine the conditions under which the hybrid geothermal systems provide positive life-cycle savings (*LCS*) when compared with conventional boiler/tower systems or conventional geothermal-only systems. Figure 58 illustrates the *LCS* associated with selecting a hybrid system over a geothermal-only system as a function of the ratio of the total annual heating to cooling load. Notice that the life cycle savings increases approximately exponentially as the ratio of the annual total heating to cooling loads for the building decreases.

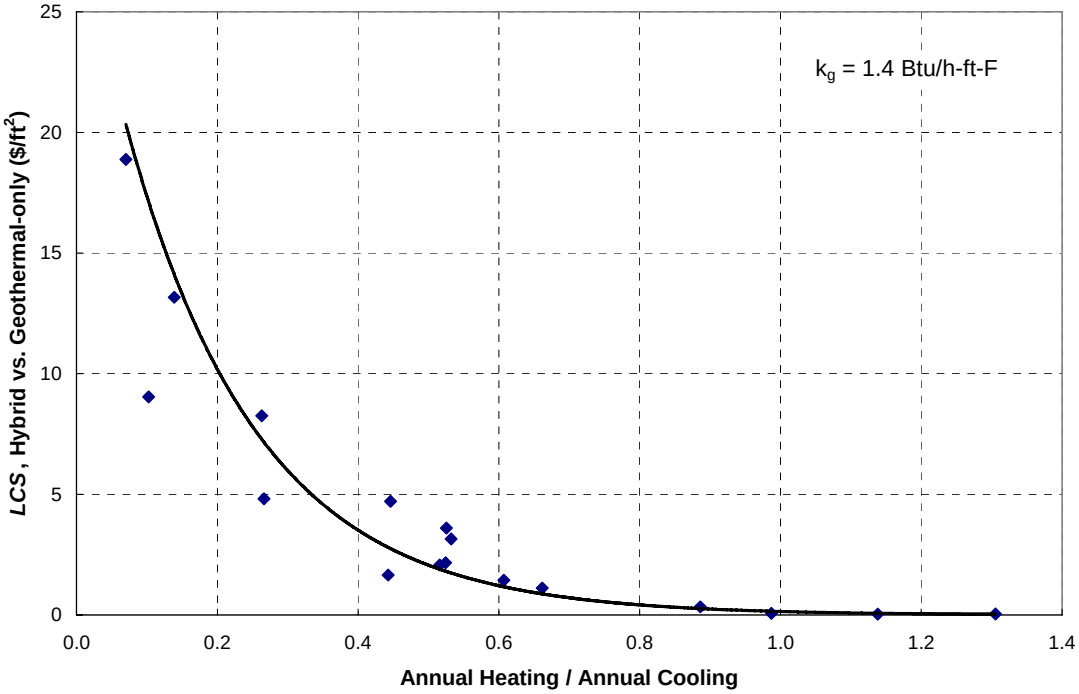

Figure 58. Life-cycle savings of hybrid systems over geothermal-only systems as a function of ratio of total annual heating load to total annual cooling load (for 35/95°F temperature limits).

This is a reasonable result, considering that hybrids have been successfully implemented in areas of heavily unbalanced climate. The more unbalanced the climate, the more benefit that the supplemental heat rejection associated with the cooling tower provides.

The *LCS* of a hybrid system when compared to a conventional boiler/tower system follows different trends; savings has no clear relationship to the ratio of the annual heating to cooling loads which introduces an imbalance in the ground load. The major difference between the hybrid and boiler/tower systems is the use of a boiler in place of a GHX (recall that the GHX in the hybrid system is sized in most cases based only on heating loads). Therefore, the LCS of a hybrid system would be expected to have some relation to peak heating load. Unfortunately, for the base case temperature limits, *LCS* appears somewhat random. When temperature limits are relaxed a more clear design trend (with peak heating load, as expected) emerges; this is

demonstrated in Section 4.4.3 below. But with more constrained temperatures, the GHX and boiler both increase in size; additionally, as the GHX size increases, it has a greater effect on the cooling which was dominated by the cooling tower. The interdependence of economic results with all three of these pieces of equipment prevents a single clear relationship from being observed.

Climatic Trends. When geographic locations are considered with the *LCC* results, there are conclusions that can be drawn regarding which equipment configurations (e.g. hybrid vs. geothermal vs. boiler/tower) have the lowest *LCC* in which climates. The best example is in Minneapolis, where the hybrid systems (using supplemental heat rejection equipment) always optimize to a cooling tower size of zero (making it a geothermal-only system). Coupled with significant savings demonstrated by geothermal over conventional boiler/tower systems, geothermal-only is clearly always the cheapest option in this northern climate (this conclusion was found to be true no matter what temperature limits are used).

Hybrid systems are generally the least expensive in all warmer climates of the United States. Figure 59 and Figure 60 demonstrate the *LCS* of hybrid systems when compared with geothermal-only and boiler/tower configurations, respectively.

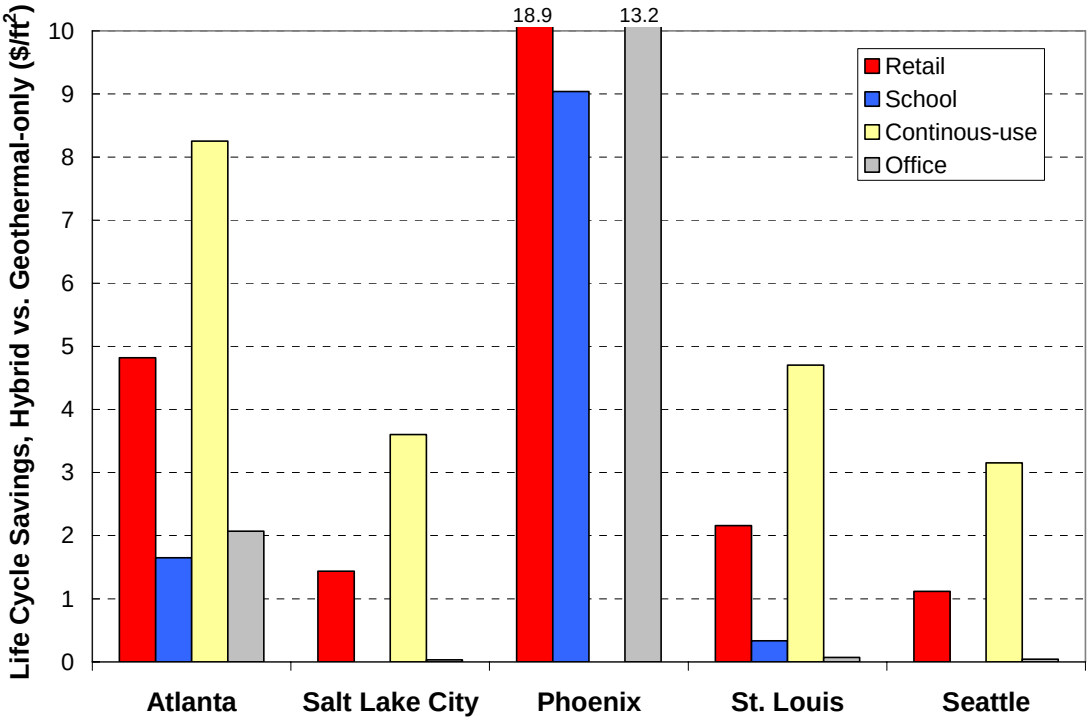

Figure 59. Life cycle savings of a hybrid system as compared with a geothermal-only system for twenty different buildings.

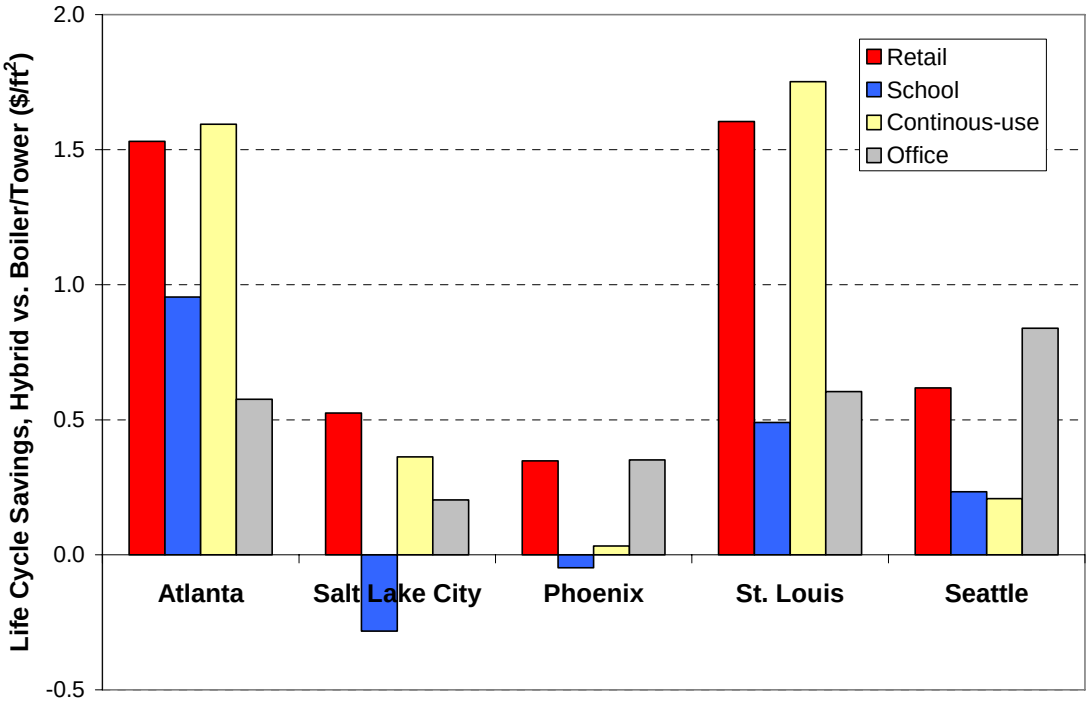

Figure 60. Life cycle savings of a hybrid system as compared with a boiler/tower system for twenty different buildings.

Note that the hybrid system is generally the most attractive option by a significant margin, with some exceptions. In Seattle and Salt Lake City, geothermal-only is cheaper (or the same cost) for both the school and office buildings. These climates are less cooling-dominated than the other climates in the study, as demonstrated in the first column of Table 10, where the cities are ranked by the ratio of total annual heating load to cooling load.

There are fewer exceptions for boiler/tower systems (shown in Figure 60). The *LCS* of hybrid versus boiler/tower systems is proportional to the peak heating load. The school in Phoenix has such a small peak heating load that the best option is a boiler/tower system, and in general, all of the buildings in Phoenix show less savings with hybrid versus boiler/tower than any of the other cities due to the small heating loads (see the second column in Table 10). Buildings in Salt Lake City yield savings with hybrid systems (for all buildings except for the school), but the savings are smaller than in other climates. Salt Lake City has a relatively high heating load, so that is not the reason for this observation. Instead, humidity differences are likely the reason. The third column in Table 10 shows that the cities with the lowest *LCS* for hybrids versus boiler/tower systems (Salt Lake City and Phoenix) are also much drier than the other four cities on the list. Though a mathematical correlation is not evident among the other four cities, it is clear that the two driest cities also exhibit the lowest life-cycle savings, likely because the cooling tower is much more effective at cooling in a dry climate, to the point that it can drive the *LCS* of a hybrid vs. conventional boiler tower to near – or below – zero in these dry climates.

Ratio: Annual Heating/Cooling		Peak Heating Load (kBtu/hr)		July Relative Humidity (%)	
Phoenix	0.10	Phoenix	906	Salt Lake City	27
Atlanta	0.37	Seattle	1172	Phoenix	31
St Louis	0.71	Atlanta	1643	St Louis	50
Salt Lake City	0.82	Salt Lake City	2099	Minneapolis	54
Seattle	0.93	St Louis	2310	Atlanta	57
Minneapolis	1.70	Minneapolis	6550	Seattle	63

Table 10. Cities in the parametric study ranked according to climate. The first column ranks cities according to the ratio of total annual heating load to cooling load (averaged for the four building types). The second column ranks them according to the peak heating load (averaged for the four building types). The third column ranks them according to the average relative humidity in the afternoon in July.

Economic Sensitivities of LCS Trends. One of the most uncertain inputs to the model is the future of energy prices. Energy price inflation was assumed to track general inflation (Rushing and Fuller, 2006); however, there is a reasonable possibility that energy prices will increase at rates that are much higher than inflation. Sensitivities were therefore run with fuel price inflation (i_F) set to 7.5% (versus 1.6% for general inflation; a more detailed discussion of sensitivities to the base case is found in Section 4.6.2). For *LCS* of hybrid versus geothermal-only, increasing the fuel inflation rate decreases the savings slightly (~10%) across the board, but the trend shown in Figure 58 is not affected. *LCS* is inversely proportional to fuel cost in this case because the hybrid cases tend to use slightly more energy than the geothermal-only configuration. This results in the *LCS* reaching (near) zero at a lower ratio of load imbalance (ratio of annual heating to cooling loads) than for the base case, which had significant savings even up to a load imbalance that is slightly greater than 1.0 (see Figure 58). Conversely, the *LCS* of hybrid versus boiler/tower systems is directly proportional to fuel inflation; additionally, because the difference in fuel consumption is large between these two systems, the increase in savings with increased fuel cost is more dramatic in this comparison. Setting i_F equal to 7.5% roughly doubles the base case curve described in Figure 70; Figure 61 compares the case of 7.5% fuel inflation with that base case curve.

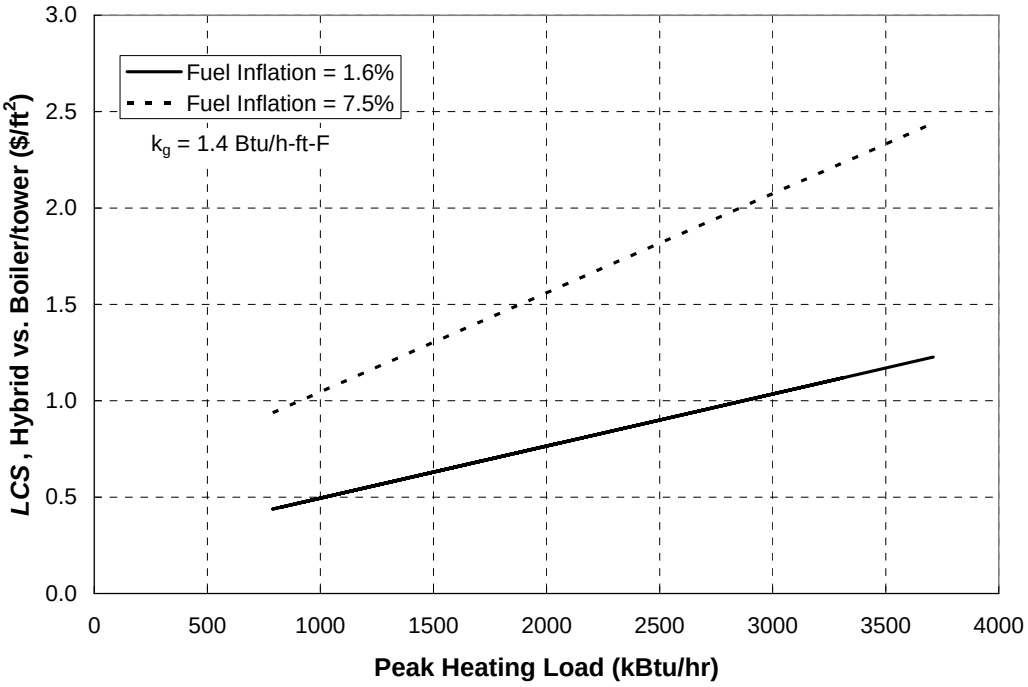

Figure 61. Life-cycle savings of hybrid systems over boiler/tower systems as a function of the peak heating load. This plot compares the base case, assuming a fuel inflation of 1.6%, to a case that assumes 7.5% fuel inflation.

The effect of the GHX cost was also examined; a sensitivity study was carried out in which the cost of installing the GHX was adjusted to be \$6/ft, and then \$20/ft (from a default of \$10/ft). As expected, the *LCS* is proportional to GHX cost for hybrid versus geothermal configurations, and inversely proportional for hybrid versus boiler/tower configurations (demonstrated in Figure 62; each data point represents an average of five random building/climate scenarios: Atlanta retail, St. Louis school, Atlanta 24-7 office, Seattle 24-7 office, Salt Lake City office).

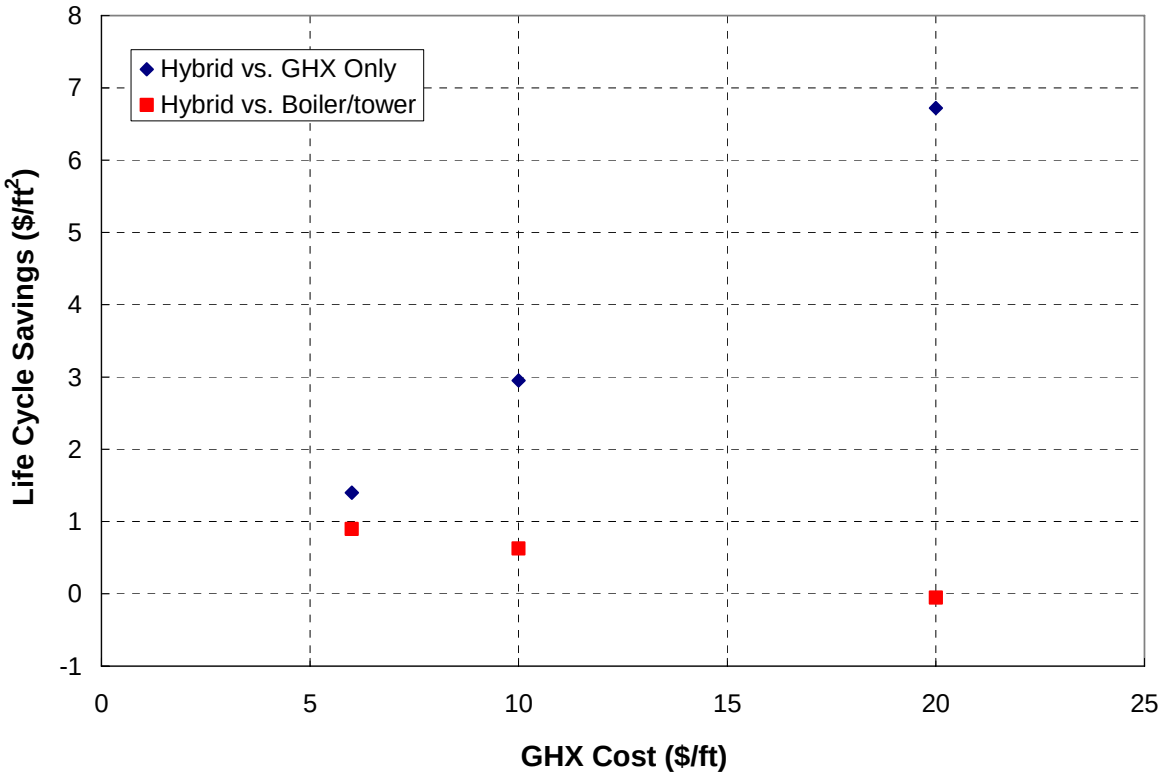

Figure 62. Life-cycle savings of hybrid systems as a function of the GHX cost. This plot shows the average values for five of the building/climate scenarios.

Additionally, a sensitivity study of the optimal design values to various simulation parameters is discussed in Section 4.6.2.

4.4.2 System with Dry Fluid Cooler

The majority of the cases that were simulated in the parametric study utilized a cooling tower for the hybrid configurations. However, other equipment can be used as the supplemental heat rejection device in order to hybridize the system. One alternative device that was simulated in this study was a dry fluid cooler (see Section 3.2.4 for a technical discussion of this device and its model). In this section, the optimum design guidelines and life cycle savings for the dry fluid cooler are compared to those for the cooling tower.

Optimal Design Trends

The dry fluid cooler is implemented in the hybrid model in the same way as the cooling tower; the only difference is in the controls; specifically, the control parameter ΔT_1 becomes the difference between the fluid temperature entering the dry fluid cooler and the ambient dry bulb temperature whereas the ambient wet bulb temperature was used for the cooling tower.

The optimal GHX size for the dry fluid cooler hybrid is found to be essentially the same as for the hybrid with the cooling tower; the design trend that was previously discussed and is shown in Figure 51 remains valid for the dry fluid cooler hybrid. The control setpoints used to control the operation of the GHX are also similar, although T_{Cool2} is slightly lower which leads to less bypass across the GHX in cooling mode.

The optimum size of the dry fluid cooler follows a trend that is similar to that of the cooling tower; the optimal dry fluid cooler is inversely proportional to the load unbalance, characterized by the ratio of the total annual heating load to the total annual cooling load. This relationship is demonstrated in Figure 63.

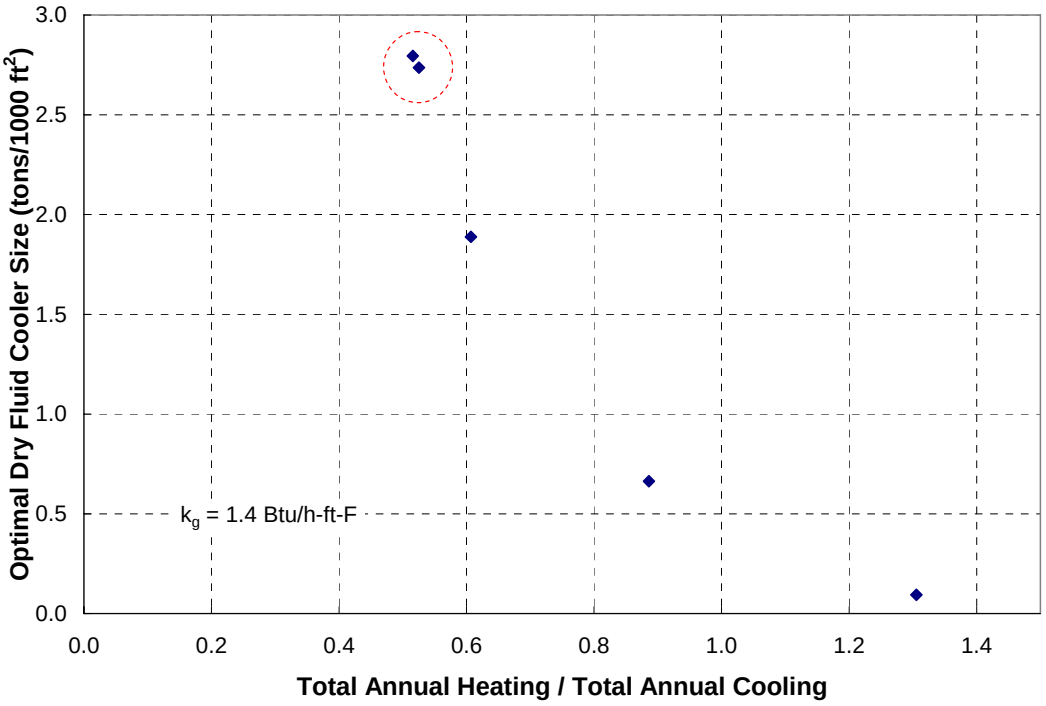

Figure 63. Optimal dry fluid cooler size as a function of the ratio of total annual heating load to total annual cooling load, which is a measure of the load unbalance.

The two data points at the largest cooler size (circled in Figure 62) represent warm climates in which the dry fluid cooler is attempting to cool the fluid to 95°F when the ambient dry bulb (the heat sink) temperature is also very near that temperature; this situation requires a very large optimal dry fluid cooler.

The main control set point for the cooler (ΔT_1) generally has an optimal value that is higher than was identified for the cooling tower. However, the largest difference in the control of a hybrid with a dry fluid cooler vs. a hybrid with a cooling tower is the set point that controls high speed operation of the cooler (T_{Cool1}). The optimal value of T_{Cool1} for the cooling tower was previously identified as being sufficiently high (~100°F) that the cooling tower operated the majority of the time at low speed (the tower only operates at high speed when the fluid temperature is greater than T_{Cool1}). Because the dry fluid cooler does not take advantage of latent heat transfer (as does the cooling tower) it must use the entire capacity of its fan in order to meet

peak cooling loads; therefore, the optimal value of T_{Cool1} is much lower for the dry fluid cooler, allowing it to operate at high speed whenever there is any significant cooling load.

Life Cycle Cost Trends

The LCC of a hybrid system with a dry fluid cooler is similar to that of a hybrid system with a cooling tower (see Figure 64). It therefore follows the same cost trends that were discussed in Section 4.4.1 for the cooling tower hybrid. In general, the life-cycle cost (*LCC*) is lower than for a conventional boiler/tower configuration, but a little higher than for the hybrid cooling tower configuration. That is, the hybrid with the cooling tower is typically the most attractive option, followed closely by the hybrid with a dry fluid cooler.

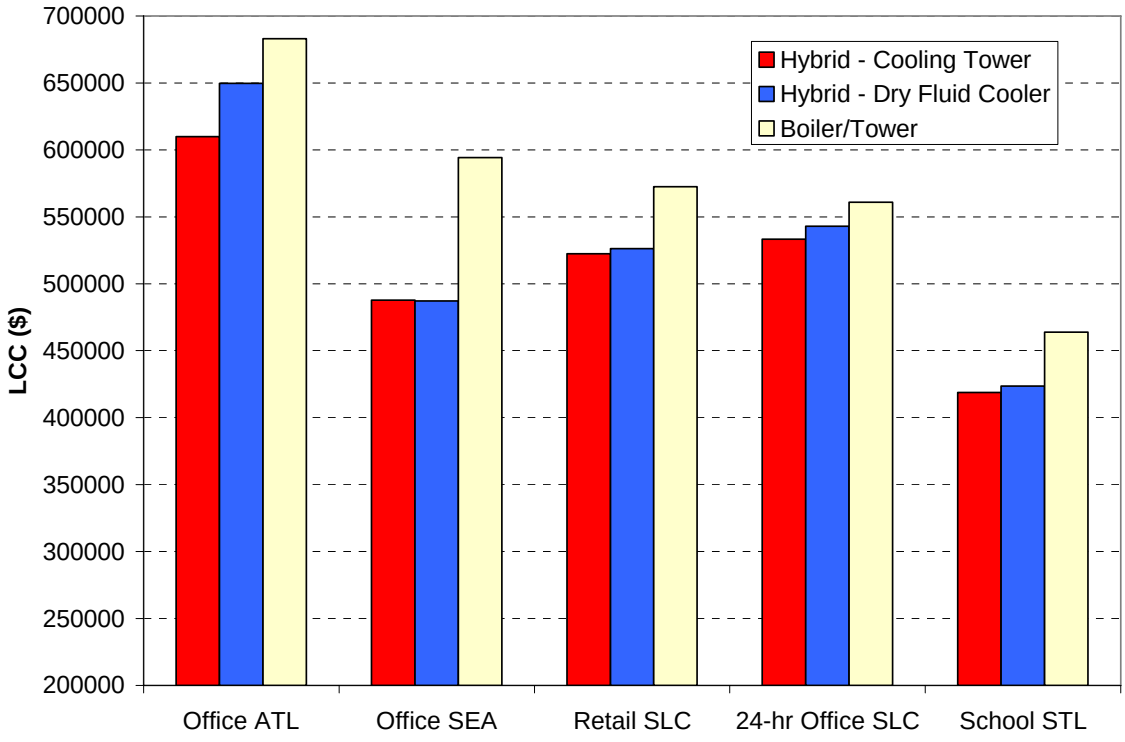

Figure 64. Life cycle cost comparison between hybrid geothermal heat pump systems with a dry fluid cooler versus a cooling tower; conventional boiler/tower system shown for reference.

4.4.3 System with Cooling Tower – Relaxed Temperature Limits

For the base case, the GHX and cooling tower are sized so that they are sufficiently large that the heat pump entering fluid temperature ($T_{fl,in}$) is always maintained within limits of 35–95°F during the simulation; this leads to efficient heat pump operation, provides some margin against particularly bad weather years, and corresponds to typical design practice. However, in this section these temperature limits are relaxed, allowing the optimizer to select a smaller GHX and supplemental equipment which results in more severe values of $T_{fl,in}$. Figure 65 illustrates the size of the ground heat exchanger (for a retail building in Salt Lake City) as a function of the lower limit imposed on the $T_{fl,in}$ and demonstrates clearly the relationship between the minimum entering fluid temperature and the equipment size. If the system is allowed to experience a 20°F entering fluid temperature as opposed to the base case value of 35°F, then the GHX size can be reduced by approximately 50%. Note that the GHX size approaches infinity as the limit of $T_{fl,in}$ approaches the ground temperature.

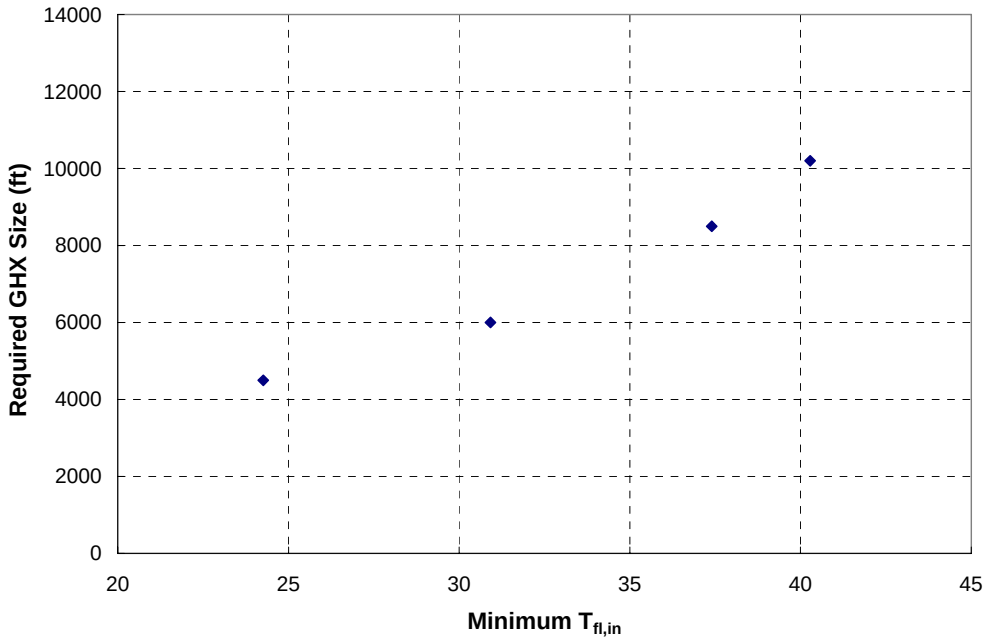

Figure 65. GHX size as a function of the lower limit on the entering fluid temperature ($T_{fl,in}$) for a retail building in Salt Lake City.

In practice, engineers design geothermal heat pump systems so that the entering fluid temperature ($T_{fl,in}$) never approaches the minimum or maximum temperature limits that are stated by the heat pump manufacturers; this allows the heat pump system to operate more efficiently and therefore be smaller (the capacity of heat pumps decreases at more extreme temperatures, as Figure 72 will demonstrate). More moderate temperatures also provide some margin for unusually extreme weather and design uncertainty. But as this section discusses, in some scenarios it may be more effective from a life cycle cost standpoint to operate the heat pumps at more 'relaxed' temperatures (i.e., allow higher $T_{fl,in}$ and lower $T_{fl,in}$ than the base case discussed above); in these cases a safety factor could be used to account for weather risk and uncertainty. Additionally, it is beneficial to investigate a range of operating temperatures in this study because designers tend to choose different operating temperatures in different projects and climates.

The parametric results are presented here for the same building/climate scenarios as those discussed in the section above, only with the minimum and maximum values of $T_{fl,in}$ set to values that are typical of manufacturer's absolute operating limits (20^{o}F for a minimum, 110^{o}F for a maximum, herein referred to as 20/110^{o}F). A comparison of these results with those from the base case concludes this section.

Optimal Design Trends

The general trends observed for optimal system design with relaxed temperature limits are similar to those discussed for the base case (in Section 4.4.1). For example, the optimal GHX size is still linearly proportional to the peak heating load in the building; however, the required bore length with the 20/110^{o}F temperature limits is approximately 70 ft/ton of heating,

which is about half of the size of the GHX that is required for the base case with the 35/95°F temperature limits. A comparison of the two trends is shown in Figure 66.

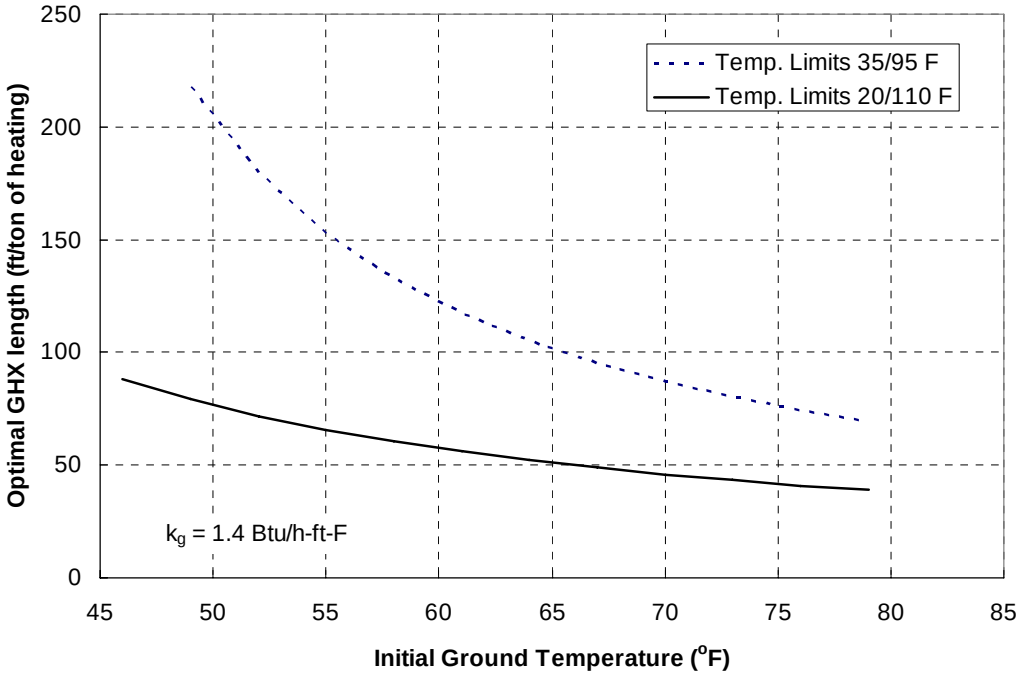

Figure 66. Optimal GHX size for cooling-dominated hybrids for two different temperature limits. Relaxed temperature limits result in a GHX size that is roughly half as large as the 35/95°F limits.

However, when the temperature limits are relaxed there are a few building/climate scenarios that result in a GHX that is sized a little *larger* than would be required to exactly satisfy the minimum temperature limit (i.e., the minimum value of $T_{fl,in}$ that is reached during the simulation is actually several degrees above the specified 20°F limit, indicating that this limit is actually not constraining the optimization). The cases in which the entering water temperature does not reach the specified 20°F limit include: the office in St. Louis, the retail building in Atlanta, and schools in Salt Lake City and Seattle.

The trend for optimal cooling tower size is similar for the relaxed temperature limits as well (as shown in Figure 67). The optimal cooling tower size is based on the cooling load that is not met by the GHX. Equation (64) is again used to represent this relationship; in this case, X =

2.25 ft /ton-^{o}F; which corresponds to 128 ft of bore per ton of cooling for the example with 57^{o}F initial ground temperature (less length is required when the operating temperature limits are set to 20°F/110°F). The optimal cooling tower size is always larger than is necessary to meet the maximum entering water temperature limit of 110^{o}F (i.e., this limit never constrains the optimization); these scenarios have an average maximum $T_{fl,in}$ of 103^{o}F.

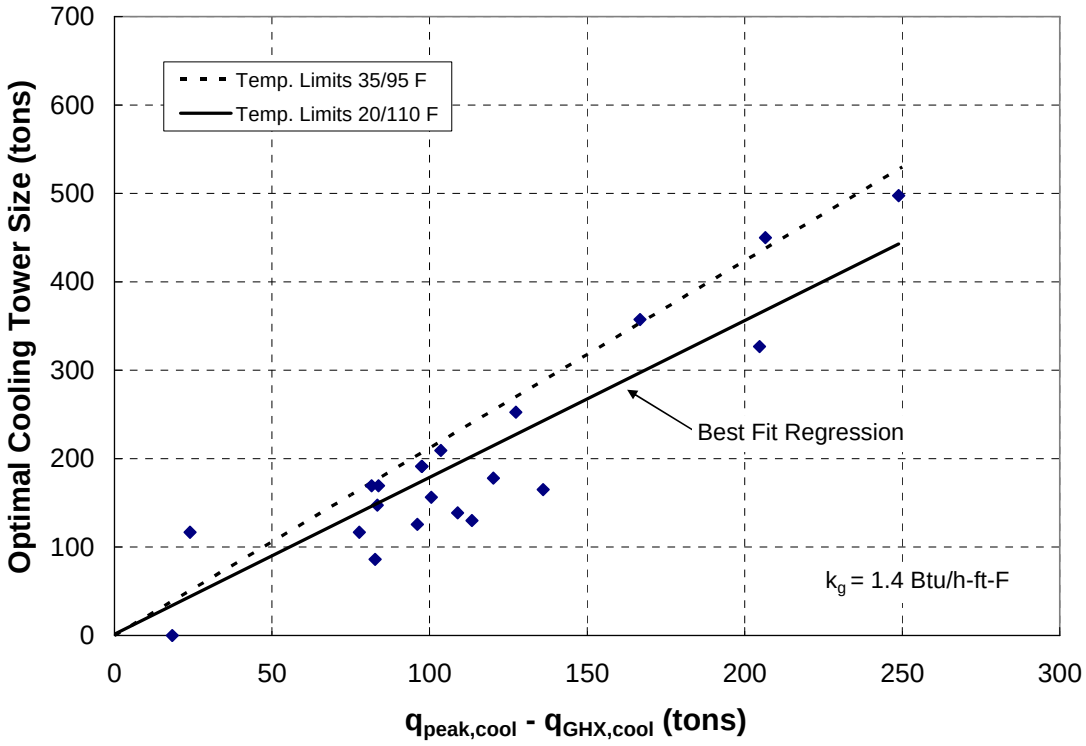

Figure 67. Optimal cooling tower size plotted as a function of the cooling load not met by the GHX, for relaxed temperature limits (20/110^{o}F).

With the relaxed temperature limits (20°F/110°F), the cooling tower is optimally sized so that it is approximately 1.7 times larger than the unmet cooling load; this factor is compared to 2.1 larger for the base case with temperature limits of 25°F/95°F. Section 4.4.1 explains why the nominal cooling tower size is so much larger than the unmet cooling load. Also, see the last part of the current section for a caveat regarding shortcomings of Figure 67.

Some subtle differences are observed for the optimal control setpoints with the relaxed temperature limits. Optimal values of ΔT_1 are generally found to be 2 to 5°F lower because the cooling tower does not have to run as often when temperature limits are relaxed (ΔT_1 remained relatively constant for different climate/building scenarios). For T_{Cool2}, the trend demonstrated in Figure **57** is not valid with relaxed temperature limits (20°F/110°F); instead, Figure 68 illustrates the optimal values of T_{Cool2} as a function of the ground temperature for both the relaxed (20/110°F) and baseline (35/95°F) temperature limits. Figure 68 demonstrates that optimal values of T_{Cool2} are generally higher for the relaxed temperature limits than for the base case. Additionally, the optimal value of T_{Cool2} is more strongly dependent on the initial ground temperature (or the related average annual ambient temperature, which is similar). For warmer climates, the value of T_{Cool2} is higher, indicating that the GHX can be bypassed slightly more often in warmer climates.

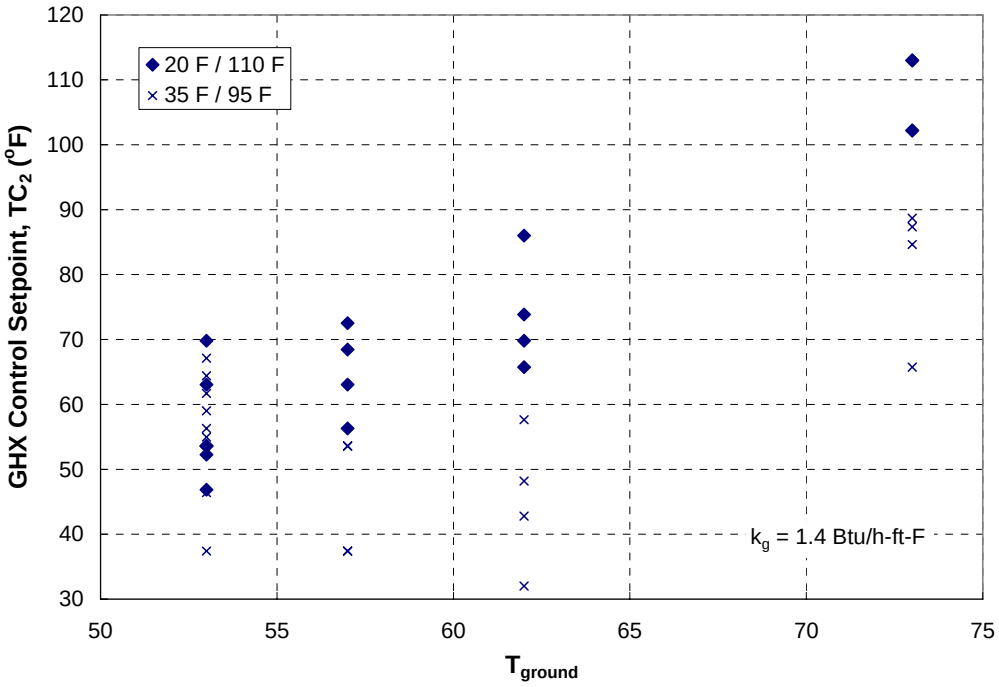

Figure 68. Optimal values of T_{Cool2} (GHX cooling setpoint) as a function of initial ground temperature (which is strongly related to the average ambient temperature).

Finally, the optimal heating control setpoint, T_{Heat1}, was found to be high enough to keep fluid diverted through the GHX whenever a significant heating load is present; this observation was also true for the base case.

Life Cycle Cost Trends

Figure 69 illustrates the life cycle savings (*LCS*) associated with a hybrid over a geothermal only system optimized using the relaxed temperature limits (20/110^{o}F) in comparison to the baseline temperature limits (35/95^{o}F). *LCS* is plotted here as a function of the heating to cooling load ratio; note that the results are similar for either set of temperature limits although *LCS* decreases somewhat for severely unbalanced climates. The dashed line in Figure 69 corresponds to the regression for the data from the 35/95^{o}F temperature limits that was shown in Figure 58.

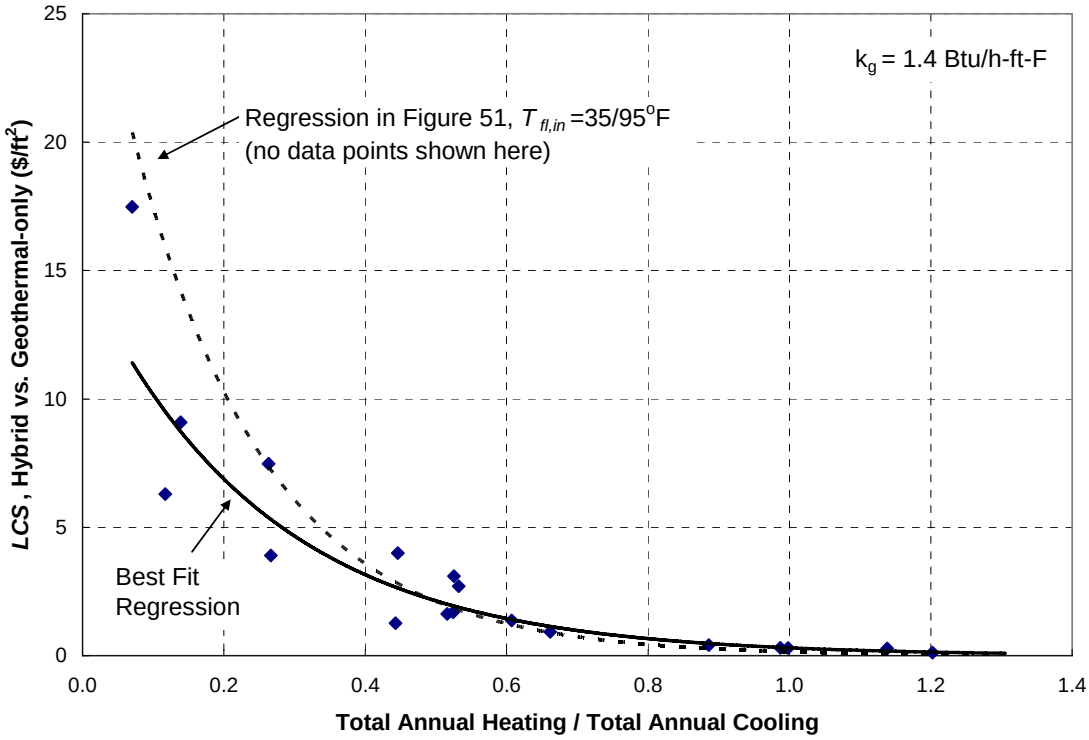

Figure 69. Life-cycle savings of hybrid systems over geothermal-only systems as a function of ratio of total annual heating load to total annual cooling load, for 20/110°F temperature limits (with results for 35/95°F temperature limits shown as the dotted line).

The *LCS* of a hybrid system relative to a conventional boiler/tower system (both optimized using the relaxed temperature limits) shows no clear relationship with the ratio of the annual heating to cooling loads. The major difference between the hybrid and boiler/tower systems is the use of a boiler in place of a GHX; therefore, the *LCS* of a hybrid system with the relaxed temperature limits relative to a boiler/tower system is shown in Figure 70 as a function of the peak heating load. Notice that the *LCS* increases approximately linearly with the peak heating load.

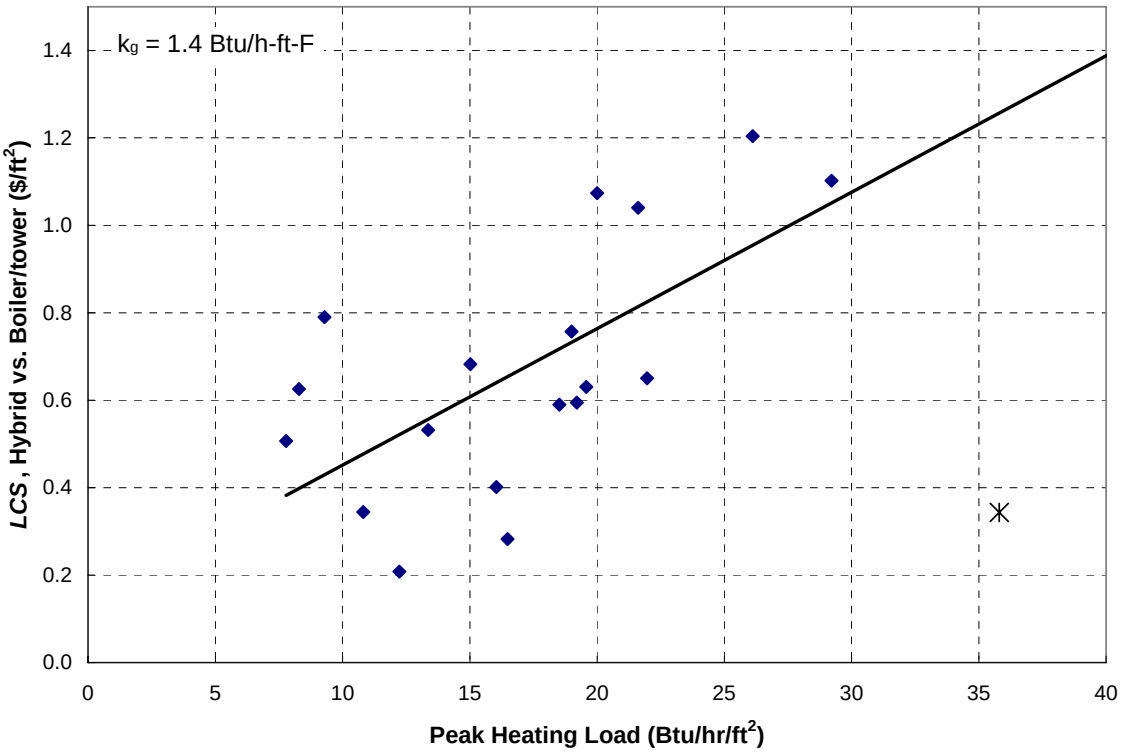

Figure 70. Life-cycle savings of hybrid systems over boiler/tower systems as a function of the peak heating load, for 20/110°F temperature limits.

Note the outlying data point in Figure 70 that is represented by a star (*); this data point represents the Phoenix school and does not appear to fit the trend for life-cycle savings. This outlier occurs because of the extremely small number of equivalent full-load hours (EFLH, the ratio of annual heating load to peak heating load) for heating in the Phoenix school; the average heating EFLH for the data points shown in Figure 70 is 1063 hr, whereas the EFLH for the Phoenix school is 83 hr (with the next lowest at 556).

The relationships between life cycle costs and climate are similar to those described for the 35/95°F cases. However, in the 20/110°F case, the hybrid configuration is *always* the most economical option in all of the climates (other than Minneapolis). The exceptions that were observed and discussed when using the 35/95°F temperature limits do not occur with relaxed

temperature limits because the GHX sizes are *much* smaller with the relaxed temperature limits. The first cost of the GHX is a smaller portion of *LCC* which allows the hybrid to be more cost effective relative to replacing the boiler for heating and the smaller GHX overlaps less with the cooling tower in cooling. (With limits of 35/95°F, the GHX meets a significant amount of the cooling load, though a cooling tower does so more cost effectively with the base case economic assumptions.)

Comparing Temperature Limits

Figure 71 illustrates the life cycle cost for the optimally designed hybrid systems in the various climate/building scenarios using both the 20/110°F and the 35/95°F temperature limits.

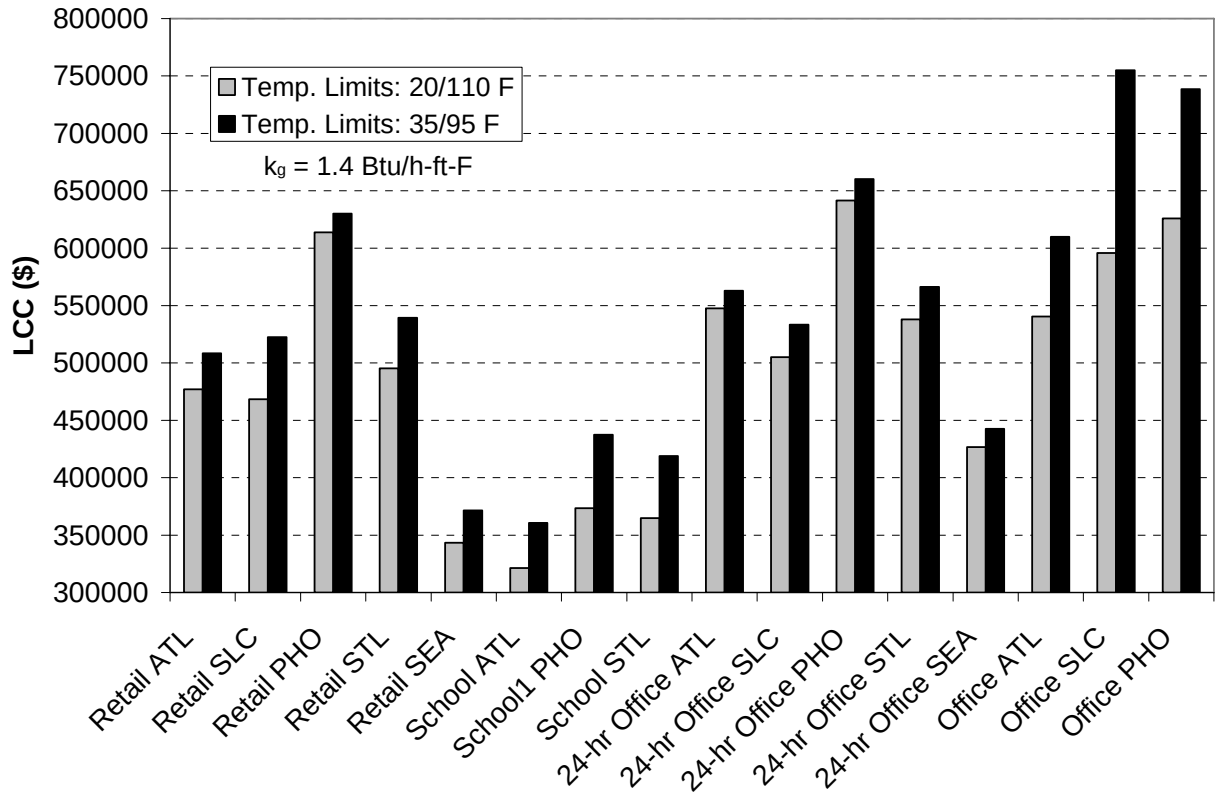

Figure 71. Life cycle cost of hybrid geothermal systems with two different sets of temperature limits, one set to 35°F and 95°F (providing some design margin) and the other set to the heat pump manufacturer's suggested temperature limits of 20/110°F.

Note that the 20/110^{o}F limits result in lower life cycle costs for all cases; in this model, the *LCC* is always lower when the design temperature limits are relaxed. This is primarily due to reduction in the optimal GHX sizes; the GHX size for the relaxed temperature limits are roughly half the size required for the scenarios with 35/95^{o}F temperature limits.

However, with the relaxed temperature limits there will be an increase in heat pump equipment cost that is not included in the *LCC* presented in Figure 71. The capacity of each heat pump is lower when the entering fluid temperature is allowed to fluctuate over a wider range (i.e., on average the heat capacity will be lower when operating with the 20/110^{o}F as opposed to the 35/95^{o}F temperature limits). Therefore, slightly larger and more expensive heat pump units are required when the relaxed temperature limits are used. As shown in Figure 72, the heat pump capacity would need to be 15-20% larger in heating constrained cases, and 5-10% larger in cooling-constrained cases (the majority of those considered). One limitation of the HyGCHP model used in the parametric study is that it does not include the cost of the equipment within the building (and therefore the cost of the individual heat pumps); therefore the change in the cost of the heat pumps that results from relaxing the temperature limit is not included in Figure 71. If this additional heat pump first cost were accounted for then the difference between the two sets of costs in Figure 71 would decrease somewhat. However, there would still be a significant difference in cost due to the larger change in GHX costs (over 50%) between the two sets of cases. This idea was tested after the parametric study by re-running some cases with a cost penalty included in the total equipment cost, equal to the cost of purchasing the slightly larger heat pumps that are required at relaxed temperatures. In almost all cases the relaxed temperature case still had a lower *LCC*. Optimal equipment sizes changed, but only slightly.

This heat pump cost penalty has been included in the distributable version of the model, so *LCC* at different operating temperatures can be compared directly by users.

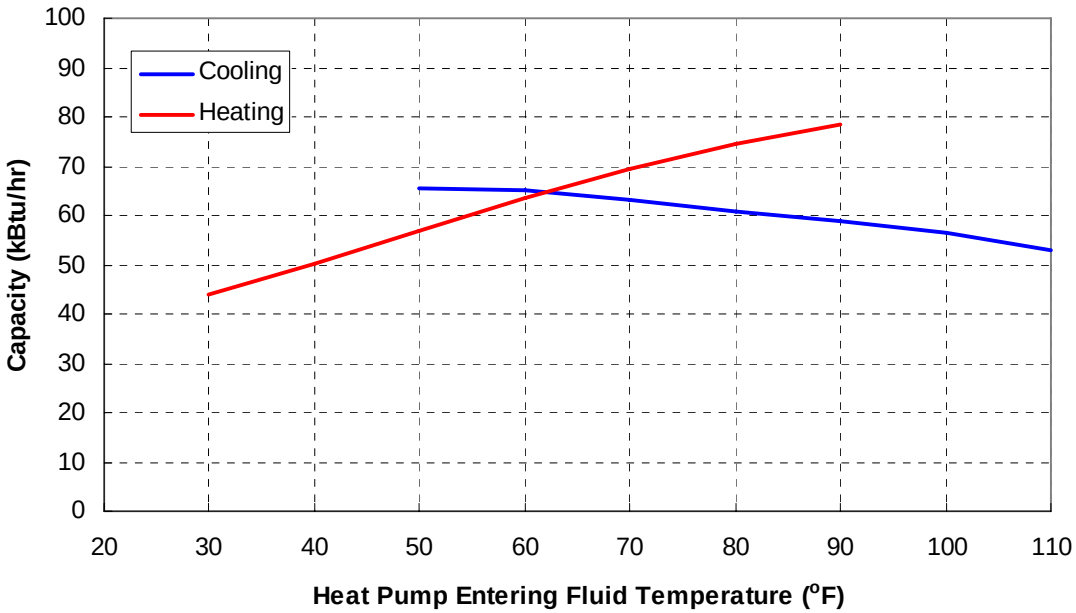

Figure 72. Cooling and heating capacity of a typical heat pump as a function of the entering fluid temperature. A 15°F increase in temperature results in a 15-20% increase in heating capacity and a 5-10% decrease in cooling capacity.

4.4.4 System with Dry Fluid Cooler – Relaxed Temperature Limits

In this section, the optimum design guidelines and life cycle savings for the dry fluid cooler are compared with those for the cooling tower, for the relaxed temperature limits of 20/110°F.

Optimal Design Trends

The dry fluid cooler is used in the hybrid model in the same way as the cooling tower; the only difference is in the controls, where ΔT_1 becomes the difference between the fluid temperature entering the dry fluid cooler and the ambient dry bulb temperature (ambient wet bulb temperature was used for the cooling tower).

The optimal GHX size for the hybrid with a dry fluid cooler is roughly the same as for the hybrid with the cooling tower (when the same temperature limits are used). The design trend in Figure 51 is therefore still valid. However, the optimal dry fluid cooler size and control setpoints are very different when the system is optimized with 20/110°F limits as compared to the 35/95°F temperature limits. This is because at 20/110°F the cooler operates with a driving temperature difference (i.e., fluid to ambient dry bulb) that is similar to the driving temperature difference seen by the cooling tower (i.e., fluid to ambient wet bulb); therefore, with the 20/110°F temperature limits the optimal size of the dry fluid cooler is similar to the optimal size of the cooling tower (this was not the case for 35/95°F; see Section 4.4.2). Figure 73 demonstrates this result by plotting several optimal dry fluid cooler sizes with the best fit curve for optimal cooling tower size.

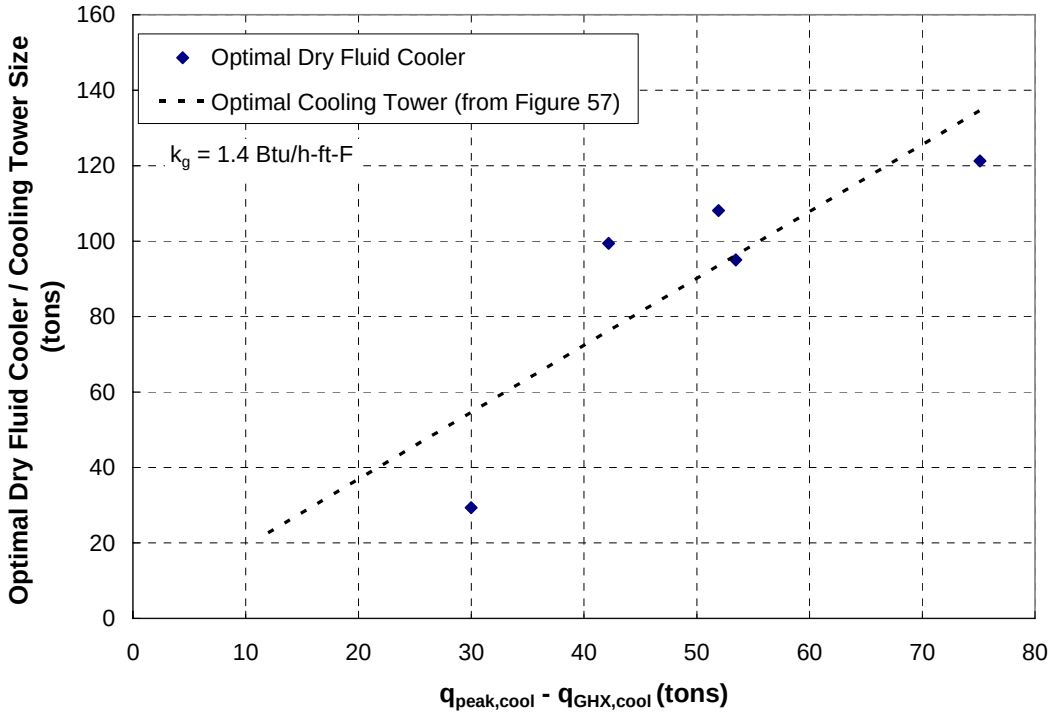

Figure 73. Optimal dry fluid cooler size plotted as a function of the cooling load not met by the GHX, for relaxed temperature limits (20/110°F). The curve represents the optimal size for the same scenarios but with a cooling tower configuration.

The optimal control setpoints with the relaxed temperature limits are different for the dry fluid cooler and cooling tower hybrid configurations. The optimal value of ΔT_1 (the differential setpoint determining operation of the dry fluid cooler) is relatively constant, at 10 to 15°F. This set point is comparable to the set point identified for the cooling tower in moderately humid climates. However, as Figure 74 demonstrates, for a drier climate (like Salt Lake City) the value of ΔT_1 increases for the cooling tower because the increased evaporation allows the cooling tower to turn on less often (which saves energy), but ΔT_1 for the dry fluid cooler remains at 10 to 15°F.

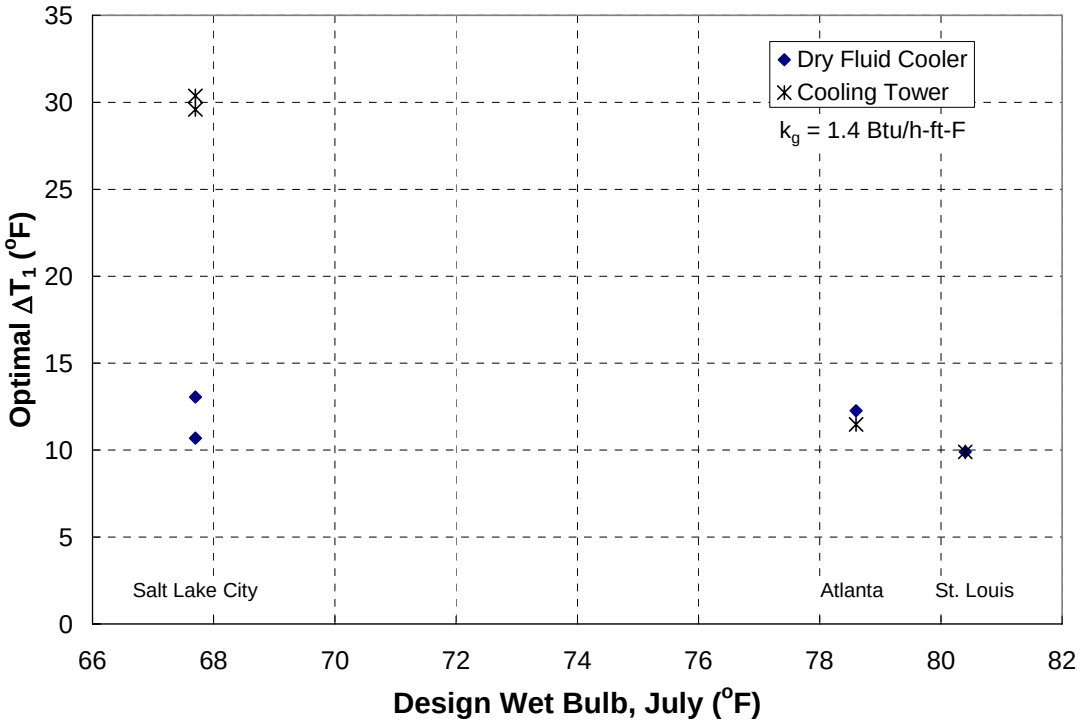

Figure 74. Optimal values of ΔT_1 plotted as a function of the ASHRAE design wet bulb temperature in July for the location in each scenario. Values are compared between cooling tower and dry fluid cooler configurations, both for 20/110°F operating temperatures.

Optimal values of T_{Cool1} (high-speed control setpoint for the dry fluid cooler) are generally found to be 60 to 70°F which allows the dry fluid cooler to operate at high speed during periods of significant cooling load.

Life Cycle Cost Trends

The *LCC* of a hybrid system with a dry fluid cooler is similar to that of a hybrid system with a cooling tower (see Figure 75); therefore, the same cost trends discussed in Section 4.4.1 for the cooling tower hybrid are observed for the dry fluid cooler hybrid. In general, the *LCC* associated with a dry fluid cooler hybrid is less than a conventional boiler/tower configuration, but a little higher than the hybrid cooling tower configuration.

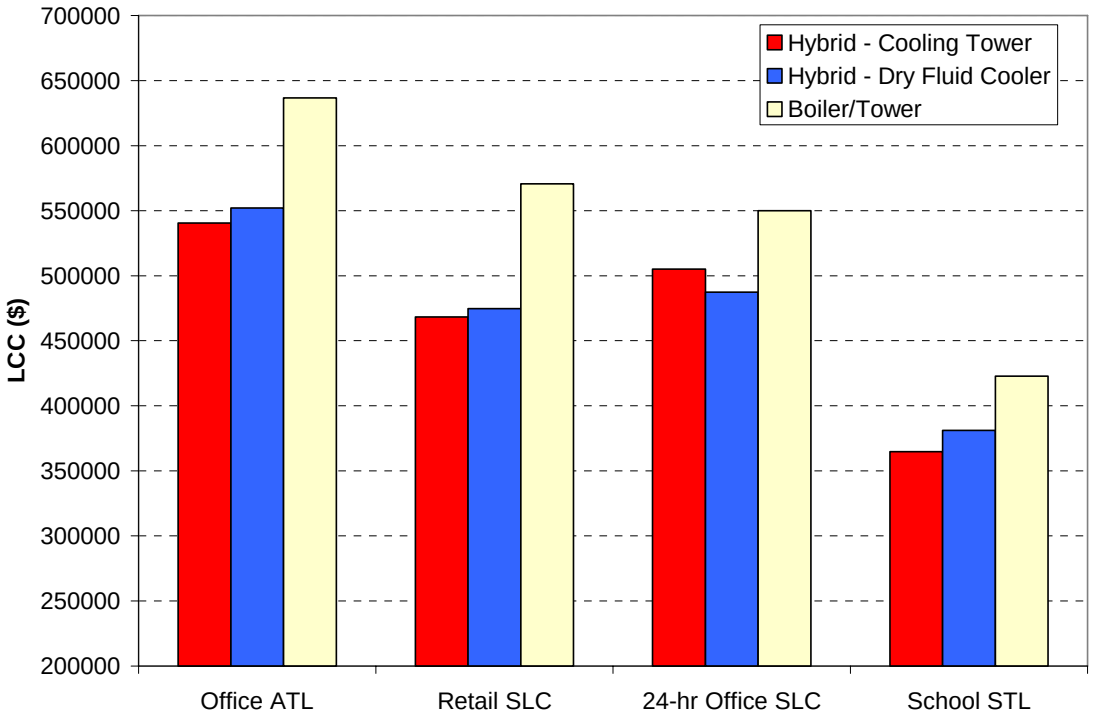

Figure 75. Life cycle cost comparison between hybrid geothermal heat pump systems with a dry fluid cooler versus a cooling tower; conventional boiler/tower system shown for reference. These results are for systems with 20/110°F temperature limits.

4.5 Results – Heating Dominated System

The primary market for hybrid ground-coupled heat pump systems in the United States is for cooling dominated buildings; however, it is possible that a similar strategy of hybridization could also result in lower *LCC* for heating dominated buildings. With this in mind, a separate model was created for studying heating-dominated hybrid systems. Three different configurations were considered: geothermal-only, a hybrid geothermal using solar panels as the supplementary heat extraction system, and a hybrid geothermal using a boiler as the supplementary heat extraction system.

The building loads used in the heating-dominated study are for the school building, which is by nature a more heating dominated building than the other three building types discussed in Section 4.2. The input parameters that were used to simulate cooling-dominated systems (summarized in Table 9) are also used for the model components in the heating-dominated systems except that a higher concentration of propylene glycol (23%) is used due to the colder temperatures. The relaxed temperature limits (20/110^{o}F) are used for these scenarios. All configurations were initially run in the Minneapolis climate; initial results demonstrated a need to study an even colder climate and therefore the Edmonton, Alberta climate was also considered.

The key *LCC* results of the heating-dominated system study are shown in Figure 76 for Edmonton and Minneapolis climates. It is immediately apparent why an additional scenario was added to study the heating dominated configurations. In the Minneapolis scenario, the boiler hybrid has only a *slightly* smaller *LCC* than the geothermal-only case. It is likely that the Minneapolis climate is very close to the breakeven climate where adding a boiler is economically justified. Though buildings in Minneapolis are heavily heating dominated, the annual unbalance

between heating and cooling is still small enough that a geothermal-only system is competitive with the hybrid and economically viable.

Also notice that the hybrid solar configurations optimized the supplemental device (i.e., the solar panels) to zero in both climates so that the hybrid solar system shown in Figure 76 is, in effect, a geothermal only system.

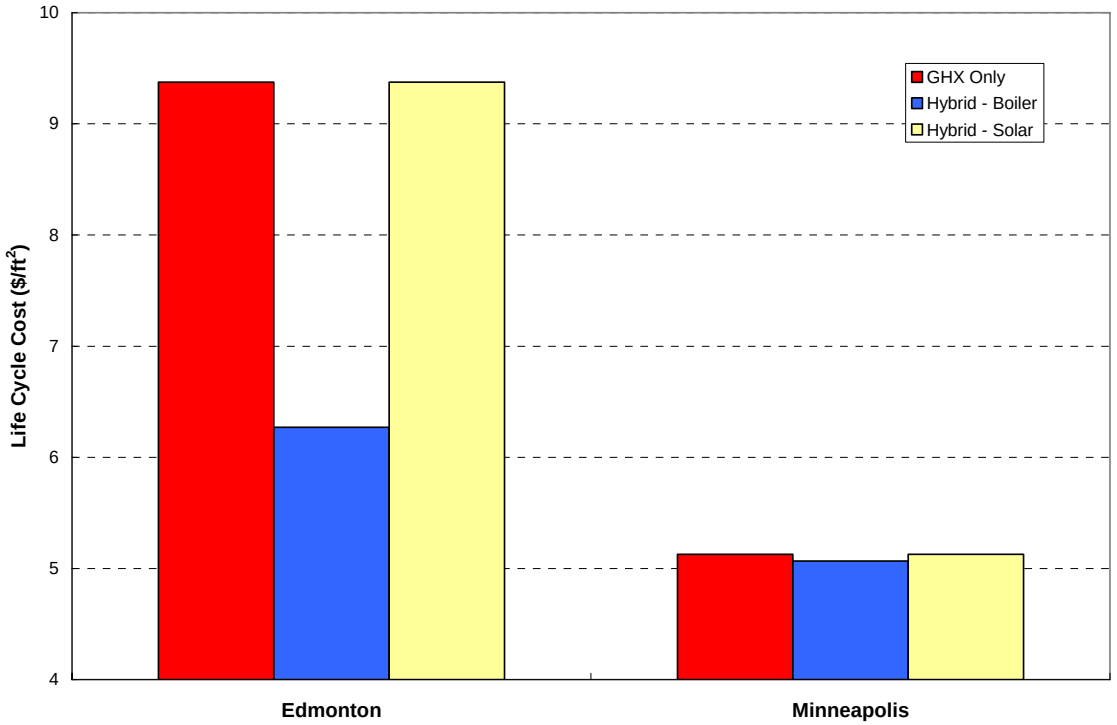

Figure 76. Life-cycle cost of different geothermal heat pump systems in Edmonton and Minneapolis.

In Edmonton, the cost of operating a geothermal-only system is significantly greater than in Minneapolis. In this heavily heating dominated climate, a significant savings ($3/ft^2) can be obtained by using a hybrid geothermal system with a boiler rather than a geothermal-only system. It is important to note that even in the heavily heating dominated Edmonton climate, the hybrid solar system still optimizes the solar system to become a geothermal-only system (by driving the solar array size to zero). The first cost of solar thermal systems is high enough that

they cannot save money against increases in GHX size. This result is a strong indication that hybrid solar systems will not be economical for any building or climate under the economic assumptions used to carry out this analysis. Note that this statement does not cover systems with direct solar heating systems that bypass the heat pumps.

Optimal Design Trends

Because only two data points were studied, it is not possible to correlate complete trends that characterize the heating dominate cases. However, based on the lessons learned by examining the optimal cooling-dominated systems, some reasonable conclusions can be drawn for the heating-dominated systems.

In geothermal-only configurations for both cities, the size of the GHX is based on the peak heating load. The GHX must be large enough to satisfy this peak load without violating the minimum entering water temperature limit. In Figure 77 the optimal GHX length (in ft/ton) is plotted as a function of the initial ground temperature (just as it was for cooling dominated systems, in Figure 66; the curve for those cooling-dominated systems is also shown in Figure 77 for reference). Note that a larger GHX is required to meet the heating load in the heating dominated systems (122 ft/ton of heating in Minneapolis and 318 ft/ton in Edmonton) than was required to meet the peak heating load in the cooling dominated cases. This is due to the unbalanced loads, which leads to a gradual cooling of the ground over time for the heating dominated cases.

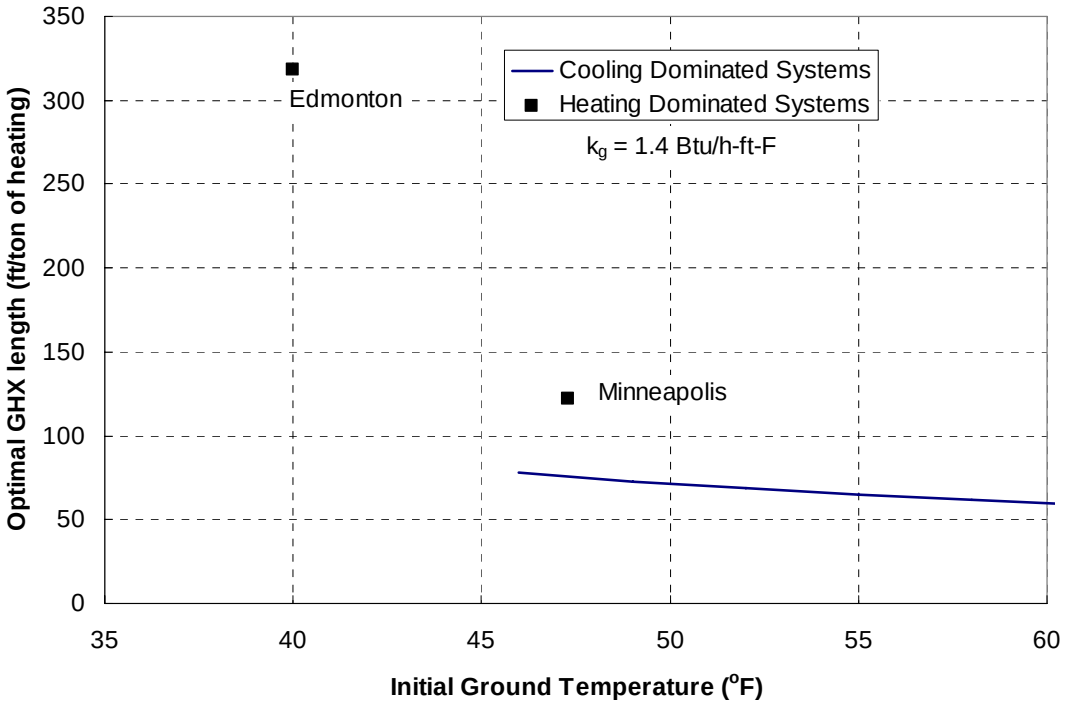

Figure 77. Optimal GHX size for heating dominated geothermal-only systems as a function of initial ground temperature, compared with the trend for cooling dominated systems. All cases are for temperature limits of 20/110°F.

In the cooling dominated systems that were studied, the optimal system resulted in a GHX that was sized to completely meet the peak heating load, and the supplementary heat rejection device (i.e., the cooling tower or dry fluid cooler) is sized to meet whatever portion of the cooling load is not met by the GHX. The hybrid systems using a boiler for the heating dominated climates studied here follow this same pattern, with the seasons reversed. The optimal GHX appears to be sized to meet the peak cooling load and the boiler is sized to meet whatever portion of the heating load is not met by the GHX. The GHX size can be estimated according to 90 to 95 ft/ton of cooling. The boiler then supplies whatever heating is not met by the GHX. This optimal boiler size varies from 69% of the peak heating load in Minneapolis to 80% of the peak heating load in Edmonton (as shown in Figure 78). This result represents a fundamental change from the other climates studied in this report. As far north as St. Louis and

Seattle, there was significant savings in using a GHX to meet the heating load in place of a boiler (for example, see Figure 70). But for the Minneapolis school, we begin to see a slight savings in using a boiler to displace the GHX for heating. Both the load unbalance *and* the ground temperature T_g likely play a role in this fundamental change (as demonstrated in Figure 79); both of these climatic parameters are significantly different from the other climates studied herein (other climates had an average T_g of 60oF and an average peak load ratio of 1.6).

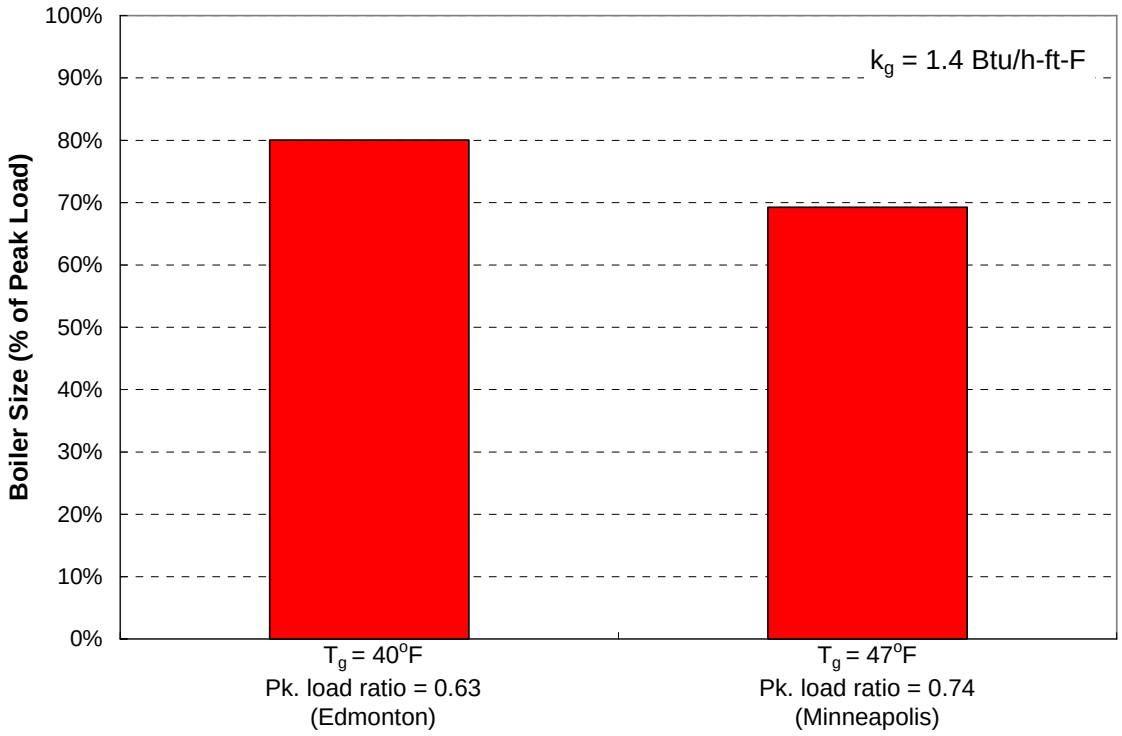

Figure 78. Optimal boiler size for heating dominated geothermal-only systems as a fraction of the peak heating load, plotted for two different climates. Peak load ratio is the ratio of peak cooling to peak heating load. Both cases are for temperature limits of 20/110°F.

Optimal control setpoints are also studied for the two systems. For the geothermal-only systems, the optimal heating setpoint (T_{Heat1}) is high enough that the GHX is never bypassed (similar to the cooling-dominated systems). In the boiler/geothermal hybrid system, the optimal value of T_{Heat1} is 50-60°F, so the GHX is still only bypassed for short periods at the beginning of

a heating period. The boiler is then operated when the temperature entering the boiler drops below about 34^{o}F (due to this low operating temperature, energy from the boiler is never lost to the ground).

4.6 Results – Other

4.6.1 Timespan of Simulation

The length of simulation time has been observed to have a significant effect on the optimal design values resulting from the HyGCHP model. The reason for this behavior is due to the build-up of energy in the ground in cooling-dominated systems and, conversely, the draw-down of energy in heating dominated systems; both of these effects lead to ground temperature change over time. Even the optimal hybrid geothermal systems are operated in a way in which the ground near the GHX changes in temperature over time (this is economically the most optimal solution for any given timespan). It is therefore informative to consider the effect of simulation timespan on the results. Figure 79 shows the required GHX size for a retail building (cooling-dominated) in Salt Lake City as a function of the number of years of simulation. In the base case, with temperature limits of 35/95^{o}F, the required GHX size increases by 50% when going from a 5 year simulation to a 20 year simulation. The effect is smaller with relaxed temperature limits, because the annual net heat rejection is smaller. The increased length required with time could be reduced somewhat if the borehole spacing was increased.

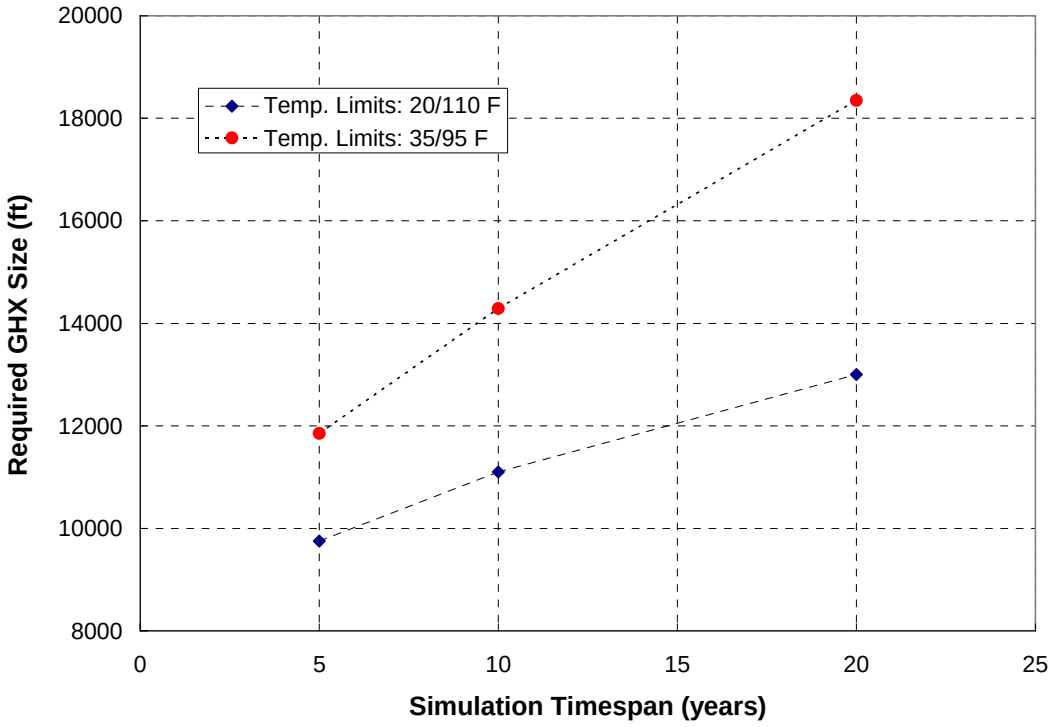

Figure 79. Required GHX size for a retail building in Salt Lake City assuming different lengths of simulation time. The results in this study assume 20 years of simulation. Values are given for two different sets of temperature limits.

Note that the slope of the 20/110°F curve in Figure 79 decreases as timespan increases, reflecting the fact that ground temperature changes are more gradual at 20 years than at 2 years though there is still significant slope even at 20 years; the same trend would likely be true for the 35/95°F curve if larger timespans were modeled. As discussed above, the parametric study results herein have been created using 20-year simulations in order to be consistent with ASHRAE (Kavanaugh, 1997) and other geothermal design tools (as discussed in Section 3.2.9). The distributable version allows for other timespans to be chosen as well, though 20 years is recommended.

It is important to consider the fact that the HyGCHP assumes low groundwater movement in these cases. For cases of significant groundwater movement, the heat buildup and resulting temperature increase would be partially mitigated. To compensate for groundwater

movement, some design algorithms have simply calculated the required GHX size for a shorter timespan, such as 1 year, for areas known to have heavy groundwater flow (Kavanaugh, 1997). Figure 79 demonstrates this approach will result in a substantially smaller GHX. There is potential for the user of the distributable version to use the timespan in the distributable as a method of compensating for groundwater flow, but additional study would be required to quantify a relationship between timespan and groundwater flow.

4.6.2 Sensitivity Studies

In addition to the parametric studies carried out at the baseline conditions over a range of buildings and climates, discussed in detail in the previous sections, a sensitivity study is carried out in which the key parameters appearing in the list of inputs in Table 9 (see Section 4.3 above) are varied from their baseline values in order to understand their importance and the impact of variations in these values. From the list of inputs in Table 6, the variables that are expected to have the largest effect on the results (i.e., on the *LCC*, equipment size, and control set points) are chosen as variables for the sensitivity study; these are summarized in Table 11. Note that the expected 'effect' on results is a function not only of the direct dependence of the results on the parameter, but also on the magnitude of the uncertainty that the parameter's assumed value will represent typical cases. For example, inputs like initial ground temperature have significant impact on results but are not varied in the sensitivity study because a reasonable, single value of initial ground temperature can be selected with some certainty for each case.

	Variable Range
GHX Cost (installed, $/ft.)	**6……..25**
Fuel cost: elec., demand, gas (% of avg.)	**75%.....150%**
Fuel inflation (%)*	**0%.....10%**
Loan: % down, rate (%)*	**5% / 3.5%.....50% / 9%**
Discount rate (%)*	**6.5%.....9%**
Tax deductibility*	**No.....Yes**
Ground conductivity (Btu/hr-ft-F)	**0.76.....1.40**

Table 11. Variables for parametric study; ranges are given for each parametric variable. (*) denotes that the parameter can be included in the non-dimensional parameters P_1 and/or P_2, discussed below.

It is important to note that the economic parameters that are denoted with an asterisk in Table 8 can be mapped onto the economic factors P_1 and P_2. As discussed in Section 3.2.9, the effect of the general economic parameters (e.g., discount rate, fuel inflation, etc.) can be represented by two non-dimensional variables, P_1 and P_2, which are defined by Duffie and Beckman (2006). This representation reduces the number of simulations that are required to study those parameters that are denoted with an asterisk. For example, if optimization results are plotted with respect to P_1, the effect of varying fuel inflation rate can be determined by mapping a change in fuel inflation rate onto a change in the variable P_1. A summary of the specific simulations that were run to accomplish the sensitivity study is shown in Table 12 below for reference (with the notation that is used to indicate each case in the remainder of this section shown in bold).

Base:	Base case, with all parameters set to default values.
GHX $:	variants of GHX cost per meter; for the Atlanta scenario varied to a low value of $6/ft or high value of $20/ft
% Fuel:	variants of default fuel cost (electricity and gas) by percentage; varied between 75% and 150% of default values, respectively.
k_g:	variant of ground conductivity; low value (0.8 Btu/hr-ft-^{o}F) is 55% of default value (1.4 Btu/hr-ft-^{o}F). (high value is used as default because geothermal projects are more likely to be sited in areas of favorable ground conductivity)
Market scenarios:	
Econ1:	fuel inflation raised to 7.5% (default is 1.6%)
Econ2:	down payment raised to 75% (default is 30%) and loan rate raised to 10% (default is 6%)
Econ3:	discount rate lowered to 4% (default is 8.5%)
Econ4:	not-for-profit (tax-exempt) organization assumed and discount rate lowered to 5%

Table 12. Parametric cases in the sensitivity study. Notation used in the remainder of this report is shown in bold.

The ten parametric studies listed in Table 9 were simulated in order to understand the impact of the variables listed in Table 11 over the associated range of values for several of the base case building/climate scenarios. These sensitivity studies were carried out for boiler/tower, geothermal-only, and hybrid configurations.

Sensitivity Example: Office building, Atlanta climate

The sensitivity study is best discussed in the context of an example; in this section, the results observed for a 127,000 ft^2 office building in Atlanta (a warm climate) are discussed. The observations presented for this example are fairly typical of the results for other climates and buildings; however, in places where substantial differences are observed, these are noted. The specific simulations discussed in this section are listed above in Table 12.

Optimized design values vs. GHX cost. The optimal value of each of the design parameters (i.e., each of the parameters controlled by the optimizer) are shown in Figure 80 as a function of the GHX cost (in $/ft) for the hybrid system. As the GHX cost rises, the optimized size of the GHX and cooling tower remain constant. This result is typical for all cases studied and indicates that the optimization of the equipment is not driven by the economics but rather by the requirement that the GHX be capable of meeting the peak heating load. It is not economically attractive to purchase additional GHX beyond what is required to meet the building loads, even at the lowest GHX cost. In a few cases, the lowest value of GHX cost ($6/ft) does lead to a slightly larger optimal GHX size, indicating that if the GHX cost is sufficiently low then the energy savings associated with a larger GHX justifies its additional cost.

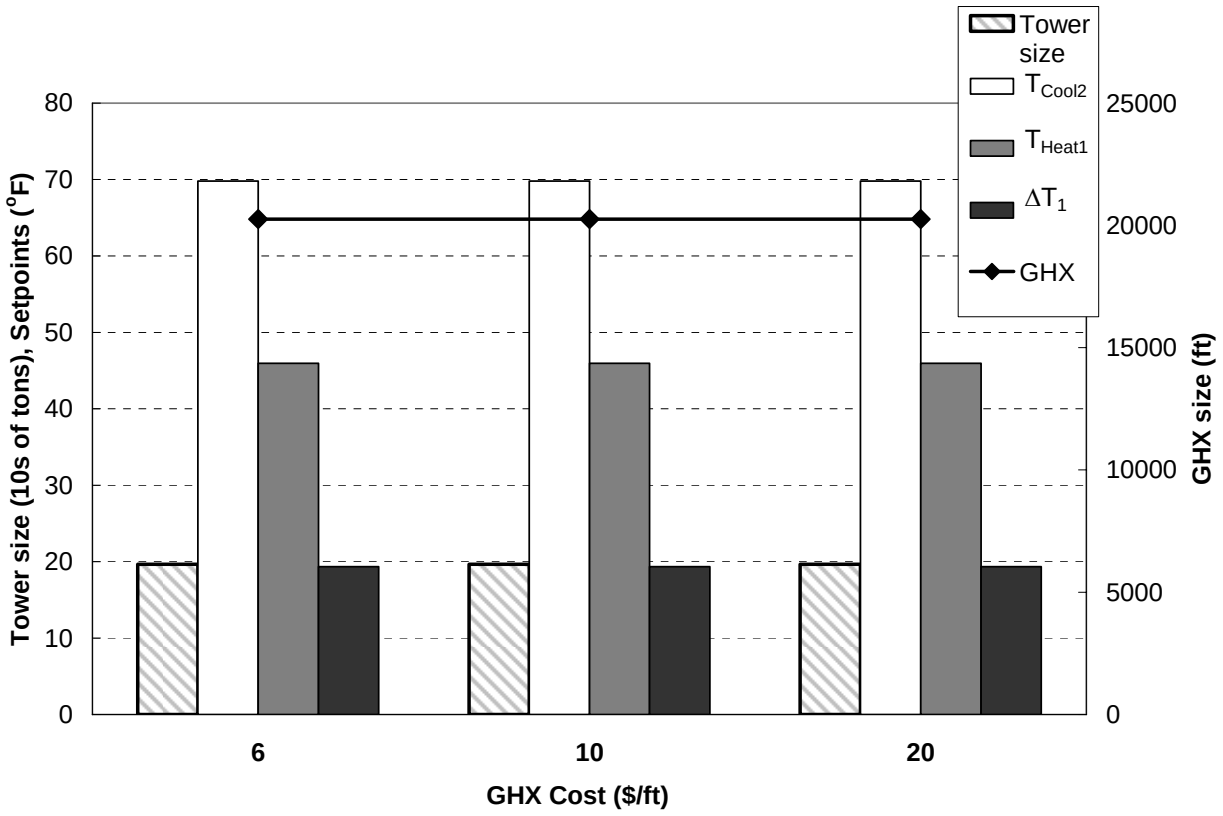

Figure 80. Optimized hybrid design values plotted as a function of GHX cost. Results are for an office building in Atlanta.

In Figure 81, the optimized values of the design parameters are shown as a function of the GHX cost (in $/ft) for the geothermal-only (i.e., non-hybrid) system. In this case the GHX size is an order of magnitude greater than in the hybrid configuration because the GHX must be sized to meet the cooling load (which is much greater than the heating load). GHX cost has no effect on the optimal design for this configuration (it is already set as low as possible to still meet the peak cooling load). This, again, is typical.

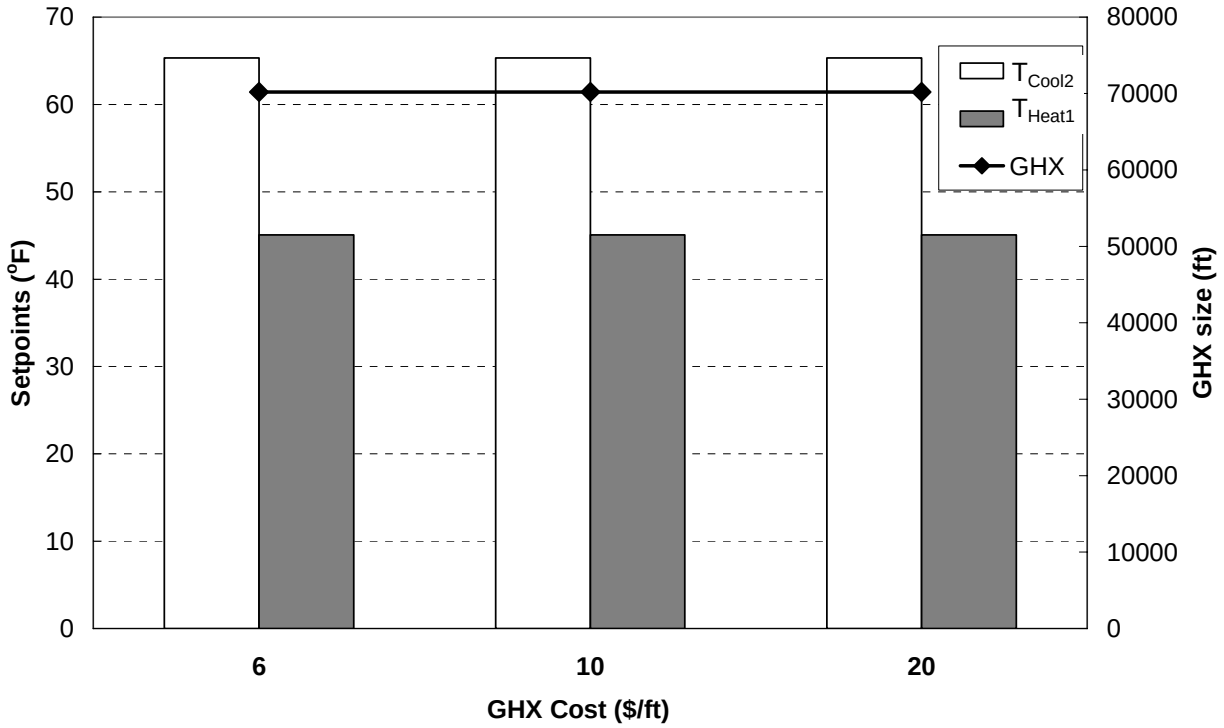

Figure 81. Optimized GCHP design values plotted as a function of GHX cost. Results are for a office building in Atlanta.

Optimized design values vs. fuel cost. In Figure 82, the optimized values of the design parameters are shown as a function of the fuel cost (the market price of electricity and gas) for the hybrid system. Notice that moderate changes in fuel cost do not cause any significant change in the optimal GHX; this observation reinforces the fact that the optimizer is sizing equipment in a way that exactly meets loads but not purchasing any additional equipment beyond this minimum requirement in order to save additional energy. At very high fuel costs (beyond the range shown in Figure 83) this trend must break down and the GHX size would increase.

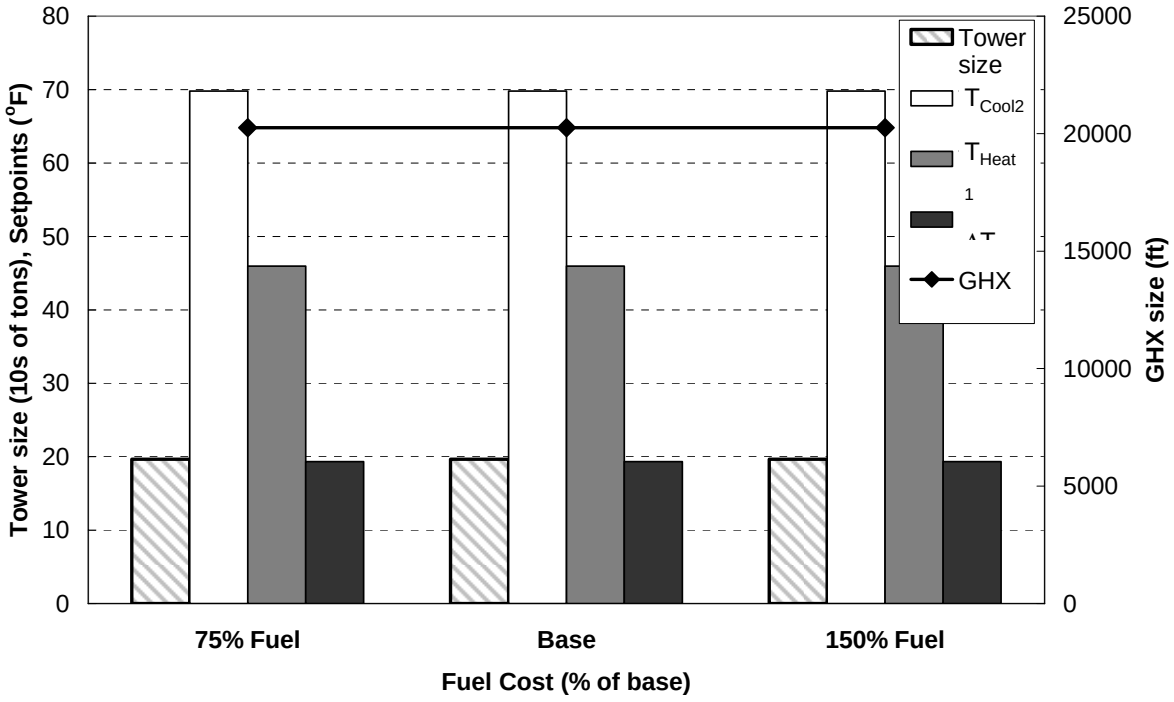

Figure 82. Optimized hybrid design values plotted as a function of fuel cost. Results are for a office building in Atlanta.

In Figure 83, the values of the optimized design parameters are shown as a function of the fuel cost for the conventional boiler/tower heat pump system. Note that boiler size is listed as the size normalized against a 35 kW (120 MBtu/h) boiler. The cooling tower size increases by about 10% when the fuel cost is increased to 150% of the default value. This result occurs in many of the scenarios; the higher fuel cost makes it economic to purchase a larger cooling tower and allow the heat pumps to operate at more moderate temperatures and thereby, higher efficiency. However, the change in the cooling tower size is not large over the range of fuel costs studied.

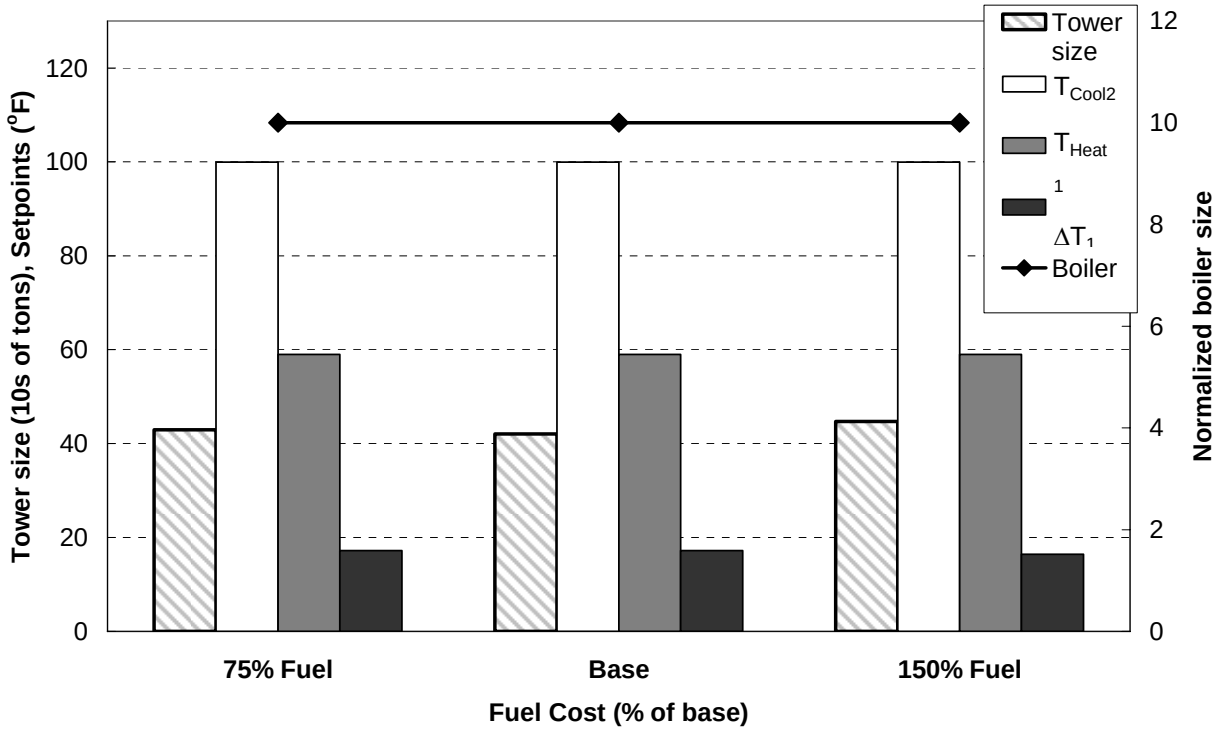

Figure 83. Optimized design values plotted as a function of fuel cost for a conventional boiler/tower system. Results are for a office building in Atlanta.

Optimized design values vs. ground conductivity. In Figure 84, the values of the optimized design parameters are shown as a function of the ground conductivity (k_g) for the hybrid system. The GHX size must increase as the ground conductivity is reduced in order to meet the peak loads. The cooling tower size decreases slightly with lower k_g; but remains relatively constant because the increase in the GHX size increase has roughly the same effect on its cooling capacity as its heating capacity and therefore the unmet cooling load that must be provided by the tower remains approximately constant. In fact, the cooling tower size may either increase or decrease slightly for the 'Low k_g' case in different climates, depending on the load balance associated with the scenario.

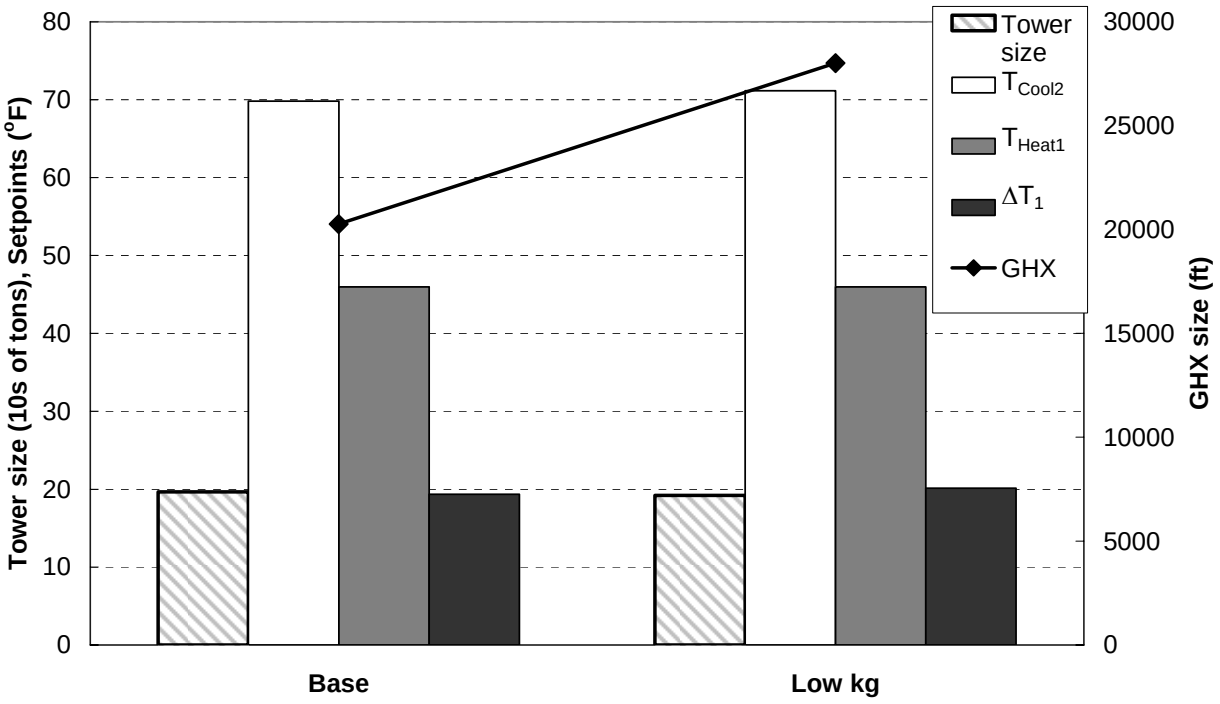

Figure 84. Optimized hybrid design values plotted as a function of ground conductivity. Results are for a office building in Atlanta.

Optimal design parameters are observed to have a much larger sensitivity to ground conductivity than to the economic parameters. The optimal GHX size increases for the low conductivity case in almost all building climate scenarios. The decrease from 1.4 Btu/hr-ft-^{o}F (in the base case) to 0.8 Btu/hr-ft-^{o}F leads to an average increase in GHX size of 29%. In other words, for every 0.1 Btu/hr-ft-^{o}F decrease in conductivity, the GHX size increased by about 5%. This increase is necessary to retain the required heating load capability of the GHX with lower ground conductivity, but it also maintains the same cooling capacity of the GHX. Therefore, the change in the cooling tower size with ground conductivity is generally smaller. The change in GHX size generally always had an impact on the optimal value of the control set point T_{Cool2} as well. T_{Cool2} decreases by an average of 9^{o}F when the ground conductivity was reduced from 1.4

Btu/hr-ft-^{o}F (in the base case) to 0.8 Btu/hr-ft-^{o}F; this decrease in the control set point serves to decrease (albeit only slightly) the amount of time in which the GHX is bypassed in cooling mode.

Optimized design values vs. economic parameters. In Figure 85, the values of the optimized parameters are shown for different market cases, labeled 'Econ1' through 'Econ4' (complete descriptions of these cases are in Table 12). As with other economic sensitivities, none of these changes in the market conditions has a significant effect of the values of the design parameters.

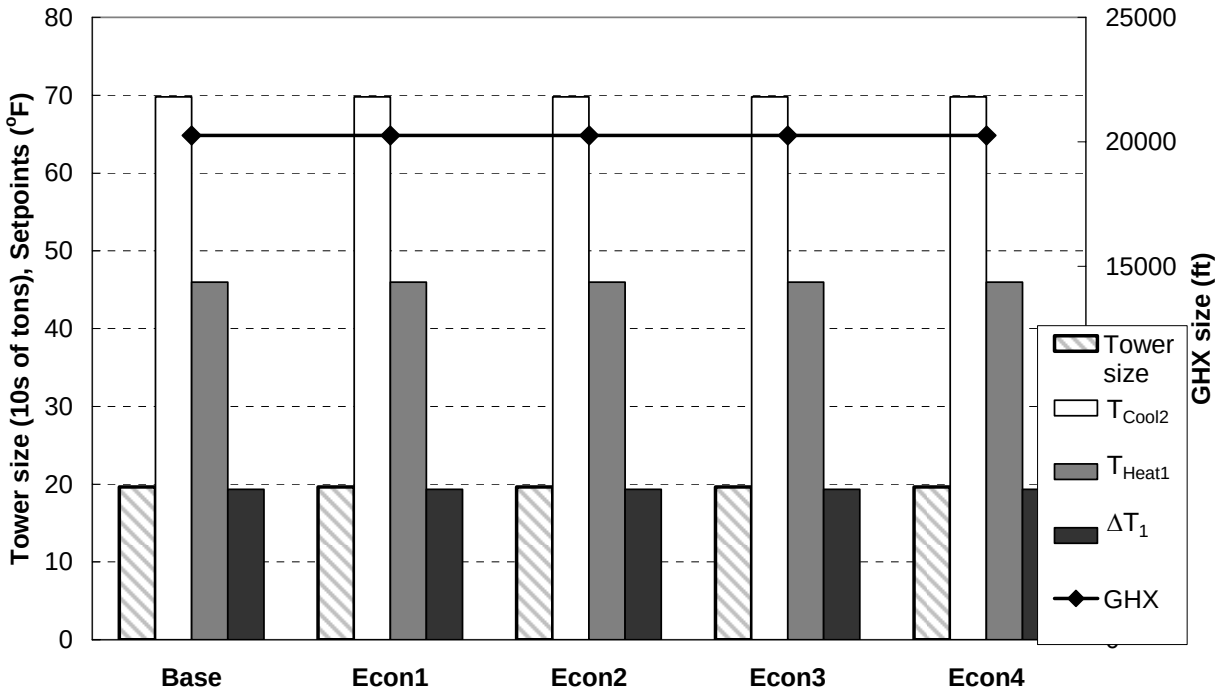

Figure 85. Optimized hybrid design values plotted for different economic scenarios. Results are for a office building in Atlanta.

In Figure 86, the values of the optimized design parameters for a conventional boiler/tower heat pump system are shown for different values of the market conditions. The only significant change occurs in the design occurs for the 'Econ1' case corresponding to an increase in fuel inflation; 'Econ1' results in a 30% increase in optimum boiler size. The larger boiler

allows the heat pumps to operate at more moderate temperatures and therefore achieve better efficiency; this is typical. In some scenarios, the cooling tower size follows a similar trend (i.e., its size increases slightly for the 'Econ1' case corresponding to higher fuel inflation).

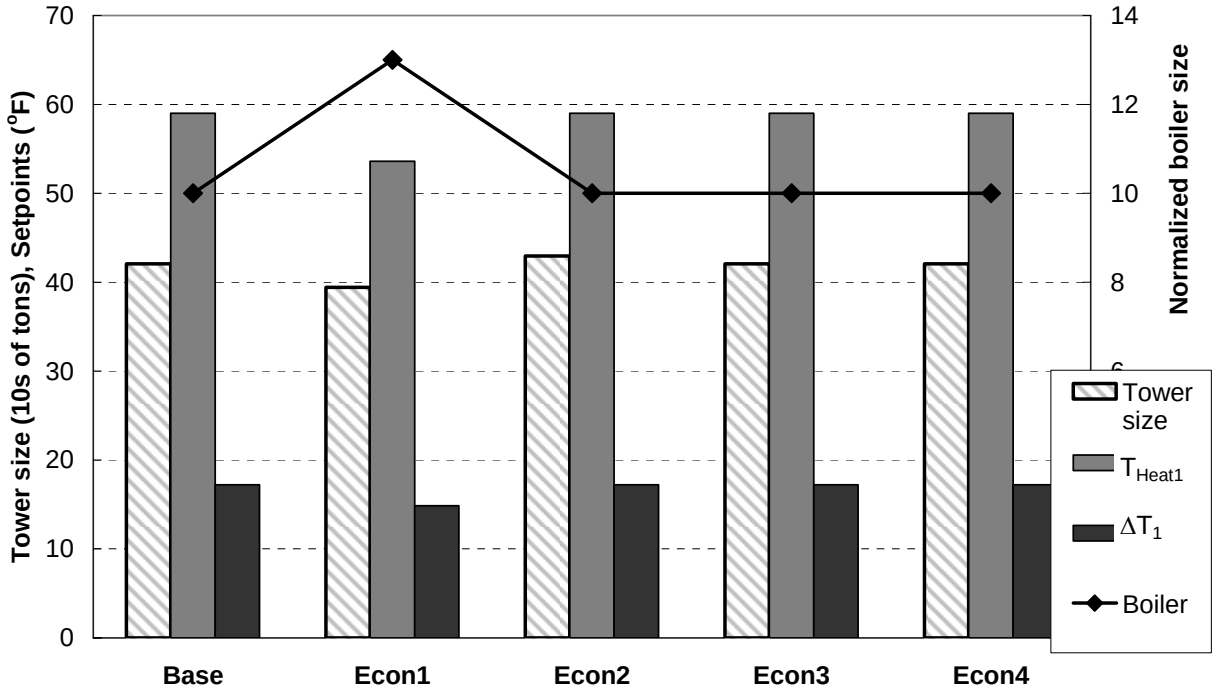

Figure 86. Optimized design values for a conventional boiler/tower system plotted for different economic scenarios. Results are for an office building in Atlanta.

Life Cycle Cost. Some specific sensitivities of the *LCC* were discussed in Section 4.4.1, but it is beneficial to describe the specific sensitivity of *LCC* for the Atlanta office case as this will allow a more complete understanding of the effects of the ten parametric cases listed in Table 12. The life cycle cost for each of the parametric cases is shown in Figure 87 for the Atlanta office building. The hybrid system generally has the lowest *LCC*, followed by the conventional boiler/tower heat pump system. The pure geothermal system is generally significantly more expensive than either of these alternatives; this is due to the large imbalance between cooling and heating loads associated with this particular building/climate combination.

(though in the parametric study corresponding to low GHX cost, the geothermal-only system is cheaper than the boiler/tower). As expected, as fuel cost or GHX cost increases, so does *LCC*. Lower *LCC* values are observed for the hybrid system (over the conventional boiler/tower) when 1) the first year fuel cost is high or 2) the GHX cost is low (and vice versa for low fuel costs and high GHX costs). This effect of fuel cost occurs because the GHX is less fuel intensive than the conventional equipment. The Low k_g case results in increased cost for the hybrid and GCHP systems due to the need for a larger GHX in order to meet the load.

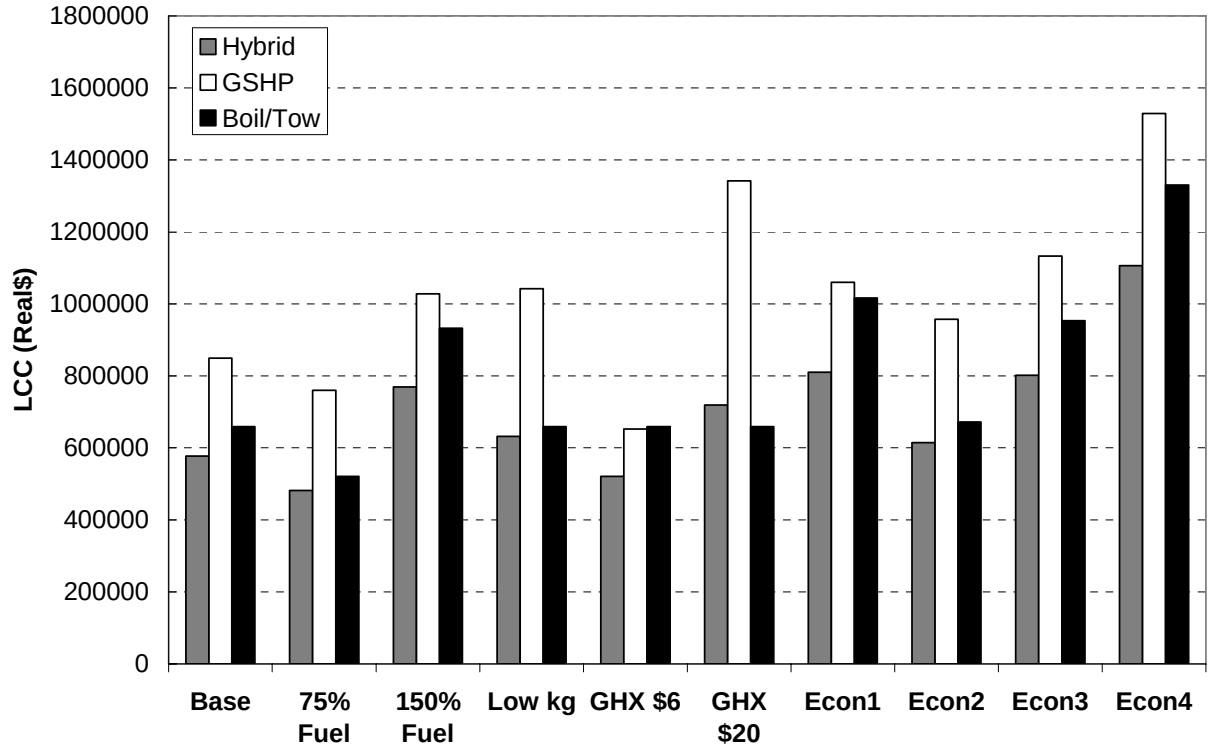

Figure 87. Life cycle costs for three heat pump systems with a range of sensitivities. Results are for a office building in Atlanta.

Varying the economic market parameters ('Econ1' through 'Econ4') affects all three configurations. The 'Econ1' scenario corresponds to larger fuel inflation and therefore leads to a result that is very similar to the 150% Fuel case; the hybrid system is more attractive, and the GHSP configuration compares more favorably to the boiler/tower system – although it is still

less attractive. In the 'Econ2' scenario, corresponding to poor loan terms, the cost of capital investment increases which closes the gap between the equipment-intensive hybrid case and the conventional boiler/tower (this also makes the very equipment-intensive geothermal-only much less attractive). In both the 'Econ3' and 'Econ4' cases, which both correspond to reduced discount rates, both of the equipment-intensive geothermal systems begin to look better compared with the boiler/tower; the lower discount rate decreases the effect of the time-value of money, thus increasing the benefits of lower operation costs (e.g. fuel savings) and mitigating the disadvantage of higher capital cost. The results are similar to the high fuel inflation case ('Econ1').

More general *LCC* sensitivity results are given at the end of Section 4.4.1.

Additional Fuel Cost Sensitivity

One of the major conclusions of the sensitivity study discussed above is that optimal design parameters are not very sensitive to the economic parameters over the range used in the parametric analysis; in other words, the optimal design is sized based on providing equipment that exactly meets the load regardless of the economic situation. Under the range of economic parameters studied in the previous section, the optimizer rarely found it attractive to buy larger equipment in order to reach higher efficiency and therefore offset fuel cost. In order to test the robustness of this conclusion, the sensitivity of the design to fuel (electricity) price was studied in more detail and over a wider range. The main result of this additional study is shown in Figure 88, which shows the optimal GHX size for a hybrid system installed in the continuous use building in St. Louis as a function of fuel price (normalized against the base case value). Note that the optimal GHX size increases only if fuel prices increase to approximately double their base case value. Similar studies carried out by varying the GHX cost and the fuel cost inflation

rate found that the optimal design was even less sensitive to these parameters. Only in severe scenarios will the economic conditions substantially effect the design guidelines presented in this report.

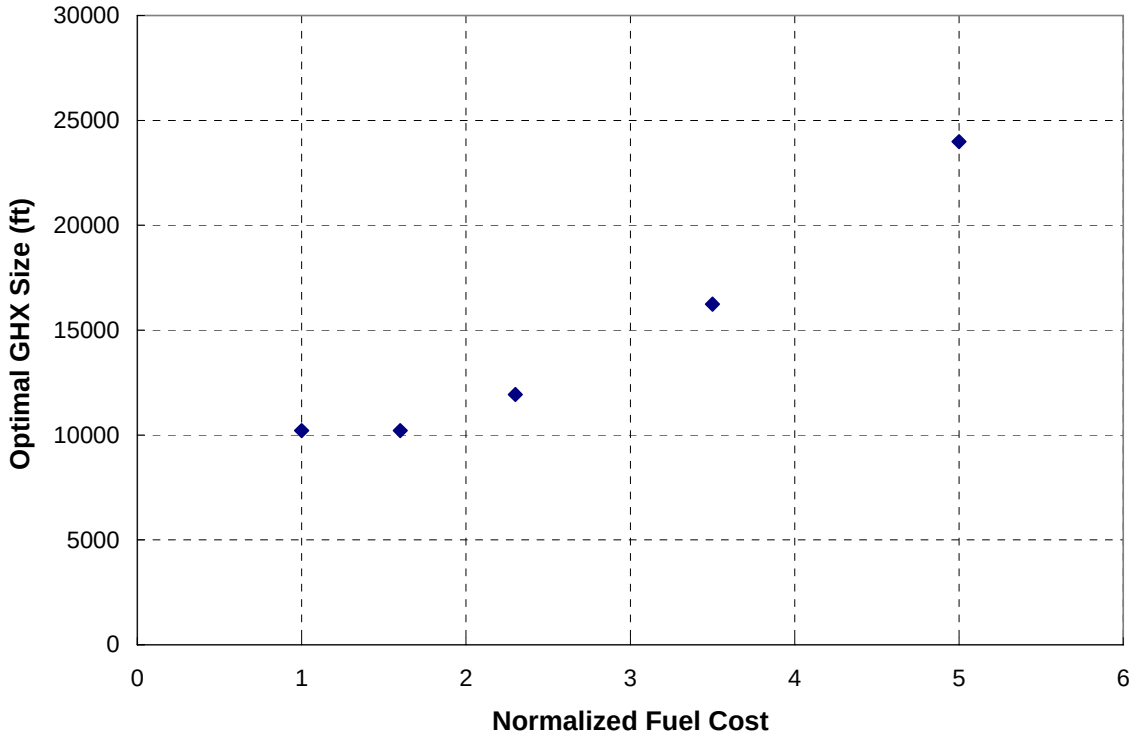

Figure 88. Sensitivity of optimal GHX size to fuel cost. The x-axis is the fuel cost normalized to the base case fuel cost (including electricity consumption, demand, and natural gas costs). Data is for a 76000 ft^2 continuous-use building in St. Louis.

Sensitivity with Relaxed Temperatures

The results discussed above indicated that in general the economic parameters selected for the analysis have a significant effect on *LCC*, but very little (if any) effect on the optimal design parameters. However, as the temperature limits are relaxed (from the base values of 35/95ºF to 20/110ºF) the economic parameters do begin to have an effect on the optimal design parameters, as discussed below in the context of the same Atlanta office building investigated in the previous section.

Figure 89 illustrates the values of the optimized design parameters for a hybrid system for several GHX costs (using the relaxed temperature limits). Note that the GHX size decreases with increasing GHX cost. Further note that the GHX size is substantially larger at the low GHX cost (6$/ft) than for the others, indicating that with the relaxed temperature limits and the low GHX cost the optimizer finds that it is economically attractive to purchase a larger GHX than would be required to simply meet the peak heating load. As the GHX cost increases, the GHX is again sized so that it exactly meets the peak heating load and therefore its size becomes insensitive to cost. This situation is common for cases run with the relaxed temperature limits: a low GHX cost allows the GHX to be larger in order to offset fuel costs.

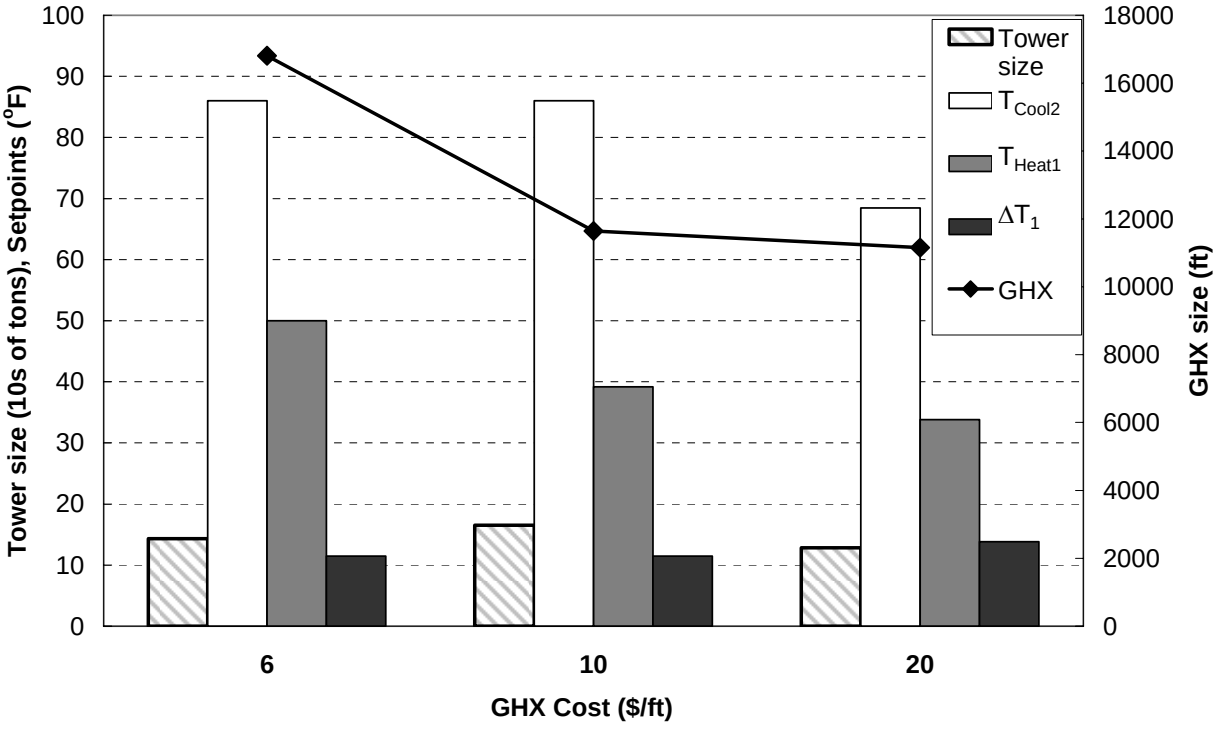

Figure 89. Optimized hybrid design values plotted as a function of GHX cost. Results are for an office building in Atlanta at relaxed temperature limits of 20/110°F.

The values of the optimized design parameters for a hybrid system are shown for the different market conditions in Figure 90. For the 'Econ1' case, corresponding to increased fuel

inflation, it is economical to purchase a larger GHX (and therefore operate the system at more moderate operating temperatures to increase equipment efficiency). For the cases 'Econ3' and 'Econ4' which correspond to reduced discount rates, the decreased effect of the time-value of money leads to an optimal system with a slightly cooler (more efficient) fluid loop; this is accomplished by purchasing a slightly larger cooling tower (though the increase in the control set point ΔT_1 means that the cooling tower is operated slightly less often). For the relaxed temperature limits it is observed that the cooling tower size often decreases slightly in the 'Econ2' case, which corresponds to poor loan terms, as the optimizer attempts to minimize the first cost of the system.

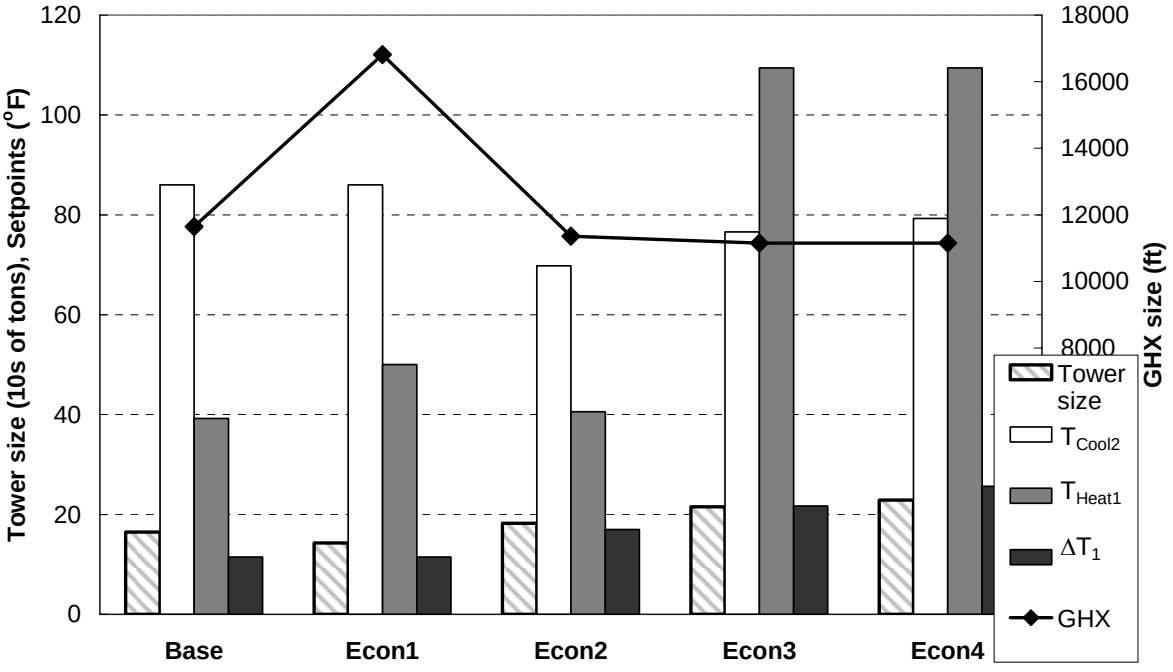

Figure 90. Optimized hybrid design values plotted for different economic scenarios. Results are for a office building in Atlanta at relaxed temperature limits of 20/110°F.

The same general trends previously discussed for *LCC* (Figure 87) are observed regardless of the temperature limits, although the *LCC* costs of the geothermal cases are

somewhat less when the relaxed temperature limits are used. The same is true for the sensitivity of the design values to conductivity (e.g. the 'low k_g' case in Figure 84).

Additional Variables Considered

In addition to the variables listed in Table 11, an investigation of the effect of uncertainties in several other variables was conducted; however, none of these additional variables studied were found to affect the results sufficiently to warrant additional study. Specifically, the impact of the first cost of the supplemental device, the grout conductivity, the maintenance cost, and the heat pump efficiency were all studied in more detail.

Maintenance cost was increased by 30%; a higher value was used in this case because some areas of the country have relatively high maintenance cost due to labor costs; maintenance costs significantly lower than the value listed in RS Means were not considered. This relatively large (30%) change in the maintenance cost had a relatively small effect on the optimized design values (a 2% increase in the *LCC* was observed).

The first cost of the supplemental device (in this case, a cooling tower) was increased by 20%. The increase in the first cost was also observed to have a small effect on the life cycle savings (a 1% change for *LCC* was observed).

The ground conductivity is included in the sensitivity study due to the large variance in this parameter that can exist from location to location, but the thermal grout is always assumed to have a conductivity of 0.8 Btu/hr-ft-^{o}F. Sensitivity to the conductivity of the grout was tested by increasing its value by 50% to a value of 1.2 Btu/hr-ft-^{o}F. This change had a negligible effect on cost, but did result in a small change in the optimal GHX control set point (T_{Cool2}). The optimal value of T_{Cool2} was found to increase by 2.5^{o}C when the high conductivity grout was used.

The heat pump efficiency was increased by 20% (in cooling *COP*); this change resulted in only a 1% decrease in *LCC* but did lead to an optimal cooling tower size that is 10% smaller than the base case. Therefore, the impact of heat pump efficiency is small in terms of *LCC* but significant in terms of cooling tower size.

5 Summary and Design Guidelines

The goal of the project is to assist practicing engineers with selecting and designing HyGCHP systems by providing a powerful simulation/optimization tool as well as a series of more approximate design guidelines based on the parametric analysis. The simulation/optimization tool is a distributable version of the HyGCHP model to be made available to practicing engineers who would like to model projects that vary significantly from those simulated and reported here. The same HyGCHP model has also been exercised over a range of conditions in order to identify design guidelines describing the optimal sizing and control strategies for these systems.

The HyGCHP model was created using the TRNSYS software, which has the ability to model geothermal systems, contains geothermal components that have been thoroughly validated, and is able to accomplish multi-year, sub-hourly simulations at reasonable speed. The HyGCHP model has been set up for cooling- and heating-dominated scenarios, as shown in Figure 11 and Figure 13. The building is modeled independently, and the resulting loads are inputs to the heat pumps in the HyGCHP model. An innovative method of modeling was utilized to model the heat pump system: two heat pump components are used to model the entire system; the performance (capacity, flow rate, power consumption, etc.) of these heat pump components is scaled appropriately to meet any peak load that is input to the model. The other

components (pumps, GHX, cooling tower, etc.) are based mainly on existing TRNSYS components.

In order to develop design guidelines, parametric studies were carried out using the HyGCHP model across a range of building/climate load scenarios. Building loads were generated for these studies using a model created in a previous ASHRAE project (ASHRAE TRP-1120, CDH, 2000). The climates were selected so that they span from cooling-dominated to heating-dominated (including a balanced case) and from wet to dry. In order to accomplish the simulation and the economic optimization it is necessary to specify a set of parameters that characterize everything from the market conditions to the soil conditions to various aspects of the equipment performance. These parameters vary according to location, year, manufacturer, designer, etc.; the value of the distributable simulation tool is that individual geothermal system designers can vary these parameters according to their situation and experience. However, for the parametric study, the key HyGCHP model parameters that were used to carry out optimizations and develop the design guidelines are summarized in Table 9. For cases resembling the economic conditions and equipment summarized in Table 9, the results of the study (as detailed in Section 4) lead to the design guidelines detailed below.

5.1 Design Guidelines and Observations – Cooling Dominated Systems

- **GHX Sizing: size the ground heat exchanger (GHX) so that it is just capable of meeting the peak heating load.** Figure 50 illustrates the optimal size of the ground heat exchanger as a function of the peak heating load (each point represents a different climate/building combination from the parametric study); notice that the optimal GHX size is essentially proportional to the peak heating load. The scatter in Figure 50 is partly due to the different

ground temperatures associated with the various climates. Figure 52 illustrates the best fit regression of the ratio of the optimal GHX size to the peak heating load as a function of the initial ground temperature; as expected, less GHX length is required to meet a given heating load in regions with high ground temperature.

Some current methods/tools for sizing hybrid systems (such as the GCHPCalc program discussed in the final section) already use this design guideline; it will be shown that the GCHPCalc software arrives at a similar GHX size as shown here.

The assumed ground conductivity (k_g) for these results is 1.4 Btu/hr-ft-^{o}F. Sensitivity studies were carried out on many of the parameters listed in Table 9, including k_g, and these studies suggest that every 0.1 Btu/hr-ft-^{o}F decrease in k_g will result in a 5% increase in the optimal GHX size.

- **Supplemental Device Size: size the supplemental cooling device based on the peak cooling load that is not met by the GHX.**
    - The rated capacity of the optimally sized cooling tower (CCCT, in tons), is 2.1x the unmet cooling load; this unmet load should be calculated according to Equation (65).
    - For the cooling tower characteristics and economic conditions considered in the parametric study, it is economically attractive to oversize the tower and then use it less frequently, almost always operating it at low speed. Low speed was chosen here as 50% speed. (The setpoint for high speed operation of the tower, T_{Cool1}, is therefore set to 5-8^{o}F above the maximum entering heat pump temperature). For single-speed towers, the tower is changed to 1.3x the unmet cooling load (from 2.1x); this unmet cooling load should be calculated according to Equation (66).

- Alternatively, the optimal cooling tower size can be estimated based on climate; specifically how balanced the building load is. Figure 54 illustrates the optimal cooling tower size (normalized by the building size) as a function of the ratio of the annual heating load to the annual cooling load of the building. Sizing the cooling tower according to Figure 54 should lead to approximately the same result as Equation (65).
- When using a dry fluid cooler as the supplementary device, the optimal sizes follow trends that are similar to those described above for cooling towers.
- It should be noted that in many of the cases, the optimal cooling tower size has a rated flow rate smaller than the maximum flow rate through the heat pump system. In these cases, it is beneficial to include a valve upstream of the tower to bypass the portion of the maximum flow that is greater than the tower's rated flow rate.

- **The optimal sizes and control setpoints identified here never balance the load on the ground**. Therefore, the ground temperature always increases over time (for the cooling-dominated climate) by an amount that is dependent on the ratio of the heating and cooling loads. The timespan of simulation (i.e., the timespan used to calculate the life cycle cost that is to be minimized) therefore has a significant impact on the results. All of the design guidelines shown here minimize the life cycle cost over 20 years. If the economic horizon is extended in the interest of sustainable design (for example, to 50 years), the optimal design will change substantially.
    - The control sequence above will be somewhat less than optimal after 20 years. After 20 years, the ground temperature will possibly have increased enough to lower the cooling capacity of the GHX. At this point, the cooling tower must be

either utilized at a higher speed (for two-speed towers) or operated more often (by lowering the setpoints) in order to maintain the desired operating temperatures.

  - For cooling dominated systems, the GHX size is therefore always set in the first year of operation, for both hybrid and geothermal-only systems.
  - Additionally, there is potential for the user of the distributable version to use the timespan in the distributable as a method of compensating for groundwater flow (as is done in some other design methods), but additional study would be required for accurate predictions.

- **The optimal design of the system does not depend substantially on the economic parameters used in the model (although the life cycle costs do)**; the equipment is sized almost entirely based on meeting the specified loads and it is rarely economically attractive to purchase larger equipment (e.g., a GHX that is larger than what is just required to meet the peak heating load) or operate equipment more often in order to improve the system efficiency.
- **Control setpoints**: c**hoose optimal control setpoints for hybrid systems as shown below.**
  - Supplemental cooling device: operate this device when conditions are favorable; that is, when the fluid temperature entering the device is greater than the ambient wet bulb (dry bulb for dry fluid cooler) + ΔT_1, where:

    ΔT_1 = 27^oF for a cooling tower, where $T_{wb,July} < 70^oF$

    23^oF for a cooling tower, where $T_{wb,July}$ 70 to 76^oF

    20^oF for a cooling tower, where $T_{wb,July} > 76^oF$

    12^oF for all dry fluid cooler scenarios

where $T_{wb,July}$ is the ASHRAE 1% design wet bulb temperature for the building's climate in July.

- GHX, cooling setpoint (T_{Cool2}): the GHX is bypassed only occasionally, generally in warmer climates (the optimal value of T_{Cool2} increases with more cooling dominated buildings). See
- Figure **57** for specific optimal values.
- GHX, heating setpoint (T_{Heat1}): the GHX is never bypassed in heating mode, so T_{Heat1} should be set to a high number that is never reached.

- **Operating temperature sensitivity: the lowest *LCC* for the HyGCHP model generally occurs at a minimum operating temperature below 35°F**. The limits on the temperature of the fluid entering the heat pump strongly drive the optimization; the equipment is sized in order to keep the entering fluid temperature within the specified limits (as presented in Table 9, the entering fluid temperature is not allowed to go below 35°F or above 95°F in the base cases). These base case temperature limits were selected with some guidance from the Project Monitoring Subcommittee and reflect "typical" design values. However, when the temperature limits are allowed to relax to 20°F and 110°F (within the manufacturers' stated operating limits) then the optimizer will typically choose an optimal minimum operating temperature that is lower than 35°F, trading off heat pump efficiency for reduced first cost (the size of the GHX is reduced by up to 50%). The effect of operating temperature limits is linked to the economic assumptions that were used for the parametric study, and it should be noted that a system designed using the more restrictive 35°F/95°F temperature limits will have some margin (against, for example, particularly severe weather or other uncertainties) that a system designed using relaxed temperature limits will not have.

- With temperatures as low as 20 – 35°F, some type of antifreeze is required. Propylene glycol was chosen as the most appropriate antifreeze. Its cost (both in initial cost and pumping power) is more than offset by the decrease in first cost that is possible with lower minimum temperature (simulations were done in several climates to confirm this).

5.2 Cost Comparisons – Cooling Dominated Systems

The parametric study considered and optimized a geothermal-only system, a boiler/tower system, and the hybrid geothermal system options for each building/climate combination. This provided an opportunity to make meaningful comparisons between these options based on life cycle costs.

- **In most moderate and southern climates, hybrid geothermal systems have a lower life cycle cost (*LCC*) than other options.**
  - The life cycle savings (*LCS*) of hybrid systems compared to geothermal-only systems is proportional to how unbalanced the climate is. Figure 58 demonstrates that the life cycle savings associated with a hybrid system compared to a geothermal-only system (normalized by the building size) decreases as a function of the ratio of the annual heating load to the annual cooling load for each building/climate scenario. Savings are negligible when this annual load ratio is greater than approximately 0.9.
  - The *LCS* of a hybrid system compared to a boiler/tower system is smaller than the *LCS* of a hybrid system compared to a geothermal-only system and increases with peak heating load (the savings is negligible when the peak heating load is near zero). See Figure 70 for some specific values.
  - A small group of buildings were also studied with a dry fluid cooler used in place of a cooling tower in the hybrid system. In this study, the life cycle cost (*LCC*) generally

changed very little from the hybrid that used a cooling tower. In some warmer climates, the *LCC* was slightly higher with the use of a dry fluid cooler.

- Unlike the optimal design parameters, the observed costs, and therefore *LCS*, are sensitive to economic parameters. For example, when fuel inflation is increased to 7.5% the *LCS* of hybrid systems as compared to boiler/tower systems *doubles*. The effect of GHX cost also has a significant effect on *LCS* (see Figure 62).

- **For climates that are like Minneapolis (7900 heating degree-days (^{o}F)) or colder, geothermal-only systems have a lower *LCC* than (cooling-dominated) hybrid or boiler/tower systems.**
- **In warm dry climates (like Phoenix), buildings with low heating loads have almost the same *LCC* for a hybrid and a boiler/tower system.**

5.3 Design Guidelines and Observations – Heating Dominated Systems

Heating-dominated systems were also studied; the hybridization of these systems occurs through the addition of either a boiler or a solar collector array; otherwise the model and control strategy are very similar to those used for the cooling-dominated systems. The heating-dominated hybrid systems were studied for climates represented by Minneapolis and Edmonton (northern Alberta, Canada). **For the assumptions listed in Table 9, the results of the heating-dominated study suggest the design guidelines detailed below.**

- Geothermal-only systems should be sized based on heating in these climates. Note that the required ft/ton of heating is significantly greater than the values shown for cooling dominated systems. This is primarily due to the small temperature difference between the deep earth temperature and the minimum heat pump entering water temperature.

- Based on the economic assumptions used here, a solar/geothermal hybrid is never a viable option; including a solar component always resulted in a larger life cycle cost than a geothermal-only system (the solar component of a hybrid system was always optimized to zero). This is likely due to the high first cost of both devices utilized in this hybrid. Note that this statement does not cover systems with direct solar heating systems that bypass the heat pumps.
- The boiler/geothermal hybrid has a slightly lower *LCC* than the geothermal-only system for a Minneapolis school; however, the boiler/geothermal hybrid was significantly more attractive than the geothermal-only system for an Edmonton school. The boiler/geothermal hybrid option is likely to become increasingly attractive going north from a Minneapolis climate.
    - To optimally design a boiler/geothermal system, the GHX should be sized to meet the peak cooling load and the boiler is sized to meet the unmet heating load (this amounts to 69% of load in Minneapolis).

5.4 Example: Use of Design Guidelines

It is instructive to demonstrate the use of the design guidelines discussed above by applying them to an example building. For this demonstration, a typical cooling-dominated building was chosen: a large office building in Atlanta. This particular building has the characteristics summarized in Table 13.

Building area (1000 ft^2)	127
Peak cooling (tons)	222
Peak heating (kBtu/hr)	2413
Annual cooling (MMBtu/yr)	3683
Annual heating (MMBtu/yr)	1905
Ground temperature (^oF)	62.0
July wet bulb (^oF)	78.6

Table 13. Characteristics of the 127,000 ft^2 office building in Atlanta.

7. An optimal design for this building starts by choosing an equipment configuration. This report has demonstrated that an optimally designed hybrid system with a GHX and a cooling tower has the lowest *LCC* in Atlanta (which is a moderate climate with some heating load). Therefore, the system should be configured as shown in Figure 11.
8. In order to size the GHX for this system, Figure 52 is used; according to this plot, the GHX size required for this location (with an initial ground temperature of 62°F) is about 115 ft/ton of peak heating load. The resulting GHX size is then 23,125 ft.
9. Next, the cooling tower is sized using Equation (65). With a L_{tot} = 23,125 ft, $q_{peak,cool}$=222 tons, and T_{ground} = 62^{o}F, the rated capacity of the cooling tower is 209 tons. Figure 54 can also be used to size the cooling tower; the ratio of the annual heating to annual cooling load is 0.52 which suggests a cooling tower size of about 1.5 tons/1000 ft^2, or about 190 tons. A size of 200 tons is chosen as the nearest 'nominal' size. Note that this is an oversized tower because the optimal system operates mainly at half speed.
10. With the equipment configured and sized, the control setpoints are now chosen. Because the summer design wet bulb temperature in Atlanta is 78.6^{o}F, the optimal value for ΔT_1 is identified as 20^{o}F.
11. T_{Cool2} is chosen to be about 60^{o}F based on
12. Figure **57**.
13. T_{Heat1} is set to 100^{o}F so that the GHX is never bypassed in heating mode, and T_{Cool1} is set to 101^{o}F (5-8^{o}F above the maximum temperature limits as discussed in this summary) so that the cooling tower operates primarily at low speed (see Section 3.2.7 for a detailed description of the control sequence).

The hybrid system for this same building was also explicitly optimized using the HyGCHP model. In Table 14, the optimal design values that were selected by the optimizer are compared with the more approximate values selected using the design guidelines, as calculated above. All values computed with the design guidelines are within 10% of the optimal for this scenario.

	Design Guidelines	HyGCHP Optimization	GCHPCalc
GHX Size (ft)	23125	23985	23600
Tower size (tons)	200	178	150
ΔT_1 (Δ^oF)	20	19.4	N/A
T_{Cool2} (^oF)	61	57.7	N/A
T_{Heat1} (^oF)	Never bypass		N/A

Table 14. Optimal design values determined with two different methods: 1) the design calculations discussed above and 2) the optimal design values determined by the HyGCHP model.

Additionally, the third column in Table 14 shows values for one commonly used GHX-sizing software that has a hybrid design feature. The software, GCHPCalc, allows for two methods of sizing the hybrid: 1) size and operate a cooling tower to meet the unmet peak cooling load or 2) size and operate a cooling tower to balance the load on the ground. As explained above, this report found that it is not economically optimal to balance the load on the ground if the objective is to minimize the 20 year life cycle cost, therefore method 1 from GCHPCalc is the preferable method, and is shown in Table 14. Note that the GHX size identified by GCHPCalc is consistent with the design guidelines presented here. The cooling tower size is somewhat smaller; however, this is at least partially an artifact of the control system that operates the cooling tower at low speed in order to achieve higher efficiency.

6 References

American Society of Heating, Refrigerating, and Air-Conditioning Engineers, Inc. (ASHRAE), *2003 ASHRAE Handbook: Applications*, Chapter. 32: Geothermal Energy, ASHRAE (2003).

ASHRAE, *2004 ASHRAE Handbook: HVAC Systems and Equipment*, Chapter. 45: Unitary Air Conditioners and Heat Pumps, ASHRAE (2004).

Baltimore Air Coil cooling tower website, October 2006, http://www.baltimoreaircoil.com/english/products/cccs/index.html

Bradley, D., *Type 582: Life Cycle Cost Economic Analysis*, Thermal Energy Systems Specialists, TRNSYS Documentation – TESS Models (2004).

CDH Energy Corp. and Thermal Energy Systems Specialists (TESS), *Development of Equivalent Full Load Heating and Cooling Hours for GCHPs Applied in Various Building Types and Locations, Final Report, ASHRAE 1120-TRP (*2000).

Chiasson, A., and C. Yavuzturk, "Assessment of the Viability of Hybrid Geothermal Heat Pump Systems with Solar Thermal Collectors", *ASHRAE Transactions: Symposia, 2003*, AHRAE (2003).

Darling, D., *Encyclopedia of Alternative Energy and Sustainability*, October 2006, http://www.daviddarling.info/encyclopedia/AEmain.html

Duffie, J. A. and W. A. Beckman, *Solar Engineering of Thermal Processes*, 3rd

edition, Wiley and Sons, Inc., (2006).

Energy Efficiency and Renewable Energy (EERE) office of the Department of Energy, Europump, and the Hydraulic Institute, *Variable Speed Pumping, A Guide to Successful Applications*, EERE (2004).

Energy Efficiency and Renewable Energy homepage (United States Department of Energy), September 2007,

http://www1.eere.energy.gov/geothermal/history.html

Energy Efficiency and Renewable Energy homepage (United States Department of Energy), *A History of Geothermal Energy in the United States*, September 2007.

Energy Information Administration (EIA), *Annual Energy Review 2006, DOE/EIA-0384(2006), EIA (2007).*

General Air Products technical info site, January 2007, http://www.generalairproducts.com/pages2/download.html

Geothermal Bore Technologies, Inc. website (GBT), February 2007, http://www.geoclip.com/

Heinonen, E., M. Wildin, A. Beall, R. Tapscott, "Assessment of Antifreeze for Ground-Source Heat Pump Systems", *ASHRAE Transactions: Symposia, 1997*, AHRAE (1997).

Hellström, G., *Duct Ground Heat Storage Model: Manual for Computer Code*, Department of Mathematical Physics, University of Lund, Sweden (1989).

Incropera, F. and DeWitt, D.., Introduction to Heat Transfer, 3rd ed., Wiley (1996).

Kavanaugh, S. and K. Rafferty, *Design of Geothermal Systems for Commercial and Institutional Buildings.* ASHRAE, (1997).

Kavanaugh, S., "A Design Method for Hybrid Ground-Source Heat Pumps", *ASHRAE Transactions: Symposia, 1998,* AHRAE (1998).

Klein et al., *TRNSYS, A Transient System Simulation Program, User's Manual,* Version 16,

Solar Energy Laboratory, University of Wisconsin-Madison (2006).

Melinder Å., *Thermophysical Properties of Liquid Secondary Refrigerants,* International Institute of Refrigeration (1997).

Mitchell, J. W. and J. E. Braun, *Design, Analysis and Control of Space*

Conditioning Equipment and Systems (unpublished edition, 1997).

Oregon Institute of Technology (OIT), Geo-Heat Center data, (2006).

Ozgener, O., and A. Hepbasli, "Experimental Performance Analysis of a Solar Assisted Ground-Source Heat Pump Greenhouse Heating System", *Energy and Buildings,* Vol 37, 2005, Elsevier (2004).

Pahud, D., and G. Hellstrom, *The New Duct Ground Heat Model For TRNSYS,* (1996).

Phetteplace, G. and W. Sullivan, "Performance of a Hybrid Ground-Coupled Heat Pump System", *ASHRAE Transactions: Symposia, 1998*, ASHRAE (1998).

Ramamoorthy, M., H. Jin, A. D. Chiasson, and J. D. Spitler, "Optimal Sizing of Hybrid Ground-Source Heat Pump Systems that Use a Cooling Pond as Supplemental Heat Rejector – A Systematic Simulation Approach," *ASHRAE Transactions 2000,* ASHRAE (2000).

R.S. Means, Facilities Maintenance and Repair Cost Data, R.S. Means (2002).

R.S. Means, Mechanical Cost Data, R.S. Means (2006).

Rushing A. and S. Fuller (of NIST), *Energy Price Indices and Discount Factors for Life-Cycle Cost Analysis,* Department of Commerce, National Institute of Standards and Technology (2006).

Shonder, J. S., P. J. Hughes, V. D. Baxter, and J. W. Thornton, "A New Comparison Of Vertical Ground Heat Exchanger Design Methods For Residential Applications," *ASHRAE Transactions,* ASHRAE (1999).

McDowell, T. and J. W. Thornton, "Simulation and Model Calibration of a Large-Scale Solar Seasonal Storage System," to be published, 2008 SimBuild Conference Proceedings, Berkeley, CA (2008).

Solar Rating and Certification Corporation ratings, November, 2007,

http://www.solar-rating.org/ratings/ratings.htm

Thermal Energy Systems Specialists (TESS), *Hybrid Geothermal Heat Pumps at Fort Polk, Louisiana*, Final Report to Oak Ridge National Laboratory for Subcontract #4000034426, (2005).

Thornton, J., *Type 504: Water Source Heat Pump*, Thermal Energy Systems Specialists, TRNSYS Documentation – TESS Models (2001).

Thornton, J., *Type 510: Closed Circuit Cooling Tower*, Thermal Energy Systems Specialists, TRNSYS Documentation – TESS Models (2004).

U.S. Department of Energy, Energy Efficiency and Renewable Energy (EERE) Industrial Technologies Program (with EuroPump and The Hydraulic Institute), *Variable Speed Pumping: A Guide to Successful Applications*, EERE (May 2004).

Value Line investment data, as compiled by A. Damodaran, New York University, December 2006,

http://pages.stern.nyu.edu/~adamodar/New_Home_Page/datafile/wacc.htm

Wetter, M., *GENOPT 2.0 Generic Optimization Program*, February 2007, http://gundog.lbl.gov/GO/

White, F., *Fluid Mechanics*, McGraw-Hill (2000).

Wrobel, J., "Predictive Model and Application of a Hybrid GSHP System for Space Conditioning, Water Heating and Deicing of a Seniors Independent Living Center", *Proceedings of International Mechanical Engineering Congress and Exposition*, ASME (2004).

Yavuzturk, C. and J.D. Spitler, "Comparative Study to Investigate Operating and Control Strategies for Hybrid Ground Source Heat Pump Systems Using a Short Time-step Simulation Model," *ASHRAE Transactions: Symposia, 2000*, ASHRAE (2000).

Zweifel G., V. Dorer, M. Koschenz, and A. Weber (of EMPA), "Building Energy and System Simulation Programs: Model Development, Coupling and Integration", *International Building Performance Simulation Association Conference Proceedings, 1995*, IBPSA (1995).

7 Appendix

7.1 Table of Results

A table of results is shown below for the main cases simulated in the parametric study.

Units
Real$: real dollars, adjusted for inflation and discount rate to today's values (*LCC* is given in real dollars).
Nom$: nominal dollars, summed across the full simulation without adjustment for inflation or discount rate.

Notes

- Hybrid and geothermal-only costs are all for 20 year simulations.
- For conventional boiler/tower configurations, costs are for a 1 year simulation, except *LCC* which is calculated for 20 years based on the 1 year simulation.

Base Case Parametric Study, Temperature Limits set to 35°F/95°F

			Costs						
	Building Type	**Climate**	**LCC**	**Equip.**	**Elec.**	**Gas**	**Water**	**Demand**	**Maint.**
			Real$	Nom$	Nom$	Nom$	Nom$	Nom$	Nom$
Hybrid									
	Retail	Atlanta	508452	177146	733121	0	84868	255224	17059
	Retail	Salt Lake City	522373	266527	685594	0	36889	225825	16077
	Retail	Phoenix	629974	133166	1022560	0	171746	297138	22762
	Retail	St. Louis	539216	255809	704960	0	47384	260983	16425
	Retail	Seattle	371522	159892	517650	0	29723	181049	14060
	Retail	Minneap.	504838	222687	725839	0	0	275675	0
	School, 9-month	Atlanta	360575	187316	331082	0	28121	281773	15672
	School, 9-month	Salt Lake City	447367	305941	325824	0	0	330050	14246
	School, 9-month	Phoenix	437491	116976	529616	0	80143	290717	18613
	School, 9-month	St. Louis	418819	258634	355231	0	8731	300434	14680
	School, 9-month	Seattle	307560	188238	253737	0	0	242883	0
	School, 9-month	Minneap.	503311	141431	311335	0	0	845072	4397
	24-hr Office	Atlanta	562796	159861	964217	0	116010	209056	16021
	24-hr Office	Salt Lake City	533351	193146	885458	0	68497	185266	15080
	24-hr Office	Phoenix	660220	123603	1189054	0	194338	246940	20816
	24-hr Office	St. Louis	566215	200653	926734	0	80449	213553	15535
	24-hr Office	Seattle	442594	119944	796686	0	64716	165171	13181
	Office	Atlanta	609892	279245	674386	0	51352	441698	18710
	Office	Salt Lake City	755061	478464	723721	0	0	428594	12452
	Office	Phoenix	677239	171226	935808	0	152491	466688	27349
	Office	St. Louis	738561	448537	696375	0	2927	502551	18785
	Office	Seattle	487884	242612	579384	0	215	318573	13426
Geothermal-only									
	Retail	Atlanta	967707	974820	626605	0	0	201925	0
	Retail	Salt Lake City	659379	518373	637261	0	0	205209	0
	Retail	Phoenix	2430001	2857719	903937	0	0	261421	68697
	Retail	St. Louis	744967	644685	629398	0	0	219931	0
	Retail	Seattle	477951	360482	483327	0	0	162631	0
	Retail	Minneap.	504838	222687	725839	0	0	275675	0
	School, 9-month	Atlanta	512390	469570	289131	0	0	231708	0
	School, 9-month	Salt Lake City	442755	301120	325818	0	0	331430	7993
	School, 9-month	Phoenix	1268993	1480660	409804	0	0	222246	36036
	School, 9-month	St. Louis	449399	331775	338516	0	0	279254	0
	School, 9-month	Seattle	307560	188238	253737	0	0	242883	0
	School, 9-month	Minneap.	503311	141431	311335	0	0	845072	4397
	24-hr Office	Atlanta	1189983	1215961	838606	0	0	171204	0
	24-hr Office	Salt Lake City	807121	676263	816588	0	0	163122	0
	24-hr Office	Phoenix	6784113	3020364	1084880	0	0	228135	72465
	24-hr Office	St. Louis	923776	839895	821252	0	0	170499	0
	24-hr Office	Seattle	682370	552822	734076	0	0	140090	0
	Office	Atlanta	873000	725066	635421	0	0	421829	0
	Office	Salt Lake City	759051	478464	723721	0	0	428594	12452
	Office	Phoenix	2349957	2695161	832510	0	0	434525	65104
	Office	St. Louis	747399	472441	700023	0	0	497796	0
	Office	Seattle	493286	251394	584085	0	0	322055	0
Boiler/tower									
	Retail	Atlanta	654396	75198	56069	7313	5463	15626	1969
	Retail	Salt Lake City	572458	81122	40349	16321	4487	11698	2064
	Retail	Phoenix	663154	95420	58922	2578	8763	14228	2224
	Retail	St. Louis	692140	83461	53374	15072	4798	16822	2118
	Retail	Seattle	430461	70567	31579	9265	2871	9797	1907
	Retail	Minneap.	651926	72643	39696	28507	3642	13370	1994
	School, 9-month	Atlanta	448391	75775	29648	6589	2465	16862	1918
	School, 9-month	Salt Lake City	421423	59921	22130	11873	2076	17286	1783
	School, 9-month	Phoenix	433065	67626	32675	2366	4243	15092	1745
	School, 9-month	St. Louis	463924	78965	26241	12502	2236	17316	1975
	School, 9-month	Seattle	329039	64538	15284	10164	1376	12768	1729
	School, 9-month	Minneap.	615686	85242	19464	12652	1017	45108	2480
	24-hr Office	Atlanta	683967	66385	66478	3611	6694	14024	1852
	24-hr Office	Salt Lake City	560936	68429	48785	7765	5107	11010	1900
	24-hr Office	Phoenix	662721	85197	62606	1060	9772	12214	2042
	24-hr Office	St. Louis	699343	76765	64350	8108	5707	14136	2037
	24-hr Office	Seattle	458399	60239	42349	3772	4225	8497	1730
	Office	Atlanta	683069	90933	44600	14845	4817	24092	2219
	Office	Salt Lake City	780900	75083	45310	29119	3953	25880	2019
	Office	Phoenix	721877	109399	56281	5648	7946	21456	2504
	Office	St. Louis	815356	103823	46096	26312	4201	28866	2405
	Office	Seattle	594352	72275	34862	21390	2478	18268	1984

	Building Type	Climate	Optimal Design Parameters (SI) GHX Length	Tower Size	Boiler Size	ΔT_1	T_{Cool1}	T_{Cool2}	T_{Heat1}
			m	kW	kW	Δ^oC	^oC	^oC	^oC
Hybrid									
	Retail	Atlanta	4150.0	759.0	0.0	12.9	38.5	9.0	13.0
	Retail	Salt Lake City	7312.5	365.2	0.0	15.6	38.5	16.5	16.8
	Retail	Phoenix	1800.0	1581.8	0.0	12.5	38.5	30.8	10.8
	Retail	St. Louis	6962.5	442.2	0.0	10.3	38.5	3.0	21.3
	Retail	Seattle	3987.5	426.8	0.0	14.7	38.5	15.0	17.5
	Retail	Minneap.	6787.5	0.0	0.0	0.0	38.5	10.3	21.5
	School, 9-month	Atlanta	4650.0	554.4	0.0	10.8	38.5	0.0	26.5
	School, 9-month	Salt Lake City	9062.5	11.0	0.0	31.8	38.5	3.0	21.3
	School, 9-month	Phoenix	1800.0	1135.2	0.0	12.5	38.5	18.8	31.0
	School, 9-month	St. Louis	7400.0	211.2	0.0	9.0	38.5	12.0	31.0
	School, 9-month	Seattle	5825.0	0.0	0.0	0.0	38.5	8.0	44.0
	School, 9-month	Minneap.	4250.0	0.0	0.0	0.0	38.5	-1.8	-1.8
	24-hr Office	Atlanta	3637.5	688.6	0.0	12.5	38.5	6.0	43.0
	24-hr Office	Salt Lake City	4950.0	468.6	0.0	15.1	38.5	19.5	18.3
	24-hr Office	Phoenix	1712.5	1381.6	0.0	12.5	38.5	31.5	43.0
	24-hr Office	St. Louis	5125.0	503.8	0.0	10.3	38.5	3.0	16.8
	24-hr Office	Seattle	2850.0	457.6	0.0	14.3	38.5	18.0	43.0
	Office	Atlanta	7312.5	627.0	0.0	10.8	38.5	14.3	29.5
	Office	Salt Lake City	14400.0	11.0	0.0	37.0	38.5	13.5	16.0
	Office	Phoenix	2587.5	2013.0	0.0	12.9	38.5	29.3	43.0
	Office	St. Louis	13175.0	134.2	0.0	16.9	38.5	12.0	16.8
	Office	Seattle	7050.0	72.6	0.0	21.7	38.5	12.8	5.5
Geothermal-only									
	Retail	Atlanta	29712.5	0.0	0.0	N/A	N/A	20.0	17.0
	Retail	Salt Lake City	15975.0	0.0	0.0	N/A	N/A	8.0	24.5
	Retail	Phoenix	86150.0	0.0	0.0	N/A	N/A	26.0	20.0
	Retail	St. Louis	19562.5	0.0	0.0	N/A	N/A	8.0	23.8
	Retail	Seattle	11075.0	0.0	0.0	N/A	N/A	8.0	20.0
	Retail	Minneap.	6787.5	0.0	0.0	N/A	N/A	10.3	21.5
	School, 9-month	Atlanta	14400.0	0.0	0.0	N/A	N/A	8.0	44.0
	School, 9-month	Salt Lake City	9062.5	0.0	0.0	N/A	N/A	12.5	21.5
	School, 9-month	Phoenix	44587.5	0.0	0.0	N/A	N/A	23.8	29.0
	School, 9-month	St. Louis	10200.0	0.0	0.0	N/A	N/A	8.0	32.0
	School, 9-month	Seattle	5825.0	0.0	0.0	N/A	N/A	8.0	44.0
	School, 9-month	Minneap.	4250.0	0.0	0.0	N/A	N/A	-1.8	-1.8
	24-hr Office	Atlanta	36975.0	0.0	0.0	N/A	N/A	19.3	21.5
	24-hr Office	Salt Lake City	20612.5	0.0	0.0	N/A	N/A	8.0	22.3
	24-hr Office	Phoenix	90962.5	0.0	0.0	N/A	N/A	26.0	4.3
	24-hr Office	St. Louis	25600.0	0.0	0.0	N/A	N/A	8.0	25.3
	24-hr Office	Seattle	16850.0	0.0	0.0	N/A	N/A	16.3	15.5
	Office	Atlanta	22100.0	0.0	0.0	N/A	N/A	20.8	5.0
	Office	Salt Lake City	14400.0	0.0	0.0	N/A	N/A	14.8	14.8
	Office	Phoenix	81250.0	0.0	0.0	N/A	N/A	24.5	5.0
	Office	St. Louis	14400.0	0.0	0.0	N/A	N/A	8.0	20.8
	Office	Seattle	7750.0	0.0	0.0	N/A	N/A	12.5	44.0
Boiler/tower									
	Retail	Atlanta	0.0	1172.6	344.1	14.4	32.5	N/A	15.8
	Retail	Salt Lake City	0.0	1311.2	384.3	14.8	39.3	N/A	25.5
	Retail	Phoenix	0.0	1850.2	303.8	11.8	47.5	N/A	5.3
	Retail	St. Louis	0.0	1295.8	437.9	13.5	32.5	N/A	28.5
	Retail	Seattle	0.0	1064.8	330.7	15.7	47.5	N/A	6.0
	Retail	Minneap.	0.0	972.4	504.9	15.7	47.5	N/A	37.5
	School, 9-month	Atlanta	0.0	1280.4	263.6	13.5	32.5	N/A	24.0
	School, 9-month	Salt Lake City	0.0	833.8	317.2	16.1	37.8	N/A	34.5
	School, 9-month	Phoenix	0.0	1172.6	156.4	10.4	37.0	N/A	22.5
	School, 9-month	St. Louis	0.0	1342.0	277.0	12.2	36.3	N/A	34.5
	School, 9-month	Seattle	0.0	1049.4	169.8	15.3	47.5	N/A	34.5
	School, 9-month	Minneap.	0.0	695.2	1992.8	11.3	47.5	N/A	6.8
	24-hr Office	Atlanta	0.0	972.4	317.2	14.8	32.5	N/A	11.3
	24-hr Office	Salt Lake City	0.0	987.8	357.5	15.7	38.5	N/A	8.3
	24-hr Office	Phoenix	0.0	1557.6	250.2	11.8	41.5	N/A	5.3
	24-hr Office	St. Louis	0.0	1126.4	424.5	14.8	32.5	N/A	9.0
	24-hr Office	Seattle	0.0	895.4	236.8	15.3	47.5	N/A	4.5
	Office	Atlanta	0.0	1573.0	397.7	9.1	37.0	N/A	25.5
	Office	Salt Lake City	0.0	1064.8	464.7	13.1	37.0	N/A	30.8
	Office	Phoenix	0.0	2358.4	357.5	10.0	47.5	N/A	6.8
	Office	St. Louis	0.0	1865.6	531.7	10.0	37.0	N/A	30.8
	Office	Seattle	0.0	1064.8	397.7	14.8	38.5	N/A	18.0

	Building Type	Climate	Optimal Design Parameters (IP) GHX Length	Tower Size	Boiler Size	ΔT_1	T_{Cool1}	T_{Cool2}	T_{Heat1}
			ft	tons	kBtu/hr	Δ^oF	^oF	^oF	^oF
Hybrid									
	Retail	Atlanta	13612.0	215.6	0.0	23.2	117.5	48.2	55.4
	Retail	Salt Lake City	23985.0	103.8	0.0	28.0	117.5	61.7	62.2
	Retail	Phoenix	5904.0	449.4	0.0	22.5	117.5	87.4	51.4
	Retail	St. Louis	22837.0	125.6	0.0	18.6	117.5	37.4	70.3
	Retail	Seattle	13079.0	121.3	0.0	26.4	117.5	59.0	63.5
	Retail	Minneap.	22263.0	0.0	0.0	0.0	117.5	50.5	70.7
	School, 9-month	Atlanta	15252.0	157.5	0.0	19.4	117.5	32.0	79.7
	School, 9-month	Salt Lake City	29725.0	3.1	0.0	57.2	117.5	37.4	70.3
	School, 9-month	Phoenix	5904.0	322.5	0.0	22.5	117.5	65.8	87.8
	School, 9-month	St. Louis	24272.0	60.0	0.0	16.2	117.5	53.6	87.8
	School, 9-month	Seattle	19106.0	0.0	0.0	0.0	117.5	46.4	111.2
	School, 9-month	Minneap.	13940.0	0.0	0.0	0.0	117.5	28.9	28.9
	24-hr Office	Atlanta	11931.0	195.6	0.0	22.5	117.5	42.8	109.4
	24-hr Office	Salt Lake City	16236.0	133.1	0.0	27.2	117.5	67.1	64.9
	24-hr Office	Phoenix	5617.0	392.5	0.0	22.5	117.5	88.7	109.4
	24-hr Office	St. Louis	16810.0	143.1	0.0	18.6	117.5	37.4	62.2
	24-hr Office	Seattle	9348.0	130.0	0.0	25.7	117.5	64.4	109.4
	Office	Atlanta	23985.0	178.1	0.0	19.4	117.5	57.7	85.1
	Office	Salt Lake City	47232.0	3.1	0.0	66.6	117.5	56.3	60.8
	Office	Phoenix	8487.0	571.9	0.0	23.3	117.5	84.7	109.4
	Office	St. Louis	43214.0	38.1	0.0	30.4	117.5	53.6	62.2
	Office	Seattle	23124.0	20.6	0.0	39.0	117.5	55.0	41.9
Geothermal-only									
	Retail	Atlanta	97457.0	0.0	0.0	0.0	117.5	68.0	62.6
	Retail	Salt Lake City	52398.0	0.0	0.0	0.0	117.5	46.4	76.1
	Retail	Phoenix	282572.0	0.0	0.0	0.0	117.5	78.8	68.0
	Retail	St. Louis	64165.0	0.0	0.0	0.0	117.5	46.4	74.8
	Retail	Seattle	36326.0	0.0	0.0	0.0	117.5	46.4	68.0
	Retail	Minneap.	22263.0	0.0	0.0	0.0	117.5	50.5	70.7
	School, 9-month	Atlanta	47232.0	0.0	0.0	0.0	117.5	46.4	111.2
	School, 9-month	Salt Lake City	29725.0	0.0	0.0	0.0	117.5	54.5	70.7
	School, 9-month	Phoenix	146247.0	0.0	0.0	0.0	117.5	74.8	84.2
	School, 9-month	St. Louis	33456.0	0.0	0.0	0.0	117.5	46.4	89.6
	School, 9-month	Seattle	19106.0	0.0	0.0	0.0	117.5	46.4	111.2
	School, 9-month	Minneap.	13940.0	0.0	0.0	0.0	117.5	28.9	28.9
	24-hr Office	Atlanta	121278.0	0.0	0.0	0.0	117.5	66.7	70.7
	24-hr Office	Salt Lake City	67609.0	0.0	0.0	0.0	117.5	46.4	72.1
	24-hr Office	Phoenix	298357.0	0.0	0.0	0.0	117.5	78.8	39.7
	24-hr Office	St. Louis	83968.0	0.0	0.0	0.0	117.5	46.4	77.5
	24-hr Office	Seattle	55268.0	0.0	0.0	0.0	117.5	61.3	59.9
	Office	Atlanta	72488.0	0.0	0.0	0.0	117.5	69.4	41.0
	Office	Salt Lake City	47232.0	0.0	0.0	0.0	117.5	58.6	58.6
	Office	Phoenix	266500.0	0.0	0.0	0.0	117.5	76.1	41.0
	Office	St. Louis	47232.0	0.0	0.0	0.0	117.5	46.4	69.4
	Office	Seattle	25420.0	0.0	0.0	0.0	117.5	54.5	111.2
Boiler/tower									
	Retail	Atlanta	0.0	333.1	1174.3	25.9	117.5	90.5	60.4
	Retail	Salt Lake City	0.0	372.5	1311.5	26.7	117.5	102.7	77.9
	Retail	Phoenix	0.0	525.6	1037.0	21.2	117.5	117.5	41.5
	Retail	St. Louis	0.0	368.1	1494.5	24.3	117.5	90.5	83.3
	Retail	Seattle	0.0	302.5	1128.5	28.2	117.5	117.5	42.8
	Retail	Minneap.	0.0	276.3	1723.3	28.2	117.5	117.5	99.5
	School, 9-month	Atlanta	0.0	363.8	899.8	24.3	117.5	90.5	75.2
	School, 9-month	Salt Lake City	0.0	236.9	1082.8	29.0	117.5	100.0	94.1
	School, 9-month	Phoenix	0.0	333.1	533.8	18.8	117.5	98.6	72.5
	School, 9-month	St. Louis	0.0	381.3	945.5	21.9	117.5	97.3	94.1
	School, 9-month	Seattle	0.0	298.1	579.5	27.5	117.5	117.5	94.1
	School, 9-month	Minneap.	0.0	197.5	6801.5	20.4	117.5	117.5	44.2
	24-hr Office	Atlanta	0.0	276.3	1082.8	26.7	117.5	90.5	52.3
	24-hr Office	Salt Lake City	0.0	280.6	1220.0	28.2	117.5	101.3	46.9
	24-hr Office	Phoenix	0.0	442.5	854.0	21.2	117.5	106.7	41.5
	24-hr Office	St. Louis	0.0	320.0	1448.8	26.7	117.5	90.5	48.2
	24-hr Office	Seattle	0.0	254.4	808.2	27.5	117.5	117.5	40.1
	Office	Atlanta	0.0	446.9	1357.3	16.4	117.5	98.6	77.9
	Office	Salt Lake City	0.0	302.5	1586.0	23.5	117.5	98.6	87.4
	Office	Phoenix	0.0	670.0	1220.0	18.0	117.5	117.5	44.2
	Office	St. Louis	0.0	530.0	1814.8	18.0	117.5	98.6	87.4
	Office	Seattle	0.0	302.5	1357.3	26.7	117.5	101.3	64.4

Base Case Parametric Study, Temperature Limits set to 20°F/110°F

Building Type	Climate	Costs						
		LCC	Equip.	Elec.	Gas	Water	Demand	Maint.
		Real$	Nom$	Nom$	Nom$	Nom$	Nom$	Nom$
Hybrid								
Retail	Atlanta	477066	119238	753685	0	91035	255206	16722
Retail	Salt Lake City	468376	148282	726453	0	54310	243648	15829
Retail	Phoenix	613802	101693	1021390	0	169959	282134	67333
Retail	St. Louis	495361	153394	749796	0	61012	280103	15824
Retail	Seattle	343370	86634	551714	0	37394	202892	13174
Retail	Minneap.	504838	222687	725839	0	0	275675	0
School, 9-month	Atlanta	321336	116412	348691	0	31191	305017	14566
School, 9-month	Salt Lake City	365441	140231	364797	0	15018	373774	13320
School, 9-month	Phoenix	373396	82706	508083	0	81665	287938	17925
School, 9-month	St. Louis	364874	123670	403562	0	21094	359632	13535
School, 9-month	Seattle	268449	97774	276239	0	7106	279886	11503
School, 9-month	Minneap.	503311	141431	311335	0	0	845072	4397
24-hr Office	Atlanta	547621	105999	986933	0	120850	214089	45978
24-hr Office	Salt Lake City	505069	123674	918216	0	78318	197833	14441
24-hr Office	Phoenix	641524	95988	1193067	0	195004	244596	19160
24-hr Office	St. Louis	538012	132389	959854	0	88530	226112	14647
24-hr Office	Seattle	426724	79334	819024	0	70811	171094	12704
Office	Atlanta	540571	149273	743272	0	58190	422390	15262
Office	Salt Lake City	595859	191271	808817	0	18024	481491	15032
Office	Phoenix	634768	141321	951002	0	148202	397213	24605
Office	St. Louis	625899	225408	770403	0	22867	531428	15786
Geothermal-only								
Retail	Atlanta	849199	750492	723099	0	0	233387	0
Retail	Salt Lake City	598699	406004	692135	0	0	226794	0
Retail	Phoenix	2279573	2482121	1148755	0	0	336429	59792
Retail	St. Louis	656335	469570	701881	0	0	255024	0
Retail	Seattle	431482	271490	519919	0	0	182581	0
Retail	Minneap.	504838	222687	725839	0	0	275675	0
School, 9-month	Atlanta	437802	345719	314958	0	0	247136	0
School, 9-month	Salt Lake City	393956	222687	345949	0	0	338172	0
School, 9-month	Phoenix	952067	986303	484068	0	0	264214	0
School, 9-month	St. Louis	402218	251394	357698	0	0	292089	0
School, 9-month	Seattle	278885	139436	264127	0	0	256477	0
School, 9-month	Minneap.	503311	141431	311335	0	0	845072	4397
24-hr Office	Atlanta	1115753	1023622	995593	0	0	209480	0
24-hr Office	Salt Lake City	740402	541339	895093	0	0	185971	0
24-hr Office	Phoenix	N/A	N/A	1128770	0	0	240055	0
24-hr Office	St. Louis	841071	667651	915707	0	0	196768	0
24-hr Office	Seattle	632052	443734	803118	0	0	162205	0
Office	Atlanta	746223	506890	700231	0	0	437736	0
Office	Salt Lake City	630761	286723	786679	0	0	440500	7906
Office	Phoenix	1789108	1826514	979050	0	0	472898	44508
Office	St. Louis	664039	342848	735211	0	0	487073	0
Boiler/tower		542107	76245	884866	133190	107387	254535	39789
Retail	Atlanta	542107	76245	44243	6659	5369	12727	1989
Retail	Salt Lake City	570726	76456	42153	14401	4239	12341	2034
Retail	Phoenix	673418	90789	58976	2293	8644	14347	4456
Retail	St. Louis	594500	74089	43550	14522	4745	14065	2005
Retail	Seattle	418685	56130	31638	8871	2715	10267	1697
Retail	Minneap.	651926	72643	39696	28507	3642	13370	1994
School, 9-month	Atlanta	358271	59342	21501	6991	2496	13397	1691
School, 9-month	Salt Lake City	400369	57260	20998	11867	2069	15794	1679
School, 9-month	Phoenix	404998	63671	30541	2179	4136	13969	1657
School, 9-month	St. Louis	422898	54012	23559	12926	2206	15587	1685
School, 9-month	Seattle	317370	46083	15706	9790	1421	13050	1490
School, 9-month	Minneap.	615686	85242	19464	12652	1017	45108	2480
24-hr Office	Atlanta	569113	63500	52215	3161	6711	10834	3380
24-hr Office	Salt Lake City	549891	66182	49120	7222	5010	9986	1891
24-hr Office	Phoenix	657325	75217	62819	993	9756	12518	1911
24-hr Office	St. Louis	587435	68611	51462	7860	5719	11416	1945
24-hr Office	Seattle	452917	49292	42622	3798	4168	8705	1587
Office	Atlanta	636704	73311	44056	13906	4386	21189	1955
Office	Salt Lake City	748758	82576	44209	28333	3799	22171	2107
Office	Phoenix	699162	92588	56533	5491	7688	20216	2152
Office	St. Louis	765852	87221	45087	25877	4036	25159	2167

	Building Type	Climate	Optimal Design Parameters (SI) GHX Length	Tower Size	Boiler Size	ΔT_1	T_{Cool1}	T_{Cool2}	T_{Heat1}
			m	kW	kW	Δ^oC	^oC	^oC	^oC
Hybrid									
	Retail	Atlanta	2150.0	888.8	0.0	14.3	47.5	21.0	13.8
	Retail	Salt Lake City	3287.5	673.2	0.0	16.9	47.5	12.0	16.0
	Retail	Phoenix	800.0	1584.0	0.0	15.4	47.5	39.0	-2.0
	Retail	St. Louis	3462.5	673.2	0.0	13.4	47.5	17.3	19.0
	Retail	Seattle	1625.0	550.0	0.0	16.0	47.5	11.3	9.3
	Retail	Minneap.	6787.5	0.0	0.0	0.0	47.5	10.3	21.5
	School, 9-month	Atlanta	2500.0	627.0	0.0	15.1	47.5	18.8	10.8
	School, 9-month	Salt Lake City	3462.5	411.4	0.0	18.2	47.5	12.0	19.8
	School, 9-month	Phoenix	750.0	1150.6	0.0	15.1	47.5	39.0	43.0
	School, 9-month	St. Louis	2850.0	457.6	0.0	5.5	47.5	20.3	31.0
	School, 9-month	Seattle	2325.0	303.6	0.0	17.3	47.5	12.0	5.5
	School, 9-month	Minneap.	4250.0	0.0	0.0	0.0	47.5	-1.8	-1.8
	24-hr Office	Atlanta	1950.0	737.0	0.0	13.8	47.5	23.3	28.8
	24-hr Office	Salt Lake City	2675.0	596.2	0.0	16.4	47.5	17.3	43.0
	24-hr Office	Phoenix	1012.5	1258.4	0.0	14.3	47.5	45.0	1.8
	24-hr Office	St. Louis	2937.5	596.2	0.0	13.4	47.5	22.5	13.8
	24-hr Office	Seattle	1450.0	519.2	0.0	14.7	47.5	21.0	10.0
	Office	Atlanta	3550.0	580.8	0.0	6.4	47.5	30.0	4.0
	Office	Salt Lake City	4950.0	442.2	0.0	21.3	47.5	12.0	6.3
	Office	Phoenix	1800.0	1751.2	0.0	14.3	47.5	45.0	-2.0
	Office	St. Louis	6000.0	411.4	0.0	14.7	47.5	13.5	9.3
Geothermal-only									
	Retail	Atlanta	22875.0	0.0	0.0	N/A	N/A	23.0	20.8
	Retail	Salt Lake City	12375.0	0.0	0.0	N/A	N/A	8.0	32.8
	Retail	Phoenix	74750.0	0.0	0.0	N/A	N/A	31.9	-1.9
	Retail	St. Louis	14400.0	0.0	0.0	N/A	N/A	21.5	11.8
	Retail	Seattle	8275.0	0.0	0.0	N/A	N/A	8.0	14.8
	Retail	Minneap.	6787.5	0.0	0.0	N/A	N/A	10.3	21.5
	School, 9-month	Atlanta	10625.0	0.0	0.0	N/A	N/A	8.0	44.0
	School, 9-month	Salt Lake City	6787.5	0.0	0.0	N/A	N/A	8.0	44.0
	School, 9-month	Phoenix	30150.0	0.0	0.0	N/A	N/A	26.8	8.0
	School, 9-month	St. Louis	7662.5	0.0	0.0	N/A	N/A	8.0	44.0
	School, 9-month	Seattle	4250.0	0.0	0.0	N/A	N/A	12.5	7.3
	School, 9-month	Minneap.	4250.0	0.0	0.0	N/A	N/A	-1.8	-1.8
	24-hr Office	Atlanta	31200.0	0.0	0.0	N/A	N/A	25.3	17.0
	24-hr Office	Salt Lake City	16500.0	0.0	0.0	N/A	N/A	8.0	27.5
	24-hr Office	Phoenix	MAX	0.0	0.0	N/A	N/A	36.5	-1.8
	24-hr Office	St. Louis	20525.0	0.0	0.0	N/A	N/A	8.0	27.5
	24-hr Office	Seattle	13525.0	0.0	0.0	N/A	N/A	8.0	23.8
	Office	Atlanta	15450.0	0.0	0.0	N/A	N/A	20.8	-1.8
	Office	Salt Lake City	8625.0	0.0	0.0	N/A	N/A	14.8	8.0
	Office	Phoenix	55000.0	0.0	0.0	N/A	N/A	29.8	-1.8
	Office	St. Louis	10450.0	0.0	0.0	N/A	N/A	14.8	9.5
Boiler/tower									
	Retail	Atlanta	0.0	1141.8	357.5	14.8	47.5	N/A	9.0
	Retail	Salt Lake City	0.0	1126.4	451.3	17.9	47.5	N/A	9.0
	Retail	Phoenix	0.0	1685.2	308.3	15.0	47.5	N/A	5.0
	Retail	St. Louis	0.0	1095.6	397.7	12.6	47.5	N/A	19.5
	Retail	Seattle	0.0	787.6	250.2	18.3	47.5	N/A	9.0
	Retail	Minneap.	0.0	972.4	504.9	15.7	47.5	N/A	37.5
	School, 9-month	Atlanta	0.0	910.8	183.2	15.3	47.5	N/A	37.5
	School, 9-month	Salt Lake City	0.0	849.2	210.0	11.8	47.5	N/A	42.8
	School, 9-month	Phoenix	0.0	1126.4	89.4	11.3	47.5	N/A	23.3
	School, 9-month	St. Louis	0.0	728.2	263.6	10.4	43.8	N/A	39.0
	School, 9-month	Seattle	0.0	695.2	116.2	17.0	47.5	N/A	36.0
	School, 9-month	Minneap.	0.0	695.2	1966.0	11.3	47.5	N/A	6.8
	24-hr Office	Atlanta	0.0	880.0	344.1	14.8	47.5	N/A	4.5
	24-hr Office	Salt Lake City	0.0	910.8	384.3	15.7	47.5	N/A	4.5
	24-hr Office	Phoenix	0.0	1265.0	236.8	13.9	47.5	N/A	6.0
	24-hr Office	St. Louis	0.0	926.2	424.5	13.9	47.5	N/A	7.5
	24-hr Office	Seattle	0.0	679.8	196.6	14.8	47.5	N/A	8.3
	Office	Atlanta	0.0	1111.0	357.5	8.3	47.5	N/A	15.0
	Office	Salt Lake City	0.0	1326.6	411.1	17.4	47.5	N/A	24.0
	Office	Phoenix	0.0	1804.0	250.2	13.5	47.5	N/A	9.0
	Office	St. Louis	0.0	1357.4	491.5	13.5	47.5	N/A	24.8

	Building Type	Climate	Optimal Design Parameters (IP) GHX Length	Tower Size	Boiler Size	ΔT_1	T_{Cool1}	T_{Cool2}	T_{Heat1}
			ft	tons	kBtu/hr	Δ^oF	^oF	^oF	^oF
Hybrid									
	Retail	Atlanta	7052.0	252.5	0.0	25.7	117.5	69.8	56.8
	Retail	Salt Lake City	10783.0	191.3	0.0	30.4	117.5	53.6	60.8
	Retail	Phoenix	5195.5	450.0	0.0	27.7	117.5	102.2	28.4
	Retail	St. Louis	11357.0	191.3	0.0	24.1	117.5	63.1	66.2
	Retail	Seattle	5330.0	156.3	0.0	28.8	117.5	52.3	48.7
	Retail	Minneap.	22263.0	0.0	0.0	0.0	117.5	50.5	70.7
	School, 9-month	Atlanta	8200.0	178.1	0.0	27.2	117.5	65.8	51.4
	School, 9-month	Salt Lake City	11357.0	116.9	0.0	32.7	117.5	53.6	67.6
	School, 9-month	Phoenix	2460.0	326.9	0.0	27.2	117.5	102.2	109.4
	School, 9-month	St. Louis	9348.0	130.0	0.0	9.9	117.5	68.5	87.8
	School, 9-month	Seattle	7626.0	86.3	0.0	31.2	117.5	53.6	41.9
	School, 9-month	Minneap.	13940.0	0.0	0.0	0.0	117.5	28.9	28.9
	24-hr Office	Atlanta	6396.0	209.4	0.0	24.9	117.5	73.9	83.8
	24-hr Office	Salt Lake City	8774.0	169.4	0.0	29.6	117.5	63.1	109.4
	24-hr Office	Phoenix	3321.0	357.5	0.0	25.7	117.5	113.0	35.2
	24-hr Office	St. Louis	9635.0	169.4	0.0	24.1	117.5	72.5	56.8
	24-hr Office	Seattle	4756.0	147.5	0.0	26.4	117.5	69.8	50.0
	Office	Atlanta	11644.0	165.0	0.0	11.5	117.5	86.0	39.2
	Office	Salt Lake City	16236.0	125.6	0.0	38.3	117.5	53.6	43.3
	Office	Phoenix	5904.0	497.5	0.0	25.7	117.5	113.0	28.4
	Office	St. Louis	19680.0	116.9	0.0	26.4	117.5	56.3	48.7
Geothermal-only									
	Retail	Atlanta	75030.0	0.0	0.0	0.0	117.5	73.4	69.4
	Retail	Salt Lake City	40590.0	0.0	0.0	0.0	117.5	46.4	91.0
	Retail	Phoenix	0.0	0.0	0.0	0.0	117.5	89.4	28.6
	Retail	St. Louis	47232.0	0.0	0.0	0.0	117.5	70.7	53.2
	Retail	Seattle	27142.0	0.0	0.0	0.0	117.5	46.4	58.6
	Retail	Minneap.	22263.0	0.0	0.0	0.0	117.5	50.5	70.7
	School, 9-month	Atlanta	34850.0	0.0	0.0	0.0	117.5	46.4	111.2
	School, 9-month	Salt Lake City	22263.0	0.0	0.0	0.0	117.5	46.4	111.2
	School, 9-month	Phoenix	98892.0	0.0	0.0	0.0	117.5	80.2	46.4
	School, 9-month	St. Louis	25133.0	0.0	0.0	0.0	117.5	46.4	111.2
	School, 9-month	Seattle	13940.0	0.0	0.0	0.0	117.5	54.5	45.1
	School, 9-month	Minneap.	13940.0	0.0	0.0	0.0	117.5	28.9	28.9
	24-hr Office	Atlanta	102336.0	0.0	0.0	0.0	117.5	77.5	62.6
	24-hr Office	Salt Lake City	54120.0	0.0	0.0	0.0	117.5	46.4	81.5
	24-hr Office	Phoenix	MAX	0.0	0.0	0.0	117.5	97.7	28.9
	24-hr Office	St. Louis	67322.0	0.0	0.0	0.0	117.5	46.4	81.5
	24-hr Office	Seattle	44362.0	0.0	0.0	0.0	117.5	46.4	74.8
	Office	Atlanta	50676.0	0.0	0.0	0.0	117.5	69.4	28.9
	Office	Salt Lake City	28290.0	0.0	0.0	0.0	117.5	58.6	46.4
	Office	Phoenix	180400.0	0.0	0.0	0.0	117.5	85.6	28.9
	Office	St. Louis	34276.0	0.0	0.0	0.0	117.5	58.6	49.1
Boiler/tower									
	Retail	Atlanta	0.0	324.4	1220.0	26.7	117.5	117.5	48.2
	Retail	Salt Lake City	0.0	320.0	1540.3	32.2	117.5	117.5	48.2
	Retail	Phoenix	0.0	478.8	1052.3	27.0	117.5	117.5	41.0
	Retail	St. Louis	0.0	311.3	1357.3	22.7	117.5	117.5	67.1
	Retail	Seattle	0.0	223.8	854.0	33.0	117.5	117.5	48.2
	Retail	Minneap.	0.0	276.3	1723.3	28.2	117.5	117.5	99.5
	School, 9-month	Atlanta	0.0	258.8	625.2	27.5	117.5	117.5	99.5
	School, 9-month	Salt Lake City	0.0	241.3	716.8	21.2	117.5	117.5	109.0
	School, 9-month	Phoenix	0.0	320.0	305.0	20.4	117.5	117.5	73.9
	School, 9-month	St. Louis	0.0	206.9	899.8	18.8	117.5	110.8	102.2
	School, 9-month	Seattle	0.0	197.5	396.5	30.6	117.5	117.5	96.8
	School, 9-month	Minneap.	0.0	197.5	6710.0	20.4	117.5	117.5	44.2
	24-hr Office	Atlanta	0.0	250.0	1174.3	26.7	117.5	117.5	40.1
	24-hr Office	Salt Lake City	0.0	258.8	1311.5	28.2	117.5	117.5	40.1
	24-hr Office	Phoenix	0.0	359.4	808.2	25.1	117.5	117.5	42.8
	24-hr Office	St. Louis	0.0	263.1	1448.8	25.1	117.5	117.5	45.5
	24-hr Office	Seattle	0.0	193.1	671.0	26.7	117.5	117.5	46.9
	Office	Atlanta	0.0	315.6	1220.0	14.9	117.5	117.5	59.0
	Office	Salt Lake City	0.0	376.9	1403.0	31.4	117.5	117.5	75.2
	Office	Phoenix	0.0	512.5	854.0	24.3	117.5	117.5	48.2
	Office	St. Louis	0.0	385.6	1677.5	24.3	117.5	117.5	76.6

Dry Fluid Cooler as supplemental device, Temperature Limits set to 35°F/95°F

Building Type	Climate	Costs						
		LCC	Equip.	Elec.	Gas	Water	Demand	Maint.
		Real$	Nom$	Nom$	Nom$	Nom$	Nom$	Nom$
Hybrid								
Office	Atlanta	649649	397734	634011	0	0	405279	14637
Office	Seattle	487171	234937	580195	0	0	330827	8730
Retail	Salt Lake City	526168	299649	663020	0	0	215892	12550
24-hr Office	Salt Lake City	542992	265114	837708	0	0	172319	11811
School, 9-month	St. Louis	423604	281642	345662	0	0	292339	10680
Geothermal-only								
Office	Atlanta	873000	725066	635421	0	0	421829	0
Office	Seattle	493286	251394	584085	0	0	322055	0
Retail	Salt Lake City	659379	518373	637261	0	0	205209	0
24-hr Office	Salt Lake City	807121	676263	816588	0	0	163122	0
School, 9-month	St. Louis	449399	331775	338516	0	0	279254	0
Boiler/tower								
Office	Atlanta	683069	90933	44600	14845	4817	24092	2219
Office	Seattle	594352	72275	34862	21390	2478	18268	1984
Retail	Salt Lake City	572458	81122	40349	16321	4487	11698	2064
24-hr Office	Salt Lake City	560936	68429	48785	7765	5107	11010	1900
School, 9-month	St. Louis	463924	78965	26241	12502	2236	17316	1975

Building Type	Climate	Optimal Design Parameters (SI)						
		GHX Length	Tower Size	Boiler Size	ΔT_1	T_{Cool1}	T_{Cool2}	T_{Heat1}
		m	kW	kW	Δ^oC	^oC	^oC	^oC
Hybrid								
Office	Atlanta	7487.5	781.0	0.0	25.6	20.5	20.3	30.0
Office	Seattle	7050.0	26.4	0.0	23.0	19.0	6.0	30.0
Retail	Salt Lake City	7400.0	396.0	0.0	37.0	19.0	10.5	30.0
24-hr Office	Salt Lake City	6000.0	457.6	0.0	21.3	47.5	18.3	30.0
School, 9-month	St. Louis	8012.5	134.2	0.0	7.7	28.0	10.5	30.0
Geothermal-only								
Office	Atlanta	22100.0	0.0	0.0	0.0	47.5	20.8	5.0
Office	Seattle	7750.0	0.0	0.0	0.0	47.5	12.5	44.0
Retail	Salt Lake City	15975.0	0.0	0.0	0.0	47.5	8.0	24.5
24-hr Office	Salt Lake City	20612.5	0.0	0.0	0.0	47.5	8.0	22.3
School, 9-month	St. Louis	10200.0	0.0	0.0	0.0	47.5	8.0	32.0
Boiler/tower								
Office	Atlanta	0.0	1573.0	397.7	9.1	47.5	37.0	25.5
Office	Seattle	0.0	1064.8	397.7	14.8	47.5	38.5	18.0
Retail	Salt Lake City	0.0	1311.2	384.3	14.8	47.5	39.3	25.5
24-hr Office	Salt Lake City	0.0	987.8	357.5	15.7	47.5	38.5	8.3
School, 9-month	St. Louis	0.0	1342.0	277.0	12.2	47.5	36.3	34.5

			Optimal Design Parameters (IP)						
	Building Type	**Climate**	**GHX Length**	**Tower Size**	**Boiler Size**	**ΔT_1**	**T_{Cool1}**	**T_{Cool2}**	**T_{Heat1}**
			ft	tons	kBtu/hr	Δ^oF	^oF	^oF	^oF
Hybrid									
	Office	Atlanta	24559.0	221.9	0.0	46.1	68.9	68.5	86.0
	Office	Seattle	23124.0	7.5	0.0	41.4	66.2	42.8	86.0
	Retail	Salt Lake City	24272.0	112.5	0.0	66.6	66.2	50.9	86.0
	24-hr Office	Salt Lake City	19680.0	130.0	0.0	38.3	64.9	67.1	86.0
	School, 9-month	St. Louis	26281.0	38.1	0.0	13.8	82.4	50.9	86.0
Geothermal-only									
	Office	Atlanta	72488.0	0.0	0.0	N/A	N/A	69.4	41.0
	Office	Seattle	25420.0	0.0	0.0	N/A	N/A	54.5	111.2
	Retail	Salt Lake City	52398.0	0.0	0.0	N/A	N/A	46.4	76.1
	24-hr Office	Salt Lake City	67609.0	0.0	0.0	N/A	N/A	46.4	72.1
	School, 9-month	St. Louis	33456.0	0.0	0.0	N/A	N/A	46.4	89.6
Boiler/tower									
	Office	Atlanta	0.0	446.9	1357.3	16.4	98.6	N/A	77.9
	Office	Seattle	0.0	302.5	1357.3	26.7	101.3	N/A	64.4
	Retail	Salt Lake City	0.0	372.5	1311.5	26.7	102.7	N/A	77.9
	24-hr Office	Salt Lake City	0.0	280.6	1220.0	28.2	101.3	N/A	46.9
	School, 9-month	St. Louis	0.0	381.3	945.5	21.9	97.3	N/A	94.1

7.2 Sequence of Operations – Cooling Dominated

The following is a general sequence of operations for the condenser loop of a cooling-dominated hybrid ground-coupled heat pump system (with a cooling tower). This system utilizes antifreeze, though a sequence for a system without antifreeze would be similar. The results of the design guidelines (or optimization using the distributable) for any specific building/climate can be used to fill in the design variables that are shown in bold, italicized font. Note that this sequence is optimal for 20 years of operation; it is possible adjustments will be required after this period (see Section 5.1).

(*Following this general sequence, an example sequence is shown for a specific scenario.*)

Hybrid Ground-Coupled Heat Pump System
Sequence of Operations

General System Description
Optimization by HyGCHP suggests installation of the following equipment: a cooling tower with a rated capacity of $\boldsymbol{C_{CCCT}}$ **(tons)**, and a bore field with a total bore length of $\boldsymbol{L_{tot}}$ **(ft)**, with bores spaced at least $\boldsymbol{d_{spacing}}$ **(ft)** apart. The cooling tower shall be installed upstream of the bore field (see Figure 2). The project designer is responsible for the final specification of the tower size and ground heat exchanger (GHX) size, spacing, and layout based on available equipment sizing, site configuration and geology.

Instrumentation
Measure fluid temperatures upstream of the cooling tower (T_{TOW}), upstream of the GHX (T_{TOW}), and upstream of the heat pumps (T_{HP}) (shown in red on Figure 2). Also measure ambient wet bulb temperature (T_{WB}).

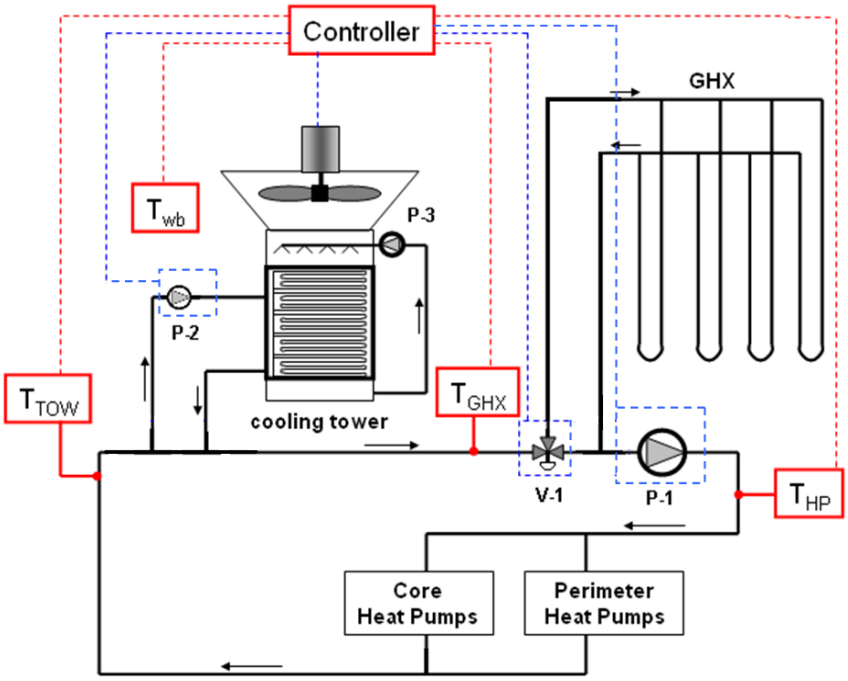

Figure 2. Setup of hybrid ground-coupled system. Required temperature measurements are shown in red, control points are shown in blue.

Sequence of Operations

Central Loop Circulation Pump Operation

Pump Operation
The central loop serving the building heat pumps and ground heat exchanger loop shall be served by one pump (P-1) with a variable frequency drive (VFD) controlled by differential pressure sensors located near the remote end of the heat pumps served. Each heat pump shall be equipped with a two-way valve (except as noted) that opens on a call for heating or cooling at the unit. Total flow/differential pressure shall be adjusted to provide 2.5 gpm/ton of building load to the heat pumps at full load (i.e. all two-way valves open).

Bypass requirement
Based on pump/drive selection and the manufacturer's recommendations there shall be a minimum central loop flow rate to avoid dead heading the pump. This minimum flow rate is determined by the pump/drive combination and the system curve. This minimum flow shall be provided by leaving out the two-way valves on the units specified in the plans and specifications (or by providing some other approved means of bypass specified by the engineer).

Notes:

a) *Some designers may want to provide redundancy in the central pumping loop. One approach sometimes used is to size two parallel pumps to meet full load requirements together. If one pump fails, the other pump can generally provide approximately 70% of the full load flow. If this approach is used, staging the pumps and duty cycling control strategies must be addressed. Pumps in parallel using VFDs shall operate at the same speed if more than one is in operation.*
b) *Propylene glycol/water mix – **X** **(%)** solution – may be recommended in order to operate at low temperatures. If a glycol mixture is used, the pump design and flow rates should take this into consideration.*

Ground Heat Exchanger Operation

The central loop circulation pump (P-1) also provides flow through the ground heat exchanger (GHX). At low loads, the overall flow-rate is reduced which greatly reduces the head loss in the GHX. The system shall include a three-way valve upstream of the GHX (V-1) to allow bypass of the GHX under some conditions.

V-1 Operation

Use temperatures upstream (T_{HP}) and downstream (T_{TOW}) of the heat pumps to determine whether the system is in cooling or heating mode. If the T_{TOW} is higher than T_{HP}, the system is in cooling mode; if T_{HP} is higher than T_{TOW}, the system is in heating mode. Note that diverse loads may result at times in heat pumps being on but T_{HP} and T_{TOW} being roughly equal (in these cases the system is in neither heating nor cooling mode, and the GHX should be bypassed).

In cooling mode

Open valve V-1 and flow all fluid through the GHX if the fluid temperature upstream of the bore field (T_{GHX}) is greater than $\boldsymbol{T_{Cool2}}$ **(°F)**.

In heating mode

Open valve V-1 and flow all fluid through the GHX if the heat pumps are in heating mode (T_{TOW} is lower than T_{HP}).

Note:

In a conventional (non-hybrid) geothermal heat pump system, the GHX is designed for the full cooling and heating load. In a hybrid like this one, the GHX is typically designed for the full heating load and part of the cooling load. In the event that there is a relatively small heating load and therefore a relatively small GHX, the designer should verify that the GHX is capable of the full flow load with all two-way valves open. This may happen when warming up the building in the winter after a weekend setback, for example. If this were to create problems, a custom control strategy such as staged warm up or partial GHX bypass may be needed.

Closed-Circuit Cooling Tower Operation

The closed-circuit cooling tower (CCCT) is connected to the central loop through a primary/secondary pumping arrangement. The pump (P-2) in the CCCT loop should be sized to produce the rated flow specified through the CCCT at the head loss for piping and fittings included the CCCT. The connection of the CCCT loop to the central loop shall be made with two close coupled T's.

CCCT Loop Pump P-2

The CCCT loop pump (P-2) shall operate if the fluid temperature upstream of the tower (T_{TOW}) is $\boldsymbol{\Delta T_1}$ **(^{0}F)** higher than the ambient wet bulb temperature (T_{WB}).

CCCT Fan

If pump P-2 is energized, the cooling tower fan shall be on. If a two-speed fan is available on the tower, the fan should operate at low – $\boldsymbol{X}$ **(%)** – speed, unless the fluid temperature upstream of the cooling tower (T_{TOW}) is greater than $\boldsymbol{T_{Cool1}}$ **(°F)**; in that case the fan should operate at full speed.

Freeze Protection

It is important that the working fluid not be allowed to freeze in the cooling tower at any time, or damage will result. It is therefore recommended that:

a) the working fluid be a water-propylene glycol solution of a concentration high enough to prevent freezing when the tower is not in operation during cold weather (ASHRAE 99.6% design dry bulb temperature). ASHRAE handbooks can be consulted for both design temperature and glycol-freezing point data.

b) If it is undesirable to use a high concentration of propylene glycol in the tower, it is also acceptable to either:

1. utilize a variable-speed pump to continually pump fluid (at minimum pump speed) through the tower during periods when the ambient temperature is below the freezing point of the working fluid, or
2. drain the tower during cold months when it is likely to freeze (note that the HyGCHP is not set-up to model this scenario).

During any freeze protection sequence, the tower fan shall be off, and all moveable dampers shall be in the closed position. It may also be beneficial to include a freeze alarm to alert the building operator when freezing conditions may occur.

Example: Atlanta Office

The following is a sequence of operations for the condenser loop of a hybrid ground-coupled heat pump system (with a cooling tower) in a 127,000 ft^2 office building in Atlanta. Section 5.4 of the final report demonstrates how the design parameters (in bold) were selected using the design guidelines for HyGCHP systems. Note that this sequence is optimal for 20 years of operation; it is possible adjustments will be required after this period (see Section 5.1).

Hybrid Ground-Coupled Heat Pump System
Sequence of Operations

General System Description
Optimization by HyGCHP suggests installation of the following equipment: a cooling tower with a rated capacity of **200 tons**, and a bore field with a total bore length of **23125 ft**, with bores spaced at least **20 - 25 ft** apart. The cooling tower shall be installed upstream of the bore field (see Figure 2). The project designer is responsible for the final specification of the tower size and ground heat exchanger (GHX) size, spacing, and layout based on available equipment sizing, site configuration and geology.

Instrumentation
Measure fluid temperatures upstream of the cooling tower (T_{TOW}), upstream of the GHX (T_{TOW}), and upstream of the heat pumps (T_{HP}) (shown in red on Figure 2). Also measure ambient wet bulb temperature (T_{WB}).

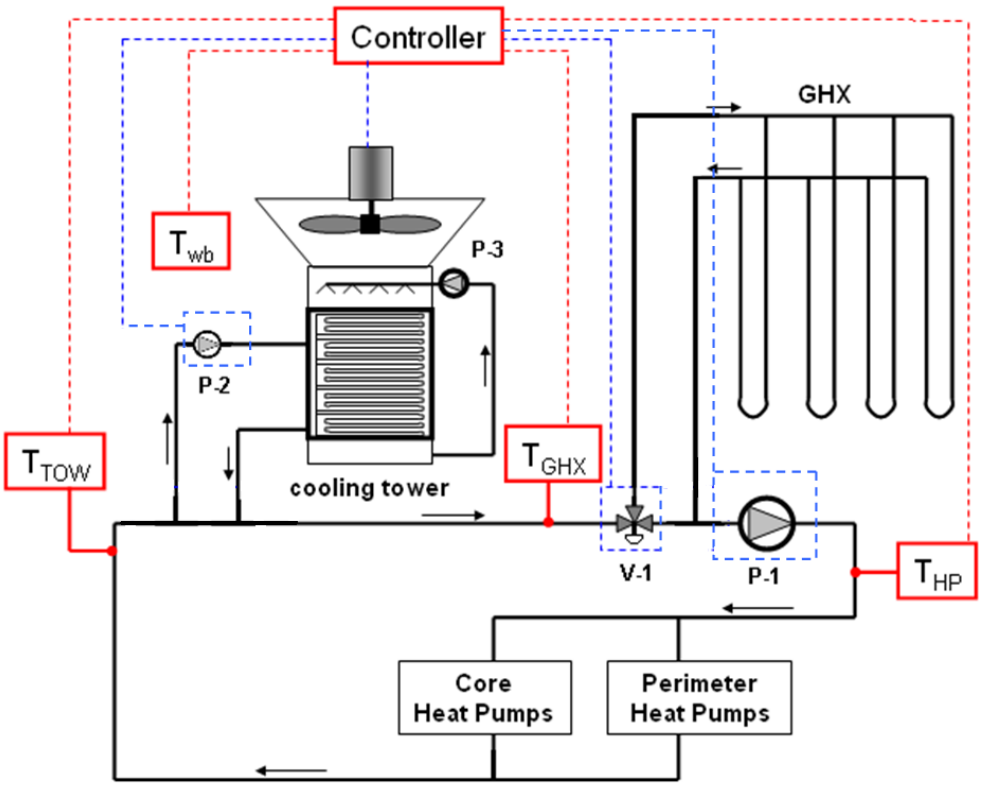

Figure 2. Setup of hybrid ground-coupled system. Required temperature measurements are shown in red, control points are shown in blue.

Sequence of Operations

Central Loop Circulation Pump Operation

Pump Operation
The central loop serving the building heat pumps and ground heat exchanger loop shall be served by one pump (P-1) with a variable frequency drive (VFD) controlled by differential pressure sensors located near the remote end of the heat pumps served. Each heat pump shall be equipped with a two-way valve (except as noted) that opens on a call for heating or cooling at the unit. Total flow/differential pressure shall be adjusted to provide 2.5 gpm/ton of building load to the heat pumps at full load (i.e. all two-way valves open).

Bypass requirement
Based on pump/drive selection and the manufacturer's recommendations there shall be a minimum central loop flow rate to avoid dead heading the pump. This minimum flow rate is determined by the pump/drive combination and the system curve. This minimum flow shall be provided by leaving out the two-way valves on the units specified in the plans and specifications (or by providing some other approved means of bypass specified by the engineer).

Notes:

c) Some designers may want to provide redundancy in the central pumping loop. One approach sometimes used is to size two parallel pumps to meet full load requirements together. If one pump fails, the other pump can generally provide approximately 70% of the full load flow. If this approach is used, staging the pumps and duty cycling control strategies must be addressed. Pumps in parallel using VFDs shall operate at the same speed if more than one is in operation.

*d) In this example a **30%** propylene glycol/water mix was recommended. If a glycol mixture is used, the pump design and flow rates should take this into consideration.*

Ground Heat Exchanger Operation

The central loop circulation pump (P-1) also provides flow through the ground heat exchanger (GHX). At low loads, the overall flow-rate is reduced which greatly reduces the head loss in the GHX. The system shall include a three-way valve upstream of the GHX (V-1) to allow bypass of the GHX under some conditions.

V-1 Operation

Use temperatures upstream (T_{HP}) and downstream (T_{TOW}) of the heat pumps to determine whether the system is in cooling or heating mode. If the T_{TOW} is higher than T_{HP}, the system is in cooling mode; if T_{HP} is higher than T_{TOW}, the system is in heating mode. Note that diverse loads may result at times in heat pumps being on but T_{HP} and T_{TOW} being roughly equal (in these cases the system is in neither heating nor cooling mode, and the GHX should be bypassed).

In cooling mode

Open valve V-1 and flow all fluid through the GHX if the fluid temperature upstream of the bore field (T_{GHX}) is greater than **61°F**.

In heating mode

Open valve V-1 and flow all fluid through the GHX if the heat pumps are in heating mode (T_{TOW} is lower than T_{HP}).

Note:

In a conventional (non-hybrid) geothermal heat pump system, the GHX is designed for the full cooling and heating load. With a hybrid, the GHX is designed for the full heating load and part of the cooling load. In the event that there is a relatively small heating load and therefore a relatively small GHX, the designer should verify that the GHX is capable of the full flow load with all two-way valves open. This may happen when warming up the building in the winter after a weekend setback, for example. If this were to create problems, a custom control strategy such as staged warm up or partial GHX bypass may be needed.

Closed-Circuit Cooling Tower Operation

The closed-circuit cooling tower (CCCT) is connected to the central loop through a primary/secondary pumping arrangement. The pump (P-2) in the CCCT loop should be sized to produce the rated flow specified through the CCCT at the head loss for piping and fittings included the CCCT. The connection of the CCCT loop to the central loop shall be made with two close coupled T's.

CCCT Loop Pump P-2

The CCCT loop pump (P-2) shall operate if the fluid temperature upstream of the tower (T_{TOW}) is **20°F** higher than the ambient wet bulb temperature (T_{WB}).

CCCT Fan

If pump P-2 is energized, the cooling tower fan shall be on. If a two-speed fan is available on the tower, the fan should operate at low – **50%** – speed, unless the fluid temperature upstream of the cooling tower (T_{TOW}) is greater than **117°F**; in that case the fan should operate at full speed.

Freeze Protection

In this example, freeze protection is provided by the 30% propylene glycol solution used as the working fluid. (See the general sequence of operations above for more details regarding freeze protection of cooling towers in hybrid systems.)

Sequence of Operations – Heating Dominated

The following is a general sequence of operations for the condenser loop of a heating-dominated hybrid ground-coupled heat pump system (with a boiler). The results of the design guidelines (or optimization using the distributable) for any specific building/climate can be used to fill in the design variables that are shown in bold, italicized font. Note that this sequence is optimal for 20 years of operation; it is possible adjustments will be required after this period (see Section 5.1).

(*Following this general sequence, an example sequence is shown for a specific scenario.*)

Hybrid Ground-Coupled Heat Pump System
Sequence of Operations

General System Description
Optimization by HyGCHP suggests installation of the following equipment: a boiler with a rated capacity of $\boldsymbol{C_{Boil}}$ **(kBtu/hr)**, and a bore field with a total bore length of $\boldsymbol{L_{tot}}$ **(ft)**, with bores spaced at least $\boldsymbol{d_{spacing}}$ **(ft)** apart. The boiler shall be installed downstream of the bore field (see Figure 1). The project designer is responsible for the final specification of the boiler size and GHX size, spacing, and layout based on available equipment sizing, site configuration and geology.

Instrumentation
Measure fluid temperatures upstream of the boiler (T_B), upstream of the ground heat exchanger (T_{GHX}), and upstream of the heat pumps (T_{HP}) (shown in red on Figure 1).

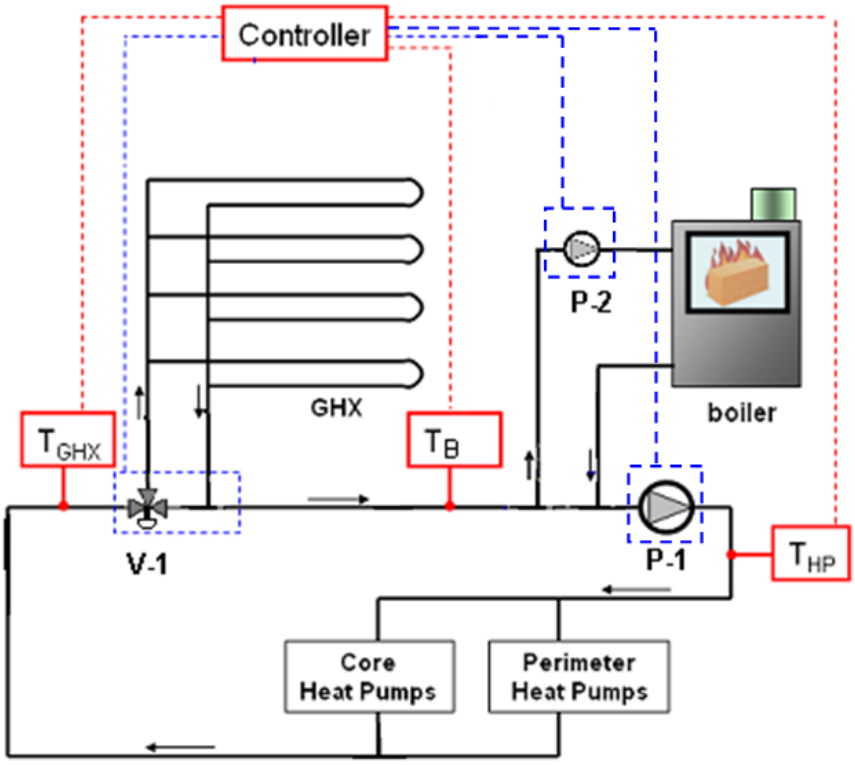

Figure 91. Setup of hybrid ground-coupled system. Required temperature measurements are shown in red, control points are shown in blue.

Sequence of Operations

Central Loop Circulation Pump Operation

Pump Operation
The central loop serving the building heat pumps and ground heat exchanger loop shall be served by one pump (P-1) with a variable frequency drive (VFD) controlled by differential pressure sensors located near the remote end of the heat pumps served. Each heat pump shall be equipped with a two-way valve (except as noted) that opens on a call for heating or cooling at the unit. Total flow/differential pressure shall be adjusted to provide 2.5 gpm/ton of building load to the heat pumps at full load (i.e. all two-way valves open).

Bypass requirement
Based on pump/drive selection and the manufacturer's recommendations there shall be a minimum central loop flow rate to avoid dead heading the pump. This minimum flow rate is determined by the pump/drive combination and the system curve. This minimum flow shall be provided by leaving out the two-way valves on the units specified in the plans and specifications (or by providing some other approved means of bypass specified by the engineer).

Notes:

e) Some designers may want to provide redundancy in the central pumping loop. One approach sometimes used is to size two parallel pumps to meet full load requirements together. If one pump fails, the other pump can generally provide approximately 70% of the full load flow. If this approach is used, staging the pumps and duty cycling control strategies must be addressed. Pumps in parallel using VFDs shall operate at the same speed if more than one is in operation.

*f) Propylene glycol/water mix – **X** **(%)** solution – may be recommended in order to operate at low temperatures. If a glycol mixture is used, the pump design and flow rates should take this into consideration.*

Ground Heat Exchanger Operation

The central loop circulation pump (P-1) also provides flow through the ground heat exchanger (GHX). At low loads, the overall flow-rate is reduced which greatly reduces the head loss in the GHX. The system shall include a three-way valve upstream of the GHX (V-1) to allow bypass of the GHX under some conditions.

V-1 Operation

Use temperatures upstream (T_{HP}) and downstream (T_{GHX}) of the heat pumps to determine whether the system is in cooling or heating mode. If the T_{GHX} is higher than T_{HP}, the system is in cooling mode; if T_{HP} is higher than T_{GHX}, the system is in heating mode. Note that diverse loads may result at times in heat pumps being on but T_{HP} and T_{TOW} being roughly equal (in these cases the system is in neither heating nor cooling mode, and the GHX should be bypassed).

In cooling mode

Open valve V-1 and flow all fluid through the GHX if the fluid temperature upstream of the bore field (T_{GHX}) is greater than $\boldsymbol{T_{Cool2}}$ **(°F)**.

In heating mode

Open valve V-1 and flow all fluid through the GHX if the fluid temperature upstream of the bore field (T_{GHX}) is less than $\boldsymbol{T_{Heat1}}$ **(°F)**.

Note:

In a conventional (non-hybrid) geothermal heat pump system, the GHX is designed for the full cooling and heating load. With a heating-dominated hybrid, the GHX is designed for the full cooling load and part of the heating laod. In the event that there is a relatively small GHX, the designer should verify that the GHX is capable of the full flow load with all two-way valves open. This may happen when warming up the building in the winter after a weekend setback, for example. If this were to create problems, a custom control strategy such as staged warm up or partial GHX bypass may be needed.

Boiler Operation

The boiler is connected to the central loop through a primary/secondary pumping arrangement. The pump (P-2) in the boiler loop should be sized to produce the full flow rate, at the head loss for piping and fittings included the boiler. The connection of the boiler loop to the central loop shall be made with two close coupled T's.

Boiler Loop Pump P-2

The boiler and boiler loop pump shall operate if the fluid temperature upstream of the boiler (T_B) is below $\boldsymbol{T_{Heat2}}$ **(°F)**. This temperature setpoint should be low enough to prevent energy added by the boiler from being transferred to the ground after the building.

Example: Minneapolis School

The following is a sequence of operations for the condenser loop of a hybrid ground-coupled heat pump system (with a boiler) in a 92,000 ft^2 school in Minneapolis. The outputs shown in bold were optimized for this building using the HyGCHP model. Note that this sequence is optimal for 20 years of operation; it is possible adjustments will be required after this period (see Section 5.1).

Hybrid Ground-Coupled Heat Pump System
Sequence of Operations

General System Description
Optimization by HyGCHP suggests installation of the following equipment: a boiler with a rated capacity of **3740 kBtu/hr**, and a bore field with a total bore length of **14,300 ft**, with bores spaced at least **20 - 25 ft** apart. The boiler shall be installed downstream of the bore field (see Figure 1). The project designer is responsible for the final specification of the boiler size and GHX size, spacing, and layout based on available equipment sizing, site configuration and geology.

Instrumentation
Measure fluid temperatures upstream of the boiler (T_B), upstream of the ground heat exchanger (T_{GHX}), and upstream of the heat pumps (T_{HP}) (shown in red on Figure 1).

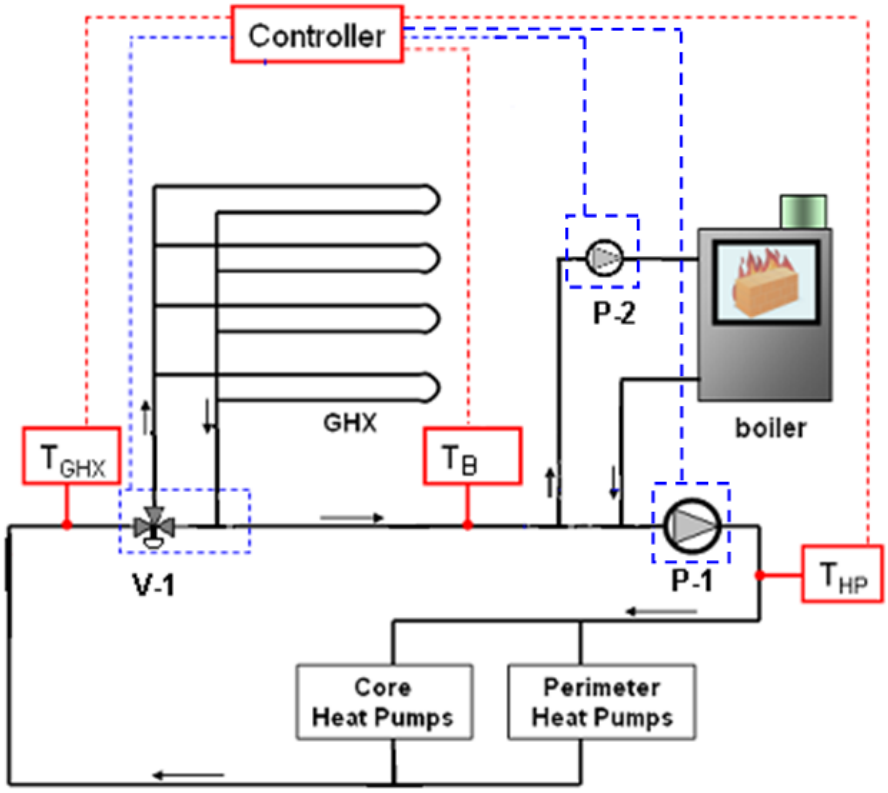

Figure 92. Setup of hybrid ground-coupled system. Required temperature measurements are shown in red, control points are shown in blue.

Sequence of Operations

Central Loop Circulation Pump Operation

Pump Operation
The central loop serving the building heat pumps and ground heat exchanger loop shall be served by one pump (P-1) with a variable frequency drive (VFD) controlled by differential pressure sensors located near the remote end of the heat pumps served. Each heat pump shall be equipped with a two-way valve (except as noted) that opens on a call for heating or cooling at the unit. Total flow/differential pressure shall be adjusted to provide 2.5 gpm/ton of building load to the heat pumps at full load (i.e. all two-way valves open).

Bypass requirement
Based on pump/drive selection and the manufacturer's recommendations there shall be a minimum central loop flow rate to avoid dead heading the pump. This minimum flow rate is determined by the pump/drive combination and the system curve. This minimum flow shall be provided by leaving out the two-way valves on the units specified in the plans and specifications (or by providing some other approved means of bypass specified by the engineer).

Notes:

g) Some designers may want to provide redundancy in the central pumping loop. One approach sometimes used is to size two parallel pumps to meet full load requirements together. If one pump fails, the other pump can generally provide approximately 70% of the full load flow. If this approach is used, staging the pumps and duty cycling control strategies must be addressed. Pumps in parallel using VFDs shall operate at the same speed if more than one is in operation.

*h) In this example a **23%** propylene glycol/water mix was recommended. If a glycol mixture is used, the pump design and flow rates should take this into consideration.*

Ground Heat Exchanger Operation

The central loop circulation pump (P-1) also provides flow through the ground heat exchanger (GHX). At low loads, the overall flow-rate is reduced which greatly reduces the head loss in the GHX. The system shall include a three-way valve upstream of the GHX (V-1) to allow bypass of the GHX under some conditions.

V-1 Operation

Use temperatures upstream (T_{HP}) and downstream (T_{GHX}) of the heat pumps to determine whether the system is in cooling or heating mode. If the T_{GHX} is higher than T_{HP}, the system is in cooling mode; if T_{HP} is higher than T_{GHX}, the system is in heating mode. Note that diverse loads may result at times in heat pumps being on but T_{HP} and T_{TOW} being roughly equal (in these cases the system is in neither heating nor cooling mode, and the GHX should be bypassed).

In cooling mode

Open valve V-1 and flow all fluid through the GHX if the fluid temperature upstream of the bore field (T_{GHX}) is greater than **57.7°F**.

In heating mode

Open valve V-1 and flow all fluid through the GHX if the fluid temperature upstream of the bore field (T_{GHX}) is less than **50.0°F**.

Note:

In a conventional (non-hybrid) geothermal heat pump system, the GHX is designed for the full cooling and heating load. With a heating-dominated hybrid, the GHX is designed for the full cooling load and part of the heating laod. In the event that there is a relatively small GHX, the designer should verify that the GHX is capable of the full flow load with all two-way valves open. This may happen when warming up the building in the winter after a weekend setback, for example. If this were to create problems, a custom control strategy such as staged warm up or partial GHX bypass may be needed.

Boiler Operation

The boiler is connected to the central loop through a primary/secondary pumping arrangement. The pump (P-2) in the boiler loop should be sized to produce the full flow rate, at the head loss for piping and fittings included the boiler. The connection of the boiler loop to the central loop shall be made with two close coupled T's.

Boiler Loop Pump P-2

The boiler and boiler loop pump shall operate if the fluid temperature upstream of the boiler (T_B) is below **34°F**. This temperature setpoint should be low enough to prevent energy added by the boiler from being transferred to the ground after the building.